DIM-ESEE CONFERENCE

organized at University of Zagreb

Faculty of Mining, Geology and Petroleum Engineering

Organized by:























PROCEEDINGS of the DIM-ESEE CONFERENCE (REVIEWED PAPERS)

Dubrovnik, October 15th – 17th, 2025

Volume 1, 2025

PUBLISHER:



University of Zagreb



Faculty of Mining, Geology and Petroleum Engineering,
Pierottijeva 6, Zagreb, Croatia

ISSN 3102-3517 (Online)

Editors:

Dalibor Kuhinek (editor-in-chief), professor, University of Zagreb, Faculty of Mining, Geology and Petroleum Engineering, Zagreb, Croatia

Mario Dobrilović (field editor), professor, University of Zagreb, Faculty of Mining, Geology and Petroleum Engineering, Zagreb, Croatia

Yann Foucaud (field editor), associate professor, University of Lorraine, Nancy, France

Josipa Kapuralić (field editor), associate professor, University of Zagreb, Faculty of Mining, Geology and Petroleum Engineering, Zagreb, Croatia

Marta Mileusnić (field editor), professor, University of Zagreb, Faculty of Mining, Geology and Petroleum Engineering, Zagreb, Croatia

Gabriela Paszkowska (field editor), professor, Wroclaw University of Science and Technology, Faculty of Geoengineering, Mining and Geology, Wroclaw, Poland

Publisher:

University of Zagreb, Faculty of Mining, Geology and Petroleum Engineering,
Pierottijeva 6, Zagreb, Croatia

Chairmen:

Assoc. prof. Vladislav Brkić, Dean of the Faculty

Scientific Committee:

Representative	Institution	Acronym
Sibila Borojević Šoštarić	University of Zagreb, Faculty of Mining, Geology and Petroleum Engineering, Croatia	UNIZG-RGNF
Ferenc Madai	University of Miskolc, Hungary	ИМ
Philipp Hartlieb	Montanuniversität Leoben, Austria	MUL
Vječislav Bohanek	University of Zagreb, Faculty of Mining, Geology and Petroleum Engineering, Croatia	UNIZG-RGNF
Karolina Adach	Faculty of Geoengineering, Mining and Geology	WUST
Eric Pirard	University of Liege, Belgium	ULiège
Davor Kvočka	Slovenian National Building And Civil Engineering Institute, Slovenia	ZAG
Alenka Mauko Pranjić	Slovenian National Building And Civil Engineering Institute, Slovenia	ZAG
Primož Oprčkal	Slovenian National Building And Civil Engineering Institute, Slovenia	ZAG
Gabriela Paszkowska	Faculty of Geoengineering, Mining and Geology	WUST
Marta Mileusnić	University of Zagreb, Faculty of Mining, Geology and Petroleum Engineering, Croatia	UNIZG-RGNF
Josipa Kapuralić	University of Zagreb, Faculty of Mining, Geology and Petroleum Engineering, Croatia	UNIZG-RGNF
Mario Dobrilović	University of Zagreb, Faculty of Mining, Geology and Petroleum Engineering, Croatia	UNIZG-RGNF
Yann Foucaud	University of Liege, Belgium	ULiège
Dalibor Kuhinek	University of Zagreb, Faculty of Mining, Geology and Petroleum Engineering, Croatia	UNIZG-RGNF

Program Committee:

Representative	Institution	Acronym
Sibila Borojević Šoštarić	University of Zagreb, Faculty of Mining, Geology and Petroleum Engineering, Croatia	UNIZG-RGNF
Ferenc Madai	University of Miskolc, Hungary	UM
Philipp Hartlieb	Montanuniversität Leoben, Austria	MUL
Vječislav Bohanek	University of Zagreb, Faculty of Mining, Geology and Petroleum Engineering, Croatia	UNIZG-RGNF
Karolina Adach	Faculty of Geoengineering, Mining and Geology	WUST
Eric Pirard	University of Liege, Belgium	ULiège
Davor Kvočka	Slovenian National Building Davor Kvočka And Civil Engineering Institute, Slovenia	
Alenka Mauko Pranjić	Slovenian National Building And Civil Engineering Institute, Slovenia	ZAG
Primož Oprčkal	Slovenian National Building And Civil Engineering Institute, Slovenia	ZAG
Gabriela Paszkowska	Faculty of Geoengineering, Mining and Geology	WUST

Published online

Published each year from 2025

Published as e-book

The proceedings will be proposed for indexation in the Scopus. Authors are solely responsible for the contents. English proofreading and formatting according to the author's instructions.

The proceedings were prepared using the Open Monograph Press tool available on the Portal of Croatian scientific and professional journals HRČAK.

CONTENS

RAW MATERIALS PROSPECTION AND DISCOVERIES

Title Authors	Page no.
Development of Engineering Methods for Slope Stabilization in Water-Infused Titanium-Zirconium Mines Oleksii Lozhnikov, Carsten Drebenstedt, Anton Bondarenko Paper No. 349	RM1-RM9
Towards Sustainable Deep Mineral Exploration: Insights from the MINOTAUR Project Magdalena Worsa-Kozak, Aurela Shtiza, Adam Wróblewski Paper No. 376	RM10-RM17
Prospections of former deposits for the purpose of protection of mining and cultural heritage Ana Maričić, Zlatko Briševac, Vladislav Brkić Paper No. 381	RM18-RM25

MINING METHODS

Title Page no. Authors Dynamic Management of Ore Body Bedding Models Based on MM1-MM7 **Machine Learning and Terrain Grid Reconstruction** Dmytro Malashkevych, Vladyslav Ruskykh, Marek Dudek, Dariusz Sala, Yuliya Pazynich Paper No. 353 MM8-MM14 **Advancing Explosion Protection in Coal** Mines Exposed to Gas-Dynamic Risks Vasyl Holinko, Oleksandr Holinko, Oleg Kuznetsov, Yulia Zabolotna Paper No. 357 Underground trial testing of NRE Support Rig MM15-MM20 Paulo Pleše, Juraj Banić, Vječislav Bohanek, Sibila Borojević Šoštarić Paper No. 358 Advancements in Oil Well Perforation Technologies Aimed at MM21-MM27 **Reducing Casing and Annular Damage** Oleksandr Pashchenko, Andrii Sudakov, Valerii Rastsvietaiev Paper No. 367 **Enhancing Rock Destruction through Viscoelastic Properties of** MM28-MM33 **Drilling Fluids** Volodymyr Khomenko, Yevhenii Koroviaka, Oleksandr Pashchenko, Andrii Ihnatov Paper No. 368 Mechanism of Gate Road Floor Heaving as the Basis for MM34-MM40 Geotechnical Stabilization of Its Section Ivan Sadovenko, Serhii Vlasov, Vladyslav Vlasov, Stanislav Hroma, Dmytro Tvilenov Paper No. 371 High-Precision 3D Scanning for the State and Stability MM41-MM51 **Assessment of Underground Mining Facilities of Various Purposes** Serhii Pysmennyi, Dmytro Brovko, Mykhailo Fedko, Svetlana Panova Paper No. 374 The variation of safety pillar's width with depth under the MM52-MM58 influence of thermo-mechanical stresses in Underground Coal Gasification Svitlana Sakhno, Ivan Sakhno, Serhii Bashynskyi, Munkhtsetseg Oidov Paper No. 377

Examples of comparative measurements of active concentration of radon (Rn) in air in Croatia

Hrvoje Vukosic, Željko Ban, Dalibor Kuhinek, Želimir Veinović Paper No. 393

MM67-MM72

MM59-MM66

Analysis of Drilling Parameters for Construction Pit Excavation

Siniša Stanković, Vinko Škrlec, Mario Dobrilović, Mihaela Fajdetić Paper No. 396

MM73-MM77

Waste organic materials in emulsion explosives-properties and possibilities

Mario Dobrilović, Ivana Dobrilović, Muhamed Sućeska, Vinko Škrlec, Romano Cardinale Paper No. 398

Geomechanical studies of the rock mass during underground block leaching of uranium

MM78-MM84

Mykola Stupnik, Olena Kalinichenko, Vsevolod Kalinichenko, Volodymyr Pilchyk Paper No. 375

MATERIALS RECYCLING & WASTE MANAGEMENT

Title Page no. Authors **Economic Assessment of Geothermal System Installation in** MR1-MR6 **Abandoned Mines** Dmytro Rudakov, Oleksandr Inkin, Rolf Schiffer Paper No. 350 **Hydrogen Recovery from Coal Industry Waste Using Pyrolysis:** MR7-MR12 **Experimental Analysis and Perspectives** Eduard Kliuiev, Ruslan Ahaiev, Vasyl Zberovskyi, Kateryna Dudlia Paper No. 354 Hybrid Approach of Neural Networks and Analog-Based Methods MR23-MR20 for Industrial Assessment of Technogenic Deposits Artem Pavlychenko, Dagmara Lewicka, Ivan Miroshnykov, Serhii Dybrin, Andrii Pererva, Roman Dychkovskyi Paper No. 356 Laboratory Investigation of Cement Kiln Dust (CKD) for MR21-MR26 Stabilization of Clay Soil from Cegléd, Hungary Sirine Trabelsi, Andrea Tóth, Tamás Kántor Paper No. 359 Red mud as geotechnical composite MR27-MR33 Primož Pavšič, Marija Đurić, Mateja Košir, Primož Oprčkal, Vesna Zalar Serjun Paper No. 361 **Development of Porous Foam Glass from End-of-Life PV Panels** MR34-MR40 **Using Secondary Raw Materials** Busra Karakas, Ildikó Fóris, Gábor Mucsi Paper No. 363 Mechanical Pretreatment of a Mild Hybrid Lithium-Ion Battery MR41-MR46 Pack - Recovery of Black Mass Tamas Kurusta, Sándor Márton Nagy Paper No. 369 Investigation of Coal Reserve Recovery Indicators in Low-MR47-MR53 **Capacity Mines Considering the Reprocessing of Mining Waste** Andrii Khorolskyi, Oleksandr Mamaikin, Iryna Lisovytska, Ivan Sheka, Svitlana Delehan Paper No. 379

Development of Waste Risk Management in Organizations

MR54-MR61

Vitaliy Tsopa, Olena Yavorska, Serhii Cheberiachko, Oleksandr Kovrov, Yuliya Pazynich, Lidia Cheberiachko Paper No. 382

Hydration and Carbonation Behaviour of Selected Recycled Materials from Slovenia

MR62-MR67

Vesna Zalar Serjun, Primož Oprčkal, Anton Meden, Marta Počka, Romana Cerc Korošec Paper No. 388

Circular Economy In Mining

MR68-MR75

Predrag Šinik, Ivo Galić, Metka Gostečnik, Viktor Kovačič, Lana Šteko, Dora Kolobara Paper No. 394

RAW MATERIALS EDUCATION

Title Page no.

Authors

Training needs of copper sector employees in the context of digital and environmental transformation: results of the SkiComCu project

ED1-ED7

Jolanta Religa, Ireneusz Woźniak, Malwina Kobylańska, Katerina Adam, Małgorzata Kowalska Paper No. 383



Development of Engineering Methods for Slope Stabilization in Water-Infused Titanium-Zirconium Mines

DIM-ESEE Conference



 $\begin{array}{l} Oleksii\ Lozhnikov^{1*},\ Carsten\ Drebenstedt^2\ , \\ Anton\ Bondarenko^1 \end{array}$

¹Dnipro University of Technology, Department of Surface Mining, 19 Yavornytskoho Ave., 49005 Dnipro, Ukraine

²TU Bergakademie Freiberg, Institute of Surface Mining and Special Structure, 09569, Freiberg, Gustav-Zeuner-Strasse, 1A, Germany

Abstract

The work aims to develop practical engineering and technical methods for strengthening the slopes of the sides of watered titanium-zirconium quarries, which will contribute to reducing the risks of landslides, considering land conservation indicators. The research was carried out using the method of modeling the stability parameters of mining massifs using specialized software Rocscience Slide. Slope stability and land conservation in the modern world are relevant and integral aspects of the sustainable development and functioning of engineering facilities. Preventing the sliding of sandy soils of pit slopes is critically essential for ensuring the safety of mining operations in mining areas. It has been determined that one of the standard methods of strengthening slopes is the use of anchor systems, which provide soil stabilization and prevent landslides and collapses. The three-dimensional modeling method is used in studies to determine the safety parameters of the mining massif, which allows for the determination of potential collapse zones. It is also used together with monitoring systems to detect early signs of slope failure. The dependence of the stability margin coefficient on the increase in the angle of inclination of the pit slope has been determined. The results of the research allow us to state that with an increase in the number of anchors from 0 to 24 units, the safety factor of the slope of the side will increase by 4.2 % from 1.16 to 1.21. It was found that sandy soils are characterized by high permeability and low cohesive strength, which makes them particularly vulnerable to sliding when the rock mass is moistened. The practical significance of the work lies in determining the effective field of application of anchor fasteners to prevent the sliding of sandy soils of the slopes of the pit, which will ensure the safety of workers and the local population. It was found that the use of the proposed engineering method of strengthening sandy-clay soils can occur in limited cases for a slight increase in the safety factor of the slopes of the pit sides.

Keywords: mining operations, slope reinforcement, anchor system, soil stabilization, massif stability

1. Introduction

Strengthening the slopes of the sides of watered pits for mining titanium-zirconium ores (Sobko et al., 2016) is a critically important task since the safety (Inthavongsa et al., 2016) and efficiency of open pit mining (Anisimov et al., 2018) of promising watered deposits depend on its solution (Kaźmierczak et al., 2022). Unstable slopes (Adamchuk et al., 2023) formed during mining operations can lead to rockslides (Koda et al., 2020), which complicate the mining process (Cherep, 2024) and create a danger to workers and equipment. Successful strengthening of slopes requires considering hydrogeological conditions (Lozhnikov et al., 2024), mechanical properties of soil (Gunawan et al., 2023), and available strengthening methods (Cherniaiev et al., 2024). In addition, it is essential to minimize the amount of soil removal during stripping operations to achieve the effect of land conservation (Moldabayev et al., 2022).

The research considered modern engineering methods for strengthening slopes (Maodin et al., 2023), emphasizing their effectiveness in the context of flooded pit rocks. Particular attention is paid to these anchor systems that provide additional slope support by securing them with steel or composite structures. This method can be especially effective in high slopes, where there is a risk of large volumes of soil collapse (Lashgari et al., 2022).

The experience of operating quarries in Germany has shown that there have been significant landslides of sand slopes during heavy rains. The lack of proper drainage systems led to oversaturation of the soil with water, which caused large-scale landslides that blocked production processes and caused significant material damage. There are also similar cases in Brazil, when landslides occurred due to insufficient strengthening of the slopes during the development of sand pits. At the same time, attempts to prevent rockslides were limited to using geotextiles without additional drainage systems. As a result, the landslide led to the loss of a significant amount of extracted material and the temporary closure of the pit. At one of the sand pits in Morocco, a rockslide occurred due to improper terracing of the slopes. It led to the destruction of part of the equipment and infrastructure, significantly affecting production activities and workers' safety.

Presented confirms the importance of applying an integrated approach to preventing the sliding of sandy soils on pit slopes, including the use of geotextiles, drainage systems, chemical additives, and terracing. Implementing these methods ensures the stability of slopes, increases the safety and efficiency of mining operations, and reduces environmental risks.

Since Ukraine has significant reserves of titanium-zirconium ores, solving the problem of ensuring the stability of alluvial rock massifs is of critical importance (**Lozhnikov et al., 2023**), since titanium and zirconium are strategic metals necessary for the development of the national economy and the country's defense capability. There are 11 titanium-zirconium deposits, 280 ore occurrences, and 1,400 mineralization points. These deposits represent a zone of concentration of minerals containing titanium and zirconium in water-saturated rocks. Their formation in Ukraine is usually associated with sedimentary processes, under the historical influence of rivers and seas.

Placers of the coastal-marine facies are developed on the Ukrainian Shield, Dnieper-Donetsk, Black Sea depressions, and form the Dnieper, Azov-Black Sea, and Kharkiv-Sumy alluvial zones. The most productive of them is the Dnieper zone, which is 50-100 km wide and over 700 km long along the northeastern slope of the Ukrainian crystalline shield.

Sedimentary deposits of titanium-zirconium ores are developed using open-pit mining, with subsequent enrichment and processing to obtain titanium and zirconium concentrates. The main difficulties in ensuring the stability of rock massifs (**Sobko et al., 2022**) arise when overburden is removed, since the overburden is represented by sandy-clayey rocks, the stability of which decreases when watered by groundwater or surface waters.

In this regard, an urgent task arises to substantiate additional measures to strengthen the slopes of mountain massifs formed from sandy and clayey rocks while exploiting titanium-zirconium mineral deposits.

2. Methods

Analysis of modern reinforcement systems in mining operations allows us to establish that anchors can increase their effectiveness if integrated with geosynthetic materials. Since anchor systems create additional adhesion between the slope and stable soil layers or rocks, which allows for the distribution of loads and reduces the risk of landslides, they can be used both temporarily and permanently, depending on the specifics of the tasks.

The main advantage of anchors is their ability to effectively strengthen slopes even in difficult geological conditions and under significant loads. The disadvantage of anchor systems is that the cost of materials and labor to install anchor systems can be substantial. This includes the costs of purchasing anchors, drilling, and installation, which can increase the overall cost of the project. Installing anchors can be technically complex, requiring highly skilled professionals and specialized equipment. This can be especially problematic in hard-to-reach areas or unstable soil conditions.

In addition, steel anchors can be susceptible to corrosion, especially in aggressive environments or in contact with groundwater (Cherniaiev et al., 2024). This requires additional protective coatings or the selection of corrosion-resistant materials, which can increase costs. In addition, regular inspections and maintenance are required to ensure the reliability of anchor systems. This includes checking the condition of the anchors and fasteners, which can be a time-consuming and expensive process. If installed incorrectly or overloaded, anchors can damage the slope structure, causing local failures or deformations, which can reduce the structure's overall stability. This factor will also affect the volume of mining reclamation work on the flooded area of the pit in the future (Lozhnikov et al., 2023).

Studying the stability of slopes in sandy-clayey soils is an essential task of engineering geology and geotechnics, mainly when additional measures are used to strengthen the slope surfaces. The Rocscience Slide software package is used to assess the stability parameters and determine the need for slope strengthening measures. This software product allows you to model complex engineering and geological conditions, take into account the influence of external loads and conduct slope stability analysis using various methods and conditions, take into account the influence of external loads and conduct slope stability analysis using various methods Bishop, Janbu, Spencer, Morgenstern-Price, etc.

When performing studies on the calculation of stability parameters, the Bishop Method was used since it is the most effective method for solving most engineering tasks in geomechanical stability. This method is more accurate than the method (Fellenius) and simpler and faster than complex methods (Morganstern-Price, finite elements). It is widely used in design of pit slopes and benches, where a circular cylindrical failure surface is possible.

The initial data for conducting research using modeling tools is the determination of possible parameters corresponding to the geometry of the slope, as well as the determination of its physical characteristics and preparation for further analysis. When performing the research, the mining and geological parameters of the development of the Motronivsko-Annivska section of the titanium-zirconium ore deposit (Sobko et al., 2016) is in commercial development Table 1.

To determine the safe geomechanical parameters of the sides during pit operation, it is necessary to establish the maximum permissible angle of inclination of natural slopes at which the slope stability reserve coefficient will remain within the allowable values. The critical value of the stability reserve coefficient in the studies is 1.15, below which the development of deformations and landslide processes is possible. The studies also study the possibility of further increasing the slope stability, which increases the stability coefficient to 1.3 or more, ensuring the absence of deformations in the slope zone.

The calculation of the safety margin factor is performed taking into account the physical and mechanical characteristics of the overburden rocks of titanium-zirconium deposits (Table 1) using Simplified Bishop Method with specified profiles for possible slope angles of the pit slopes α_S from 14° (**Figure 1a**) up to 29° (**see Figure 1b**), which allows determining safe parameters of geomechanical stability of a given pit overall slope.

Table 1. Physical and mechanical properties of overburden bench rocks the of titanium-zirconium deposits (**Sobko** et al., 2016)

#	Name	Average layer thickness, m	Unit weight, kN/m³	Cohesion, kPA	Angle of internal friction, φ, degrees
1	Forest-like loams	7	26.9	30	22
2	Red-brown clay	10	27	75	24
3	Plastered striped clay	10	23	50	30
4	Samara sand with clay	10	26	100	21.74
5	Sands of the Poltava series	10	26	25	30
6	Sand of the Kharkiv layer	6	20	30	35
7	Kyiv tier	10	27	10	20
8	Crystalline foundation	-	26	200	40

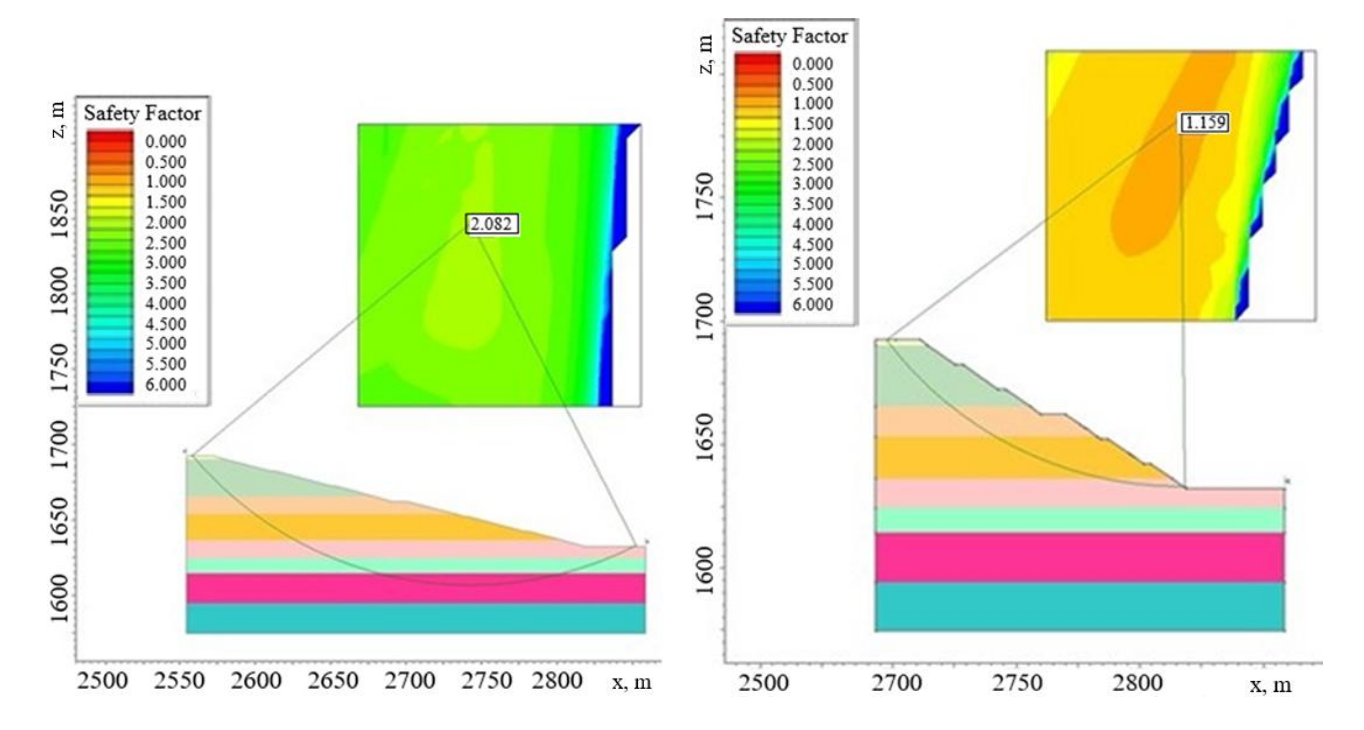


Figure 1. Results of the Factor of Safety (FOS) calculation for overall slope a) 14°, b) 29°

Analysis of the calculation results (**Figure 1**) allows us to determine the influence of the slope angle of the overall slope of the titanium-zirconium pit on the safety factor. The results of the safety factor indicator were obtained when changing the slope angle of the pit slope from 14° to 29°.

To determine the influence of the slope angle of the pit slope on the index of the stability reserve coefficient of the rock massif, studies were carried out in the range from 14° to 29°. The results (**Figure 2**) allow us to establish a safe slope angle of the pit side for the conditions of development of the Motrono-Annivska section of the titanium-zirconium deposit. The results obtained are the initial data for further determination of the effectiveness of using reinforcing structures to increase the stability of slopes of sides composed of sedimentary rocks exposed to waterlogging.

The obtained research results (**Figure 2**) allow us to establish that increasing the height of the overburden slope during the development of titanium-zirconium deposits by 2.07 times from 14 to 29° leads to a decrease in the value of the factor of stability by 1.79 times from 2.08 to 1.16. Thus, it can be confirmed that the stability of the titanium-zirconium pits' overall slopes can be achieved only at small angles of inclination of their slopes or using engineering methods of strengthening.

Special software was used to investigate the effectiveness of a simple end-mounted system, such as mechanically secured anchor bolts or blind anchors. The slide provides the opportunity to simulate the stability of the mountain massif. When performing the research, the dependencies of the stability reserve coefficient on the length of soil anchors L_A (from 5 m to 40 m) were also established, which allowed for determining the effective parameters of engineering structures. The number of anchors taken in the research is 6 to 24 units. The distance between the anchors is 7 m to 20 m in the horizontal and vertical directions. Pull-out or failure load of the anchor mechanism (Anchor Capacity) in 150 kN.

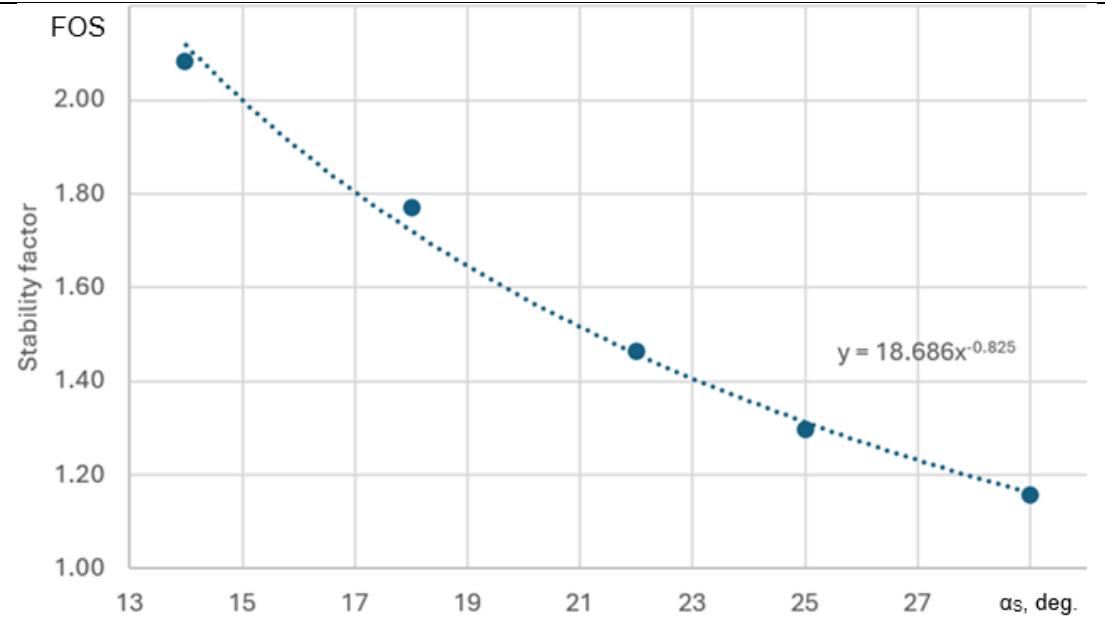


Figure 2. Dependence of the safety factor (FOS) of the rock mass on the slope angle of the pit slope (α_S)

3. Results

3.1. Determination of the influence of the anchors' length on the stability factor of rock

To determine the effectiveness of anchor systems on a slope composed of sedimentary rocks, a possible increase in the length of the anchors from 5 m to 40 m was considered. The specified range of the length of the anchor systems allows us to determine the optimal value of its length at which the stability margin coefficient will stop growing. The schematic diagram of the placement of anchor systems of different lengths with the number of anchors in a row of six units is presented in (Figure 3).

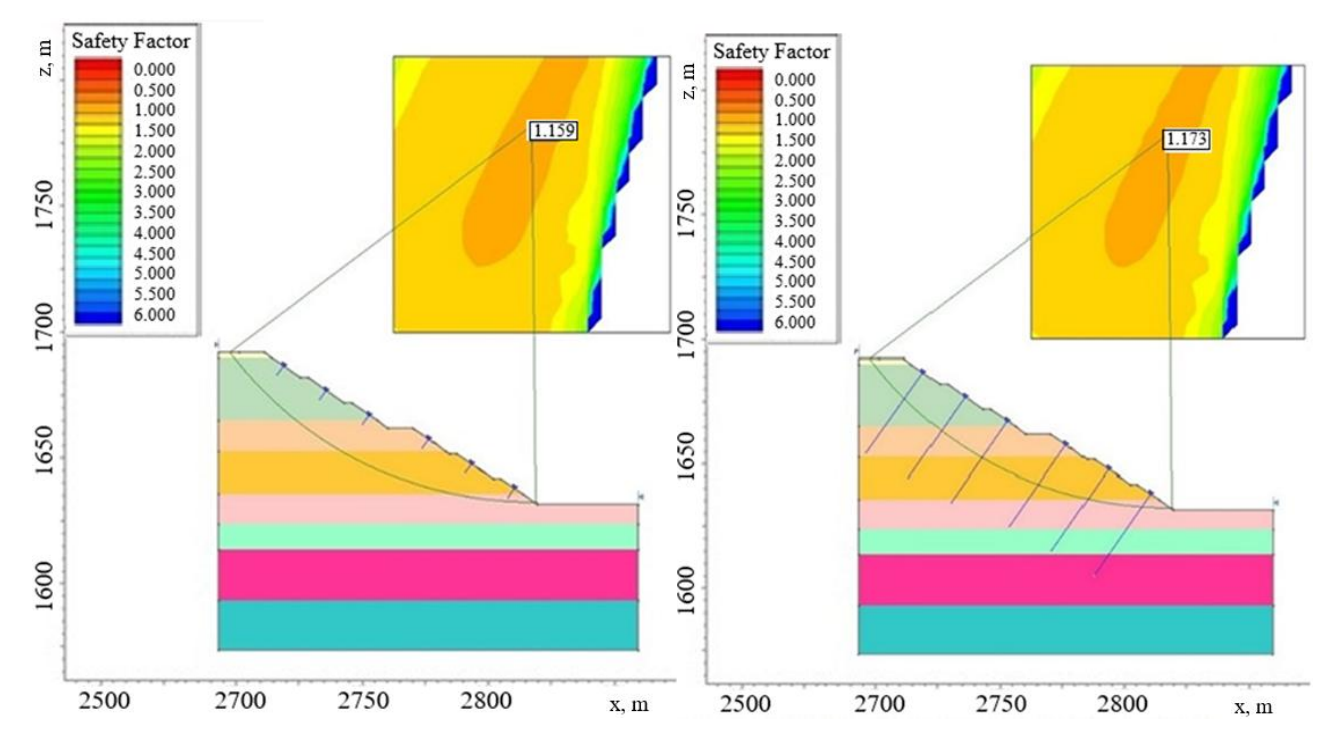


Figure 3. Calculation schemes for the stability factor when using anchors of different lengths a) 5 m, b) 40 m

A similar calculation with the determination of the safety factor for the conditions of development of the Motrono-Annivska section of the titanium-zirconium deposit was performed for the range of anchor lengths from 5 m to 40 m. The obtained dependences are shown in (**Figure 4**).

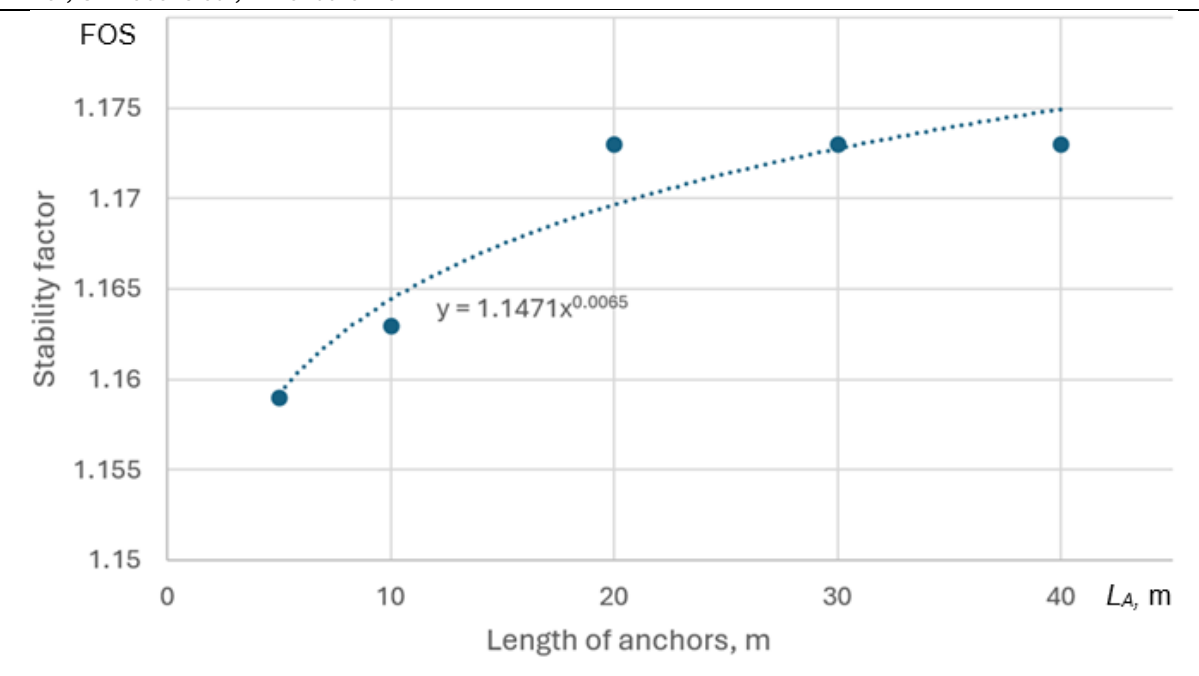


Figure 4. Influence of anchor length (L_A) on the safety factor (FOS) of the rock massif at a pit slope angle of 29°

According to the established dependence (**Figure 4**), the use of anchor systems longer than 20 m is ineffective, since they will not increase the safety factor, but the cost of their manufacture and installation will increase due to the increase in the mass of the metal structure. At the same time, expanding the anchor length four times from 5 m to 20 m will lead to an increase in the safety factor by 1.2 % from 1.159 to 1.173. The results obtained allow us to determine that in subsequent studies, it is advisable to consider the range of anchor lengths from 5 m to 20 m.

3. 2. Determination of the influence of the anchors number on the coefficient of rock stability

The next step of the research is to determine the impact of the number of soil anchors on the stability of the rock massif during the development of a similar section of the titanium-zirconium deposit. When performing calculations, the range of increasing the number of soil anchors is assumed from 0 to 24 units. The diagram of the pit slope in its normal state is shown in (**Figure 5a**. At the same time, when using six anchors (**Figure 5b**) and 24 anchors (**Figure 5c**), which allows for analyzing their location for further stability modeling work.

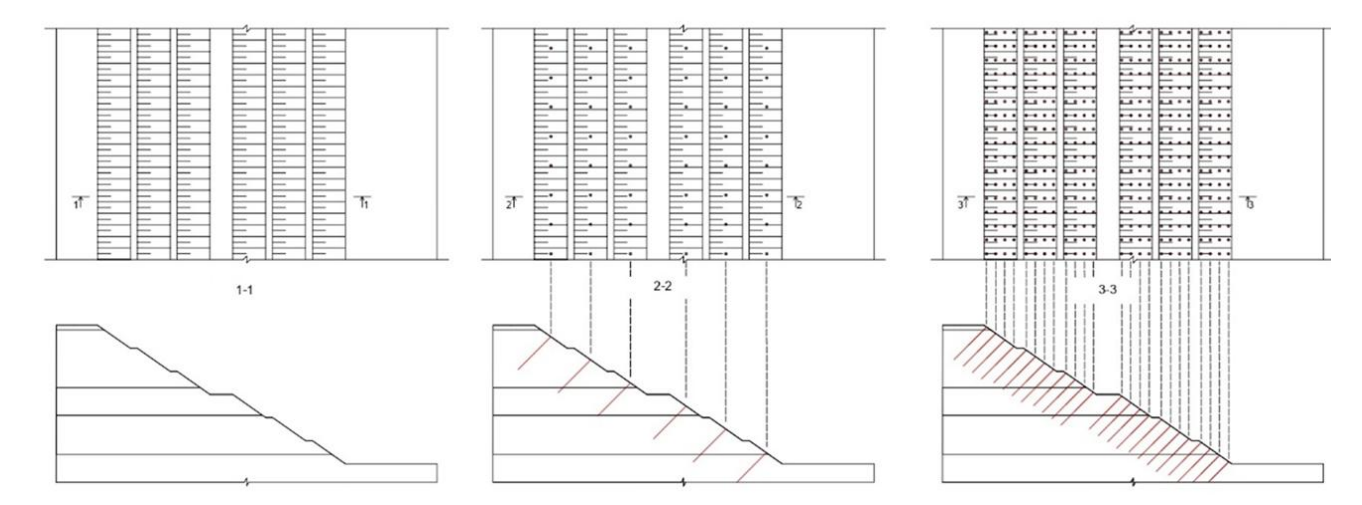


Figure 5. The overall slope of the pit a) Without installation of reinforcing elements, b) With the installation of a reduced number of reinforcing elements, c) With the installation of an increased number of reinforcing elements

According to the schemes considered (**Figure 5**), the reinforcement of the side rocks will be carried out using soil anchors of different lengths. The method of arrangement of the anchor system is assumed to be perpendicular to the slope. Under the arrangement of various numbers of anchors from 6 to 24 pieces, the distance between them can be from 7 m to

20 m in the horizontal and vertical directions. When modeling the functioning of the anchor system installed in the side rocks of the pit, the load on pulling out or destruction of the anchor mechanism is assumed (Anchor Capacity) in 150 kN.

The results of the calculations obtained to determine the stability reserve coefficient of the pit slope rocks when installing anchors from 6 to 24 units are shown in (**Figure 6**).

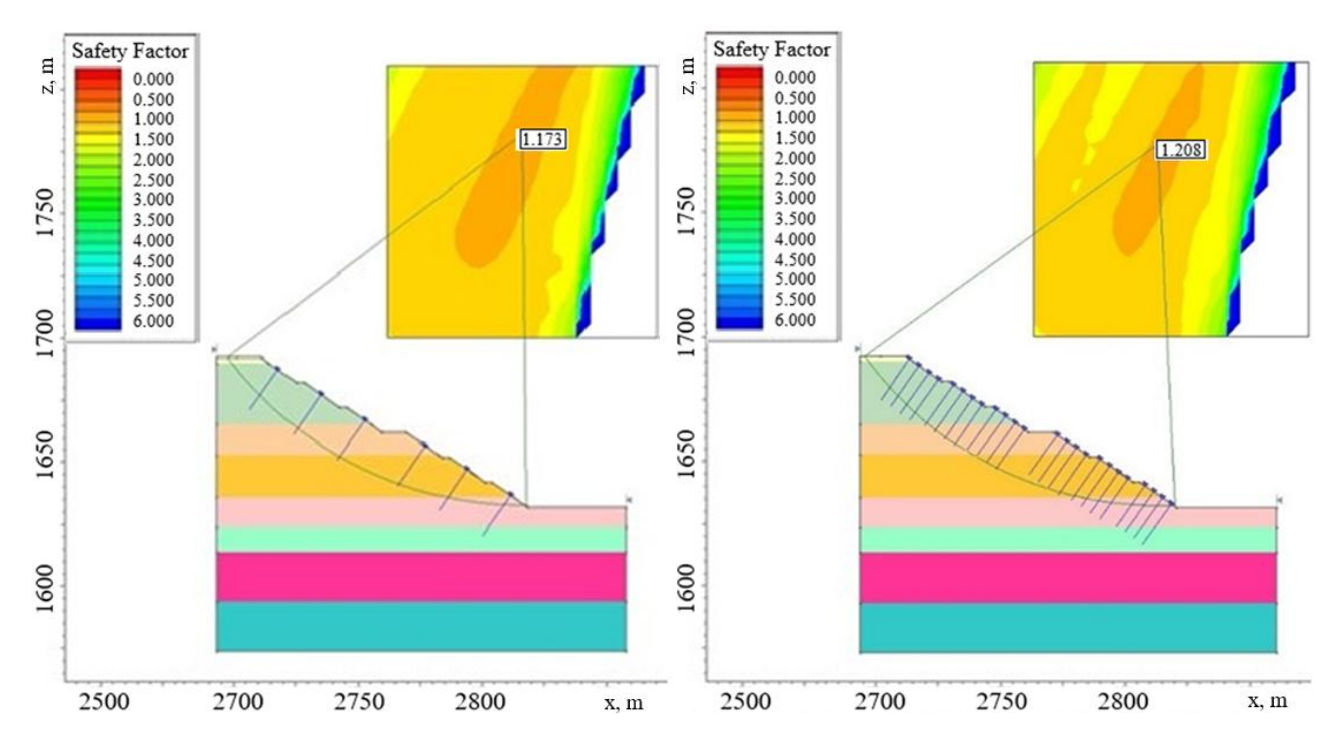


Figure 6. Schemes for determining the safety factor of the rock side of a titanium-zirconium pit when installing different numbers of anchors a) 6 units, b) 24 units

The calculations of the indicators of the reserve coefficient of stability of the rocks of the pit slope with different numbers of anchors allow us to establish the dependence between these parameters. On (**Figure 7**) shown the influence of the number of anchors on the indicator of the reserve coefficient of stability of the rocks of the titanium-zirconium pit slope.

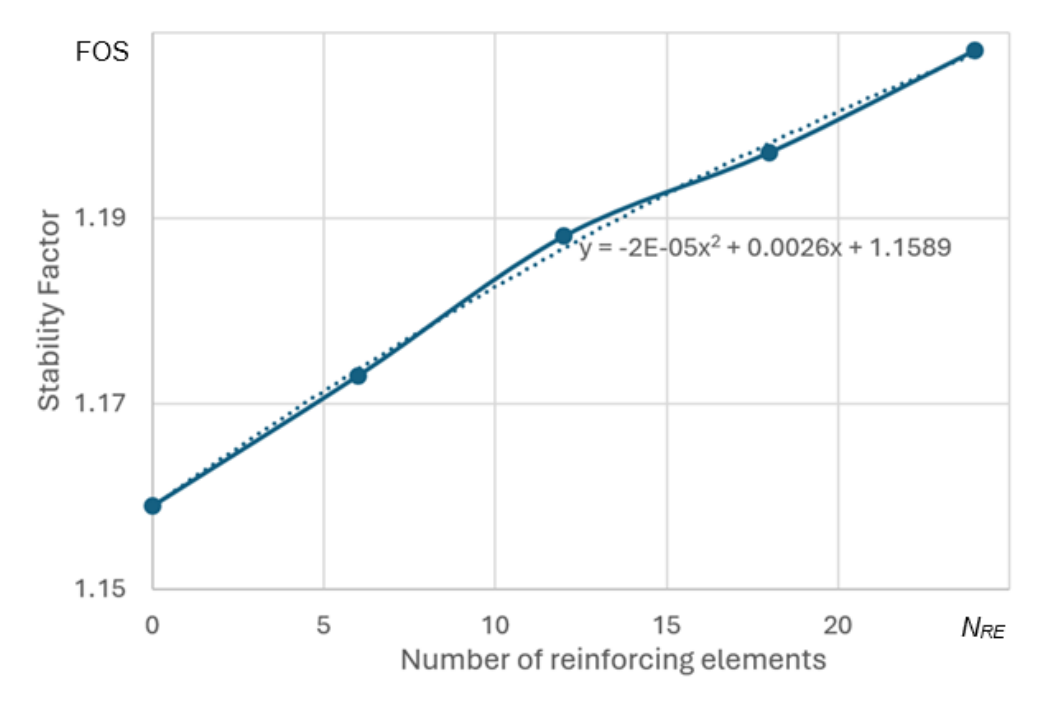


Figure 7. Dependency of the Factor of Safety (FOS) on the number of reinforcing elements (N_{RE})

According to the obtained research results (**Figure 7**), it was found that increasing the number of anchors in the system to 24 units allows for an increase in the stability reserve of the rocks of the pit slope with a slope angle of 29° by 4.2 % from 1.159 to 1.208. Thus, the stability of the slope of the side composed of sedimentary rocks is increased; however, the safe value of the stability reserve coefficient (1.3) is not achieved.

The results allow us to choose the most effective solution when justifying the parameters of anchor systems used to secure sedimentary rocks in the sides of the exit and main trench of a titanium-zirconium pit.

4. Discussion

The studies that were conducted allow us to determine the scope of work involved in constructing anchor systems to increase the pit slopes' stability during the development of a titanium-zirconium deposit. During the calculations, soil anchors of various lengths and quantities were considered. The range of anchor lengths from 5 m to 40 m was studied, and the number of units from 6 to 24. The method of installing anchors is provided perpendicular to the slope, with a distance between them from 7 m to 20 m in horizontal and vertical directions. When modeling the load indicators for pulling out or destruction of the anchor mechanism (Anchor Capacity), a force of 150 kN was assumed. The general results of the studies on establishing the dependence of the number and length of reinforcing elements on the stability reserve coefficient of the pit slope rocks are shown in (**Figure 8**).

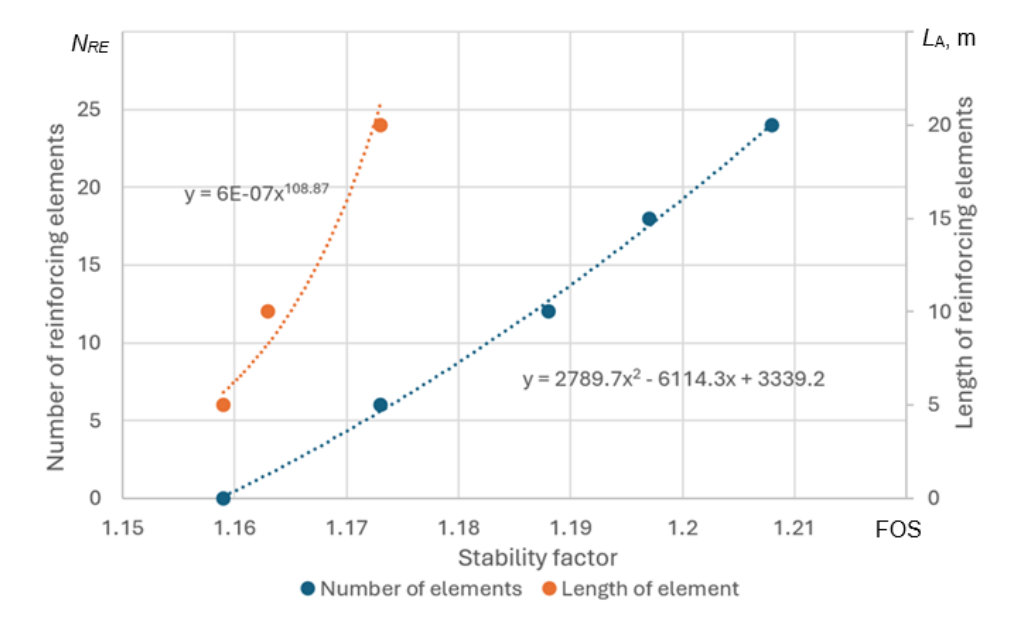


Figure 8. Dependence of the number and length of reinforcing elements on the rock stability factor

According to the established dependencies (**Figure 8**), it is proposed to use anchor systems with a length of no more than 20 m, since a further increase in this indicator does not affect the stability factor. At the same time, an additional increase will lead to increased manufacturing and installation costs. It is determined that an increase in the length of anchors from 5 m to 20 m will increase the stability factor by 1.2 % from 1.159 to 1.173, which has minimal effectiveness.

At the same time, increasing the number of anchors on the slopes of the sides of titanium-zirconium quarries will increase the safety factor. If 24 units increase the number of anchors at a slope angle of the side of the titanium-zirconium pit of 29°, its safety factor will increase by 4.2 m% from 1.16 to 1.21. Thus, increasing the number of reinforcing units in the anchor system is more effective than increasing their length. It can be considered as one of the methods of strengthening sandy-clayey soils in limited cases.

5. Conclusions

The modeling results obtained in the work allow us to establish that an increase in the height of the overburden ledge during the development of the Motrono-Annivska section of the titanium-zirconium deposits by 2.07 times from 14° to 29° leads to a decrease in the value of the stability reserve factor by 1.79 times from 2.08 to 1.16. Thus, it is confirmed that the stability of the sides of these quarries can be achieved only at small angles of inclination of their slopes, or with the use of engineering methods of strengthening.

The established dependencies allowed us to determine that the installation of anchor systems with a length of more than 20 m is ineffective, since in this case, the stability reserve coefficient does not increase, but the cost of their manufacture and installation increases. It was determined that expanding the anchor length four times from 5 m to 20 m

at a slope angle of the titanium-zirconium pit slope of 29° will lead to an increase in the stability reserve coefficient by 1.2% from 1.159 to 1.173, which is not effective enough to introduce the relevant technologies into the production process. It is determined that increasing the number of reinforcing elements on the slopes of titanium-zirconium quarries leads to their moderate strengthening and an increase in the safety factor. When the number of anchors is increased to 24 units, the safety factor of the side slope will increase by 4.2 % from 1.16 to 1.21, which is more effective than increasing the length of the anchor structures.

6. References

- Sobko B.Y. Laznikov O.M., Haidin A.M., Lozhnikov O.V. (2016). Substantiation of rational mining method at the Motronovsky titanium-zirconium ore deposit exploration. *Scientific Bulletin of National Mining University*, 2016. 6 (156). P. 41-49.
- Inthavongsa, I., Drebenstedt, C., Bongaerts, J., & Sontamino, P. (2016). Real options decision framework: Strategic operating policies for open pit mine planning. *Resources Policy*, 47, 142-153. https://doi.org/10.1016/j.resourpol.2016.01.009
- Anisimov, O., Symonenko, V., Cherniaiev, O., & Shustov, O. (2018). Formation of safety conditions for development of deposits by open mining. Web of Conferences. E3S Web of Conferences forthcoming. https://doi.org/10.1051/e3sconf/20186000016
- Sobko, B., Haidin, A., Lozhnikov, O., & Jarosz, J. (2019). Method for calculating the groundwater inflow into pit when mining the placer deposits by dredger. In E3S Web of Conferences (Vol. 123, p. 01025). EDP Sciences. https://doi.org/10.1051/e3sconf/201912301025
- Anisimov, O., Slyvenko, M., and Cherniaiev, O. (2025). Modeling and determination of rock displacement parameters on the internal waterlogged dump. *IOP Conf. Series: Earth and Environmental Science*, 1481 (2024) 012011 IOP Publishing. p.1-9 https://doi.org/10.1088/1755-1315/1481/1/012011
- Kaźmierczak, U., Bartlewska-Urban, M., & Strzałkowski, P. (2022). Slope Shape Optimization of Water Reservoirs Formed Due to the Reclamation of Post-Mining Excavations. *Applied Sciences*, *12*(3), 1690. https://doi.org/10.3390/app12031690
- Adamchuk, A., & Shustov, O. (2023). Control of Dump Stability Loading Rock on its Edge. Inżynieria Mineralna Journal of the Polish Mineral Engineering Society, 1(51), 91–96. https://doi.org/10.29227/IM-2023-01-11
- Koda, E., Kiersnowska, A., Kawalec, J., & Osiński, P. (2020). Landfill slope stability improvement incorporating reinforcements in reclamation process applying observational method. *Applied Sciences*, 10(5), 1572. https://doi.org/10.3390/app10051572
- Cherep A. (2024). Determination of rational technological schemes for the completion of open-pits taking into account land reclamation March 2024 *IOP Conference Series Earth and Environmental Science*, 1319(1):012013 http://dx.doi.org/10.1088/1755-1315/1319/1/012013
- Lozhnikov, O.V., Adamova, V.O., & Slivenko, M.M. (2024). Justification of the safe parameters of recreational zones during the reclamation of watered residual quarry spaces. *Natsional'nyi Hirnychyi Universytet. Naukovyi Visnyk*, (5), 85-92. https://doi.org/10.33271/nyngu/2024-5/085
- Gunawan, M., Hidayati, & Adam, R. (2023). Slope Stability Analysis Using Bishop Method and Slide 2D Software at Sand Stone Mining in Sedau Village, Narmada District, Lombok Barat Regency. *IOP Conference Series: Earth and Environmental Science*, 1175(1), 012010. https://doi.org/10.1088/1755-1315/1175/1/012010
- Cherniaiev, O., Anisimov, O., Dreshpak, O., & Borodina, N. (2024). Substantiation the safety open pit wall parameters in the conditions of a reduced protective zone near State critical infrastructure. *E3S Web of Conferences*, 526, 01014. https://doi.org/10.1051/e3sconf/202452601014
- Moldabayev, S. K., Sultanbekova, Z. Z., Adamchuk, A. A., Sarybaev, N. O., & Nurmanova, A. N. (2022). Technology of an open pit refinement under limit stability of sides. *Naukovyi Visnyk Natsionalnoho Hirnychoho Universytetu*, 6, 5–10. https://doi.org/10.33271/nvngu/2022-6/005
- Maodin, M. A., Faryansah, Ariadi, S. D., Verlandi, G. S., Alpiana, & Hidayati. (2023). Analysis of Andesite Rock Slope Stability with Bishop Method. *IOP Conference Series: Earth and Environmental Science*, 1175(1), 012007. https://doi.org/10.1088/1755-1315/1175/1/012007
- Lashgari, M., & Ozturk, C. A. (2022). Slope failure and stability investigations for an open pit copper mine in Turkey. *Environmental Earth Sciences*, 81, 1-17. https://doi.org/10.1007/s12665-021-10125-7
- Lozhnikov, O., Sobko, B., Pavlychenko A. (2023). Technological Solutions for Increasing the Efficiency of Beneficiation Processes at the Mining of Titanium-Zirconium Deposits. *Inzynieria Mineralna*, (1), 61–68. http://doi.org/10.29227/IM-2023-01-07
- Sobko B., Lozhnikov O., M. Chebanov, D. Vinivitin. (2022). Substantiation of the optimal parameters of the bench elements and slopes of iron ore pits. *Naukovyi Visnyk Natsionalnoho Hirnychoho Universytetu*, 5, 26-32. https://doi.org/10.33271/nvngu/2022-5/026
- Cherniaiev, O., Anisimov, O., Saik, P., & Akimov, O. (2024). Theoretical substantiation of water inflow into the mined-out space of quarries mining hard-rock building materials. *IOP Conference Series: Earth and Environmental Science*, 1319(1), 012002. https://doi.org/10.1088/1755-1315/1319/1/012004.

Lozhnikov, O., & Adamova, V. (2024). Methodology for determining the scope of reclamation works when forming recreational zone in the quarry residual space. *IOP Conference Series: Earth and Environmental Science*, 1348(1), 012043. https://doi.org/10.1088/1755-1315/1348/1/012043

Funding

This research was funded by the Ministry of Education and Science of Ukraine, grant number 0123U101759.

Author's contribution

Oleksii Lozhnikov (professor): conceptualization, investigation and supervision.

Carsten Drebenstedt (professor): methodology, resources, supervision, validation.

Anton Bondarenko (postgraduate student): data curation, formal analysis, original draft, and writing.

All authors have read and agreed to the published version of the manuscript.



Towards Sustainable Deep Mineral Exploration: Insights from the MINOTAUR Project

DIM-ESEE Conference



Magdalena Worsa-Kozak¹* □⊠, Aurela Shtiza² □⊠, Adam Wróblewski¹ □⊠

¹Wroclaw University of Science and Technology (WUST), Faculty of Geoengineering, Mining and Geology, Wybrzeże Wyspiańskego 27, 50-370 Wrocław, Poland.

²Industrial Minerals Association Europe (IMA-Europe), Rue de Deux Églises 26, 1000 Brussels, Belgium.

Abstract

Deep land-based mineral exploration faces persistent technological and societal challenges. Traditional methods such as drilling, seismic imaging, and downhole logging have advanced in resolution and efficiency, yet remain capital-intensive, slow, and environmentally intrusive. This paper reviews the past developments on onshore deep exploration technologies, identifies their main limitations, and evaluates recent innovations that seek to overcome them. We present a comparative framework that assesses current methods across five criteria: technical performance, geological accuracy, economic efficiency, environmental footprint, and social acceptance.

The analysis shows that while geophysical imaging and airborne surveys expand depth penetration and reduce drill risk, they require high investment and specialist processing. Drone-enabled and proximal sensing methods provide cost-efficient and socially accepted surface data, yet lack subsurface resolution. Even advanced directional drilling remains costly and intrusive, limiting its acceptability despite improved precision. This paper situates MINOTAUR explorer concept within the broader technological evolution of deep mineral exploration and demonstrates how autonomous robotic approaches could directly address the core bottlenecks of cost, environmental footprint, and social acceptance. The study highlights the potential of robotics-based exploration to contribute to more sustainable and socially accepted access to (critical) raw materials in Europe.

Keywords: Deep Mineral Deposits, Sustainable Mineral Exploration, Breaktrough Innovation, Mining, Deep Land Deposits

1. Introduction

The secure and sustainable supply of Critical Raw Materials (CRMs) has become one of the most pressing strategic challenges for Europe's green and digital transition. CRMs are indispensable in renewable energy technologies, electric vehicles, digital devices, and defense applications. Yet their supply chains are vulnerable due to import dependency and geopolitical risks (European Parliament and the Council, 2024). To mitigate these vulnerabilities, strengthening Europe's domestic exploration and extraction capabilities for deep mineral deposits is crutial. Deep exploration represents the frontier of mineral discovery, offering opportunities to access previously untapped resources, but it also brings significant technological, environmental, and societal challenges (Malehmir et al., 2017; Golani, 2021; An et al., 2023; Singh & Malinowski, 2023).

Historically, deep on-land mineral exploration has relied on surface mapping, geochemical sampling, and drilling (core and reverse-circulation) to probe subsurface targets. The early roots of exploration include stream-sediment geochemistry, till sampling, and outcrop mapping, evolving into regional geochemical and geophysical surveys (e.g. airborne magnetics, gravity, electromagnetic) as the search spaces expanded with time. Over the past decades, geophysical techniques—such as electrical resistivity, induced polarization (IP), magnetotellurics, gravity, and seismic imaging—have matured and become standard tools for subsurface characterization. Complementarily, downhole well logging (e.g. resistivity, sonic, gamma) and core logging became widely used to directly probe rock properties. Yet, despite technological advances, these methods remain limited due to higher costs, constraints related to depth penetration, resolution ambiguity and environmental or social impact.

Current onshore exploration technologies rely on drilling, geophysics, and downhole logging to characterize subsurface mineral systems. While advances in seismic imaging, directional core drilling, and physical property logging have improved the overall exploration efficiency (Bellefleur et al., 2004; Maries et al., 2017; Okada, 2022; Rodríguez et al., 2023), these methods remain capital-intensive, slow, and environmentally intrusive – especially the drilling. Exploration drilling is further constrained by limited social acceptance, significant surface disturbance, and high carbon and water footprints (Prno & Slocombe, 2012). Consequently, the raw materials sector is increasingly seeking novel

approaches that combine improved and accurate geological insights with automation, digitalisation, artificial intelligence (AI), and sustainability principles (Yang et al., 2024).

Persistent challenges include: (I) Cost and risk: Drilling still represents the most expensive and uncertain phase in exploration campaigns, often dominating budgets. (II) Environmental and social constraints: Infrastructure, site preparation, waste and drill cuttings, access roads, and surface disturbance provoke opposition and regulatory hurdles. (III) Uncertainty and resolution: Geophysical and geochemical anomaly signals are often ambiguous, requiring multiple passes and integration with drilling for confirmation. (IV) Time lag and feedback latency: Sequential workflows (survey \rightarrow modelling \rightarrow drilling \rightarrow reinterpretation) slow down responsiveness to emerging data and preclude adaptive strategies.

To alleviate these constraints, recent research emphasizes integrative, data-driven, and less invasive approaches. For example, Yang et al. (2024) highlights how artificial intelligence (AI) is applied across ten mineral exploration tasks (e.g. data fusion, predictive targeting, estimation), pointing out the promise and challenges of coupling domain knowledge with machine learning. Moreover, the geosciences broadly are reckoning with how to translate AI advances into practical, interpretable, robust systems (e.g. practical geospatial AI) rather than black-box models (Du et al. 2025). In the mining sector specifically, the automation and robotics pin point the increasing deployment of intelligent systems (e.g. robotic inspection, sensor networks) and the challenges related to navigation, coordination, and autonomy in complex underground environments (Konieczna-Fulawka et al. 2025).

Yet, existing robotic systems typically focus on inspection tasks (visual, structural, mechanical) rather than actively performing exploration (drilling, sensing, decision feedback). For example, mobile inspection robots in deep mines (Konieczna-Fulawka et al., 2025) survey tunnels and infrastructure, but do not autonomously probe subsurface mineralization. Similarly, advances in mining robotics more broadly examine autonomy in haulage, drilling rigs, and earthmoving systems, but fall short of integrated in-situ exploration solutions (Du et al., 2025).

In response to these gaps, this article presents the MINOTAUR concept — miniature robotic explorers with integrated geophysical/geochemical sensing, autonomous navigation, and digital twin modelling — as a possible approach to address the core bottlenecks of cost, environmental disturbance, and social legitimacy in deep land exploration (CORDIS, 2024; MINOTAUR Consortium, 2024). We situate MINOTAUR within the lineage of exploration technology and then apply a five-criteria comparative framework (technical performance, geological accuracy, economic efficiency, environmental footprint, social acceptance) to benchmark it against conventional and emerging approaches. Our results suggest that MINOTAUR could reduce exploration times and costs by about 30%, significantly lower surface disturbance through use of small robotic units instead of large rigs, and improve targeting success via continuous in-situ data fusion driven by AI logic.

By embedding the MINOTAUR advancements in the broader evolutionary arc of exploration technologies, we delineate both its potential advantages and its limitations. The remaining sections unfold as follows: first we describe the methodology behind our comparative analysis; second we present recent technological developments; third we apply the comparative framework to benchmark methods; and finally we discuss implications, challenges, and future pathways.

2. Methods

The methodological approach began with a comprehensive literature review of scientific and policy publications to establish the state of the art in deep mineral exploration. This review covered recent advances in seismic imaging, downhole logging, directional drilling, and remote sensing, as well as their integration with digital data processing techniques. Particular attention was given to identifying how these technologies are currently applied in exploration campaigns, the limitations they face when targeting mineralization at great depths, and their potential for further improvement. The outcome of this review provided the setting for a structured state-of-the-art synthesis, which served as the baseline for developing a comparative framework. The assessment framework evaluated each technology across multiple dimensions: 1. Technical performance, 2. The geological accuracy, 3. Economic efficiency, 4. Environmental footprint, and last but not least - 5. The social acceptance. These criteria were then applied to compare conventional methods with the innovative MINOTAUR concept of miniaturized robotic systems, as enhanced by artificial intelligence and digital twin technology. The analysis emphasized how combining advanced sensing, automation, and data-driven modelling can improve geological resolution, enhance targeting accuracy, reduce surface disturbance, and ultimately increase the sustainability of deep mineral exploration.

3. State-of-the-art

Mineral exploration technologies have evolved rapidly in response to the dual challenge of declining quality of resources being exploited; lower discovery rates, and the overall growth of societal and environmental constraints. Present day approaches combine traditional geological expertise with advanced geophysics, geochemistry, remote sensing, robotics, and artificial intelligence to improve efficiency, accuracy, and sustainability across the exploration value chain. Global demand for energy transition and technology metals is compelling exploration at depth to comply with tighter environmental and social constraints, which in turn are pressuring a new generation of sensing, modelling, and targeting workflows. Across methods, the state-of-the-art converges on (i) higher-replicability geophysical imaging (including passive approaches), (ii) drone-enabled and spectral remote sensing, (iii) deeper-penetrating airborne systems, (iv) objective mineralogical measurements via proximal spectroscopy, and (v) more surgical drilling supported by directional

technologies—each judged here along technical performance, geological accuracy, economic efficiency, environmental footprint, and social acceptance.

Remote sensing and airborne geophysics represent crucial frontiers. Hyperspectral imaging, multispectral satellite data, and UAV-based sensors provide detailed mineralogical and alteration maps with minimal environmental impact. These methods significantly enhance large-scale reconnaissance, especially in inaccessible terrains, while their depth penetration remains limited (Okada, 2022). Airborne innovations, such as electromagnetic (EM) systems, gravity gradiometry (AGG), and the emerging airborne induced polarization (IP), allow the detection of concealed mineralization under deeper top layers. These systems improve geological accuracy and reduce the need for invasive ground surveys, although they require substantial capital investment and specialist data processing capacity (Alcalde et al., 2022; Okada, 2022).

At the surface, high-resolution drone campaigns fusing magnetics with multispectral/hyperspectral imaging deliver centimetre-to-metre-scale mapping of alteration and structure, enabling accurate mineral system vectoring where outcrop is limited. Technically, UAVs enhance coverage and repeatability; economically, they cut mobilisation costs and improve safety; environmentally, they are low-impact; socially, they minimise on-ground disturbance—yet payload, endurance, and airspace regulations can restrict their deployment (Alcalde et al., 2022; Okada, 2022).

Airborne geophysics is seeing breakthrough performance at depth. Contemporary EM systems, including SQUID-enhanced TDEM and the emergence of practical airborne IP, improve the detectability of concealed conductive sulfides under thick cover; AGG (FALCON/FTG) uniquely images density contrasts—iconic for IOCG systems—where conventional airborne gravity was below the noise floor. Technically, these systems expand the depth of investigation and target fidelity; economically, they front-load value by shrinking the drill search space but demand high-capex platforms; environmentally, they are non-invasive; socially, they limit land access yet may encounter concerns over low-flying surveys. UAV-based EM receiver concepts (with ground-based transmitters) point to further cost reductions but are payload-limited today (Alcalde et al., 2022; Okada, 2022).

Seismic imaging has also advanced, with active and passive approaches complemented by full-waveform inversion and reverse-time migration, enabling high-resolution imaging in crystalline environments. Such methods reduce drilling risk and environmental footprint, but their effectiveness is sensitive to acquisition geometry and data noise (Alcalde et al., 2022). Recent syntheses highlight that active hard-rock seismics now leverages sparse 3D acquisition with pre-stack depth migration, full-waveform inversion, and reverse-time migration to track mineralized horizons to ~1 km in crystalline terranes; the technical gains are balanced by sensitivity to irregular land geometries and acquisition gaps, which can degrade image reliability and hence geological accuracy if not mitigated in processing. Passive seismic methods based on ambient noise increasingly complement or substitute active sources, lowering cost and surface impact while extending shear-wave velocity models to greater depths; their resolution is typically coarser, but integration with active data and other geophysics improves targeting confidence and cost-effectiveness. Together, these developments reduce drill-out risk and stakeholder disturbance relative to traditional reconnaissance, which supports social acceptance.

Drilling remains the only definitive technique for confirming mineralization directly, yet it is also the most expensive and environmentally intrusive. The development of deep and ultra-deep drilling systems has expanded access to resources. However technical challenges such as high temperature, pressure, and borehole stability persist (Dvoynikov et al., 2022). Directional drilling and rotary steerable systems, adapted from the petroleum sector, increase the precision and geological accuracy while reducing unnecessary meters drilled (Ma et al., 2016, Zhang et al., 2025). Nonetheless, their high operational costs and complexity limit widespread application in greenfield exploration. Finally, drilling remains the rate-limiting step for discovery and the largest lever on footprint and social acceptance. Directional and deep-targeting technologies (RSS, MWD/LWD) increase technical precision and geological hit-rate, reduce metres drilled, and lower disturbance per discovery. However, HPHT environments, tool reliability, specialist crews, and day-rate premiums constrain economic efficiency (Ma et al., 2016; Caers et al., 2022; Dvoynikov et al., 2022; Rodríguez et al., 2023). The industry response—use non-invasive seismic/airborne/spectral methods to tighten uncertainty before committing steel—embodies the prevailing "less-drill, smarter-drill" ethos.

Meanwhile, proximal sensing and automated spectral scanning of drill cores standardize mineralogical datasets, reducing operator bias and increasing comparability across projects (Okada, 2022). Benefits occur by providing information directly at drill sites through automated proximal spectroscopy (e.g., HyLogger/NVCL), which standardises core mineralogy, reduces operator bias, and scales to regional knowledge systems—though spectral resolution, calibration, and data management remain practical limits.

New decision-analytic frameworks, including value of information (VOI) and efficacy of information (EOI), improve the cost-effectiveness of exploration by guiding optimal drillhole placement. These approaches reduce uncertainty and unnecessary drilling, aligning technical performance with both economic efficiency and social acceptance (Caers et al., 2022; Yang et al., 2024). Within geochemical and mapping domains, integrated "vectors-to-ore" and big-data workflows—paired with machine learning where appropriate—are now a routine for anomaly detection and target ranking. The frontier is not merely the algorithmic accuracy but the geological plausibility and transferability across domains; here, physics- and mineral-system-informed features, together with uncertainty quantification, are central to improve decision making and social license, because they support transparent, minimally invasive programmes that focus drilling where it matters most. Complementing these developments, artificial intelligence and deep learning are increasingly applied to integrate large, heterogeneous datasets, from geophysics to geochemistry. Such methods enable

predictive geological modelling and anomaly detection, though their reliability strongly depends on training data quality and geologically informed validation (Alcalde et al., 2022; Okada, 2022).

Despite the advances of the above-described technologies, mineral exploration still faces several persistent gaps and challenges. Drilling remains the critical but still the most costly and most environmentally intrusive step in the discovery pipeline, accounting for the largest share of budgets and ecological disturbance (Ma et al., 2016; Dvoynikov et al., 2022; Zhang et al., 2025). Even with more precise geophysical and remote sensing tools, exploration campaigns often require extensive drill programs to validate targets, leading to inflated costs, high energy use, and land disturbance. This raises social acceptance barriers, particularly in regions sensitive to environmental impacts. Moreover, while machine learning and advanced imaging enhance predictive accuracy, their outcomes are often constrained by data quality, incomplete geological knowledge, and the difficulty of transferring models across mineral systems (Okada, 2022; Alcalde et al., 2022). These factors combine to perpetuate inefficiencies: excessive drilling, elevated risks of dry holes, and reliance on a shrinking pool of specialized technical staff to interpret data and model development.

The urgent need, therefore, is for technologies that limit the number of drillholes while maximizing geological confidence, thereby reducing costs, environmental footprint, and workforce demands. This is precisely where the MINOTAUR project offers a transformative solution. By deploying miniaturized robotic explorers with integrated sensing and digital twin capabilities (**Figure 1**), MINOTAUR enables in-situ characterization of ore bodies in real time, minimizing the need for conventional drilling campaigns (**MINOTAUR Consortium, 2024**). Its approach reduces operational inefficiencies, addresses social concerns by lowering visual/surface disturbance, and increases the reliability of subsurface models through continuous data fusion and AI-based geological interpretation. In this sense, MINOTAUR directly targets the core bottlenecks of modern exploration—drilling intensity, cost escalation, environmental impact, and limited human resources—paving the way for a more sustainable and socially acceptable future of mineral exploration.

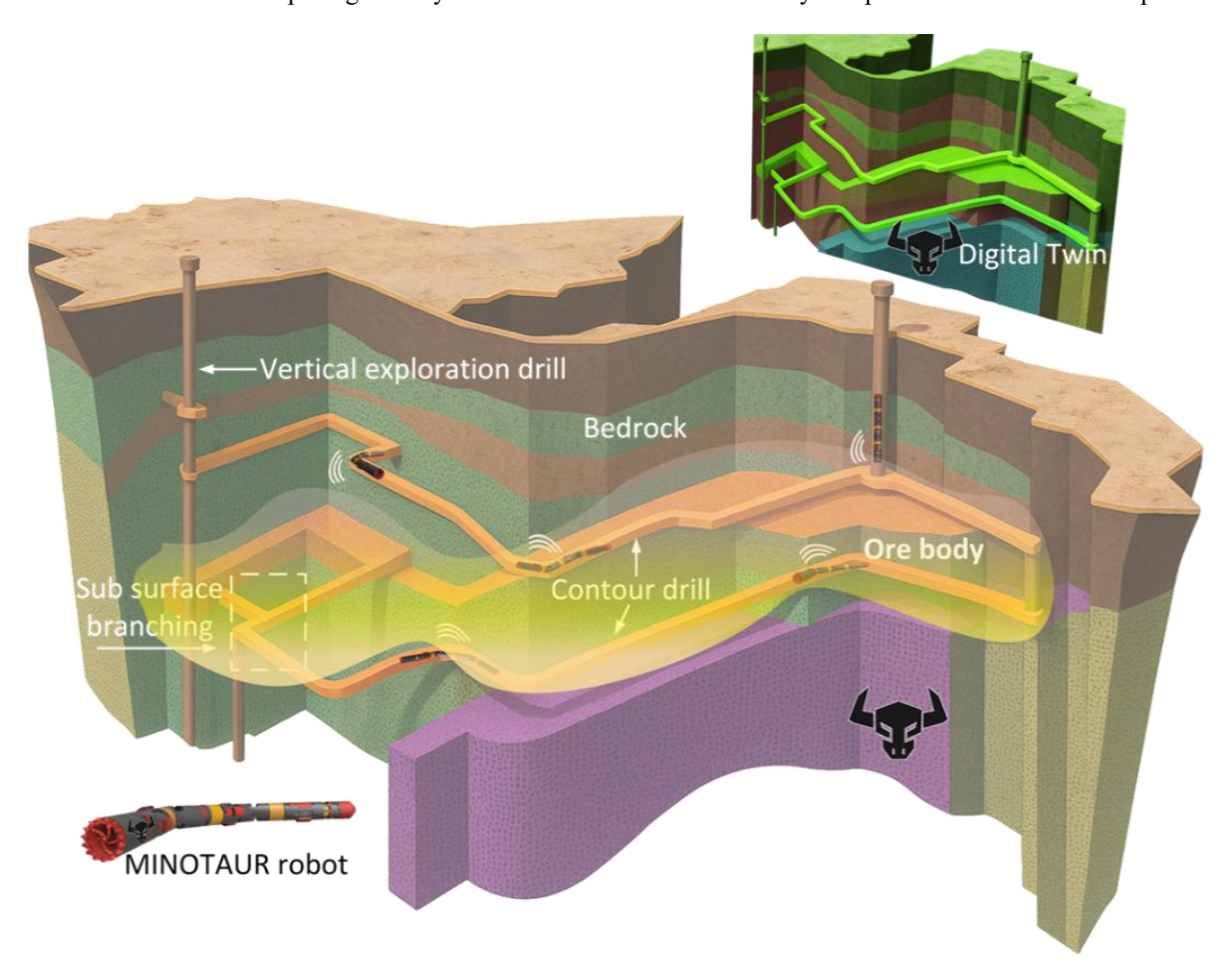


Figure 1. MINOTAUR Explorer Concept (MINOTAUR Consortium, 2024)

3. Comparative Analysis of Mineral Exploration Technologies and The MINOTAUR Concept

The MINOTAUR system is built on a modular robotic architecture specifically designed for contour drilling and autonomous in-situ geological sensing. Each robotic explorer consists of discrete modules—a steering module, locomotion module, sensing module, control module, and drilling head—that can be configured according to mission requirements. This modularity enables rapid adaptation to varying geological and operational conditions, improving resilience and reducing downtime in the field. The explorers are designed to penetrate cohesive soils and hard rock formations, avoid obstacles, monitor borehole stability, and adjust drilling performance dynamically. Equipped with geophysical and geochemical sensors (LIBS, XRF, XRD, magnetic susceptibility, sonic velocities), the system acquires high-resolution data directly from the rock mass, feeding it into a digital core representation that substitutes traditional physical core handling.

Operationally, the explorers leverage advanced autonomy principles described in the robotics literature. **Cranford et al. (2023)** emphasize the integration of digital twin technology, allowing MINOTAUR to update geological and geomechanical models in real time based on sensor feedback, creating a continuously refined 3D subsurface representation. **Kokkinis et al. (2024)** outline the value of multi-agent robotic fleets for subsurface tasks, highlighting how MINOTAUR can deploy multiple explorers to coordinate drilling, sensing, and logistics. Nikolakopoulos et al. (2025) show that such systems rely on robust navigation in GPS-denied environments, achieved through tightly coupled sensor fusion, SLAM (simultaneous localization and mapping), and LoRaWAN-based mesh communication. This ensures precise localization, safe coordination, and resilience in complex underground conditions.

The MINOTAUR explorers follow a sequential operational workflow: (i) mapping the local geometry and identifying target drilling sites; (ii) anchoring and stabilizing in the rock mass; (iii) executing contour drilling while adjusting parameters based on real-time rock property sensing; and (iv) updating digital twins and transmitting data to surface operators for decision-making. Real-time autonomy allows local drill planning, adaptive response to unexpected geological features, and long-horizon mission execution without constant human supervision. These principles mark a departure from conventional drilling, where core recovery and manual interpretation dominate. By digitizing the entire exploration workflow, MINOTAUR reduces physical sample handling, accelerates geological interpretation, and enables a more sustainable, low-impact mode of resource characterization.

Table 1. Comparison of modern mineral exploration technology with the MINOTAUR Explorer concept.

Technology	Technical	Geological	Economic	Environmental	Social
	Performance	Accuracy	Efficiency	Footprint	Acceptance
High-fidelity geophysical imaging (active & passive seismic, FWI, RTM)	Advanced imaging to ~1 km in crystalline terranes; sensitive to noise and acquisition geometry (Alcalde et al., 2022).	High accuracy in mapping horizons but limited by irregular geometries; requires integration with other datasets.	Moderate – reduces drilling needs but requires costly data acquisition and processing.	Low surface impact compared to drilling; non-invasive.	Generally positive, though public concerns may arise from seismic sources.
Drone-enabled & spectral remote sensing	High-resolution (cm-m scale) mapping of alteration/structure; limited depth penetration (Okada, 2022).	Good for surface mineralogy; weak for subsurface targets.	High efficiency – low cost and flexible deployment; UAV limits (payload, airspace).	Minimal impact; low emissions and disturbance.	Very positive due to small footprint and reduced field activity.
Deeper- penetrating airborne systems (EM, AGG, airborne IP)	SQUID-TDEM, AGG (FALCON/FTG) detects concealed mineralization (Okada, 2022).	Improved fidelity for conductive/dense bodies; still ambiguous without drilling.	Economically efficient for narrowing targets; requires high CAPEX aircraft.	Non-invasive; minor environmental footprint.	Limited concerns, though low-flying surveys may raise local issues (Alcalde et al., 2022).
Proximal spectroscopy (e.g., HyLogger/NV CL)	Automated mineralogy logging, spectral scanning of cores (Okada, 2022).	Objective datasets; high comparability; calibration needed.	Cost-effective in reducing manual core handling; requires drill cores first.	Minimal – occurs in labs or drill sites.	Well accepted due to transparency and reduced bias.

Technology	Technical Performance	Geological Accuracy	Economic Efficiency	Environmental Footprint	Social Acceptance
Surgical drilling (directional, RSS, MWD/LWD)	High precision drilling, adaptable trajectories (Ma et al., 2016).	Increases geological hit- rate; essential for validation.	Costly day rates; reduces unnecessary drilling meters.	Smaller footprint per discovery; but drilling remains intrusive (Dvoynikov et al., 2022).	Mixed – essential but often resisted by communities due to visible disturbance.
MINOTAUR Explorer	Modular robotic design with in-situ sensing, autonomous navigation, and real-time digital twin integration	Continuous in-situ geophysical & geochemical sensing, along with digital cores replacing physical samples, improves reliability.	Expected to cut timelines and costs by ~30% vs. traditional campaigns	Minimal surface footprint; robotic contour drilling reduces disturbance, eliminates large rigs	High potential – autonomy, transparency, and reduced impact align with societal expectations for sustainable exploration

The comparative analysis (**Table 1**) shows that while traditional exploration technologies each contribute towards specific strengths—such as the depth penetration of airborne EM and gravity systems, the high-resolution mapping of UAV-based spectral sensing, or the precision of directional drilling—they are also constrained by limitations in cost, depth accuracy, or environmental and social acceptance. Geophysical imaging and airborne systems reduce drill risk but require significant investment and specialist expertise; drone and proximal sensing provide low-impact, cost-efficient data but lack subsurface reach; and even advanced drilling technologies, though more precise, remain costly and intrusive. In contrast, the MINOTAUR Explorer system integrates modular robotics, in-situ sensing, and digital twin technologies to simultaneously improve technical performance, geological accuracy, and cost efficiency of mineral exploration, while substantially lowering its environmental footprint and enhancing the societal acceptance. This positions MINOTAUR not merely as an incremental improvement but as a transformative approach to mineral exploration aligned with the EU's goals towards sustainability and critical raw materials strategic autonomy.

4. Conclusions

The state of the art in mineral exploration demonstrates rapid convergence of high-resolution sensing, automation, and data-driven analytics are necessary to support the decision making process. Collectively, these advances improve technical performance, geological accuracy, and cost efficiency, while offering new pathways to reduce environmental footprint and increase societal acceptance. However, their practical integration into deep onshore exploration remains partial and fragmented.

Compared with conventional technologies, the comparative analysis conducted in this study indicates that MINOTAUR's autonomous, modular robotic systems could deliver tangible performance gains. By combining continuous in-situ sensing, real-time digital twin updates, and adaptive navigation, such systems may cut operational costs and timelines by up to one-third relative to traditional campaigns, while sharply reducing surface disturbance and safety risks. The resulting improvement in environmental and social performance strengthens alignment with the EU Critical Raw Materials Act and its sustainability goals.

Nonetheless, these results remain preliminary and conceptual. The proposed advantages are contingent upon successful system miniaturization, robustness under geological and mechanical stress, and seamless data integration between robotics, sensors, and geological models. Future work should therefore focus on validating the robotic exploration framework in field conditions, benchmarking it against active industrial drilling systems, and quantifying lifecycle environmental and economic metrics. Hybrid strategies—where robotic systems complement rather than replace existing methods—may prove most feasible in the medium term.

Ultimately, the shift toward robotic, autonomous, and digitally integrated exploration represents a significant step forward rather than a total paradigm replacement. It reflects a broader trend toward smarter, lower-impact resource discovery consistent with European strategic autonomy and the global sustainability agenda.

5. References

Alcalde, J., Carbonell, R., Pospiech, S., Gil, A., Bullock, L. A., Tornos, F. (2022). Preface: State of the art in mineral exploration, Solid Earth, 13, 1161–1168, https://doi.org/10.5194/se-13-1161-2022

An, Z., Zhao, Y., Zhang, Y. (2023). Mineral exploration and the green transition: Opportunities and challenges for the mining industry. *Resources Policy*, 86, 104263. https://doi.org/10.1016/j.resourpol.2023.104263

Bellefleur, G., Müller, C., Snyder, D., Matthews, L. (2004). Downhole seismic imaging of a massive sulfide orebody with mode-converted waves, Halfmile Lake, New Brunswick, Canada. Geophysics, 69(2), 318–329. https://library.seg.org/doi/10.1190/1.1707051

Caers, J., Scheidt, C., Yin, Z., Wang L., Mukerji T., House K. (2022)Efficacy of Information in Mineral Exploration Drilling. Nat Resour Res 31, 1157–1173. https://doi.org/10.1007/s11053-022-10030-1

CORDIS (European Commission). (2024). MINOTAUR — Miniaturized Robotic Systems for Autonomous In-Situ Exploration and Mining Operations of Small Deposits and Urban Mines (Project ID 101178775). Retrieved from https://cordis.europa.eu/project/id/101178775 (Access: 2025.08.30)

Cranford, R. (2023). Conceptual application of digital twins to meet ESG targets in the mining industry. Frontiers in Industrial Engineering, 9, 1223989. https://doi.org/10.3389/fieng.2023.1223989

Du, H., Chan, L., Tong, J. Raad R., Naghdy F., Guo Q., Yu Y., Islam M.R., Tubball F., Ros M, Li Z., Ritz C., (2025) Industrial Progress of Robotic Automation in Mining Applications: A Survey. Mining, Metallurgy & Exploration 42, 537–556. https://doi.org/10.1007/s42461-025-01219-yDvoynikov, M. V., Sidorkin, D. I., Yurtaev, S. L., Grokhotov, E. I., Ulyanov, D. S. (2022). Drilling of deep and ultra-deep wells for prospecting and exploration of new raw mineral fields. Записки Горного института, 258, 945-955. https://doi.org/10.31897/PMI.2022.55

European Parliament and the Council. (2024). Regulation (EU) 2024/1252 of 11 April 2024 establishing a framework for ensuring a secure and sustainable supply of critical raw materials. Official Journal of the European Union. Retrieved from http://data.europa.eu/eli/reg/2024/1252/oj

Golani, P.R. (2021). Challenges in Mineral Exploration. In: Assessment of Ore Deposit Settings, Structures and Proximity Indicator Minerals in Geological Exploration. Springer Mineralogy. Springer, Cham. https://doi.org/10.1007/978-3-030-65125-1 6

Kokkinis, A., Frantzis, T., Skordis, K., Nikolakopoulos, G., Koustoumpardis, P. (2024). Review of automated operations in drilling and mining. Machines, 12(12), 845. https://doi.org/10.3390/machines12120845

Konieczna-Fuławka, M., Koval, A., Nikolakopoulos, G., Fumagalli, M., Santas Moreu, L., Vigara-Puche, V., Müller, J., & Prenner, M. (2025). Autonomous Mobile Inspection Robots in Deep Underground Mining—The Current State of the Art and Future Perspectives. Sensors, 25(12), 3598. https://doi.org/10.3390/s25123598

Nikolakopoulos, G., Koval, A., Fumagalli, M., Konieczna-Fuławka, M., Santas Moreu, L., Vigara-Puche, V., Verma, K., Waard, B. d., Deutsch, R. (2025). Autonomous drilling and the idea of next-generation deep mineral exploration. Sensors, 25(13), 3953. https://doi.org/10.3390/s25133953

Ma, T., Chen, P. Zhao, J. (2016). Overview on vertical and directional drilling technologies for the exploration and exploitation of deep petroleum resources. Geomech. Geophys. Geo-energ. Geo-resour. 2, 365–395 https://doi.org/10.1007/s40948-016-0038-y

Malehmir, A., Maries, G., Bäckström, E., Schön, M., Marsden, P. (2017). Developing cost-effective seismic mineral exploration methods using a landstreamer and a drophammer. Scientific Reports, 7, 10325. https://doi.org/10.1038/s41598-017-10451-6

Maries, G., Malehmir, A., Bäckström, E., Schön, M., Marsden, P. (2017). Downhole physical property logging for iron-oxide exploration, rock quality, and mining: An example from central Sweden. Ore Geology Reviews, 90, 1–13. https://doi.org/10.1016/j.oregeorev.2017.10.012

MINOTAUR Consortium. (2024). MINOTAUR Project website. Retrieved from https://www.minotaur-mining.eu/Okada, K. (2022). Breakthrough technologies for mineral exploration. Mineral Economics, 35(3), 429–454. https://doi.org/10.1007/s13563-022-00317-3

Prno, J., & Slocombe, D. S. (2012). Exploring the origins of "social license to operate" in the mining sector: Perspectives from governance and sustainability theories. Resources Policy, 37(3), 346–357. https://doi.org/10.1016/j.resourpol.2012.04.002

Rodríguez, R., Fernández, V., Bascompta, M., Garcia-Gonzalez, H. (2023). Directional core drilling as an approach to reduce uncertainty in tunneling construction. Applied Sciences, 13(19), 10998. https://doi.org/10.3390/app131910998

Singh, B., Malinowski, M. (2023). Seismic imaging of mineral exploration targets: Evaluation of ray- vs. wave-equation-based pre-stack depth migrations for crooked 2D profiles. Minerals, 13(2), 264. https://doi.org/10.3390/min13020264

Yang, F., Zuo, R., Kreuzer, O. P. (2024). Artificial intelligence for mineral exploration: A review and perspectives on future directions from data science. Earth-Science Reviews, 258, 104941. https://doi.org/10.1016/j.earscirev.2024.104941

Zhang, J., Wang, H., Ji, G., Cui, M., Chen, L., Li, W., Liu, L. (2025, February). Technologies and Achievements for Drilling and Completion of Onshore Deep and Ultra-Deep Wells in China. In International Petroleum Technology Conference (p. D032S009R016). IPTC. https://doi.org/10.2523/IPTC-24918-MS

Acknowledgment

This research was conducted in the frame of MINOTAUR project that has received funding from the European Union's Horizon Europe Research and Innovation Programme under the Grant Agreement No. 101178775

Author's contribution

Magdalena Worsa-Kozak (Dr.): conceptualization, investigation, writing – original draft. **Aurela Shtiza** (Dr.): conceptualization, investigation, writing – original draft, writing – review & editing. **Adam Wróblewski** (MSc Eng.): writing – review & editing.

All authors have read and agreed to the published version of the manuscript.



Prospections of former deposits for the purpose of protection of mining and cultural heritage

DIM-ESEE Conference



Ana Maričić^{1*} D, Zlatko Briševac¹ D, Vladislav Brkić¹ D

1 University of Zagreb, Faculty of Mining Geology and Petroleum Engineering Pierottijeva 6, 10000 Zagreb, Croatia

Abstract

The scientific investigation of former raw material deposits is becoming increasingly important in the context of cultural heritage protection. From a geological and mining perspective, and depending on the research objectives, such investigations can generally be divided into two categories. The first concerns the exploration of sites where mineral raw materials and hydrocarbons were historically extracted, with emphasis on assessing deposit reserves and the potential for renewed exploitation. The second focuses on the restoration of culturally significant buildings and monuments, where the properties of the construction material must be carefully examined in order to identify suitable original or substitute stone. This paper presents examples of both research approaches in Croatia, a country with a long tradition of mineral resource exploitation. Particular attention is given to the recent restoration needs following the Zagreb earthquake, which have highlighted the critical demand for authentic natural stone in conservation practice.

Keywords: Prospection, raw materials deposits, hydrocarbons and mining heritage, cultural heritage, geotechnology

1. Introduction

In Croatia, numerous sites hold considerable potential to be recognized as geotechnological heritage (Briševac et al., 2021a; Briševac et al., 2021b). Geotechnological heritage consists of quarrying and industrial minerals heritage, Coal mining heritage, Metal mining heritage and Petroleum exploitation heritage (Figure 1).

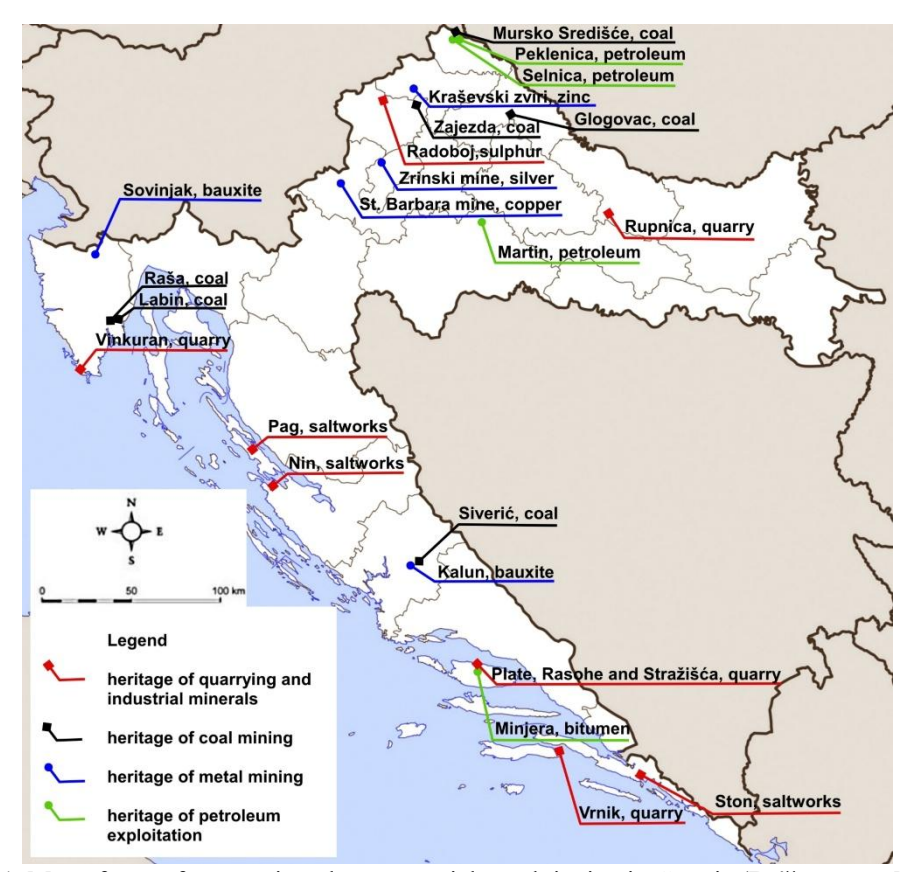


Figure 1. Map of some former mineral raw materials exploitation in Croatia (Briševac et al., 2021a)

The quarrying and use of natural stone for construction purposes has a long tradition throughout the Mediterranean (Calvo & Regueiro, 2010). In Croatia, carbonate stone has historically been the dominant building material (Crnković & Jovičić, 1993; Briševac et al., 2021b), and it continues to play the same role in modern quarrying activities (Briševac & Bohanek, 2023; Briševac et al., 2023). However, due to stone susceptibility to physical and chemical weathering, particularly under fluctuating climatic and temperature conditions, its long-term performance must be carefully considered in both heritage conservation and contemporary construction. In this context, previous studies (Smirčić et al., 2020; Velić & Velić, 2020; Mišur et al., 2021; Moro et al., 2023; Grgasović, 2024; Velić & Velić, 2025) provide valuable insights into natural stone characteristics and thus contribute to the broader understanding and presentation of geological heritage in Croatia.

Besides stone exploitation, former oil and gas fields also form part of Croatia's geotechnological heritage. These sites, with preserved infrastructure and historical records, reflect the early development of the petroleum industry and its cultural and socio-economic significance (Briševac et al., 2021a).

The renovation of historic buildings poses a particular challenge, as authenticity often requires the use of the original stone types. In practice, however, sourcing adequate material is frequently hindered by technical, logistical, and economic constraints (Maričić et al., 2023). Quarrying sites once extended along the Adriatic coast, from Istria through Dalmatia to Dubrovnik, with especially prominent extraction on the islands of Brač and Korčula, as well as in selected inland regions (Donelli et al., 2009). Archaeological and historical records from ancient Istria and Dalmatia confirm the existence of highly developed quarrying, construction, and artistic techniques, which contributed to the prosperity of local economic and cultural centres. Many ancient monuments along the eastern Adriatic coast were built from locally sourced stone, each quarry providing material with distinctive properties and quality that shaped the durability and aesthetics of these structures (Buzov, 2009).

In this context, it is essential to systematically document and preserve the legacy of quarrying and oil exploitation in Croatia. The aim of this paper is to present the research methodology developed to record sites of former mineral resource extraction, to analyse the challenges associated with the restoration of historic buildings using original stone, and to discuss the wider implications of these issues for heritage preservation and sustainable resource management.

2. Research methods

The research focused on documenting historical exploitation of natural resources with the aim of preserving and presenting associated cultural heritage. The methodology (**Figure 2**) combined literature review, field investigation, laboratory analysis, and community engagement to capture both tangible and intangible aspects of heritage.



Figure 2. Graphic structure of the methodology

The applied mentioned methodology follows a structured, multi-step approach integrating both historical and contemporary research techniques. The process begins with a literature and archival review (Step 1), which provides the historical context of mining activities and establishes the foundation for further analyses. Subsequently, field surveys

(Step 2) ensure direct documentation of sites and collection of representative samples, which are then subjected to laboratory analyses (Step 3) to assess their physical and mechanical properties. Complementary to these technical steps, industrial infrastructure documentation (Step 4) and community involvement (Step 5) supply essential contextual data, linking material characteristics with socio-cultural knowledge and heritage value.

All gathered information converges in the integrated evaluation and mapping phase (Step 6), which synthesizes archival sources, field data, laboratory results, and stakeholder perspectives into a comprehensive framework. Such an approach ensures not only scientific rigor but also relevance for heritage preservation and practical decision-making.

For stone resources, the study involved analysing scientific publications, geological maps, and archival data to identify former quarrying sites. Field inspections included photographic documentation and the collection of representative samples. The literature published so far (Briševac et al., 2023; Maričić et al., 2025; Donelli et al., 2009) shows that laboratory tests have been carried out to determine the geological, physical, and mechanical properties of the stone in accordance with relevant European standards (EN 1926:2006; EN 1936:2006; EN 13755:2008; EN 12440:2019; EN 12407:2019; EN 12670:2019), supporting evaluation for restoration and conservation purposes.

For oil and gas sites, the approach emphasized the documentation of historical extraction infrastructure, including wells, pipelines, and processing installations. Fieldwork consisted of on-site surveys, photographic and videographic documentation, and non-invasive assessment of materials and technologies. Interviews with former workers, local historians, and community representatives provided additional insight into the socio-economic and cultural significance of these sites.

Finally, all collected data were systematically integrated to evaluate the heritage value of each site, support conservation and restoration strategies, and inform the presentation of both stone and hydrocarbon sites for educational and interpretive purposes.

3. Results

The study identified significant former natural resource sites in Croatia, emphasizing their relevance for cultural heritage preservation and potential reuse in restoration projects.

3.1 Stone Quarries

Field surveys and laboratory analyses revealed that several historical quarries along the Adriatic coast and selected inland regions produced stone with mechanical and physical properties suitable for restoration. Notably, Brač and Korčula limestones exhibited high compressive strength and low porosity, confirming their historical use in prominent monuments. Archival sources and previous studies (**Briševac et al., 2021b; Donelli et al., 2009**) provided additional information on the historical significance and current operational status of these quarries.

Brač limestone and other regional carbonates were evaluated for compatibility, considering compressive strength, porosity, and weathering behaviour. The study confirmed that these materials meet the necessary criteria for restoration, ensuring both structural stability and historical authenticity. The integration of geological assessment, archival research, and material testing demonstrates the practical application of the proposed methodology in high-profile conservation projects, emphasizing the importance of systematically documenting former quarries and quarry areas for sustainable heritage management.

Table 1. Selected former quarry areas and stone characteristics (adapted from Briševac et al., 2023; Donelli et al., 2009).

Quarry area Co	mpressive Strength (MPa)	Porosity (%)	Heritage Significance	Current Status
Brač	75	4	High	Operational
Korčula	90	2	High	Inactive with limited access
Istria	65	6	High	Operational and inactive
Benkovac	125	3	Medium	Operational
Zagreb	29	16	High	Inactive

3.2 Zagreb Cathedral Restoration

Zagreb Cathedral has been renovated several times, including the replacement of stone parts (Crnković & Poggi, 1995; Maričić et al., 2023). The use of travertine to replace the local lithothamnium limestone is shown in Figure 3.

The 2020 earthquake in Zagreb highlighted the urgent need for authentic natural stone in heritage restoration. The cathedral, as one of Croatia's most significant cultural and religious monuments, suffered structural damage requiring careful conservation of its stone elements. Field and laboratory analyses of historical quarries were crucial to identify materials matching the original stone in both mechanical properties and aesthetic characteristics. This is particularly important because the damaged stone cannot be replaced at the original sites, such as the Vrapče quarry, due to bureaucratic obstacles and nature conservation (**Figure 4**).



Figure 3. Stone ornaments removed from the cathedral, showing the replacement of lithothamnium limestone with travertine.



Figure 4. The current appearance of the Vrapče quarry, from which most of the stone material came during Bolle's renovation.

3.3 Hydrocarbon Sites

Documentation of former oil and gas extraction sites highlighted the industrial heritage of these locations. Mapping, photographic surveys, and interviews with former workers revealed sites of high cultural and educational value, some of which retain original infrastructure dating back to the early 20th century (**Briševac et al., 2021a; 2021b**). These findings support heritage preservation, public education, and potential tourism initiatives.

The documentation and assessment of former oil and gas extraction sites in Croatia revealed their significant value as part of the nation's industrial and cultural heritage. These sites, some of the earliest examples of petroleum infrastructure in the region, offer unique insights into the technological evolution and economic development associated with hydrocarbon exploitation. Many of these locations preserve original features such as drilling rigs, wellheads, pipelines, separation units, and processing facilities, which serve as tangible reminders of early 20th-century energy production (Figure 5).



Figure 5. Peklenica oil field (NW Croatia)

Despite the historical importance, challenges for conservation include exposure to weathering, loss of technical documentation, and ownership/legal status uncertainties. Nevertheless, systematic documentation and preliminary conservation proposals developed during this research lay the groundwork for future protection and valorisation of hydrocarbon heritage in Croatia, aiming to integrate these sites into wider heritage management strategies and public engagement initiatives.

3.4 Integrated Heritage Evaluation

Combining results from stone and hydrocarbon sites enabled the creation of a preliminary heritage map (**Figure 6**), identifying areas of historical, geological, and cultural significance. This approach provides a practical framework for conservation, sustainable resource management, and sourcing authentic materials for restoration.

Three large areas of high historical, geological and cultural significance are Zagreb, Papuk and Istria. The Zagreb area, encompassing the country's largest and most populous city and situated between two protected areas, the Žumberak-Samobor Highlands and Medvednica Nature Parks (Briševac et al., 2021a; Maričić et al., 2023; URL 1; URL 2), thus represents a site of exceptional importance. Papuk Nature Park, which contains the Rupnica geological monument in its western sector (Briševac et al., 2021a) and the Radlovac d.d. quarries in its eastern sector, further illustrates the close interaction between natural and industrial heritage. Moreover, Papuk Geopark is part of the European Geoparks Network and UNESCO Global Geoparks Network (URL 3). The Istrian peninsula is also a large area with a rich heritage of stone quarrying and the use of stone for the construction of historical buildings (Mileusnić et al., 2019; Briševac et al., 2021a). In addition to these three large areas, the islands of Brač and Korčula (Moro, et al., 2023) are also of high historical, geological and cultural significance, and the Geopark of the Vis Archipelago, which is on the UNESCO list of geoparks (Briševac et al., 2021a; Mišur, et al., 2021; URL 4).

Four areas on and near the Adriatic Sea are of medium significance. These are the dimension stone quarries in the hinterland of Trogir. The Benkovac area with a special type of natural stone slabs. Velebit Nature Park, which contains a special geological heritage (Smirčić, et al., 2020; Velić & Velić, 2020; Grgasović, 2024; Velić & Velić, 2025), also belongs to this group.

Only one area on the Croatian mainland was categorised as being of low significance. The area of Mursko Središće, where there are traces of coal and oil extraction (**Briševac et al., 2021a**).

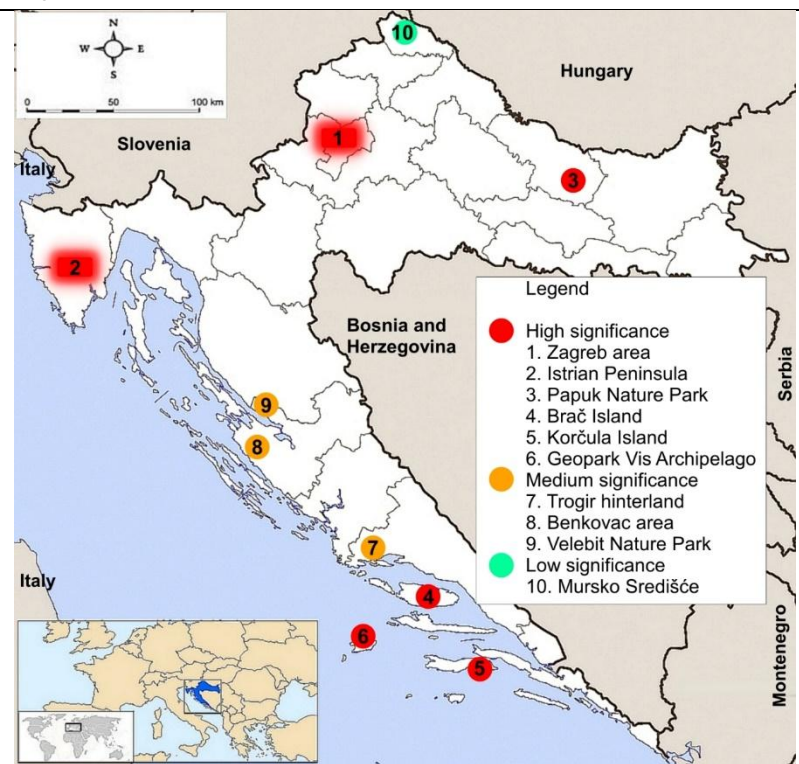


Figure 6. Integrated map of former natural resource exploitation and heritage value in Croatia

4. Discussion

Compared to previous approaches, the proposed methodology provides a more holistic and replicable framework that links geological, historical, and social dimensions of heritage. Importantly, this methodology proved effective in identifying quarries with suitable stone for restoration, evaluating hydrocarbon sites for industrial heritage value, and integrating these findings into a comprehensive heritage map (**Figure 6**).

Historical quarries along the Adriatic coast, particularly carbonate varieties from Brač and Korčula, remain crucial for restoring cultural monuments due to their proven durability and historical significance. Laboratory analyses confirmed their mechanical and physical properties, supporting the selection of authentic materials for conservation projects (Briševac et al., 2021b; Maričić et al., 2023). Field and archival data also highlight the historical and economic importance of these quarries, which contributed to the construction of numerous notable monuments along the coast. The systematic documentation facilitated by the methodology allows for easier identification of quarries that can reliably supply material, addressing both conservation needs and sustainable resource use.

The recent restoration of Zagreb Cathedral following the earthquake provides a practical example of the methodology in action. Identification of suitable stone, limestone and other regional carbonates, relied on field surveys, laboratory testing, and historical data to ensure both structural stability and authenticity. This case underscores the critical role of systematically documenting former quarries and evaluating material properties for high-profile conservation projects, illustrating the direct applicability of the proposed approach.

Hydrocarbon sites, often overlooked, represent an important aspect of industrial heritage. Retained infrastructure and equipment offer insights into early 20th-century extraction technologies and socio-economic impacts. These sites not only document the technological evolution of the petroleum industry but also reflect the broader historical context of regional economic development and community life associated with resource extraction. The methodology enabled the identification, documentation, and preliminary evaluation of these sites, supporting education, tourism, and interdisciplinary heritage preservation. However, challenges such as physical degradation of structures, environmental contamination, and gaps in archival records pose significant obstacles for conservation efforts. Addressing these requires coordinated strategies involving heritage specialists, engineers, local stakeholders, and policymakers to ensure the sustainable preservation and adaptive reuse of hydrocarbon heritage sites, thereby integrating them effectively into regional cultural narratives and development plans.

Integrating stone and hydrocarbon site data enabled the creation of a preliminary heritage map, identifying areas of high historical, geological, and cultural value. This map not only provides a practical framework for conservation and sustainable resource management but also serves as a strategic tool for planning future restoration projects by guiding the selection of authentic materials and prioritizing sites of high heritage significance.

Challenges remain, including limited quarry access, economic constraints, and stone weathering. Future research should focus on predictive durability models, alternative materials for restoration, and comprehensive documentation of

industrial heritage. Overall, protecting former deposits supports both cultural preservation and responsible management of natural resources.

The mining sector in Croatia today is primarily focused on the production of non-metallic mineral raw materials for the construction industry and has proven to be very resilient in the many crises it has gone through (Briševac & Bohanek, 2023). This also represents a potential for geotechnological heritage in the future, as parts of this current exploitation can be presented to the public. Further research could also focus on the valorisation of sites where materials were used for pottery production during historic and prehistoric periods (Neral et al., 2023).

5. Conclusions

- 1. Historical quarries in Croatia, particularly along the Adriatic coast, remain valuable sources of authentic stone for heritage restoration. Brač and Korčula limestone demonstrated high durability and suitable mechanical properties, confirming their historical and ongoing relevance in conservation projects.
- 2. The recent restoration of Zagreb Cathedral following the earthquake illustrates the practical application of the proposed methodology. Systematic documentation of quarries, combined with laboratory testing and archival research, enabled the selection of stone that ensured both structural stability and historical authenticity.
- 3. Former oil and gas extraction sites constitute a vital component of industrial heritage, safeguarding infrastructures that date back to the early 20th century. These sites offer significant potential for educational programs, heritage tourism, and active community involvement, thereby fostering greater public appreciation of the historical and technological evolution of the petroleum industry in Croatia
- 4. The integrated approach, combining literature review, field surveys, laboratory analyses, and community engagement, proved effective in identifying and evaluating sites of geological, cultural, and industrial significance. This methodology offers a replicable framework for future heritage documentation and restoration projects.
- 5. Challenges remain, including limited quarry access, economic constraints, and stone weathering. Addressing these issues requires strategic planning, predictive evaluation of material durability, and exploration of alternative or supplementary materials when original sources are unavailable.
- 6. Protecting and systematically documenting former deposits supports both cultural preservation and sustainable resource management. The combination of heritage mapping, scientific analysis, and applied restoration practice provides a foundation for informed decision-making in conservation and ensures the long-term protection of Croatia's geotechnological and cultural heritage.

6. References

- Briševac, Z., Maričić, A., Brkić, V., & Bralić, V. (2021a). An overview and future prospects of Croatian geotechnological heritage. *Rudarsko-geološko-Naftni Zbornik*, 36(1). https://doi.org/10.17794/rgn.2021.1.7
- Briševac, Z., Maričić, A. & Brkić, V. (2021b). Croatian Geoheritage Sites with the Best-Case Study Analyses Regarding Former Mining and Petroleum Activities. *Geoheritage* 13, 95. https://doi.org/10.1007/s12371-021-00620-5
- Briševac, Z., Maričić, A., Kujundžić, T., & Hrženjak, P. (2023). Saturation Influence on Reduction of Compressive Strength for Carbonate Dimension Stone in Croatia. *Minerals*, 13(11), 1364. https://doi.org/10.3390/min13111364
- Briševac, Z., & Bohanek, V. (2023). Impact of the COVID-19 crisis on the mining sector in Croatia. *Rudarsko-geološko-Naftni Zbornik*, 38(4), 63–74. https://doi.org/10.17794/rgn.2023.4.6
- Buzov, M. (2009). The Ancient Quarries in Croatia: The Technology of Extracting Stone. IX. International Conference ASMOSIA, Tarragona, 628-635.
- Calvo, J. P., & Regueiro, M. (2010). Carbonate rocks in the mediterranean region-From classical to innovative uses of building stone. Geological Society Special Publication, 331, 27-35. https://doi.org/10.1144/SP331.3
- Crnković, B. & Jovičić, D. (1993). Dimension stone deposits in Croatia. *Rudarsko-geološko-naftni zbornik*, 5, 139–163. Crnković, B. & Poggi, F. (1995). Travertine the restoration stone for the Zagreb Cathedral. *Rudarsko-geološko-naftni zbornik*, 7, 77–85.
- Donelli, I., Matijaca, M., Paduan, I. (2009). Ancient quarries on the eastern Adriatic coast with specific reference to the island of Brač (Croatia), IX. International Conference ASMOSIA, Tarragona, 636-640.
- EN 1926:2006 (2006): Natural Stone Test Methods—Determination of Uniaxial Compressive Strength. European Committee for Standardization: Brussels, Belgium.
- EN 12440:2019 (2019): Natural Stone—Denomination Criteria. European Committee for Standardization: Brussels, Belgium.
- EN 12407:2019 (2019): Natural Stone Test Methods—Petrographic Examination. European Committee for Standardization: Brussels, Belgium.
- EN 12670:2019 (2019): Natural Stone—Terminology. European Committee for Standardization: Brussels, Belgium.
- EN 1936:2006 (2006): Natural Stone Test Methods—Determination of Real Density and Apparent Density, and of Total and Open Porosity. European Committee for Standardization: Brussels, Belgium.

- EN 13755:2008 (2008): Natural Stone Test Methods—Determination of Water Absorption at Atmospheric Pressure. European Committee for Standardization: Brussels, Belgium.
- Grgasović, T. (2024). New Dasycladal algae from the Anisian (Middle Triassic) of Lika (Croatia). *Rudarsko-geološko-Naftni Zbornik*, 39(5), 101-108. https://doi.org/10.17794/rgn.2024.5.7
- Maričić, A., Briševac, Z., Hrženjak, P., & Jezidžić, H. (2023). Natural building stone in the construction and renovation of the Zagreb Cathedral. *Rudarsko-geološko-Naftni Zbornik*, 38(3), 29–42. https://doi.org/10.17794/rgn.2023.3.3
- Maričić, A., Briševac, Z., & Barudžija, U. (2025). Resistance to salt crystallization of thin-bedded or platy limestone from the town of Benkovac in Croatia. *Mining of mineral deposits*, 19(1), 98-106. https://doi.org/10.33271/mining19.01.098
- Mileusnić, M., Maričić, A., & Hruškova Hasan, M. (2019). Croatian geological heritage related to historical mining and quarrying. *European geologist*, (48), 5-9.
- Mišur, I., Budić, M., Kurenčić, T., & Korbar, T. (2021). Tectonic influence on speleogenesis of sea caves on Biševo Island (UNESCO Global Geopark Vis Archipelago, Adriatic Sea, Croatia). *Geosciences*, 11/8, 341. https://doi.org/10.3390/geosciences11080341
- Moro, A., Mezga, A., Mikša, G. & Kalemarski, N. (2023). Characteristics of the facies and radiolitid paleoenvironment of the Upper Cenomanian shallow-water succession from the southern part of the Adriatic Carbonate Platform, northwestern side of Korčula Island, Croatia. *Rudarsko-geološko-naftni zbornik*, 38 (5), 19-30. https://doi.org/10.17794/rgn.2023.5.2
- Neral, N., Kudelić, A., Maričić, A. & Mileusnić, M. (2023). Pottery technology through time: Archaeometry of pottery and clayey raw material from the multi-period site in eastern Croatia. *Rudarsko-geološko-Naftni Zbornik*, 38(2), 1-21. https://doi.org/10.17794/rgn.2023.2.1
- Smirčić, D., Japundžić, D., Gaberšek, N., Aljinović, D., Prlj-Šimić, N., Krizmanić, K., Pavić, I., & Barudžija, U. (2020). First record of the upper Illyrian ammonoid subzone marker Reitziites reitzi in the Karst Dinarides. *Rudarsko-geološko-Naftni Zbornik*, 35(2). https://doi.org/10.17794/rgn.2020.2.7
- Velić, I., Valić, J. (2020). The geological significance of Majstorska Cesta a historical road on Velebit Mt. with a special review of Jurassic carbonate rocks. (2020). *Rudarsko-geološko-Naftni Zbornik*, 35(3). https://doi.org/10.17794/rgn.2020.3.5
- Velić, J. i Velić, I. (2025). Stratigraphic age and morphometric features of upper pleistocene flow till pebbles from the Papuča gravel pit (Gospić, Croatia). *Rudarsko-geološko-naftni zbornik*, 40 (4), 171-184. https://doi.org/10.17794/rgn
- URL 1. https://www.pp-zumberak-samoborsko-gorje.hr/about-the-park/geology/?lang=en (accessed 21st August 2025).
- URL 2. https://www.pp-medvednica.hr/en/ (accessed 21st August 2025).
- URL 3. https://www.pp-papuk.hr/papuk-unesco-geopark/?lang=en (accessed 21st August 2025).
- URL 4. https://www.geopark-vis.com/eng/geopark-vis-archipelago-homepage (accessed 21st August 2025).

Acknowledgment

This research was partially carried out within the framework of the institutional project Geomathematical methods in geology approved as part of the Recovery and resilience plan for Croatia implemented at the Faculty of Mining, Geology and Petroleum Engineering University of Zagreb in 2025.

Author's contribution

Ana Maričić (associate professor): conceptualization, investigation, data curation, methodology, writing – original draft and writing – review & editing. Zlatko Briševac (associate professor): conceptualization, data curation, formal analysis, investigation, methodology, project administration, resources, supervision, validation, visualization, writing – original draft and writing – review & editing. Vladislav Brkić (associate professor): conceptualization, supervision, validation, writing – review & editing.

All authors have read and agreed to the published version of the abstract.



Dynamic Management of Ore Body Bedding Models Based on Machine Learning and Terrain Grid Reconstruction

DIM-ESEE Conference



Dmytro Malashkevych¹* □□, Vladyslav Ruskykh¹ □□, Marek Dudek² □□, Dariusz Sala² □□, Yuliya Pazynich¹,² □□,

¹ Dnipro University of Technology, 19 Dmytra Yavornytskoho Ave., Dnipro, 49005, Ukraine

Abstract

Accurate three-dimensional modeling of ore bodies is fundamental for effective mine planning, reserve estimation, and production management. However, due to the limitations of exploration methods, geological survey data are often incomplete, making it necessary to continuously update deposit models as new information becomes available. This study presents a methodology for the dynamic updating of ore body models that integrates geological data analysis with machine learning algorithms and mesh reconstruction techniques. The approach was applied to the Southern Bilozerka iron ore deposit, developed by PJSC Zaporizhzhia Iron Ore Plant. The methodology combines Linear Regression and Random Forest algorithms to enhance predictive accuracy. Linear Regression provides interpolation functions describing the general ore body geometry, while Random Forest improves the robustness of forecasts by reducing errors under heterogeneous geological conditions. Using Python-based tools in the Google Colab environment, predictive points of ore body distribution were calculated and then incorporated into wireframe and block models. This allowed not only the refinement of ore body geometry but also reliable reserve estimation, which for the studied level reached approximately 22 million tonnes. Furthermore, the constructed models formed a basis for calendar-based planning of development and stoping operations. The results confirmed that combining regression and ensemble approaches is an effective solution for dynamically updating geological models of ore bodies. The methodology ensures the integration of mine surveying and exploration data into digital models, improving the reliability of long-term planning and mine design.

Keywords: geological modeling, ore body modeling, model updating, mesh reconstruction, machine learning, random forest.

1. Introduction

In the process of mineral extraction, geological exploration data serve as the foundation for constructing 3D models of mineral deposits structures. Modeling plays a critical role throughout the entire life cycle of deposit development, including deposit exploration, complexity analysis, mine design and planning, and production process management (**Deutsch**, **2023**). Due to the limitations of technical conditions and exploration technologies, comprehensive data on ore bodies cannot be fully obtained through geological surveying to accurately describe the shape and distribution of the ore body. Therefore, ore body modeling is a dynamic process that is continuously refined as the geological database is updated. It must be gradually modified and revised in parallel with ongoing exploration and mining operations.

For instance, in the case of the Pivdenno-Bilozerske iron ore deposit, the characteristics of the ore body change continuously during extraction. Resource models become obsolete rapidly as geological information is collected along the mineralized zones. Consequently, short-term models must be regularly reconstructed to enhance modeling accuracy and optimize long-term planning (Dychkovskiy & Bondarenko, 2006). However, due to the complexity and uncertainty inherent is 3D geological modeling, it is often difficult to perform accurate mineral resource estimation, which significantly affects the efficiency and reliability of mine design and operation optimization. Therefore, the dynamic updating of geological models has become a crucial task for optimizing mining operations in modern mineral extraction (Kamiński et al., 2021).

In the context of continuous geological data updates, model reconstruction based on implicit modeling (Sherstyuk, 1999) is one of the possible solutions. Within this method, the geometric body is constructed from cross-sectional data. Mathematical functions can be used to represent the 3D surface model, which can be converted into a mesh model for visualization purposes (Dychkovskyi et al., 2018). For geological models, if implicit models and boundary lines are available, they can be used as constraints for spatial interpolation, and the implicit modeling method can be directly applied for dynamic updating. However, the updated geological model can be constructed using various methods. For a similar model built using the contour splicing method, it is difficult to update the model by using reinterpreted contour polylines (Li et al., 2019). The dynamic management of ore body bedding models using machine learning and terrain

² AGH University of Krakow, Al. Mickiewicza 30, 30059, Krakow, Poland

grid reconstruction supports more environmentally responsible mining practices (Polyanska et al., 2024). By improving the accuracy of geological models, it reduces unnecessary excavation and minimizes the disturbance of surrounding ecosystems (Pan et al., 2025). Continuous updates of the model allow early detection of geotechnical risks, which helps prevent slope instability, erosion, and excessive land degradation. Integrating ecological parameters into the modeling process enhances resource extraction efficiency while lowering waste generation and greenhouse gas emissions (Dychkovskyi et al., 2019). Thus, this approach contributes to sustainable mine planning, balancing mineral recovery with environmental protection and long-term land management.

For local updating of a geological model, the interactive mesh deformation method (Huang et al., 2006) may be a feasible approach. First, this method requires the refinement of mesh vertices in the area of interest on the surface of the updated mesh models, including both constrained and unconstrained points. Second, a target updated position must be specified for each constrained point, and the deformation constraints must be defined at the target position of each constrained point (Kyrylenko et al., 2025). During the deformation process, the coordinates of the unconstrained points are updated using Laplacian deformation algorithm (Sun et al., 2018). Machine learning techniques offer major improvements in ore body forecasting, with the Random Forest algorithm (Breiman, 2001) demonstrating significant effectiveness in reducing prediction errors compared to linear regression, particularly in geologically heterogeneous environments. Finally, previous work on mining-technogenic object forecasting is in line with our findings and confirms the potential of mesh-based model updating based on dynamically acquired geological data (Petlovanyi et al., 2021).

The authors propose the use of a geological information database for predicting the spatial distribution of a mineral deposit. Unlike existing methods, the proposed approach is based on the manipulation of the vertices of the 3D surface mesh of the deposit. These points can be determined either instrumentally during geological exploration or predicted using regression analysis or the random forest algorithm. The advantage of linear regression lies in its ability to generate an interpolation function that optimally describes the variability of the data (Pazynich et al., 2024). This function can also be used to determine the location for the development of mine workings intended to prepare the deposit for extraction. The main drawback of linear regression is the significant error margin when predicting data. To reduce the forecasting error, the random forest algorithm is employed.

To address the aforementioned challenges, we focus on a method of local updating of 3D ore body models based on real geological interpretation data obtained during mining operations. Based on mesh reconstruction, we consider the local update process of ore body models as a restructuring of mesh models guided by the predicted spatial distribution of the ore body using regression methods (**Dychkovskyi et al., 2013**). This approach enables the automatic updating of the specified 3D ore body model using continuously enriched geological data. It provides an effective solution to the problem of high-frequency model updates during extraction and exploration and has broad potential for application and dissemination in geological modeling.

The methodology was tested at PJSC Zaporizhzhia Iron Ore Plant, exploiting the Pivdenno-Bilozerske deposit accessed via vertical shafts and level drifts from 340 to 1140 meters depth. The mine's design capacity is 4.5 million tons of ore per year, with extraction conducted between the 840- and 1140-meter levels. A level-based preparation system is applied, using sublevel ore blasting and subsequent hardening backfill. Operational levels are 100 meters high, and chambers are 30 meters wide, mined in a two-stage checkerboard pattern. The forecasting approach begins with creating a coordinate table of ore body points, obtained through measurements in development or exploration workings. **Figure 1** illustrates the spatial contours of the ore body at the working levels, referenced to relative coordinates.

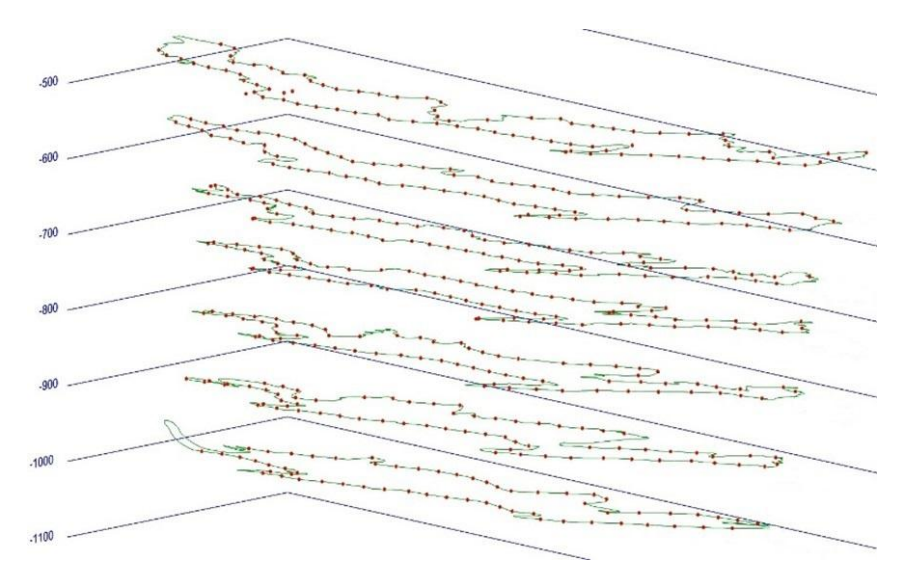


Figure 1. Technological contours of the ore body

The methodology for dynamically updating ore body models using machine learning and topographic mesh reconstruction involves several key stages. First, a database is created by compiling surveying and geological data on

ore—host rock contact points, with additional parameters such as strength or ore concentration included when available. Machine learning models are then constructed, using linear regression for interpolating ore body geometry and Random Forest to predict contours while minimizing errors from data gaps and heterogeneity. Predictive points for ore distribution at specific horizons are generated, and CAD files in .dxf format are produced for integration into computer-aided design systems.

Next, a three-dimensional wireframe model is built by connecting the predictive points, with extraction chambers distinguished by mining stage and visualized in different colors. This wireframe is then converted into a block model, allowing calculation of ore reserves per chamber, assessment of preparatory work, and planning of production schedules. The method's strength lies in combining regression with ensemble forecasting, providing flexibility and robustness even with incomplete geological data, while automated updates and repeated recalculations enable real-time refinement of ore body geometry during exploration and mining operations.

3. Results

The research was conducted for the conditions of the 1040-1140 m ming level of the Pivdenno-Bilozerske iron ore deposit, which has been prepared for further exploration. The initial dataset consisted of the spatial coordinates of ore body-host rock contact points obtained during previous mining operations.

Based on the regression analysis and performed calculations, the following empirical dependencies for the hanging wall and footwall of the ore body were derived:

for the hanging wall:

$$y = 0.08x - 0.4z + 83900 \tag{1}$$

for the footwall

$$y = 0.08x - 0.4z + 83900 \tag{2}$$

This made it possible to determine the directional dip angles of the footwall and hanging wall of the deposits (Fig. 2). Unlike linear regression, the Random Forest method does not provide an explicit function for ore body distribution, but it predicts the reference points of mineral occurrence with smaller errors, which are then used to construct the surface. In the Colab environment, a Python script was developed that, based on statistical observations of ore body geometry, generated predictive control points for the layout of development workings at each of the projected horizons. By connecting these predictive points, operational contact lines between the footwall and hanging wall of the ore body and the host rocks were obtained. A comparative analysis of this method with contour derived from geological surveys of the Pivdenno-Bilozerske iron ore deposit for the 1140 m horizon is presented in Fig. 3.

The application of Linear Regression and Random Forest algorithms made it possible to construct predictive contours of the ore body at the designed horizons. Linear Regression provided interpolating functions that describe the overall geometry of the ore body, while the Random Forest method significantly reduced prediction errors. Comparative analysis showed that the average deviation between the predicted and actual contours did not exceed 1 m, which confirms the reliability of the obtained models.

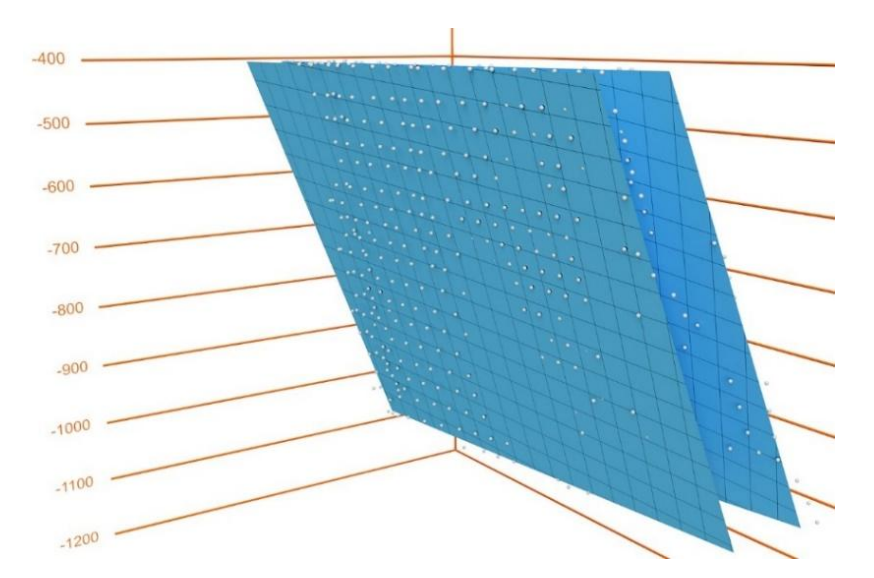


Figure 2. Approximated surfaces of the footwall and hanging wall of the Pivdenno-Bilozerske iron ore deposit

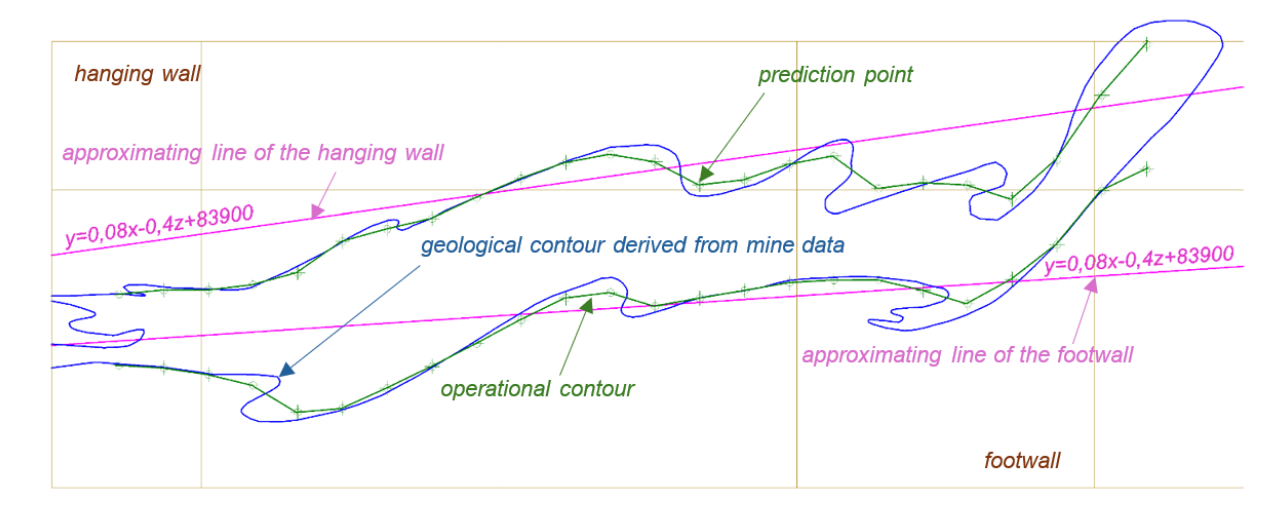


Figure 3. Prediction of the Pivdenno-Bilozerske iron ore deposit distribution at the 1140 m horizon

The next stage of the study involved constructing a wireframe model of the ore body at the designed mining level prepared for extraction. For this purpose, graphical information from each projected horizon was integrated into a unified three-dimensional ore body model. Separate three-dimensional meshes were generated for the hanging wall and footwall of the deposit, with vertices corresponding to the predictive points. The extraction chambers of the first and second stages were distinguished by color coding (Fig. 4).

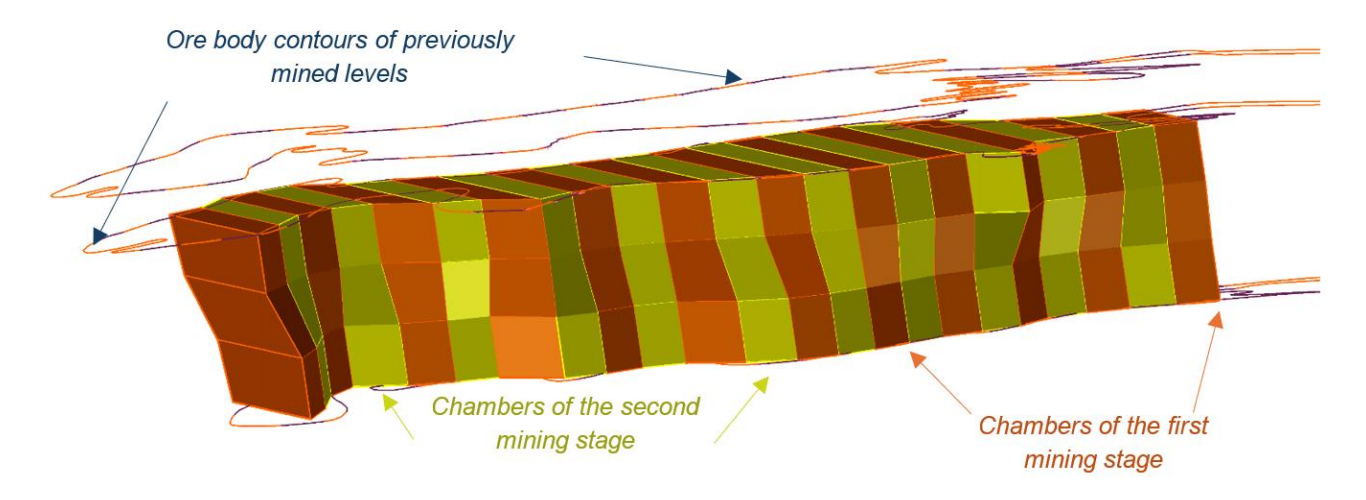


Figure 4. Prediction of the Pivdenno-Bilozerske iron ore deposit distribution at the 1040-1140 m mining level

The subsequent transformation of the wireframe model into a block model made it possible to determine the volume of the prepared ore reserves, which was approximately 5.52 million cubic meters or 22 million tons. This block model enabled a more detailed analysis of the ore body, providing not only the total volume but also the spatial distribution pattern of the ore. By converting the wireframes of the footwall and hanging wall into blocks, each extraction chamber could be examined individually. This approach allowed for the calculation of ore reserves and the assessment of preparatory work volumes for each chamber.

The block model also facilitated the planning of production schedules based on the estimated ore volumes, allowing for more efficient allocation of mining resources. In addition, it supported detailed visualization of the ore body structure, which enhanced understanding of its geometry and the sequence of mining stages. By integrating information from both the wireframe and block models, each extraction chamber could be analyzed individually, providing precise data for operational decision-making. This combination improved the ability to assess ore distribution patterns and optimize preparatory and extraction work. Overall, the integration of these modeling approaches increased both the accuracy and the practical utility of ore body evaluations for mining operations.

Chamber reserve modeling using both the wireframe and block models is presented in Figure 5. The wireframe model provides a detailed spatial representation of the ore body, showing the contours of the footwall and hanging wall. By transforming the wireframe into a block model, the volume of ore reserves in each extraction chamber can be accurately

calculated. This approach allows for separate analysis of individual chambers, supporting the assessment of preparatory work and production planning. Overall, combining wireframe and block models enhances the precision and practical utility of ore reserve evaluations.

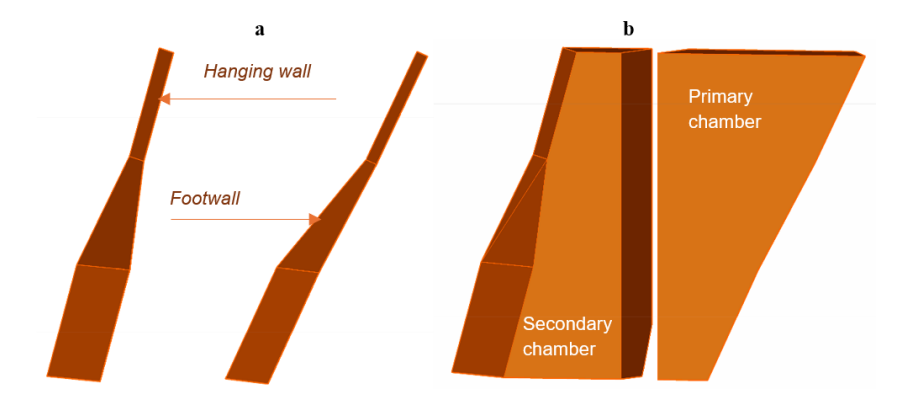


Figure 5. Chamber reserve modeling: (a) wireframe model; (b) block model

The proposed approach not only refined the geometry of the ore body but also enabled the calculation of work volumes for each individual extraction chamber. This provides the basis for:

- determining the locations of capital workings at each horizon;
- optimizing the length and number of development workings;
- preparing production schedules for development and stoping operations;
- forecasting extraction volumes step by step.

Thus, the research results confirmed the practical feasibility of applying machine learning techniques for the dynamic updating of geological ore body models.

4. Discussion

The results obtained confirm the effectiveness of applying machine learning methods for the dynamic updating of geological ore body models. The combined use of Linear Regression and the Random Forest algorithm made it possible to integrate the advantages of analytical interpretation with the robustness of predictive modeling, while minimizing errors (Petlovanyi et al., 2021; Dychkovskyi et al., 2019; Sala & Bieda, 2021). Comparative analysis with geological survey observations showed that the average deviation did not exceed 1 m, which indicates the high reliability of the predictive models.

The application of the proposed methodology in mining practice offers several important advantages. First, dynamic updating of the 3D model allows for the rapid incorporation of new exploration and mine surveying data, thereby improving the accuracy of long-term planning. Second, the construction of both wireframe and block models of the ore body enables stage-wise reserve evaluation and the determination of optimal parameters for the mining system (Petlovanyi et al., 2021; Deutsch, 2023; Sala & Bieda, 2021; Kamiński et al., 2021; Lewicka, 2010). Third, the methodology provides a foundation for integrating machine learning results into computer-aided mine planning systems.

At the same time, the results also highlight certain limitations. Machine learning methods require high-quality and representative datasets, which necessitates systematic monitoring of the completeness and reliability of geological information (**Deutsch**, 2023; **Kamiński et al.**, 2021;. Sala& Richert, 2025) Moreover, a promising direction for future research involves the use of neural networks and advanced ensemble forecasting techniques, which could further enhance the robustness of models under heterogeneous geological conditions.

5. Conclusions

This study has developed and validated a methodology for the dynamic updating of geological ore body models based on the integration of machine learning techniques with topographic mesh reconstruction. The use of Linear Regression and Random Forest algorithms improved the accuracy of predicting ore body geometry and enabled the regular adjustment of models throughout the mining process. The construction of wireframe and block models for the Southern Bilozerka deposit made it possible to estimate reserves of approximately 22 million tonnes and to establish a reliable basis for calendar-based planning of development and stoping operations.

The proposed methodology ensures the effective integration of mine surveying and geological exploration data into digital models, which significantly enhances the efficiency of mine production management. It provides a robust framework for accurately representing ore body geometry and supports informed decision-making in planning and operational processes. Furthermore, the results highlight promising directions for future research, including the

application of deep learning methods and the expansion of datasets to improve the modeling of complex geological structures.

6. References

Breiman, L. (2001). Random forests. Machine Learning, 45(1), 5–32. https://doi.org/10.1023/A:1010933404324

Deutsch, C. V. (2023). The Place of Geostatistical Simulation through the Life Cycle of a Mineral Deposit. Minerals, 13(11), 1400. https://doi.org/10.3390/min13111400

Huang, J., Zhang, H., Shi, X., Liu, X., & Bao, H. (2006). Interactive mesh deformation with pseudo material effects. Computer Animation and Virtual Worlds, 17(5), 383–392. https://doi.org/10.1002/cav.154

Li, C., Li, F., Guo, J., Liu, C., & Liu, Y. (2019). 3D geological map modeling technology based on a geological route and geological object wireframe model. *Acta Geologica Sinica - English Edition*, 93(1), 231–235.

Petlovanyi, M., Ruskykh, V., Sai, K., & Malashkevych, D. (2021). Prompt determination of predictive parameters for mining-technogenic landscape objects. IOP Conference Series: Earth and Environmental Science, 1348(1), 012035.

Sherstyuk, A. (1999). Fast ray tracing of implicit surfaces. Computer Graphics Forum, 18(2), 139–147. https://doi.org/10.1111/1467-8659.00343

Sun, J., Ding, Y., Huang, Z. D., Wang, N., Zhu, X. L., & Xi, J. T. (2018). Laplacian deformation algorithm based on mesh model simplification. In Proceedings of the 3rd IEEE International Conference on Image, Vision and Computing (ICIVC) (pp. 209–213). IEEE.

Dychkovskiy, R., & Bondarenko, V. (2006). Methods of Extraction of Thin and Rather Thin Coal Seams in the Works of the Scientists of the Underground Mining Faculty (National Mining University). International Mining Forum 2006, New Technological Solutions in Underground Mining, 21–25. https://doi.org/10.1201/noe0415401173.ch3

Kamiński, P., Dyczko, A., & Prostański, D. (2021). Virtual Simulations of a New Construction of the Artificial Shaft Bottom (Shaft Safety Platform) for Use in Mine Shafts. Energies, 14(8), 2110. https://doi.org/10.3390/en14082110

Dychkovskyi, R., Falshtynskyi, V., Ruskykh, V., Cabana, E., & Kosobokov, O. (2018). A modern vision of simulation modelling in mining and near mining activity. E3S Web of Conferences, 60, 00014. https://doi.org/10.1051/e3sconf/20186000014

Kyrylenko, O., Denysiuk, S., Bielokha, H., Dyczko, A., Stecuła, B., & Pazynich, Y. (2025). Smart Monitoring and Management of Local Electricity Systems with Renewable Energy Sources. Energies, 18(16), 4434. https://doi.org/10.3390/en18164434

Pazynich, Y., Kolb, A., Korcyl, A., Buketov, V., & Petinova, O. (2024). Mathematical model and characteristics of dynamic modes for managing the asynchronous motors at voltage asymmetry. Polityka Energetyczna – Energy Policy Journal, 27(4), 39–58. https://doi.org/10.33223/epj/191779

Dychkovskyi, R.O., Tymoshenko, Y.V., Astafiev, D.O. (2014). Method of analytical investigation of wall advance speed and forms of line face influence on stress-strain state of a rock massif. Naukovyi Visnyk Natsionalnoho Hirnychoho Universytetu, (1), pp. 11–16

Psyuk, V., & Polyanska, A. (2024). The usege of artificial intelligence in the activities of mining enterprises. E3S Web of Conferences, 526, 01016. https://doi.org/10.1051/e3sconf/202452601016

Vladyko, O., Maltsev, D., Cabana, E. C., Shavarskyi, I., & Dychkovskyi, R. (2022). Formation of the models of mining enterprise management. Naukovyi Visnyk Natsionalnoho Hirnychoho Universytetu, 3, 30–36. https://doi.org/10.33271/nvngu/2022-3/030

Polyanska, A., Pazynich, Y., Petinova, O., Nesterova, O., Mykytiuk, N., & Bodnar, G. (2024). Formation of a Culture of Frugal Energy Consumption in the Context of Social Security, pp. 60-87. The Journal of the International Committee for the History of Technology, 29(2), 60-87. https://doi.org/10.11590/icon.2024.2.03

Pan, F., Zhao, X., Dudek, M., Rehman, M. Z., & Shahzad, U. (2025). Ecological Impacts of Cultivated Land Conversion and Urban Eco-Resilience in the COP29 Era. Land Degradation and Development, Portico. https://doi.org/10.1002/ldr.70080

Dychkovskyi, R., Tabachenko, M., Zhadiaieva, K., & Cabana, E. (2019). Some aspects of modern vision for geoenergy usage. E3S Web of Conferences, 123, 01010. https://doi.org/10.1051/e3sconf/201912301010

Sala, D., & Bieda, B. (2021). Role of Stochastic Approach Applied to Life Cycle Inventory (LCI) of Rare Earth Elements (REEs) from Secondary Sources Case Studies. Towards a Sustainable Future - Life Cycle Management, 107–120. https://doi.org/10.1007/978-3-030-77127-0 10

Lewicka, D. (2010). The impact of HRM on creating proinnovative work environment. International Journal of Innovation and Learning, 7(4), 430. https://doi.org/10.1504/ijil.2010.032932

Sala, D., & Richert, M. (2025). Perspectives of Additive Manufacturing in 5.0 Industry. Materials, 18(2), 429. https://doi.org/10.3390/ma18020429

Author's contribution

Dmytro Malashkevych (associate professor): conceptualization, methodology, formal analysis, data visualization, writing – original draft. **Vladyslav Ruskykh** (associate professor): investigation, validation, resources, supervision, writing – review & editing. **Marek Dudek** (professor): conceptual framework, **Dariusz Sala** (associate professor): data curation & formal analysis, **Yuliya Pazynich** (associate professor): literature review & editing process.

All authors have read and agreed to the published version of the manuscript.



Advancing Explosion Protection in Coal Mines Exposed to Gas-Dynamic Risks

DIM-ESEE Conference



Vasyl Holinko¹®⊠, Oleksandr Holinko¹*®⊠, Oleg Kuznetsov¹®⊠ Yulia Zabolotna¹®⊠

¹ Dnipro University of Technology, 49005 Dnipro, 19 Dmytro Yavornytskoho Ave.

Abstract

This study focuses on enhancing explosion protection in coal mines affected by gas-dynamic risks, where high methane levels and dust contamination reduce the performance of monitoring systems. Conventional optical sensors are prone to rapid fouling, resulting in reduced accuracy and reliability. To address this, a hybrid approach is proposed that integrates a stable thermocatalytic sensor with a selective optical unit. The thermocatalytic sensor provides reliable baseline monitoring and protective shutdown functions, while the optical element records rapid surges rates of methane concentration rather than absolute values. This change in function minimizes the impact of dust deposition and improves the system's ability to detect hazardous gas surges. Analytical modeling based on Boucher's law confirms the feasibility of this method. A prototype device was developed using ATmega8 microcontrollers with automated calibration, diagnostics, and service alerts. The results demonstrate enhanced responsiveness, stability, and reliability of methane monitoring, offering a practical basis for upgrading existing mine safety systems and strengthening explosion protection.

Keywords: "mine operations", "explosion protection", "methane", "gas-dynamic phenomena", "sensors detection"

1. Introduction

The complex geological structure of coal deposits located in Ukraine, combined with high levels of gas in the seams, their tendency to spontaneous combustion, and frequent sudden emissions of mixtures of coal, gas, and rock, significantly increases the likelihood of emergencies (Bondarenko et al., 2007). Incidents such as explosions of methane-air mixtures are particularly dangerous, posing a threat to the lives of miners and the safety of mining equipment. One of the key causes of such explosions is the improper or untimely operation of mine equipment, in particular stationary gas analyzers, which are designed to detect exceedances of permissible methane concentration levels in the air of underground workings (Tabachenko et al., 2012). Often, these devices do not respond quickly enough or do not work at all in critical situations that arise during sudden gas-dynamic emissions, when the level of methane in the air rises sharply. The most dangerous type of such sudden events are explosive emissions, during which the concentration of methane can rise to a maximum value of 100% in a very short time interval. At the same time, the rate of increase in methane saturation in the air sometimes reaches extremely high values – up to 5 percent per second, which makes it impossible for most existing technical means to respond in time(Golinko & Kotlyarov, 2010).

In modern conditions, both domestic and foreign mining industries have accumulated significant practical experience in the creation and implementation of automated gas monitoring systems (Lunca et al., 2013). In Ukrainian coal mines with seams prone to sudden gas-mechanical phenomena, the use of fast-acting thermocatalytic analyzer (ATB-type) has been widely implemented. These devices function as central nodes of systems for continuous measurement of methane concentration in workings and determination of its growth rate. In addition, these devices have an emergency power shutoff function in case of critical exceedances of the concentration threshold or methane growth rate, which is an element of automatic protection (Fong et al., 2018).

However, a significant problem with the use of existing gas analysis systems is their frequent activation in cases where there are no real conditions for the emergence of threatening situations. Such false alarms lead to the unwanted stoppage of the work process at coal mining facilities, which ultimately causes significant economic losses, reduces overall production, disrupts planned indicators, and complicates the organization of mining operations. In addition, the technical equipment currently used to detect and prevent the consequences of sudden gas-dynamic emissions in high-risk mines does not fully meet the requirements of modern operation, in particular in terms of speed, reliability, resistance to external factors, and ease of maintenance (Golinko & Kotlyarov, 2010).

In view of the above, further development of technologies in the field of automated rapid response systems is extremely important, involving both the thorough modernization of existing devices and the introduction of fundamentally new engineering solutions for high-speed protective systems capable of effectively preventing the development of hazardous situations (**Dychkovskyi et al., 2019**). In order to minimize the risk of methane-air mixture explosions in the mining industry, it is necessary to continue targeted scientific and technical research, the main goal of which should be to

improve the accuracy, stability, and adaptability of gas environment monitoring systems. Particular attention should be paid to improving their response to changes in the concentration of fouling impurities in real time.

An analysis of existing approaches to detecting methane in mine air has shown that the highest rate of detection of changes in the gas environment can be achieved by using optical absorption techniques (Lapshyn et al., 2025). However, this technology has a number of significant limitations, including its high sensitivity to external conditions such as temperature, humidity, atmospheric pressure, and the presence of other gases that can affect measurement accuracy (Fedoreiko et al., 2025). In addition, one of the main factors hindering the widespread use of this method is the increased dustiness of the air in mine workings where monitoring devices are installed.

Recent scientific experiments in the field of optical measurement have made it possible to design compact, highly sensitive methane sensors (**Vovna & Zori**, **2013**). Such devices use a metal mesh that acts as a filter, inside which there is a channel for optical reading. With a wire diameter of 0.1 mm and holes with an area of 0.01 mm², the time response is about one second. In experimental prototypes of devices operating on the principle of light absorption, it was possible to improve dynamic sensitivity by introducing software signal processing methods. It was also possible to partially reduce the influence of negative external factors, including air pollution (**Vovna et al., 2017**).

However, the use of such solutions significantly complicates the design of analyzers, necessitates the use of additional sensors with different spectral parameters, and does not solve the problem of automatic monitoring of the technical condition of the devices themselves (Fedoreiko et al., 2014). Thus, the question of creating a fully functional self-diagnostic system for methane analyzers based on optical principles remains open today.

At the current stage of development of technical safety measures in the coal industry, the vast majority of devices for determining the methane content in the air environment of mines, which are part of automatic gas hazard response systems, operate on the basis of a relatively inertial method of thermocatalytic analysis (Golinko & Kotlyarov, 2010). The popularity of this approach is explained by the high accuracy of methane-responsive sensors, as well as their resistance to the influence of accompanying external factors, such as air humidity, changes in temperature conditions, the presence of dust particles, and the gas composition in the environment.

The results of experiments and theoretical studies of the thermocatalytic principle of operation have contributed to a significant increase in the durability and stability of such sensor systems (Alekseev & Golinko, 2018; Alekseev & Golinko, 2020). One of the advantages of thermocatalytic elements is the ability to control their functional characteristics by adjusting the power supply parameters. In combination with the capabilities of modern microprocessor-based computing devices, this allows for the implementation of a remote self-diagnostic function for analyzers, as well as effective verification of automatic power shut-off systems in the event of a detected hazard.

As part of experimental research, a method for monitoring the technical condition of stationary thermocatalytic gas analyzers was developed and substantiated, which involves automatic verification of zero readings of devices by reducing the voltage supplied to the thermocouple (Alekseev & Golinko, 2018). This disconnection of the power supply to a level at which the methane oxidation reaction on the working element cannot occur, allows the accuracy of the device's "zero" to be determined without operator intervention. The use of modern digital technologies allows not only to monitor the stability of these indicators, but also to automatically correct them (Kyrylenko et al., 2025).

An algorithm for the operation of the sensor device was developed based on the results obtained, , which implements the specified functions in an automated mode. In addition, another diagnostic method was substantiated: checking the sensitivity of primary sensors by analyzing changes in their output parameters in the process of varying the electric current in the so-called "plateau" section of the output characteristic, where a stable bridge voltage is formed (Golinko & Kotlyarov, 2010). This allows the accuracy of the sensor element's response to changes in methane concentration to be assessed. Thanks to the use of modern microprocessor computing modules, it has become possible not only to automatically evaluate the performance of primary transducers, but also to quickly adjust the analyzer's readings if there are changes in its sensitivity. (Golinko & Kotlyarov, 2010). As a result, a functional algorithm and software have been created that ensure continuous self-diagnosis of the device under operating conditions.

It is worth noting that improvements in the design characteristics of sensor elements, namely, reducing their size and optimizing their shape and geometry, have made it possible to significantly improve the speed parameters of gas analyzers. In particular, the reduction in the response time of thermocatalytic sensors, combined with the introduction of improved methods of digital signal processing, has made it possible to increase the overall dynamics of gas control devices. Despite the progress achieved, a complete and final solution to this problem has not yet been found and it remains relevant for further scientific research...

2. Methods of the Research in Advancing Explosion Protection

In view of these circumstances, the main objective of the study is to find innovatory approaches that can ensure a higher response rate and long-term stability of automated methane monitoring systems in hazardous mine workings and areas (Vladyko et al., 2025). The best results in achieving maximum performance of optical sensors can be achieved in cases where the radiation source together with the receiving element, is placed directly in the flow of the air-gas mixture to be analyzed. This design configuration ensures high sensitivity and instantaneous response of the sensor. At the same time, this design has a significant drawback: intense dust particle deposition on the surface of light-emitting and receiving components. This inevitably leads to distorted results, reduced accuracy, and ultimately to device failure or loss of functionality.

The problem is particularly acute in production environments with excessive dust. For example, in the cleaning areas of preparatory tunnels or at the intersections of main and auxiliary workings, the concentration of dust particles can reach 500 mg/m³ or even more.. The use of protective screens or barriers partially slows down the contamination process, but at the same time worsens the responsiveness of the system, increases the time constant, and creates additional difficulties in maintenance and enterprise management (Polyanska et al., 2024; Vladyko et al., 2022).

Thus, present practice confirms that it has not yet been possible to create a reliable high-speed gas analyzer based solely on the optical principle of methane detection. That is why a combined approach, an example of which is described in, is attracting more and more attention. In such a system, the main working module is a thermocatalytic sensor, although with lower dynamics. Its signal is used as the basis for forming the system's output data, including telemetry information indicators and emergency power shutdown commands (Golinko & Kotlyarov, 2010). It acts as a corrective element for the results received from a fast-acting but more susceptible to dust deposits optical sensor.

The function of the optical element is to ensure the prompt generation of power cut-off commands in case of critically high methane concentrations or excessively rapid changes in its content in the gas environment. At the same time, the weak point of such a solution remains the problem of gradual loss of sensitivity which cannot be fully compensated for even by software signal processing methods, due to contamination of optical surfaces. This can lead to delayed or false activation of the emergency protection system.

To minimize these shortcomings, here is proposed to change the approach: namely to switch the optical sensor from the mode of measuring the absolute level of methane to the mode of recording its growth rate during sudden gas-dynamic processes. This method makes it possible to reduce the dependence of measurement accuracy on the contamination of optical elements and at the same time increase the reliability of determining hazardous trends.

The theoretical basis of this concept is based on Bouguer's law (Oshina & Spigulis, 2021), which describes the relationship between the intensity of radiation J and the amount of energy Jn absorbed by a gas phase layer of thickness dx in a selected spectral range. It is this relationship that allows us to formalize the processes of optical absorption and explain changes in the sensor signal under conditions of dynamic gas flows.

$$J_{\pi} = -K \cdot J \cdot dx \cdot d\nu,$$
 where are:

K – coefficient characterizing the attenuation of the radiation flux.

If the wavelength of the emitted radiation remains unchanged, and the optical path length of the gas mixture with methane concentration C is constant, then the mathematical resolution of equation (1) takes the following form

$$J_{\Pi} = J_0 \cdot (1 - e^{-A \cdot Cx}),$$
 where are:

A – spectral absorption parameter at wavelength λ , intrinsic to the molecular structure of methane, which is determined by its physical properties and does not vary with the amount of substance in the medium.

When monitoring potentially hazardous methane accumulations and assuming that the distance separating the radiation source from the detector lies within the range of several decimeters, expression (2) can be approximated by a proportional dependence

$$J_{\pi} = J_0 \cdot (1 - A \cdot Cx). \tag{3}$$

From relation (3) it follows that a variation in methane concentration by a value ΔC will induce a corresponding variation in the measured radiation energy flux by a magnitude of

$$\Delta J_{\Pi} = A \cdot \Delta C x \cdot J_{0}. \tag{4}$$

From which one can obtain the subsequent functional relationship

$$\Delta C = a \cdot \frac{\Delta J}{J_0},\tag{5}$$

a – proportionality constant, reflecting both the absorbing capacity of methane molecules and the optical path length between emitter and receiver.

3. Research Results and Discussion

Analysis of equation (1)-(5) (Vovna et al., 2017) indicates that if the initial radiation power incident on the gaseous environment is precisely known, and the attenuated signal after propagation over a certain spatial interval is reliably measured, then it becomes possible to determine short-term changes in methane concentration that accompany rapid gasdynamic events. A particularly significant outcome is that the fraction of energy absorbed within the methane-containing medium remains insensitive to gradual fluctuations in the baseline emission intensity. As a result, the method ensures robust measurements that are not distorted by external factors such as temperature shifts, barometric pressure changes, or progressive dust deposition on the optical components of the monitoring system.

This conclusion provides a conceptual basis for reexamining the design principles of methane detection and control units, especially those integrated into automated safety systems intended to disconnect electrical power during critical gas buildup. An effective strategy in this regard is the application of a hybrid analytical module that combines both thermocatalytic and optical sensing elements operating in parallel (see Figure. 1). In such a configuration, under conditions where no abrupt increases in methane levels occur (for instance, in the absence of sudden outbursts or emissions), the dominant role in concentration measurement is assigned to the thermocatalytic detector D1. The output of this sensor is processed to evaluate the degree of methane saturation in the atmosphere and to generate a protective command that disables the power supply once the established safety thresholds are surpassed.

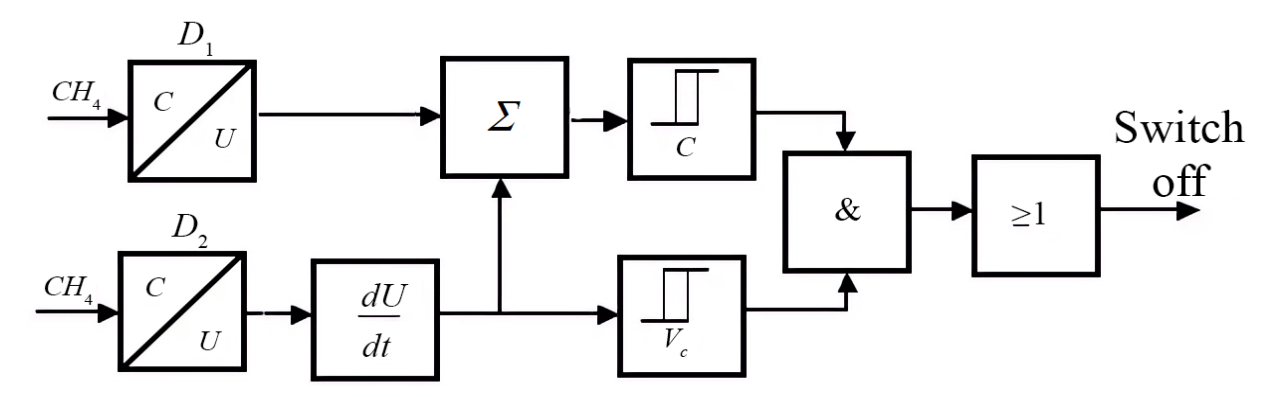


Figure 1. Generalized signal formation scheme for the operation of high-speed gas protection systems

The high-precision optical detector D2 integrated into the system is not engaged in permanent operation. Instead, it is activated selectively, only under conditions when it is necessary to register an abrupt and extremely fast escalation in the concentration of methane within the mine atmosphere during a very short observation interval. If the velocity of growth in methane content surpasses a pre-defined critical rate (for instance, an increment greater than 1% per second), the control unit, regardless of the absolute concentration at that specific moment, instantly issues a command to disconnect the power supply to all electrical installations. Conversely, when the rate of increase is more moderate (for example, within the interval from approximately 0.2 %/s up to 1.0 %/s), the decision-making algorithm relies on an integrated evaluation: the incremental concentration detected optically is added to the baseline measurement provided by the thermocatalytic sensor. Should the resultant value exceed the established safety margin, the protective mechanism is again triggered, ensuring that power delivery to equipment is terminated in advance of a potential hazard.

The conceptual innovation proposed for enhancing the responsiveness of the monitoring system does not involve the design of a completely novel device from the ground up. Instead, the approach consists in a targeted modernization of the already existing methane detection module, which has been extensively tested in mining practice. This analyzer is equipped with a number of auxiliary functions, such as the capacity for continuous self-diagnostics, automated compensation of baseline drift (zero correction), and adjustment of sensitivity parameters of the primary thermocatalytic element. Into this proven architecture a miniature optical unit is incorporated, and following this integration, modifications are introduced both to the operational logic and to the embedded software of the system. This dual refinement guarantees coordinated functioning between the two measurement channels, thereby improving overall reliability.

The technical realization of the upgraded methane analyzer is founded on the use of microcontrollers belonging to the ATmega8 family, which provide centralized control of all functional modules. The device is configured to work in two basic regimes: the initialization stage (calibration procedure) and the principal working stage (real-time monitoring). Importantly, the calibration procedure is fully automated, without the necessity for direct operator's intervention. For this purpose, two gas mixtures are employed: purified ambient air and a specially prepared calibration mixture with a strictly regulated methane content, such as a 1% concentration sample.

When the analyzer is switched into the calibration mode, the system automatically displays the indication "Air" on the interface screen, accompanied by additional data concerning the remaining time until the commencement of the calibration sequence. At this moment, the methane-sensitive detectors are inserted into a compact, hermetically sealed chamber, which has been preliminarily filled with purified air. Such an arrangement establishes reference baseline conditions, indispensable for subsequent re-calibration procedures and for achieving precise adjustment of the zero level of the measuring channels.

The subsequent operational sequence of the system during the calibration cycle of the optical sensor is schematically illustrated in Figure. 2. Within this procedure, the control software incorporates specially programmed pauses that eliminate the influence of transient processes. During these intervals, the nominal electrical current is applied to the light-emitting diode (LED), after which the actual output signal of the optical sensor, expressed as voltage U₀, is registered. This reference parameter is stored in the internal memory of the microcontroller and later serves as the baseline indicator for all subsequent computational routines.

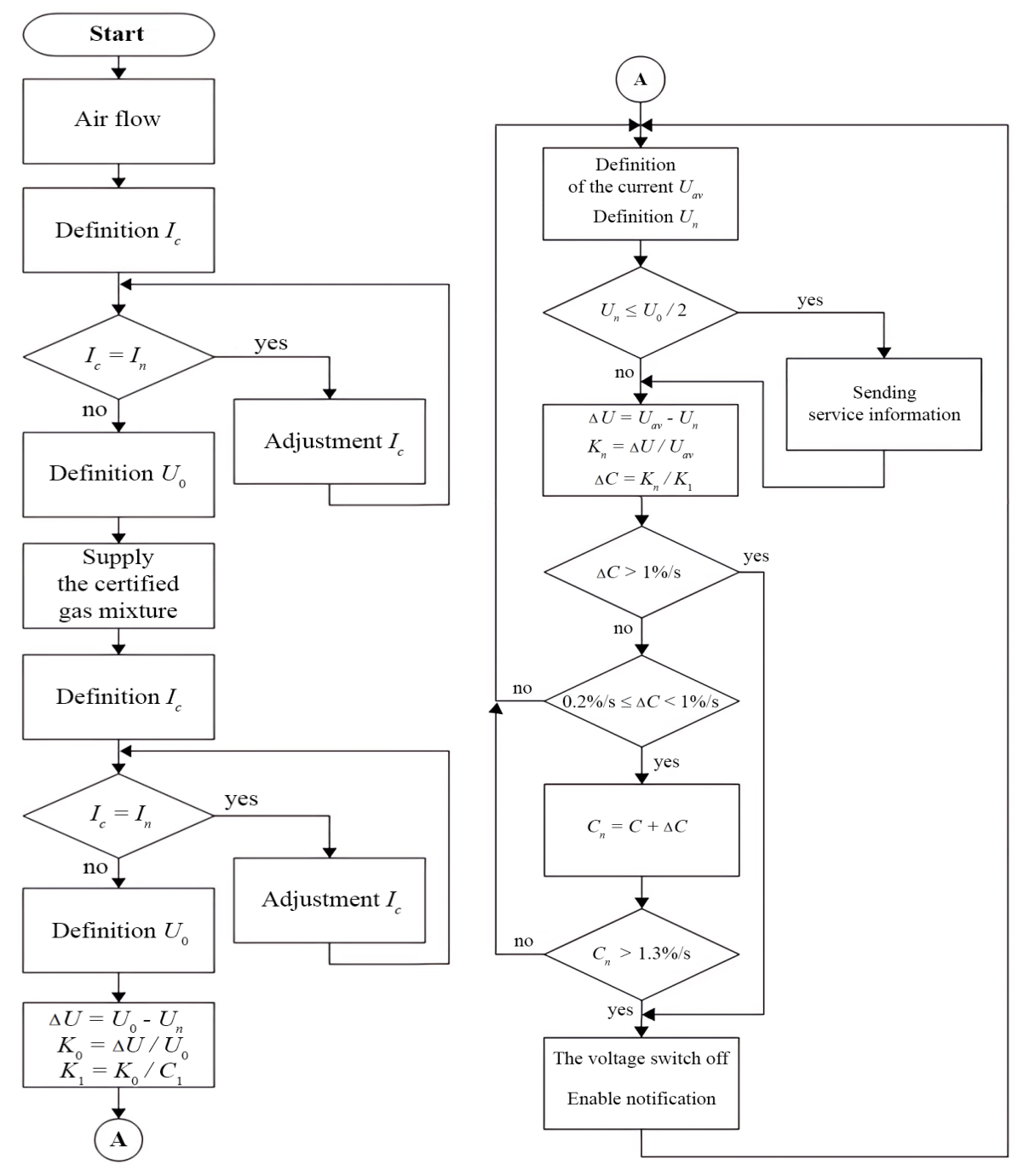


Figure 2. Functional algorithm of the gas analyzer during calibration and subsequent routine operation

Once the time required for the complete stabilization and adjustment of the inertial thermocatalytic detector has passed, the system automatically displays a new notification on the interface screen: "Certified mixture", accompanied by a countdown timer to the continuation of the calibration protocol. At this stage, the measuring chamber is purged and filled with a reference calibration mixture of gases, typically containing methane at a concentration of 1 % by volume. The system simultaneously verifies the current delivered to the LED and, if discrepancies are detected, executes an automatic correction routine. Parallel to this process, the optical channel records a new output voltage value denoted as Uff. The difference between the initial and the newly measured voltages is then computed according to the relation: $\Delta U = U_0 - Uff$. Based on this, the relative deviation in signal level is expressed as a dimensionless coefficient: $K_0 = \Delta U / U_0$. If the real methane concentration in the calibration mixture differs from the nominal standard of 1 vol.%, the obtained result undergoes mathematical correction. For this purpose, the coefficient is normalized to the conditional value corresponding to exactly 1 % methane according to the expression: $K_1 = K_0 / C_a$, where C_a designates the actual methane content in the certified calibration gas. The final coefficient K_1 is then written into the non-volatile memory of the microcontroller, functioning as a calibration constant that quantitatively characterizes the sensitivity of the optical sensor by accounting for relative shifts in its output signal.

Upon successful completion of all calibration stages, the device automatically transitions into its standard measurement mode. From this point onward, the analyzer continuously evaluates the gaseous environment, detecting both gradual changes and sudden surges in methane content. This guarantees a high level of reliability and operational safety under potentially explosive conditions typically present in underground mining operations.

In addition to its primary task of quantifying methane levels, the analyzer also performs ongoing diagnostics of the optical measurement channel. This is essential since, during long-term usage, the optical window and associated elements may accumulate particulate contamination, dust deposits, or condensed aerosols, which can distort the accuracy of the readings. Should the registered output voltage decline to a value not exceeding half of the original baseline (i.e., Uo/2), the control system automatically generates a service alert directed to the supervisory dispatcher. The message recommends preventive maintenance, specifically the cleaning of the optical assembly.

This preventive diagnostic approach effectively minimizes systemic errors, preserves the stability of measurement accuracy, and ensures that even after extended periods of continuous operation, the gas analyzer remains capable of promptly detecting the emergence of explosive methane concentrations in the industrial environment.

4. Conclusions

Maintaining the efficiency and dependable operation of current gas monitoring equipment remains a fundamental requirement for safety in explosive mining environments. One effective solution for improving the performance of methane analyzers is the integration of two types of sensors that differ in their working principles and functional properties. The first element is a thermocatalytic detector, which provides stable and accurate readings but reacts relatively slowly to rapid changes in the gas medium. The second is an optical sensor, characterized by its ability to respond almost instantly, though its precision in determining the absolute concentration is lower. Combining these two measurement devices makes it possible to establish an effective compromise: reliable determination of the average methane level together with fast response to sudden fluctuations in the atmosphere.

The research work introduces a methodical approach for identifying potentially explosive environment. The core idea is as follows: when no external disturbances caused by gas-dynamic phenomena are present in mine tunnels, the primary and most trustworthy source of information about methane levels is the thermocatalytic sensor. Based on its measurements, the system generates a control signal, which, when required, disconnects electrical installations to eliminate the ignition risk. Within the same configuration, the optical sensor acts as a supplementary element. Instead of determining the exact methane percentage, it records short-term rises in concentration, thereby providing additional monitoring and protectionfunction. This aspect is especially critical in emergency cases, such as the sudden release of methane pockets into mine workings, when gas-dynamic conditions may change unpredictably.

If the detected growth rate of methane content exceeds a pre-defined safety threshold, the system instantly sends a command to de-activate electrical devices – even if the thermocatalytic sensor has not yet registered a hazardous average level. When the growth remains moderate and within acceptable boundaries, a cumulative value is calculated. This parameter represents the sum of the thermocatalytic sensor's current readings and the short-term increase fixed by the optical detector. Should this integrated figure exceed the allowable safety concentration, the equipment is again automatically shut down, which establishes a multi-tiered system of protection against explosions.

Further justification demonstrates that big methane concentration variations can be effectively tracked through analyzing the relative change in the intensity of the optical radiation reaching the sensor. This principle is particularly important because it neutralizes the impact of slow-acting external factors: such as gradual temperature fluctuations, shifts in barometric pressure, or dust accumulation on optical surfaces of the device. Thus measurement results remain invariable to environmental influences, which greatly enhances both precision and reliability of the monitoring system.

The study also presents a detailed outline of the algorithm developed for the ATmega8 microcontroller, which forms the technical basis of the high-speed methane analyzer. The embedded software manages the simultaneous operation of the two sensors, carries out real-time calculations, evaluates data against safety-critical limits, and generates emergency shutdown signals. This demonstrates the effectiveness of combining different sensor functions within one measurement system and emphasizes the potential of integrated measuring technologies for mining safety. Consequently, the proposed solution not only provides accurate and rapid detection of hazardous air/gas mixtures also this article should be considered as a basis for further research aimed at the technical implementation of the method under consideration.

5. References

- Alekseev, M., Golinko, O. (2018). Automatic diagnostics of the state of stationary thermocatalytic gas analyzers. (Avtomatychna diahnostyka stanu statsionarnykh termokatalitychnykh hazoanalizatoriv) *Zbirnyk naukovykh prats'* NHU, 53, 223 229 https://ir.nmu.org.ua/handle/123456789/152372 (In Ukrainian)
- Alekseev, M., Golinko, O. (2020) Automatic sensitivity control of sensors of stationary thermocatalytic methane analyzers. (Avtomatychnyy kontrol' chutlyvosti datchykiv statsionarnykh termokatalitychnykh analizatoriv metanu) *Hirnychyy visnyk KHI*, 107, 16 22. http://iomining.in.ua/ua/homeua/journal/107ua/#107 (In Ukrainian)
- Bondarenko, V.I., Griadushchiy, Y.B., Dychkovskiy, R.O., Korz, P.P., Koval, O.I. (2007). Advanced experience and direction of mining of thin coal seams in Ukraine. *Technical, Technological and Economic Aspects of Thin-Seams*

- Coal Mining International Mining Forum 2007, 1–7
- Dychkovskyi, R., Tabachenko, M., Zhadiaieva, K., & Cabana, E. (2019). Some aspects of modern vision for geoenergy usage. E3S Web of Conferences, 123, 01010. https://doi.org/10.1051/e3sconf/201912301010
- Fedoreiko, V., Zahorodnii, R., Lutsyk, I., Rutylo, M., & Bureha, N. (2025). Modelling of resource-saving control modes of a bioheat generator using neuro-fuzzy controllers. IOP Conference Series: Earth and Environmental Science, 1457(1), 012005. https://doi.org/10.1088/1755-1315/1457/1/012005
- Fedoreiko, V.S., Rutylo, M.I., Lutsyk, I.B., & Zahorodnii, R.I. (2014). Thermoelectric modules application in heat generator coherent systems, Naukovyi Visnyk Natsionalnoho Hirnychoho Universytetu, (6), 111–116
- Golinko, V., Kotlyarov, A. (2010) Control of explosiveness of the environment in mine workings and equipment of coal mines. Monograph. (Kontrol' vzryvoopasnosti sredy v gornykh vyrabotkakh i oborudovanii ugol'nykh shakht). *D.: Lira*, 368 p. ISBN 978-966-383-269-2 (In Russian).
- Golinko, V., Kotlyarov, A. (2010) Use of low-inertia methane sensors in automatic gas control systems. *Naukovyi Visnyk NHU*. 4. 85 89. https://nvngu.in.ua/index.php/uk/component/jdownloads/viewdownload/25/289 (In Russian).
- Fong, S., Ashasi-Sorkhabi, A., Prakash, G., Narasimhan, S., & Riseborough, M. (2018). Automated Condition-Based Monitoring of Automated People Movers. *Automated People Movers and Automated Transit Systems*, 57–67. https://doi.org/10.1061/9780784481318.007
- Kyrylenko, O., Denysiuk, S., Bielokha, H., Dyczko, A., Stecuła, B., & Pazynich, Y. (2025). Smart Monitoring and Management of Local Electricity Systems with Renewable Energy Sources. Energies, 18(16), 4434. https://doi.org/10.3390/en18164434
- Lapshyn, Y., Shevchenko, O., Dybrin, S., & Dychkovskyi, R. (2025). Feasibility of Fine Classification in Processing Watered Coal Sludge from Storage: A Case Study of the Dnipro Coke Chemical Plant. Acta Montanistica Slovaca, 30(1), 100–113. https://doi.org/10.46544/ams.v30i1.07
- Lunca, E., Salceanu, A., & Ursache, S. (2013). Automated Measurement and Monitoring of the Electromagnetic Fields from GSM Systems. *Journal of Clean Energy Technologies*, 174–177. https://doi.org/10.7763/jocet.2013.v1.40
- Muhammad, T., Ni, G., Chen, Z., Mallek, S., Dudek, M., & Mentel, G. (2024). Addressing resource curse: How mineral resources influence industrial structure dynamics of the BRI 57 oil-exporting countries. *Resources Policy*, 99, 105420. https://doi.org/10.1016/j.resourpol.2024.105420
- Polyanska, A., Pazynich, Y., Mykhailyshyn, K., Babets, D. & Toś, P. (2024). Aspects of energy efficiency management for rational energy resource utilization. Rudarsko-Geološko-Naftni Zbornik, 39(3), 13–26. https://doi.org/10.17794/rgn.2024.3.2
- Polyanska, A., Pazynich, Y., Mykhailyshyn, K., Babets, D. & Toś, P. (2024). Aspects of energy efficiency management for rational energy resource utilization. *Rudarsko-Geološko-Naftni Zbornik*, 39(3), 13–26. https://doi.org/10.17794/rgn.2024.3.2
- Tabachenko, N.M., Dychkovskiy, R.Ye., Falshtynskiy, V.S. (2012). About extraction of methane and slate gas from coal and slate deposits. *Naukovyi Visnyk Natsionalnoho Hirnychoho Universytetu*, 2, 44–48
- Vladyko, O., Maltsev, D., Cabana, E. C., Shavarskyi, I., & Dychkovskyi, R. (2022). Formation of the models of mining enterprise management. Naukovyi Visnyk Natsionalnoho Hirnychoho Universytetu, 3, 30–36. https://doi.org/10.33271/nvngu/2022-3/030
- Vladyko, O., Maltsev, D., Gliwiński, Ł., Dychkovskyi, R., Stecuła, K., & Dyczko, A. (2025). Enhancing Mining Enterprise Energy Resource Extraction Efficiency Through Technology Synthesis and Performance Indicator Development. Energies, 18(7), 1641. https://doi.org/10.3390/en18071641
- Vovna, O., Zori, A., Akhmedov, R. (2017) Increasing the accuracy of the optoelectronic methane concentration meter of coal mines. (Pidvyshchennya tochnosti optoelektronnoho vymiryuvacha kontsentratsiyi metanu vuhil'nykh shakht) Zbirnyk naukovykh prats'. «Elektroenerhetyka ta peretvoryuval'na tekhnika». *Kharkiv. NTU "KhPI"*, 4(1226), 19–24. https://repository.kpi.kharkov.ua/server/api/core/bitstreams/b14d9ec7-0fc8-4ff9-974d-26da69298c11/content (In Ukrainian).
- Vovna, O., Zori, A., Khlamov, M. (2010) Method of compensating for dynamic error of infrared methane concentration meter for coal mines. (Sposib kompensatsiyi dynamichnoyi pokhybka infrachervonoho vymiryuvacha kontsentratsiyi metanu dlya vuhil'nykh shakht) Zbirnyk naukovykh prats'. «Elektroenerhetyka ta peretvoryuval'na tekhnika». *Kharkiv. NTU "KhP1"*, 2. 65–70. https://core.ac.uk/download/pdf/162886053.pdf (In Ukrainian)
- Vovna, A., Zori, A. (2013) High-speed meter of methane concentration in the mine atmosphere of coal mines (Bystrodeystvuyushchiy izmeritel' kontsentratsii metana v rudnichnoy atmosfere ugol'nykh shakht). *Visn. Kremenchutsk. nat. un-tu im. Mikhail Ostrogradsky. Kremenchuk*, 6(83), 114-119. https://visnikkrnu.kdu.edu.ua/statti/2013-6(83)/114.pdf (In Russian).
- Oshina, I., Spigulis, J. (2021) Beer–Lambert law for optical tissue diagnostics: current state of the art and the main limitations. *Journal of Biomedical Optics*, 26 (10). https://doi.org/10.1117/1.JBO.26.10.100901

Author's contribution

Vasyl Holinko (Professor) conceptualization, review & editing; Oleksandr Holinko (Associate Professor) original draft and writing; Oleg Kuznetsov (PhD student) data curation, formal analysis; Yulia Zabolotna (Associate Professor) supervision, validation.

All authors have read and agreed to the published version of the manuscript.



Underground trial testing of NRE Support Rig

DIM-ESEE Conference

Paulo Pleše^{1*}, Juraj Banić¹, Vječislav Bohanek², Sibila Borojević Šoštarić²

- ¹ DOK -ING Ltd., Slavonska Avenija 22 G, 10000 Zagreb, Croatia
- ² University of Zagreb, Faculty of Mining, Geology and Petroleum Engineering Pierottijeva 6, 10000 Zagreb, Croatia



Abstract

Narrow Reef Mining (NRM) is a modern method developed to extract valuable minerals such as platinum group metals (PGMs) and gold from narrow ore bodies. The Narrow Reef Equipment (NRE) fleet, made by DOK-ING, includes three main machines: a drill rig, a dozer, and a support rig. The support rig plays a key role in roof safety, but roof bolting has often been identified as the main bottleneck of the mining cycle. This study presents results from efficiency trials of the NRE support rig conducted at two South African mines: Tumela and Bokoni. Although the same machines were used, the Bokoni mine achieved better performance. The reasons included redesigned machine parts, more experienced operators, and improved training. The study shows that combining technical improvements with skilled operators leads to safer and more efficient mining in narrow reef conditions.

Keywords: NRE fleet, NRE Support rig, breast mining; utilization, efficiency

1. Introduction

The South African mining sector has, for more than 100 years, been considered a labour intensive industry with a mining method characterised by physically demanding manual drilling methods, and operations completed by blasting and cleaning process (**Dludlu & Meyer, 2021; Pickering, 2004**). Two main reasons driving the need for change in PGE mining are safety and economic factors. Mechanised methods, including advanced drilling, rock bolting, and ore transport systems, are seen as necessary to prolong the viability of platinum mines. The NRE fleet is a unique, innovative, electric robotic solution for underground mining, aiming to increase safety and productivity while reducing capital and operating costs (**Bohanek et al, 2023**). The Narrow Reef Equipment (NRE) made by DOK-ING conists of three main machines, each designed for a specific part of the mining cycle (drilling, cleaning and bolting) in narrow reef environments (**Bohanek et al, 2025**). The Support Rig is crucial for ensuring the safety of the mining process, but research clearly shows that the roof bolting activity is a significant bottleneck within the mining cycle (**Andrews & Pickering, 2010**). Mechanised bolting not only increases safety by removing operators from direct exposure to unstable hanging walls but also enhances productivity through faster installation of support elements (**Marek et al., 2012**).

The paper presents the results of trial efficiency testing conducted on the NRE Support Rig in two different underground mines located in South Africa.

2. NRE Fleet and NRE Support Rig

The NRE Fleet represents a new class of ultra-low-profile equipment tailored for stope widths below 2.2 m. Its ability to operate in confined reef conditions minimizes ore dilution, improves production efficiency, and reduces costs, while remote-controlled functionality enhances worker safety. Growing demand for critical metals requires mining of increasingly complex deposits. NRE units, operating within 0.9–1.7 m, are fully electric, remote-controlled, and automated, making them the only mechanized option for reefs thinner than 1.7 m or with dips greater than 14°.

DOK-ING's NRE Support Rig is purpose-built for narrow-reef mining, enabling the automated installation of self-drilling resin bolts (SDRs) from a remote, safe distance. With a profile height of just 790 mm, battery power, and fully electric drive, it fits into stopes as narrow as 0.9 m and can function at reef inclinations of up to 22°. ts dual-tool arrangement allows simultaneous drilling and resin injection of two bolts. Compact tracks, divided maintenance compartments, low noise, and zero emissions further enhance its underground suitability. The rig is designed to address the traditional bottleneck of roof bolting in narrow reef operations, providing consistent and reliable ground support. Its remote-controlled functions reduce operator exposure to hazardous conditions, significantly improving mine safety.

The NRE Fleet including NRE Support Rig is shown on Figure 1 and NRE Support Rig technical characteristics are shown in **Table 1**.



Table 1. NRE Support Rig technical characteristics				
	Prime Mover	Toolset		
Dimensions	4150 x 1976 x 745 mm	2185 x 1950 x 793 mm		
Weight	10000 kg	3000 kg		
Power system	Battery Type LiFePO4	Battery Type LiFePO4		
	Battery Pack Nominal Voltage	Battery Pack Nominal Voltage 346 V		
	Electrical grid via trailing cab	Electrical grid via trailing cable 380 – 550 VAC 3ph		
On board fast charger	Charging time 1 h	Charging time 1 h		
	Charging source 380 – 550 V	AC 3ph		
Drilling system	Drifters type - electric			
	Drifters power up to 80kW each.			
	Maximum drill thrust force 40	0kN		
	Drifters per tool 1, 2 tools per	machine		

3. Testing

Underground trials have two key aspects: proving that the equipment performs its intended function and ensuring that the mining method used is sufficiently productive (**Pickering and Moxham**). The four NRE support rigs (SR0003, SR004, SR008 and SR009) were tested in two underground mine, where their performance, availability, and utilization were systematically assessed. The testing of the four NRE support rigs was carried out at two sites: Tumela 15 shaft, which forms part of the Amandelbult mining complex, and Bokoni Platinum Mine. Amandelbult, positioned on the Western Limb of the Bushveld Igneous Complex and managed by Anglo American Platinum, continues steady production through its Tumela and Dishaba shafts. Bokoni, by contrast, is located on the Eastern Limb in Limpopo and, after being placed on care and maintenance in 2017, is now undergoing a revival under the ownership of African Rainbow Minerals (ARM). In both Amandelbult and Bokoni, the machines were tested within a breast mining layout. This layout follows a panel structure where stoping advances face by face along the reef, supported by systematic drilling and blasting. Access is provided through strike gullies, and support installation closely follows the face to maintain stability. Breast mining layout is shown on Figure 2.

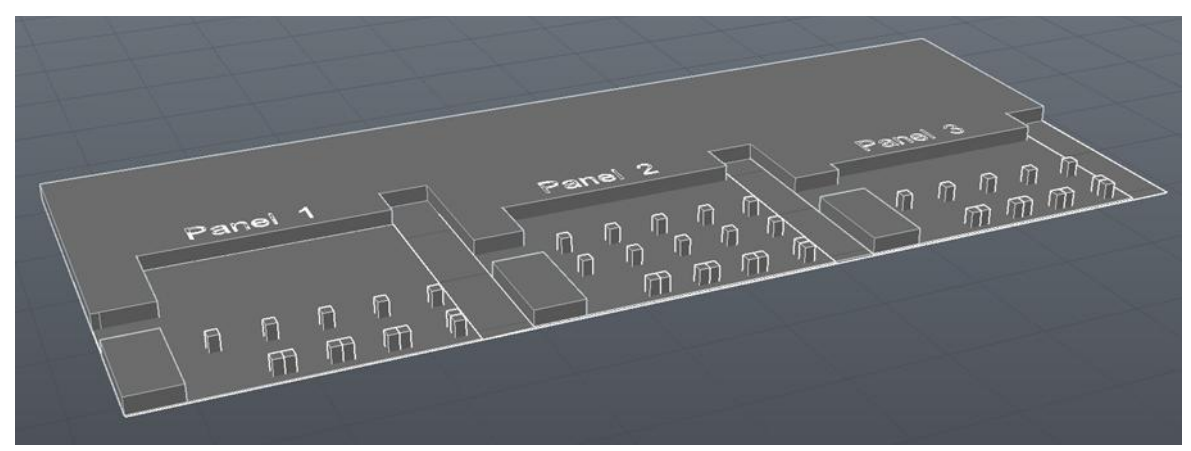


Figure 2. Brest mining layout

The panels in Bokoni more or less correspond to the panels in which NRE worked in the Tumela mine. The length of the faces of the panel were between 25 and 30 meters. In Tumela and Bokoni, 2 m long SDR anchors were installed in a 1 m × 1 m grid arrangement. Each individual anchor consists of consists of 5 segments of 40 cm, The first segment contains a cutting insert followed by 3 middle segments, and the last segment contains a mixing insert which is responsible for evenly mixing the two components of the resin. Unfortunate circumstance for testing the machines in Bokoni mine was the thin reef horison and targeted profile height of 100cm, while in Tumela the profile was 140cm on average. Lower profile mean that it is difficult to eliminate breakdowns that occure in the panel, lower profile makes it difficult to maneuver the machine while driving, and finally it increases the time required to fill the machine with bolts and resin. In general, it can be stated that the working conditions in the Bokoni mine were more challenging. A cross section of the panel with installed anchors is presented in Figure 3, while Figure 4 shows the NRE Support Rig in operation during bolting.

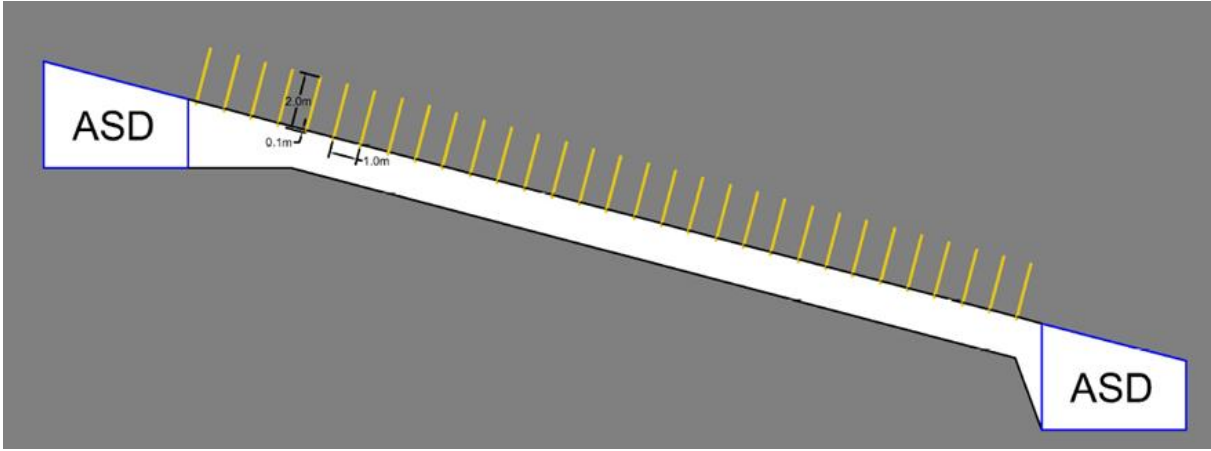


Figure 3. Cross section of panel



Figure 4. NRE support rig in operation

At Tumela 15 shaft, trials are conducted with the first-generation NRE machines, whereas at Bokoni mine the second, upgraded version was tested, showcasing design refinements aimed at improving reliability and efficiency.

Beyond technical upgrades, the difference in operator experience was notable. At Tumela, workers were new to the NRE machines and had to build their experience from the ground up. At Bokoni, most operators already had a background with NRE or ULP machines, and an improved training program was provided to help them develop the required skills more quickly.

4. Results

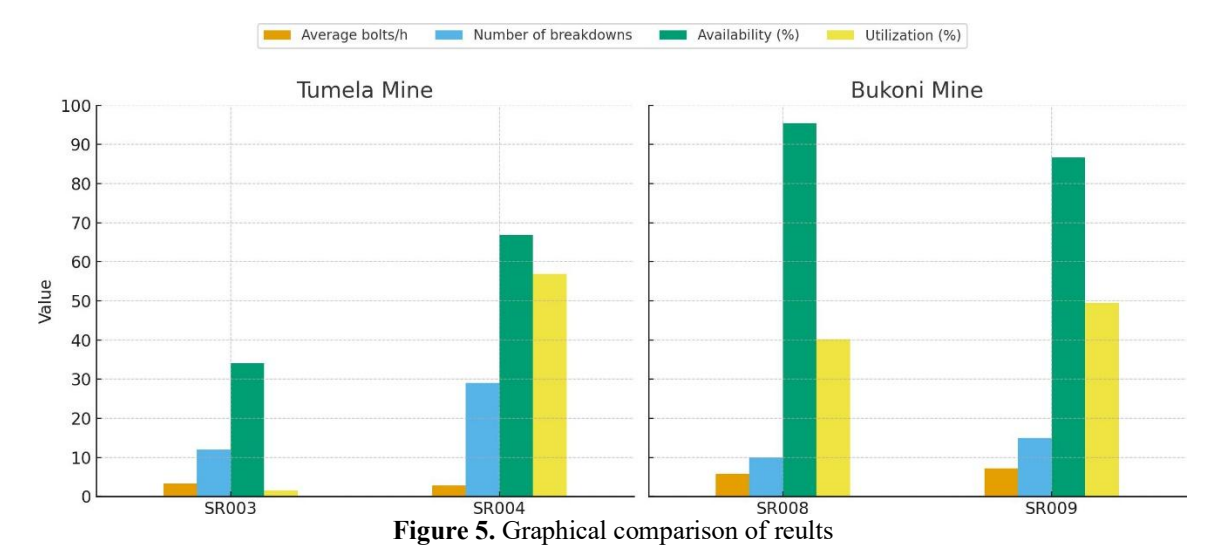
During the testing, several key performance indicators were recorded to evaluate the support rigs. These included the total number of installed bolts, the face time in hours, the average number of bolts installed per hour, the number of breakdowns, the total breakdown duration, and the overall recorded time. From these values, additional reliability measures were derived: Mean Time Between Failures (MTBF), representing the average operating time between two breakdowns, and Mean Time To Repair (MTTR), indicating the average time required to restore a machine to operation. Together with availability and utilization, these metrics provided a comprehensive view of machine performance both mines. Results of testing for Tunmela and Bukoni miner are shown in Table 2 and Table 3 and a graphical comparison of the results is shown in **Figure 5**.

Table 2. Results of testing in Tumela mine

	SR003	SR004		
Installed bolts	279	500		
Face time (h)	88:38:00	179:52:00		
Average bolts/h	3.35	2.78		
Number of breakdowns	12	29		
Total breakdown duration (h)	3636:00:00	1312:00:00		
Total time (h)	5512:00:00	3960:00:00		
Utilization time (h)	83:21:00	2251:14:00		
MTBF (h)	6:56:00	77:37:43		
MTTR (h)	303:00:00	45:14:28		
Availability	34.03%	66.87%		
Utilization	1.51%	56.85%		

Table 3. Results of testing in Bukoni mine

	Table 5. Results of testing in Dukoni inine		
	SR008	SR009	
Installed bolts	498	856	
Face time (h)	85:30:00	119:25:00	
Average bolts/h	5.82	7.17	
Number of breakdowns	10	15	
Total breakdown duration (h)	11:30:00	39:45:00	
Total time (h)	245:30:00	296:45:00	
Utilization time (h)	98:45:00	146:50:00	
MTBF (h)	9:52:30	17:08	
MTTR (h)	1:09:00	2:39:00	
Availability	95.39%	86.60%	
Utilization	40.22%	49.48%	



In Tumela, the first-generation rigs (SR003 and SR004) showed modest drilling productivity, with average installation rates of 3.35 and 2.78 bolts/h. High numbers of breakdowns, long repair times, and frequent component failures resulted in very low availability for SR003 (34.03%) and only moderate availability for SR004 (66.87%). Utilization was also poor, especially in SR003, where only 1.51% of the total recorded time was effectively used for production. From the other, in Bokoni, the second-generation rigs (SR008 and SR009) delivered much better results. Productivity nearly doubled, with average drilling rates of 5.82 and 7.17 bolts/h, and breakdowns were fewer and repaired

more quickly. Availability rose sharply to 95.39% for SR008 and 86.60% for SR009, while utilization improved to 40.22% and 49.48%, respectively.

According to feedback from the sites, improved performance depends not only on technical upgrades of the machines but also on the experience of the personnel operating them, which is consistent with previous research. Operator training and the acceptance of mechanized bolting are equally critical factors, as insufficient skills may negatively affect both productivity and safety outcomes (Hattingh et al., 2010). Furthermore, maintenance practices and supply chain support play a decisive role, since frequent breakdowns, prolonged repair times, or shortages of spare parts can substantially reduce the availability and utilisation of bolters (Fourie, 2015). In addition to the experience of the operator and the maintenance habits of the technical staff, the mine infrastructure, such as water supply, access to compressed air and a workshop, also plays a major role in the support rig performance. The lack of any of the above-mentioned makes the machine maintenance difficult and therefore the results will not be as expected.

5. Conclusions

The trials of the NRE Support Rig at Tumela and Bokoni mines showed both the promise and the difficulties of bringing mechanised bolting into narrow reef conditions. At Bokoni, the newer generation of rigs worked far better than the older units at Tumela, with higher productivity, better availability, and steadier utilisation. These gains came not only from technical upgrades, but also from stronger maintenance routines and the fact that operators already had more experience with the machines.

At the same time, the results made it clear that better technology alone is not enough. How well people are trained, how readily they adapt to mechanised bolting, and how reliably spare parts and service are available all play just as big a role. Without that support, even the most advanced rig is at risk of frequent stoppages and long repair times, which quickly eat away at efficiency.

The results of the trial testing will be used to guide improvements and support the development of the third generation of machines, designed to deliver higher performance and more reliable maintenance. Future measurements will also track infrastructure conditions and environmental factors to assess their effect on machine and operator performance.

6. References

- Andrews, M., & Pickering, R. G. B. (2010). A systematic approach to the optimization of extra low profile (XLP) mine productivity for narrow reef platinum mines. 267–276.
- Bohanek, V., Petro, L., & Borojević Šoštarić, S. (2023). Narrow Reef Mining (NRM)—Innovative Mining Technology for Narrow, Sub-Horizontal PGE Ore Bodies. Materials Proceedings, 15(1), 9. https://doi.org/10.3390/materproc2023015009
- Bohanek, V., Pleše, P., Šoštarić, S. B., Purkić, R., & Vokić, E. (2025). Influence of Mining Layout on Efficiency of NRE Drill Rig. Mining, 5(1), 6. https://doi.org/10.3390/mining5010006
- Dludlu, N., & Meyer, L. (2021). Sustaining the South African mining industry through technology-driven productivity improvements. Journal of the Southern African Institute of Mining and Metallurgy, 121(7), 373-380.
- Fourie, H. (2015). Improvement in the overall efficiency of mining equipment: a case study. Journal of the Southern African Institute of Mining and Metallurgy, 116, 445–482.
- Hattingh, T.S., Sheer, T.J., & Du Plessis, A.G. (2010). Human factors in mine mechanization. 4th International Platinum Conference, SAIMM.
- Marek, A., Thorley, S., Dawson, L., & Pickering, R. (2012). Mechanized bolting on-board drilling automation and a change in the support regime in low-profile mechanized mining. Platinum 2012, SAIMM.
- Pickering, R. G. B., & Moxham, K. (2007). The development and implementation of the Lonmin mechanized breast mining. Journal of the Southern African Institute of Mining and Metallurgy, 107(1), 5–14.

Acknowledgment

Many thanks to the Bokoni team for their contribution in collecting data on the performance of the NRE fleet.

Funding

The research is funded by EIT RawMaterials.as part of project 23024—NRE-ElectRA (Electric, Remote Control, Automatic Narrow Reef Mining Equipment).

Author's contribution

Paulo Pleše (mag.ing.min.): testing, formal analysis and original draft and writing. Juraj Banić (univ. bacc. ing. min): testing, and original draft and writing. Vječislav Bohanek (associate professor): conceptualization and methodology. Sibila Borojević Šoštarić (professor): conceptualization and review & editing.

All authors have read and agreed to the published version of the paper.



Advancements in Oil Well Perforation Technologies Aimed at Reducing Casing and Annular Damage

DIM-ESEE Conference



Oleksandr Pashchenko¹* □⊠, Andrii Sudakov² □⊠, Valerii Rastsvietaiev² □⊠

¹ Dnipro University of Technology, Dmytra Yavornytskoho Ave., 19, Dnipro, 49005, Ukraine

Abstract

Perforation is a vital process in oil and gas well completion, creating channels through casing, cement, and formation to enable hydrocarbon flow. The goal of this research is to develop and evaluate a hybrid perforation technology that minimizes casing and annular damage while enhancing formation permeability. Conventional shaped-charge perforation often damages the casing and cement sheath, causing cracks, deformations, and compromised integrity, which reduce well longevity and increase maintenance costs. This study presents a hybrid perforation technology integrating shapedcharge perforation, mechanical drilling, and adaptive energy control to minimize structural damage while enhancing formation permeability. Using numerical fluid-structure interaction modeling and laboratory experiments on scaled casing and cement samples, the technology's performance was evaluated. Simulations show a 24.4% reduction in peak casing stresses compared to traditional methods, keeping stresses below the material's yield limit and reducing radial deformation by 38.1%. Experimental results indicate a 20.2% smaller perforation hole diameter, a 44.8% decrease in crack depth, and a 57.1% improvement in cement sheath integrity, evidenced by reduced permeability. The hybrid approach also reduces annular debris by 30%, mitigating flow obstructions, and increases formation permeability by 18%, boosting hydrocarbon recovery. The adaptive energy control system adjusts perforation parameters in real-time based on formation and casing properties, ensuring stability and minimizing damage. Compared to existing methods, such as perforation by drilling and optimized shaped-charge systems, this technology offers superior damage mitigation and productivity. Laboratory conditions limit result generalizability, necessitating field trials to validate performance across diverse geological settings. This hybrid technology promises reduced repair costs and enhanced production efficiency, particularly in high-density reservoirs.

Keywords: hybrid perforation technology, casing damage, annular space, formation permeability, adaptive energy control

1. Introduction

Perforation of oil and gas wells is a pivotal process in well completion, facilitating hydrocarbon flow from the reservoir to the wellbore by creating channels through the casing, cement sheath, and formation. Conventional perforation methods, particularly shaped-charge perforation, are widely used for their ability to form deep tunnels but often cause significant collateral damage, including cracks, deformations, and material loss in the casing, as well as compromised cement sheath integrity, leading to fluid leaks and debris accumulation in the annular space (Maksymovych et al, 2021; Fituri et al, 2024; Zholbassarova et al., 2024). These issues reduce well longevity, increase maintenance costs', and impair production efficiency, especially in complex geological settings like high-pressure, high-temperature wells or high-density formations. Alternative techniques, such as mechanical drilling, laser perforation, and hydro-abrasive perforation, offer distinct advantages, greater precision, cleaner channels, or reduced thermal damage, but face limitations in penetration depth, energy requirements, or effectiveness in hard formations (Khomenko et al., 2023; Pashchenko et al., 2024; Lukin & Kondrat, 2024). Traditional perforation methods cause microfractures, debris obstruction, and compromised zonal isolation. These issues reduce well longevity and increase maintenance costs. They are particularly problematic in complex geological settings, such as high-pressure, high-temperature wells or high-density formations. (Robey et al., 2019; Ihnatov et al., 2023).

Efforts to mitigate perforation-induced damage have included directed perforation to align tunnels with reservoir stress fields, optimization of charge parameters to control penetration, and the use of advanced casing materials like high-strength alloys (**Zhang et al., 2021**). However, these approaches often address specific issues without comprehensively tackling the combined effects on casing, cement, and annular space. For instance, directed perforation enhances flow but does not reduce debris, and advanced materials increase costs, limiting adoption (**Sala et al., 2023**). Previous studies (**Robey et al., 2019**). reported that traditional shaped-charge perforation causes significant damage, with hole diameters up to 32.1 mm, consistent with this study's findings. However, their combined mechanical and explosive method achieved only an 11.37% reduction in damage, less effective than the hybrid approach proposed here. Recent research also

highlights the impact of annular debris on well productivity, which the hybrid method addresses through a 30% reduction in debris volume (Pivnyak et al., 2020; Nemati et al., 2025). Unlike studies focused on optimizing charge parameters without integrating mechanical methods, the hybrid approach offers a more comprehensive solution by addressing both causing damage and formation connectivity (Lozynskyi, 2023). Moreover, few studies integrate real-time adaptive control or predictive modeling to dynamically adjust perforation parameters, leaving a gap in achieving holistic damage mitigation. Fluid-structure interaction (FSI) modeling, which analyzes the interplay of fluid jets, shockwaves, and structural responses, offers a promising tool to optimize perforation processes but remains underutilized (Bahrami et al. 2009; Bondarenko et al., 2024). These findings underscore the need for integrated solutions like the proposed hybrid technology.

This research aims to develop and evaluate a novel hybrid perforation technology that integrates shaped-charge perforation with mechanical drilling techniques to minimize damage to the casing and annular space. By combining the high-energy penetration of shaped charges with the precision of mechanical methods, the proposed system creates perforation channels with reduced collateral harm. A key innovation is adaptive energy control, which adjusts perforation parameters in real time based on formation and casing properties, ensuring optimal penetration while mitigating stress on well components. The approach incorporates advanced FSI modeling to predict and optimize stresses and deformations during perforation, enhancing precision and formation permeability for improved hydrocarbon recovery. Unlike traditional methods that rely on fixed high-energy charges, this technology dynamically tailors energy output to match the mechanical properties of the casing, cement, and formation, addressing the limitations of existing techniques. By integrating adaptive control and predictive modeling, this hybrid system represents a significant advancement in perforation technology, promising safer, more efficient well completion practices in challenging geological environments.

2. Methods

The proposed hybrid perforation system integrates shaped-charge perforation with mechanical drilling to combine the deep penetration capabilities of explosive jets with the precision of mechanical methods. Shaped charges generate high-velocity metallic jets to initiate perforation tunnels, while a mechanical drilling component, equipped with a high-strength bit, refines the tunnel geometry and removes debris. The system operates under adaptive energy control, which dynamically adjusts the explosive energy and drilling parameters based on real-time data about the formation and casing properties. The energy of the shaped charge, E_c , is calculated as:

$$E_c = \frac{1}{2}m_j v_j^2 \tag{1}$$

where is:

 m_i – mass of the metallic jet (kg),

 v_i – velocity (m/s).

The adaptive control system modulates E_c to ensure that the jet velocity remains below the threshold that induces excessive casing damage, typically determined by the casing's yield strength, σ_y (Xiao et al., 2024). For mechanical drilling, the torque, T, and axial force, F_a , are optimized based on the formation's unconfined compressive strength, σ_c :

$$T = k_r \sigma_c d_b^2 \tag{2}$$

$$F_a = k_a \sigma_c A_b \tag{3}$$

where:

 k_r , k_a – empirical coefficients,

 d_b – bit diameter (m),

 A_b – bit contact area (m²).

 σ_c – formation unconfined compressive strength (Pa)

The control system uses formation data, such as porosity ϕ and Young's modulus E, obtained from well logs, to adjust these parameters, ensuring minimal stress on the casing and cement sheath.

Numerical modeling is employed to simulate the perforation process and assess its impact on the casing and annular space. The study utilizes fluid-structure interaction modeling to capture the dynamic interplay between the high-velocity jet, shockwaves, and the structural response of the casing and cement. The governing equations for FSI include the Navier-Stokes equations for the fluid domain:

$$\rho_f \left(\frac{\partial \mathbf{v}}{\partial t} + \mathbf{v} \cdot \nabla \mathbf{v} \right) = -\nabla p + \mu \nabla^2 \mathbf{v} + \mathbf{f} \tag{4}$$

where:

 ρ_f – fluid density (kg/m³),

v - velocity (m/s),

p – pressure (Pa),

 μ – viscosity (Pa·s), and f – represents external forces (N), coupled with the structural dynamics equation.

The coupling occurs at the fluid-structure interface, where continuity of velocity and stress is enforced. Simulations were conducted using ANSYS (version 2024 R1), a computational fluid dynamics (CFD) software that supports fluid-structure interaction (FSI) modeling through coupled solvers for fluid flow and structural mechanics. This software was chosen for its robust multiphysics capabilities, including the ability to handle high-velocity jets and shockwaves via the Navier-Stokes equations and finite element analysis for stress distribution. It enables accurate prediction of dynamic interactions between the perforation jet and well components, supporting optimization of parameters like stress and deformation in the casing and cement. The model inputs include casing material properties (e.g., yield strength $\sigma_y = 550 \,\mathrm{MPa}$), cement compressive strength ($\sigma_{cc} = 30 \,\mathrm{MPa}$), and formation characteristics ($E = 20 \,\mathrm{GPa}$, $\phi = 0.15$). The output parameters include stress distribution, deformation, and crack propagation in the casing and cement.

The experimental setup involves laboratory tests on scaled model samples to validate the numerical results. Cylindrical casing samples, made of API-grade steel (e.g., P110, with $\sigma_y = 758$ MPa), are encased in a cement sheath and placed within a simulated formation block. The hybrid perforation system is deployed in a controlled environment, with shaped charges delivering energies ranging from 10 to 50 kJ and mechanical drilling at rotational speeds of 100–300 RPM (10.5–31.4 rad/s). High-speed cameras and acoustic sensors monitor the perforation process, capturing jet penetration and debris generation. Post-perforation, the samples are analyzed using non-destructive testing (e.g., ultrasonic imaging) and destructive methods (e.g., sectioning) to measure damage parameters. The experimental setup is designed to replicate downhole conditions, with confining pressures up to 20 MPa and temperatures up to 80°C. The cement sheath, composed of Class G cement with a compressive strength of 30 MPa, was cast around the casing to a thickness of 25 mm to simulate typical well conditions. The simulated formation block was constructed using a sandstone-like material with a porosity of 0.15 and Young's modulus of 20 GPa, designed to replicate the mechanical properties of a medium-hard reservoir rock.

The evaluation parameters focus on quantifying the performance of the hybrid perforation system compared to conventional methods. The degree of casing damage is assessed by measuring the perforation hole diameter, d_h , and crack depth, l_c , using the relationship:

$$l_c = k_c \sqrt{\frac{E_c}{\sigma_y}} \tag{5}$$

where:

 k_c – material-specific constant (m²).

Cement sheath integrity is evaluated through the presence of microcracks, detected via ultrasonic wave attenuation, and fluid leakage tests, where permeability k_c (equivalent to approximately 9.87×10^{-16} m² for 1 mD) is calculated as:

$$k_c = \frac{Q\mu L}{A\Delta P} \tag{6}$$

where:

Q – flow rate (m³/s),

 μ – fluid viscosity (Pa·s),

L – sample length (m),

A - cross-sectional area (m²),

 ΔP - pressure differential (Pa).

Formation permeability, k_f , post-perforation is measured using core samples, applying Darcy's law:

$$k_f = \frac{Q\mu L}{A\Delta P} \tag{7}$$

Finally, debris accumulation in the annular space is quantified by collecting and weighing residual particles, with volumes normalized to the perforation tunnel volume. These parameters collectively provide a comprehensive assessment of the technology's ability to minimize damage while enhancing well productivity.

3. Results

The numerical simulations, conducted using fluid-structure interaction modeling in ANSYS, provide insights into the stress and deformation profiles induced by traditional shaped-charge perforation and the proposed hybrid perforation system. The hybrid system integrates shaped-charge perforation with mechanical drilling, employing adaptive energy control to optimize penetration while reducing collateral damage. The maximum von Mises stress (σ_{vm}) in the casing was calculated as:

$$\sigma_{vm} = \sqrt{\sigma_x^2 + \sigma_y^2 + \sigma_z^2 - \sigma_x \sigma_y - \sigma_y \sigma_z - \sigma_z \sigma_x + 3(\tau_{xy}^2 + \tau_{yz}^2 + \tau_{zx}^2)}$$
(8)

where:

 σ_x , σ_y , σ_z – normal stresses (Pa),

 τ_{xy} , τ_{yz} , τ_{zx} – shear stresses (Pa).

For traditional perforation, the peak stress reached 820 MPa, exceeding the yield strength of the P110 casing ($\sigma_y = 758$ MPa), leading to plastic deformation. In contrast, the hybrid system, with adaptive energy control limiting the charge energy to 30 kJ, reduced the peak stress to 620 MPa, staying within the elastic limit. Deformation, measured as radial displacement (u_r), was reduced from 2.1 mm in traditional perforation to 1.3 mm in the hybrid approach. The adaptive control system adjusted the explosive energy based on real-time formation data, reducing stress concentrations by 24.4%. Table 1 summarizes the stress and deformation results, visualization you can see on Figure 1.

Table 1. Comparison of Stress and Deformation in Casing

Perforation Method	Peak von Mises Stress (MPa)	Radial Deformation (mm)
Traditional	820	2.1
Hybrid	620	1.3

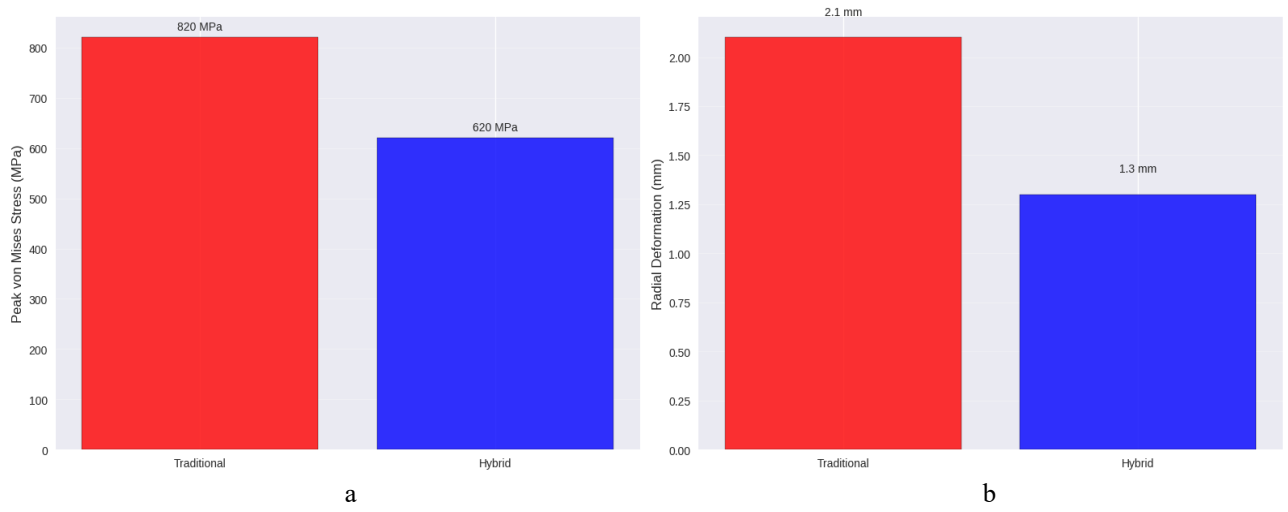


Figure 1. Stress (a) and Deformation (b) Comparison by Perforation Method

Experimental tests were conducted on scaled casing samples (P110 steel, $\sigma_y = 758$ MPa) encased in a cement sheath ($\sigma_{cc} = 30$ MPa). The tests compared damage to the casing and cement sheath under traditional shaped-charge perforation, perforation by drilling, and the hybrid method. Damage to the casing was quantified by the perforation hole diameter (d_h) and crack depth (l_c), measured using ultrasonic imaging and sectioning. Traditional perforation resulted in an average hole diameter of 32.1 mm and crack depth of 5.8 mm, while the hybrid method reduced these to 25.6 mm and 3.2 mm, respectively, representing a 20.2% reduction in hole diameter and 44.8% reduction in crack depth. The cement sheath integrity was assessed through microcrack detection and permeability tests. The hybrid method reduced microcrack density by 35%, with a cement permeability (k_c) of 0.12 mD (1.18 × 10⁻¹⁶ m²) compared to 0.28 mD (2.76 × 10⁻¹⁶ m²) for traditional perforation. Formation permeability (k_f) post-perforation, measured using Darcy's law (8) increased by 18% with the hybrid method (from 15 mD (1.48 × 10⁻¹⁴ m²) to 17.7 mD (1.75 × 10⁻¹⁴ m²)) due to cleaner perforation tunnels. Table 2 and Figure 2 present experimental results, showing damage and permeability metrics for traditional, drilling, and hybrid perforation methods.

Table 2. Experimental Damage and Permeability Results

Table 2. Experimental Banage and I emicaemy results				
Method	Hole Diameter (mm)	Crack Depth (mm)	Cement Permeability	Formation Permeability
Traditional	32.1	5.8	$0.28 \text{ mD} (2.76 \times 10^{-16} \text{ m}^2)$	$15.0 \text{ mD} (1.48 \times 10^{-14} \text{ m}^2)$
Perforation by Drilling	28.5	4.1	$0.20 \text{ mD} (1.97 \times 10^{-16} \text{ m}^2)$	$16.2 \text{ mD} (1.60 \times 10^{-14} \text{ m}^2)$
Hybrid	25.6	3.2	$0.12 \text{ mD} (1.18 \times 10^{-16} \text{ m}^2)$	$17.7 \text{ mD} (1.75 \times 10^{-14} \text{ m}^2)$

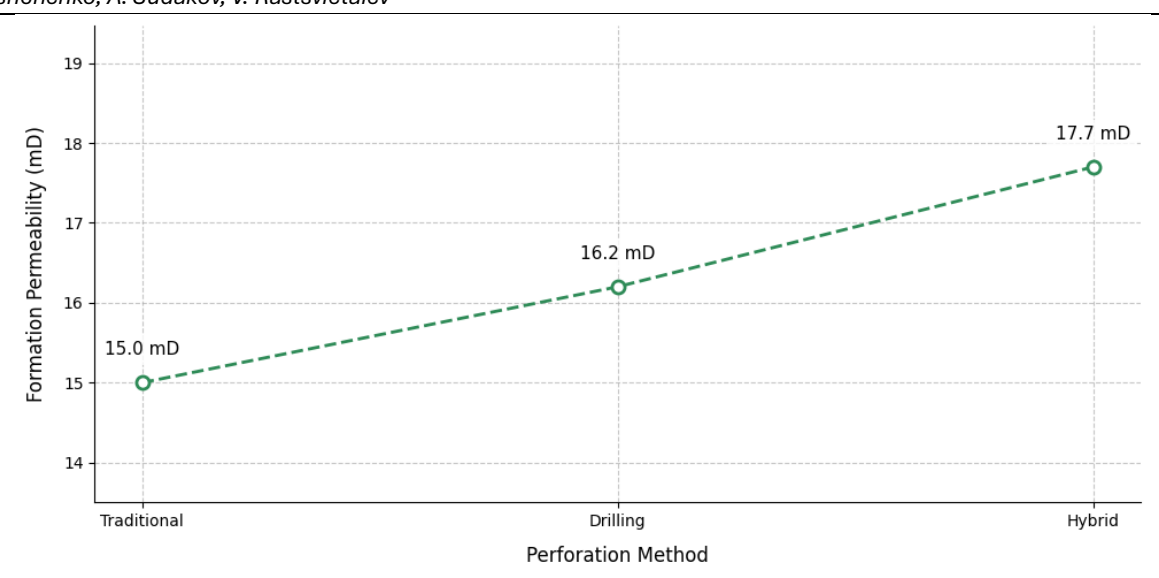


Figure 2. Formation Permeability Post-Perforation

The hybrid technology outperforms traditional shaped-charge perforation and perforation by drilling. It reduces casing hole diameter by 20.2% and crack depth by 44.8% compared to traditional methods, and by 10.2% and 22.0% compared to drilling. Cement sheath permeability decreased by 57.1% and 40% compared to traditional and drilling methods, respectively. Additionally, the hybrid method increased formation permeability by 18% and reduced annular debris by 30%, enhancing well productivity. These results demonstrate that hybrid technology, with adaptive energy control, effectively balances deep penetration with minimal structural damage, offering a significant improvement over existing methods.

4. Discussion

The results of this study demonstrate the efficacy of the proposed hybrid perforation technology, which integrates shaped-charge perforation with mechanical drilling and adaptive energy control, in minimizing damage to the casing and annular space while enhancing formation permeability. This control mechanism stabilizes the perforation process by maintaining stress below the casing's yield limit ($\sigma_{vm} = 620 \,\mathrm{MPa}$ vs. 820 MPa for traditional methods), reducing the likelihood of plastic deformation and crack propagation. The mechanical drilling component further contributes by refining tunnel geometry and removing debris, which mitigates annular space blockages.

Despite the promising results, this study has certain limitations due to its laboratory setting. The experiments were carried out on scaled casing samples under controlled conditions of up to 20 MPa pressure and 80 °C temperature. Such models, although representative, cannot fully capture the complex stresses and interactions present in actual wells with variable casing thickness and formation properties. The FSI modeling also relied on simplified boundary conditions, assuming uniform formation properties ($\phi = 0.15$, E = 20 GPa). These assumptions may overlook geological heterogeneities and reduce the accuracy of predictions. To overcome these limitations, field trials are necessary to validate hybrid technology under real downhole conditions and assess its impact on integrity and productivity.

The practical significance of hybrid perforation technology is substantial, particularly for high-density reservoirs where traditional methods often cause excessive damage. By reducing casing and cement damage, the technology can decrease the frequency and cost of well repairs, which are significant expenses in field operations. For instance, minimizing crack depth by 44.8% and cement permeability by 57.1% can extend well lifespan and reduce the risk of fluid migration, which is critical in environmentally sensitive areas. The 18% increase in formation permeability also enhances production efficiency, making the technology suitable for tight reservoirs with low natural permeability ($k_f < 0.20 \, mD$ (1.97 × $10^{-16} \, m^2$)). Furthermore, the adaptive energy control system can be integrated into existing perforation tools, offering a cost-effective upgrade for operators. The reduction in annular debris by 30% further simplifies post-perforation cleanout operations, potentially lowering operational downtime. These benefits position hybrid technology as a viable solution for improving well completion practices in challenging geological settings.

5. Conclusions

Perforation is critical for oil and gas well completion but often causes casing and annular damage, reducing well longevity and productivity. This study developed a hybrid perforation technology integrating shaped-charge perforation, mechanical drilling, and adaptive energy control to address these challenges. The methodology combined fluid-structure interaction modeling and laboratory experiments on scaled casing and cement samples to evaluate performance.

The key findings demonstrate that hybrid technology significantly reduces damage compared to traditional methods. It achieves a 20.2% reduction in perforation hole diameter, a 44.8% reduction in crack depth, and a 57.1% decrease in cement sheath permeability, improving zonal isolation. Technology also reduces annular debris by 30%, mitigating flow obstructions, and increases formation permeability by 18% (from 15 mD to 17.7 mD), enhancing hydrocarbon recovery. The adaptive energy control system ensures stresses remain below the casing's yield limit (620 MPa vs. 820 MPa for traditional methods), minimizing plastic deformation.

Practically, this technology reduces repair costs and enhances production efficiency, particularly in high-density reservoirs. It can be integrated into existing perforation tools, offering a cost-effective solution. However, the laboratory setting limits result generalizability, as scaled models may not fully capture downhole complexities. Future work should focus on field trials to validate performance across diverse geological conditions and develop automated control systems for broader industry adoption.

6. References

- Bahrami, H., Siavoshi, J., Veisi, M. S., & Bahraie, R. (2009). Numerical simulation of wellbore dynamics during underbalanced perforation. *Latin American and Caribbean Petroleum Engineering Conference*. https://doi.org/10.2118/120162-ms
- Biletskiy, M. T., Ratov, B. T., Khomenko, V. L., Borash, A. R., & Muratova, S. K. (2024). The choice of optimal methods for the development of water wells in the conditions of the Tonirekshin field (Kazakhstan). *Naukovyi Visnyk Natsionalnoho Hirnychoho Universytetu*, 1, 13–19. https://doi.org/10.33271/nvngu/2024-1/013
- Bondarenko, V., Kovalevska, I., Krasnyk, V., Chernyak, V., Haidai, O., Sachko, R., & Vivcharenko, I. (2024). Methodical principles of experimental-analytical research into the influence of pre-drilled wells on the intensity of gas-dynamic phenomena manifestations. *Mining of Mineral Deposits*, 18(1), 67-81. https://doi.org/10.33271/mining18.01.067
- Fituri, M. A., Munoz, J., Al Harbi, A., & Abouganem, A. (2024). Improving well productivity through better perforation design. *Proceedings of the International Petroleum Technology Conference (IPTC 2024)*. https://doi.org/10.2523/IPTC-24199-MS
- Nemati, N., Ahangari, K., Goshtasbi, K., Shirinabadi, R., & Azadpour, M. (2025). Investigating the effect of wellbore perforation on sand production using hybrid numerical modeling in an Iranian oil field. *Scientific Reports*, 15(1). https://doi.org/10.1038/s41598-025-04411-8
- Ihnatov, A. O., Haddad, J., Stavychnyi, Y. M., & Plytus, M. M. (2022). Development and implementation of innovative approaches to fixing wells in difficult conditions. *Journal of the Institution of Engineers (India) Series D*, 104(1), 119–130. https://doi.org/10.1007/s40033-022-00402-5
- Khomenko, V. L., Ratov, B. T., Pashchenko, O. A., Davydenko, O. M., & Borash, B. R. (2023). Justification of drilling parameters of a typical well in the conditions of the Samskoye field. *IOP Conference Series Earth and Environmental Science*, 1254(1), 012052. https://doi.org/10.1088/1755-1315/1254/1/012052
- Lozynskyi, V. (2023). Critical review of methods for intensifying the gas generation process in the reaction channel during underground coal gasification (UCG). *Mining of Mineral Deposits*, 17(3), 67-85. https://doi.org/10.33271/mining17.03.067
- Lukin, O., & Kondrat, O. (2024). Utilizing well-reservoir pseudo-connections for multi-stage hydraulic fracturing modeling in tight gas saturated formations. *Mining of Mineral Deposits*, 18(2), 113-121. https://doi.org/10.33271/mining18.02.113
- Xiao, Q., Huang, Z., Zu, X., & Jia, X. (2015). Influence of drift velocity and distance between jet particles on the penetration depth of shaped charges. *Propellants Explosives Pyrotechnics*, 41(1), 76–83. https://doi.org/10.1002/prep.201500051
- Maksymovych, O., Solyar, T., Sudakov, A., Nazar, I., & Polishchuk, M. (2021). Determination of stress concentration near the holes under dynamic loadings. *Naukovyi Visnyk Natsionalnoho Hirnychoho Universytetu*, (3), 19–24. https://doi.org/10.33271/nvngu/2021-3/019
- Pashchenko, O. A., Khomenko, V. L., Ratov, B. T., Koroviaka, Y. A., & Rastsvietaiev, V. O. (2024). Comprehensive approach to calculating operational parameters in hydraulic fracturing. *IOP Conference Series Earth and Environmental Science*, 1415(1), 012080. https://doi.org/10.1088/1755-1315/1415/1/012080
- Pivnyak, G., Falshtynskyi, V., Dychkovskyi, R., Saik, P., Lozynskyi, V., Cabana, E., & Koshka, O. (2020). Conditions of Suitability of Coal Seams for Underground Coal Gasification. *Key Engineering Materials*, 844, 38–48. https://doi.org/10.4028/www.scientific.net/kem.844.38
- Robey, R., Suire, D., & Grove, B. (2019). Developing and Fielding Perforating Systems: A Comparison in High-Pressure Wells. *Offshore Technology Conference*. https://doi.org/10.4043/29582-ms
- Sala, D., Pavlov, K., Pavlova, O., Dychkovskyi R., Ruskykh, V., & Pysanko, S. (2023). Determining the Level of Efficiency of Gas Distribution Enterprises in the Western Region of Ukraine. *Inżynieria M*ineralna, 2(2 (52)), 109–122. https://doi.org/10.29227/im-2023-02-64
- Zhang, H., Wang, H., Yu, Q., Zheng, Y., Lu, G., & Ge, C. (2021). Perforation of Double-Spaced Aluminum Plates by Reactive Projectiles with Different Densities. *Materials*, 14(5), 1229. https://doi.org/10.3390/ma14051229

Zholbassarova, A. T., Bayamirova, R. Y., Ratov, Gusmanova, A. G., & Koroviaka, Ye. A. (2024). Development of technology for intensification of oil production using emulsion based on natural gasoline and solutions of nitrite compounds. SOCAR Proceedings, 2, 48–55. https://doi.org/10.5510/OGP20240200965

Author's contribution

Oleksandr Pashchenko (associated professor): conceptualization, methodology, writing and visualization. Andrii Sudakov (professor): project administration and supervision. Valerii Rastsvietaiev (associated professor): software and investigation.

All authors have read and agreed to the published version of the manuscript.



Enhancing Rock Destruction through Viscoelastic Properties of Drilling Fluids

DIM-ESEE Conference

Volodymyr Khomenko^{1*} □⊠, Yevhenii Koroviaka¹ □⊠, Oleksandr Pashchenko¹ □⊠, Andrii Ihnatov¹ □⊠



¹ Dnipro University of Technology, Dmytra Yavornytskoho Ave., 19, Dnipro, 49005, Ukraine

Abstract

This study examines the viscoelastic properties of drilling fluids and their impact on rock fragmentation during oil and gas well drilling. Focusing on fluid-rock interaction, we investigated how viscoelastic parameters – storage modulus (G'), loss modulus (G''), and relaxation time (τ) – affect the rate of penetration (ROP) and torque in sandstone, limestone, and shale. Three water-based fluids (Fluid A: G'=10 Pa, $\tau=0.1$ s; Fluid B: G'=50 Pa, $\tau=1$ s; Fluid C: G'=100 Pa, $\tau=10$ s) were tested on rock cores under controlled conditions (WOB=5000 N, 60 RPM, flow rate=10 L/min). Rheometer measurements quantified viscoelasticity, while a custom drilling rig recorded ROP and torque. Finite element simulations, using a generalized Maxwell model, analyzed stress distribution and crack propagation. Results showed that higher viscoelasticity (Fluid C) increased ROP by up to 63% in sandstone (8.5 mm/min vs. 5.2 mm/min for Fluid A) and reduced torque by 19% (10.1 N·m vs. 12.5 N·m). Strong correlations (r>0.95, p<0.01) linked storage modulus to ROP, with effects most pronounced in sandstone (UCS=50 MPa) and least in shale (UCS=100 MPa). Simulations indicated 20% higher shear stress in sandstone with viscoelastic fluids, enhancing crack initiation. These findings underscore the elastic component's role in stress transfer, challenging viscosity-centric models. Tailored fluid formulations could optimize drilling across lithologies. Limitations include ambient testing conditions, suggesting future research into high-pressure, high-temperature settings and field applications. This work provides a framework for designing advanced drilling fluids to improve efficiency and sustainability.

Keywords: "viscoelastic properties", "drilling fluids", "rock destruction", "rate of penetration", "storage modulus"

1. Introduction

The efficiency of drilling operations in the oil and gas industry, as well as in subsurface exploration, depends on optimizing interconnected processes, with drilling fluids (or drilling muds) playing a critical role. These fluids perform essential functions, including cooling and lubricating the drill bit, transporting cuttings to the surface, stabilizing the borehole, and controlling formation pressures (Mnzool et al., 2024; Ratov et al., 2021; Stavychnyi et al. 2024). Beyond these well-established roles, the viscoelastic properties of drilling fluids, characterized by their ability to exhibit both viscous and elastic behaviors under stress, are increasingly recognized for their influence on the mechanical destruction of rock formations during drilling (Pashchenko et al., 2024a; Ihnatov et al., 2023, Biletskiy et al., 2019). These properties affect stress distribution and energy transfer at the rock-tool interface, potentially amplifying rock fracturing, particularly in challenging geological environments like hard or heterogeneous formations (Muratova et al., 2025; Maksymovych et al., 2021). In mining practices, these viscoelastic enhancements can directly improve borehole drilling for mineral exploration, blasting hole preparation, or tunneling in sedimentary rocks such as sandstone and shale, leading to higher penetration rates and reduced energy consumption. For instance, applying fluids with optimized storage modulus and relaxation time could accelerate rock destruction in open-pit or underground mining operations, minimizing downtime and operational costs while adapting to varying lithologies. Despite their importance, the specific contribution of viscoelastic properties to rock destruction remains underexplored, with limited studies addressing the underlying mechanisms or practical implications. Understanding and optimizing these properties can enhance the rate of penetration (ROP), reduce operational costs, and minimize environmental impacts, thereby improving overall well construction efficiency.

The study of drilling fluids has long been central to petroleum engineering and geotechnical research, with extensive literature on their rheological properties, such as viscosity, yield stress, and shear-thinning behavior, which govern fluid flow under shear and stress. Foundational work by (Guo et al., 2021) established models linking viscosity and flow behavior to cuttings transport and wellbore pressure losses, while later studies, like those by (Ronaes et al., 2012) emphasized shear-thinning properties for optimizing fluid performance across varying flow regimes. More recent research, including (Chudyk et al., 2023 and Yang et al., 2023, Symanovych et al., 2024), demonstrated how tailoring rheological profiles to specific formations can enhance ROP, cuttings transport, and borehole stability. However, while rheology has been thoroughly investigated, viscoelasticity, particularly its role in rock destruction, has received less attention. Studies by (Ettehadi, et al. 2022; Pashchenko et al., 2024b; Fedoreiko et al. 2013) provided initial insights,

suggesting that viscoelastic fluids can enhance rock fracturing under high-pressure, high-temperature conditions by amplifying stress waves. Yet, the mechanisms linking viscoelastic parameters (e.g., relaxation time, storage modulus) to rock failure remain poorly quantified, and systematic investigations across diverse rock lithologies are scarce.

Gaps remain in understanding the role of viscoelasticity in drilling fluids, as most studies emphasize steady-state rheology while neglecting dynamic, time-dependent behavior. This research addresses the issue by combining experiments and numerical modeling to investigate how viscoelastic parameters, viscosity, elasticity, and relaxation, affect rock fragmentation during drilling. Laboratory tests will measure fluid properties and their impact on rock samples under simulated field conditions, while simulations will analyze stress and strain dynamics at the drilling interface. The integrated approach aims to quantify the link between viscoelasticity and rock destruction, providing practical recommendations for fluid design and improving drilling performance.

2. Methods

To investigate the role of viscoelastic properties of drilling fluids in enhancing rock destruction, a combined approach integrating laboratory experiments and numerical modeling was employed. This methodology aims to systematically evaluate how viscoelastic parameters influence the mechanical interaction between drilling fluids and rock formations under controlled and simulated drilling conditions. The experimental component focuses on measuring the viscoelastic properties of drilling fluids and their impact on rock samples, while numerical modeling provides insights into the stress and strain dynamics at the fluid-rock interface. This dual approach ensures a comprehensive understanding of the underlying mechanisms and allows for validation of experimental results against theoretical predictions. Laboratory experiments were conducted using a rheometer to characterize the viscoelastic properties of drilling fluids. The storage modulus G', which represents the elastic component, and the loss modulus G'', which indicates the viscous component, were measured as functions of oscillatory shear frequency. Moduli are defined as:

$$G' = \frac{\sigma_0}{\gamma_0} \cos \delta \tag{1}$$

$$G'' = \frac{\sigma_0}{\gamma_0} \sin \delta \tag{2}$$

where:

 σ_0 – stress amplitude (Pa),

 γ_0 – strain amplitude (dimensionless),

 δ – phase angle between stress and strain (rad).

The relaxation time τ , a key viscoelastic parameter, was calculated using the Maxwell model:

$$\tau = \frac{\eta}{G} \tag{3}$$

where:

 η – viscosity (Pa·s),

G – shear modulus (Pa).

Drilling fluids with varying polymer concentrations were tested to achieve a range of viscoelastic behaviors, from predominantly viscous to highly elastic. These fluids were prepared using water-based formulations with additives such as xanthan gum and polyacrylamide, commonly used in drilling operations.

Rock samples included sandstone, limestone, and shale, selected to represent a range of mechanical properties and lithologies encountered in drilling. Uniaxial compressive strength (UCS) tests were performed to determine the baseline mechanical properties of each rock type, with UCS defined as:

$$\sigma_c = \frac{F}{A} \tag{4}$$

where:

F – maximum force applied (N),

A – cross-sectional area of the sample (m^2).

Laboratory drilling tests were conducted using a custom rig equipped with a rotary drill bit, where rock samples were subjected to drilling under controlled fluid flow conditions. The rate of penetration and torque were measured to assess the efficiency of rock destruction, with ROP calculated as:

$$ROP = \frac{\Delta d}{\Delta t} \tag{5}$$

where:

 Δd – depth drilled (m),

 Δt – time interval (s).

Numerical modeling was performed using finite element analysis (FEA) to simulate the fluid-rock interaction during drilling. The viscoelastic behavior of the drilling fluid was modeled using a generalized Maxwell model, which describes stress relaxation as a sum of exponential decays:

$$\sigma(t) = \int_{-\infty}^{t} G(t - t')\dot{\gamma}(t')dt'$$
(6)

where:

G(t) – relaxation modulus (Pa),

 $\dot{\gamma}$ – shear rate (s⁻¹).

The rock was modeled as a brittle elastic material with failure criteria based on the Mohr-Coulomb model:

$$\tau_f = c + \sigma_n \tan \phi \tag{7}$$

where:

 τ_f – shear strength (Pa),

c – cohesion (Pa),

 σ_n – normal stress (Pa),

 ϕ – friction angle (rad).

The drilling fluids tested included three formulations with distinct viscoelastic profiles, characterized by relaxation times ranging from 0.1 to 10 seconds and storage moduli from 10 to 100 Pa. Rock samples were cylindrical cores (50 mm diameter, 100 mm length), sourced from outcrops to ensure consistency. All experiments were conducted at ambient temperature and pressure, with plans to extend conditions to high-pressure, high-temperature (HPHT) environments in future studies. This methodology provides a framework for quantifying the influence of viscoelastic properties on rock destruction, bridging experimental observations with theoretical insights.

3. Results

To evaluate the influence of viscoelastic properties of drilling fluids on rock destruction, a series of laboratory experiments and numerical simulations were conducted. The results provide insights into how variations in viscoelastic parameters, such as storage modulus, loss modulus, and relaxation time, affect the rate of penetration and rock fragmentation efficiency across different rock types. The data are presented through tables summarizing key experimental outcomes and graphs illustrating trends and correlations. Statistical analysis was applied to identify patterns and quantify relationships between fluid properties and drilling performance.

Experimental tests involved three water-based drilling fluids with distinct viscoelastic profiles, labeled Fluid A, Fluid B, and Fluid C. Fluid A had a low storage modulus (10 Pa) and short relaxation time (0.1 s), Fluid B exhibited moderate viscoelasticity (50 Pa, 1 s), and Fluid C was highly viscoelastic (100 Pa, 10 s). These fluids were tested on cylindrical core samples of sandstone, limestone, and shale, each with a diameter of 50 mm and length of 100 mm. Drilling was performed using a rotary rig at a constant weight-on-bit (WOB) of 5000 N and rotational speed of 60 RPM, with fluid flow rate maintained at 10 L/min. The ROP was calculated in the equation (5). Torque was also recorded to assess energy requirements for rock destruction (Table 1).

Table 1. Experimental Results for ROP and Torque

Rock Type	Fluid	Storage Modulus (Pa)	Relaxation Time (s)	ROP (mm/min)	Torque (N·m)
Sandstone	A	10	0.1	5.2 ± 0.3	12.5 ± 0.8
Sandstone	В	50	1.0	6.8 ± 0.4	11.2 ± 0.6
Sandstone	С	100	10.0	8.5 ± 0.5	10.1 ± 0.5
Limestone	A	10	0.1	4.1 ± 0.2	14.8 ± 0.9
Limestone	В	50	1.0	5.5 ± 0.3	13.0 ± 0.7
Limestone	С	100	10.0	7.0 ± 0.4	11.5 ± 0.6
Shale	A	10	0.1	3.8 ± 0.2	16.2 ± 1.0
Shale	В	50	1.0	4.9 ± 0.3	14.5 ± 0.8
Shale	С	100	10.0	6.2 ± 0.4	12.8 ± 0.7

The results indicate that ROP increases with higher storage modulus and relaxation time, with Fluid C consistently achieving the highest ROP across all rock types. Sandstone exhibited the highest ROP, followed by limestone and shale, reflecting differences in uniaxial compressive strength (UCS: sandstone 50 MPa, limestone 80 MPa, shale 100 MPa). Torque decreased with increasing viscoelasticity, suggesting that elastic properties reduce frictional energy losses.

Figure 1 shows a positive correlation between storage modulus and ROP, with sandstone displaying the steepest increase, indicating greater sensitivity to viscoelasticity.

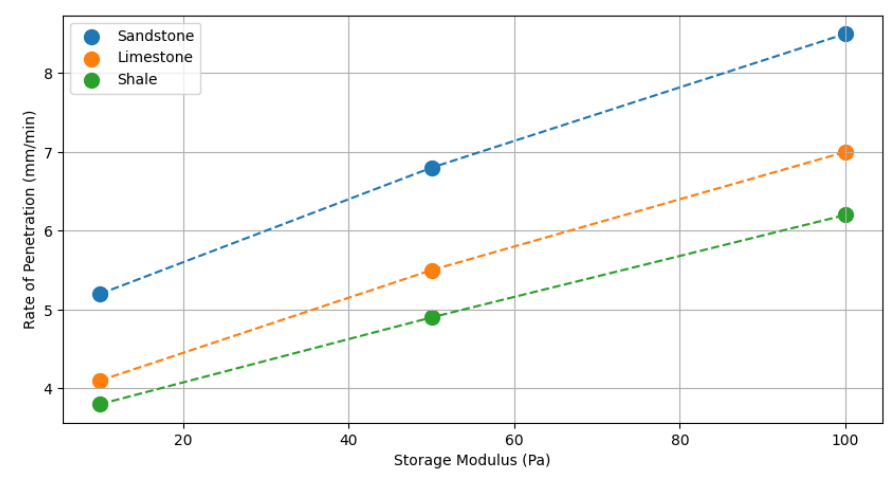


Figure 1. ROP vs Storage Modulus for Different Rock Types

Numerical simulations provided additional insights into stress dynamics. The maximum shear stress at the rock-fluid interface was calculated as:

$$\tau_{\text{max}} = \frac{\sigma_1 - \sigma_3}{2} \tag{8}$$

where:

 σ_1 , σ_3 – major and minor principal stresses (Pa).

Simulations showed that Fluid C induced 20% higher shear stress in sandstone compared to Fluid A, correlating with experimental ROP trends. A bar plot (fig. 2) comparing simulated shear stress across fluids for sandstone is showed below.

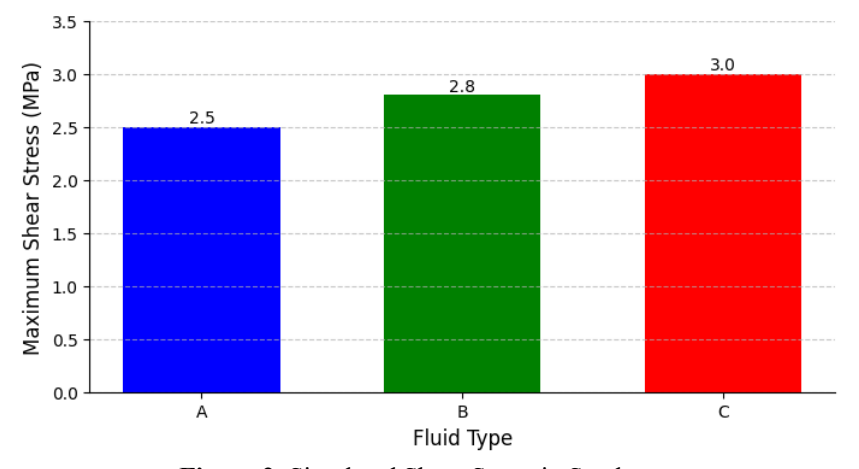


Figure 2. Simulated Shear Stress in Sandstone

Statistical analysis was performed using Pearson's correlation coefficient to quantify the relationship between storage modulus and ROP. The coefficient r is defined as:

$$r = \frac{\sum (x_i - \bar{x})(y_i - \bar{y})}{\sqrt{\sum (x_i - \bar{x})^2 \sum (y_i - \bar{y})^2}} \tag{9}$$

where:

 x_i , y_i – paired measurements of G' and ROP,

 \bar{x} , \bar{y} – values of G' and ROP.

For sandstone, r = 0.98, indicating a strong positive correlation (p < 0.01). Limestone and shale yielded r = 0.96 and r = 0.95, respectively, confirming consistent trends across rock types. A one-way ANOVA test revealed significant differences in ROP between fluids (F = 15.2, p < 0.001), with post-hoc Tukey tests identifying Fluid C as significantly outperforming Fluid A. The analysis reveals that higher viscoelasticity, characterized by increased storage modulus and relaxation time, enhances ROP and reduces torque, particularly in softer rocks like sandstone. The elastic

component of the fluid amplifies stress transfer, promoting crack propagation. These findings align with simulation results, where higher shear stresses correlate with improved rock destruction. However, effectiveness diminishes in harder rocks like shale, suggesting lithology-specific fluid optimization is necessary.

4. Discussion

The experimental and numerical results provide compelling evidence that the viscoelastic properties of drilling fluids significantly enhance rock destruction during drilling, with implications for optimizing drilling efficiency. The observed increase in the rate of penetration (ROP) with higher storage modulus (G') and relaxation time (τ) underscores the critical role of elasticity in facilitating rock fragmentation. Comparing these findings to existing theories, the results partially corroborate models of fluid-rock interaction proposed by (**Pashchenko et al., 2024b**), who suggested that viscoelastic fluids enhance rock fracturing under high-pressure conditions through dynamic stress amplification. However, Livescu's model primarily focused on high-pressure, high-temperature environments, whereas the current study was conducted at ambient conditions. The consistency of viscoelastic effects at lower pressures suggests broader applicability, extending the model's relevance to conventional drilling scenarios. Similarly, (**Ettehadi et al., 2022**) noted that viscoelastic fluids could improve rock fragmentation by transmitting stress waves, a hypothesis supported by the current findings. However, the present study advances these theories by quantifying the relationship between specific viscoelastic parameters (G', τ) and ROP across multiple lithologies, revealing a lithology-dependent response not explicitly addressed in prior models.

The results also challenge traditional rheological models that emphasize viscous properties, such as those by (Yang et al., 2023), which focused on yield stress and plastic viscosity for cuttings transport and ROP optimization. While viscous properties remain critical for hydraulic performance, the current findings highlight the overlooked contribution of elasticity in rock destruction (Lapshyn et al., 2025; Fedoreiko et al., 2025). This discrepancy suggests that conventional non-Newtonian models, such as the Herschel-Bulkley model, may need modification to incorporate viscoelastic effects, potentially through a generalized Maxwell model (6). Such a model better captures the time-dependent behavior observed in the experiments.

A novel pattern emerging from this study is the interaction between viscoelasticity and rock mechanical properties. The stronger effect in sandstone compared to shale suggests that viscoelastic fluids are more effective in rocks with lower UCS and higher brittleness, where elastic energy can exploit existing microfractures. This finding opens a new avenue for research into lithology-specific fluid design, potentially integrating viscoelasticity with formation evaluation data to optimize drilling parameters. Additionally, the reduction in torque with higher viscoelasticity indicates energy efficiency gains, which could lower operational costs and environmental impacts, a practical implication not fully explored in prior studies.

5. Conclusions

This study has demonstrated that the viscoelastic properties of drilling fluids play a significant role in enhancing rock destruction during drilling operations. The key findings indicate that fluids with higher storage modulus (G') and longer relaxation time (τ) substantially improve the rate of penetration and reduce torque across different rock types, with the most pronounced effects observed in sandstone. Specifically, Fluid C, characterized by a storage modulus of 100 Pa and a relaxation time of 10 s, achieved up to 63% higher ROP in sandstone compared to Fluid A (10 Pa, 0.1 s), alongside a 19% reduction in torque. These results highlight the elastic component of viscoelastic fluids as a critical factor in amplifying stress transfer and promoting crack propagation at the rock-tool interface. The positive correlation between G' and ROP (r > 0.95, p < 0.01) across sandstone, limestone, and shale underscores the robustness of this relationship, though the effect diminishes in harder rocks like shale (UCS 100 MPa) compared to softer sandstone (UCS 50 MPa). Numerical simulations further confirmed that higher viscoelasticity induces greater shear stress, supporting the experimental observations.

The findings suggest that viscoelasticity enhances drilling efficiency by enabling dynamic stress wave transmission, which augments the mechanical action of the drill bit. This mechanism is particularly effective in brittle rocks, where elastic energy exploits microfractures to facilitate fragmentation. The reduction in torque with increased viscoelasticity also indicates potential energy savings, offering both operational and environmental benefits. These outcomes challenge traditional focus on viscous properties in drilling fluid design and advocate for incorporating viscoelastic parameters into fluid formulations to optimize performance in diverse geological settings.

Future research should examine viscoelastic fluid performance under real drilling conditions, accounting for temperature, pressure, and circulation effects. Efforts are also needed to optimize viscoelastic parameters for harder formations and to validate results through large-scale field trials. Additionally, the development of eco-friendly viscoelastic additives could ensure both operational efficiency and environmental sustainability. To bridge laboratory and numerical insights to practical applications, future work should complement these with in-situ implementations in real drilling operations, such as pilot tests in oil/gas wells or mining sites. In mining contexts, the results can be applied to enhance rock destruction efficiency in methods like rotary drilling for ore body access or shaft sinking, where higher ROP in sandstone-like formations could reduce project timelines by up to 60% based on our data, while torque reductions minimize equipment wear in shale-heavy environments.

6. References

- Biletskiy, M. T., Ratov, B. T., Syzdykov, A. Kh., & Delikesheva, D. N. (2019). Express method for measuring the drilling muds rheological parameters. 19th International Multidisciplinary Scientific GeoConference SGEM 2019 (Vol. 19, No. 1.2, pp. 861–868). International Multidisciplinary Scientific GeoConference. https://doi.org/10.5593/sgem2019/1.2/S06.109
- Chudyk, I., Sudakova, I., Dreus, A., Pavlychenko, A., & Sudakov, A. (2023). Determination of the thermal state of a block gravel filter during its transportation along the borehole. Mining of Mineral Deposits, 17(4), 75-82. https://doi.org/10.33271/mining17.04.075
- Ettehadi, A., Ülker, C., & Altun, G. (2021). Nonlinear viscoelastic rheological behavior of bentonite and sepiolite drilling fluids under large amplitude oscillatory shear. Journal of Petroleum Science and Engineering, 208, 109210. https://doi.org/10.1016/j.petrol.2021.109210
- Fedoreiko, V.S., Rutylo, M.I., & Iskerskyi, I.S. (2013). Improvement of energy performance of the electrotechnological complex for production of solid biofuels using neural controller. Naukovyi Visnyk Natsionalnoho Hirnychoho Universytetu, 5, 78–85.
- Fedoreiko, V., Zahorodnii, R., Lutsyk, I., Rutylo, M., & Bureha, N. (2025). Modelling of resource-saving control modes of a bioheat generator using neuro-fuzzy controllers. IOP Conference Series: Earth and Environmental Science, 1457(1), 012005. https://doi.org/10.1088/1755-1315/1457/1/012005
- Guo, B., Meng, Y., & Wei, N. (2021). Applied gaseous fluid drilling engineering: Design and field case studies (pp. 1–323). Elsevier. https://doi.org/10.1016/B978-0-323-85675-1.00017-6
- Ihnatov, A. O., Haddad, J., Stavychnyi, Y. M., & Plytus, M. M. (2022b). Development and implementation of innovative approaches to fixing wells in difficult conditions. Journal of the Institution of Engineers (India) Series D, 104(1), 119–130. https://doi.org/10.1007/s40033-022-00402-5
- Lapshyn, Y., Shevchenko, O., Dybrin, S., & Dychkovskyi, R. (2025). Feasibility of Fine Classification in Processing Watered Coal Sludge from Storage: A Case Study of the Dnipro Coke Chemical Plant. Acta Montanistica Slovaca, 30(1), 100–113. https://doi.org/10.46544/ams.v30i1.07
- Maksymovych, O., Solyar, T., Sudakov, A., Nazar, I., & Polishchuk, M. (2021). Determination of stress concentration near the holes under dynamic loadings. Naukovyi Visnyk Natsionalnoho Hirnychoho Universytetu, 2021(3), 19–24. https://doi.org/10.33271/nvngu/2021-3/019
- Mnzool, M., Al-Mukhtar, A., Majeed, A.J., Arafat, A., & Gomaa, E. (2024). Simulation and performance characteristics of rock with borehole using Visual Finite Element Analysis. *Mining of Mineral Deposits*, 18(3), 33-41. https://doi.org/10.33271/mining18.03.033
- Muratova, S., Ratov, B., Khomenko, V., Pashchenko, O., & Kamyshatskyi, O. (2025). Improvement of the methodology for measuring plastic viscosity and dynamic shear stress of drilling fluids. Iop Conference Series Earth and Environmental Science, 1491(1). https://doi.org/10.1088/1755-1315/1491/1/012026
- Pashchenko, O., Ratov, B., Khomenko, V., Gusmanova, A., & Omirzakova, E. (2024a). Methodology for optimizing drill bit performance. International Multidisciplinary Scientific GeoConference Surveying Geology and Mining Ecology Management (SGEM). https://doi.org/10.5593/sgem2024/1.1/s06.78
- Pashchenko, O. A., Borodina, N. A., Yavorska, O. O., Ishkov, V. V., & Cherniaiev, O. V. (2024b). Application of polymer flooding to increase oil recovery. IOP Conference Series: Earth and Environmental Science, 1415(1). https://doi.org/10.1088/1755-1315/1415/1/012054
- Ratov, B. T., Fedorov, B. V., Syzdykov, A. Kh., Zakenov, S. T., & Sudakov, A. K. (2021). The main directions of modernization of rock-destroying tools for drilling solid mineral resources. International Multidisciplinary Scientific GeoConference Surveying Geology and Mining Ecology Management, SGEM, 21(1.1), 335–346. https://doi.org/10.5593/sgem2021/1.1/s03.062
- Ronaes, E., Fossdal, T., & Stock, T. (2012). Real-time drilling fluid monitoring and analysis Adding to integrated drilling operations. SPE/IADC Drilling Conference Proceedings. https://doi.org/10.2118/151459-MS
- Stavychnyi, Y., Koroviaka, Y., Ihnatov, A., Matyash, O., & Rastsvietaiev, V. (2024). Fundamental principles and results of deep well lining. IOP Conference Series: Earth and Environmental Science, 1348(1). https://doi.org/10.1088/1755-1315/1348/1/012077
- Symanovych, H., Lisovytska, I., Odnovol, M., Ahaiev, R., & Poimanov, S. (2024). Rationale and modeling of technology for complex bottom-hole zone de-stressing of gas-dynamically active rock mass. *Mining of Mineral Deposits*, 18(2), 83-92. https://doi.org/10.33271/mining18.02.083
- Yang, H., Zhang, P., Meng, X., Gao, S., & Liang, H. (2023). On the online calibration of drilling fluid rheological parameters using EMD and MLE. IEEE Sensors Journal, 23(17), 19861–19870. https://doi.org/10.1109/jsen.2023.3297392

Author's contribution

Volodymyr Khomenko (associated professor): conceptualization, writing and methodology. Yevhenii Koroviaka (associated professor): project administration. Oleksandr Pashchenko (associated professor): editing and formal analysis. Andrii Ihnatov (associated professor): investigation and software.

All authors have read and agreed to the published version of the manuscript.



Mechanism of Gate Road Floor Heaving as the Basis for Geotechnical Stabilization of Its Section

DIM-ESEE Conference



Ivan Sadovenko¹* [©]⊠, Serhii Vlasov¹ [©]⊠, Vladyslav Vlasov² ⊠, Stanislav Hroma¹ ⊠, Dmytro Tvilenov³ ⊠

- ¹ Dnipro University of Technology, Dnipro, Ukraine
- ² LLC «NATIFE», Dnipro, Ukrane
- ³ Coal-mine LW Bogdanka S.A., Leczna, Poland

Abstract

Gate road stability in layered rock masses is significantly affected by temporal loosening, stress redistribution, and rheological changes in rock strength during initial mining operations. Conventional support systems often fail to prevent floor heaving under intensive rock pressure, particularly in soft wall rocks. This study aims to optimize gate road geometry and support design in Western Donbas mines by integrating physico-mathematical modeling, empirical measurements, and analytical approaches. The physico-mathematical model was developed to describe radial compaction, support leg deepening, and time-dependent changes in rock strength. Empirical data from twenty full-scale measurement stations were analyzed to derive calculation ratios for gate road sections. Stable correlations were established between non-linear regression parameters, lithological and structural indices, and the required support leg extensions to compensate for floor heaving. The analysis identified that excessive displacements occur when wall rocks are loosened, with extreme deformation zones determining displacement distribution along mine boundaries. Application of the proposed methodology allowed for calculation of support leg extensions of 0.5 m - 0.7 m, which were confirmed through industrial testing to maintain gate road stability under technological load conditions. The combined empirio-analytical approach provides a scientifically justified and practically validated methodology for designing gate road sections in layered rock masses. It accounts for geometry, rock structure, and rheological strength changes, offering a reliable basis for improving safety and operational efficiency in Western Donbas mines.

Keywords: rock mass, gate road support parameters, mine working floor heaving, stress-strain state, rheological changes in rock strength

1. Introduction

The study of gate road floor heaving is highly relevant due to its direct impact on mine safety, operational efficiency, and the longevity of underground workings. In layered rock masses subject to temporal loosening and stress redistribution, uncontrolled floor heaving can lead to deformations, damage to support structures, and interruptions in mining operations (Tsolas, 2021). Understanding the mechanisms driving these displacements provides a scientific basis for geotechnical stabilization, enabling the design of support systems that maintain gate road integrity under complex geological and rheological conditions. In regions such as the Western Donbas, where extensive mining occurs in heterogeneous rock formations, developing predictive models and empirically validated support strategies ensures both safe and cost-effective extraction practices, highlighting the practical and theoretical significance of this research (Haidai et al., 2022).

The current scientific and practical trends in mining development increasingly focus on the construction and operational use of gate roads within layered and nonhomogeneous carboniferous rock masses, taking into account their geometrical coordinates as well as transverse and isotopic characteristics (Dychkovskyi et al., 2019). Within this context, determining the geotechnical effectiveness of extraction pillar preparation, considering parameters spatially and temporally correlated with gate road dimensions, emerges as a critical task that significantly influences both the technical performance and economic efficiency of coal mining operations (Bondarenko et al., 2018; Pivnyak et al., 2015). Effective gate road design ensures stability under complex rock mass conditions while optimizing resource extraction and reducing operational risks.

Recent studies have emphasized the importance of selecting optimal mining methods and understanding the influence of rock fragmentation processes on operational efficiency. A comprehensive approach to decision-making in mining operations has been proposed, involving the simultaneous evaluation of multiple criteria and case studies to determine the most effective mining methods (Namin and Amou, 2024). The significance of blast design and its impact

on rock breakage, energy consumption, and downstream processing efficiency has also been thoroughly examined (Sahlabadi et al., 2025).

These studies collectively demonstrate how advanced analytical and numerical approaches can enhance the accuracy of mining method selection and blasting optimization. Their findings provide valuable insights that align with the objectives of the present research, supporting the development of more efficient and sustainable mining practices.

Over recent years, several research findings have gained recognition within the scientific community and have been successfully implemented in practice (Bondarenko et al., 2014; Mondal et al., 2024). Among these, geomechanical forecasting of in-seam working rock floor heaving has been emphasized, particularly studies that explain the process mechanism under varied mining and geomechanical conditions and propose geotechnical measures to minimize negative operational factors, thereby improving the possibilities for gate road reuse (Sakhno and Sakhno, 2023). Such approaches provide predictive insights into rock mass behavior, supporting safer and more efficient underground operations.

Another important research direction involves the analysis of the stress-strain state at the interface between longwall workings and gate roads (Dychkovskyi et al., 2014). Studies have considered both the static phase of gate road parameters and their temporal changes under the influence of the advancing stope. Additionally, geotechnical control measures have been developed to maintain the opening section and enable its reuse, ensuring operational continuity while mitigating deformation-related risks (Vlasov et al., 2022; Rahimi 2020; Snihur et al., 2022). These investigations highlight the dynamic interaction between mining operations and gate road stability, emphasizing the need for timely intervention.

Furthermore, geomechanical and technological substantiation of measures to maintain gate road sections during the mining of gently sloping seams has been extensively studied (Shamganova et al., 2021). Research has particularly addressed layered rock masses with transverse-isotropic heterogeneity in strength characteristics, proposing design and support solutions that account for both lithological variability and operational loading conditions (Malkowski et al., 2016). These findings contribute to the methodological basis for designing gate road support systems capable of withstanding complex geological conditions while maintaining operational efficiency.

A cumulative analysis of these scientific and practical trends demonstrates their overall positive impact on mining safety and efficiency (Muhammad et al., 2025). However, certain limitations remain, particularly regarding the geotechnical locality of some studies and the insufficient analytical generalization of tasks. In many cases, theoretical models and practical implementation are insufficiently harmonized, emphasizing the need for further integrative research to bridge the gap between predictive geomechanics and field applications, particularly under the specific conditions of Ukrainian mines (Dychkovskyi et al., 2024). Addressing these gaps will enhance the reliability of gate road design and the sustainable development of underground coal mining operations.

Consequently, the research purpose is to optimize geometrical configuration of a gate road section under the conditions of the layered rock mass experiencing its loosening in space and time and being impacted by stress redistribution during development operations.

Formulation of the task of geotechnical locality of the available solution avoidance to select adequate configuration of a gate road section under the conditions of the layered rock mass experiencing its loosening in space and time and being impacted by stress redistribution during development operations is quite reasonable. It can be done while harmonizing physico-mathematical description of conditionally radial gate road compaction with a support leg deepening into a foot as well as a result of rheological change in the rock strength. The selection of rational support design should involve regularities of rock pressure manifestation; characteristics and structure of enclosing rocks; and nature of their interaction with the support.

2. Methodology of research

The research methodology combines theoretical modeling, numerical simulations, and field investigations to study the mechanism of gate road floor heaving and to develop stabilization measures. A physico-mathematical model of conditionally radial compaction was constructed, considering the deepening of support legs into the floor and rheological changes in rock strength under long-term loading. This model accounts for lithological variability, anisotropy of strength parameters, and stress redistribution caused by mining operations, allowing the identification of deformation zones and prediction of floor heaving.

To quantitatively analyze these phenomena, numerical simulations were performed using both finite-element and finite-difference methods. These simulations provided detailed spatial and temporal distributions of stress and strain within the mine working and surrounding rock mass. Regression analyses were applied to establish correlations between non-linear deformation parameters, lithological indices, and the required support leg extensions. The simulation results were then systematically compared with field measurements and analytical solutions, allowing assessment of model accuracy and calibration of semi-empirical parameters (see formulas 1-8).

The methodological framework was further validated through experimental studies and full-scale field measurements in Western Donbas mines. Monitoring data from multiple stations provided insights into the temporal dynamics of gate road displacement and floor heaving, which were then used to refine theoretical models and simulations. By integrating analytical descriptions, numerical modeling, and empirical observations, the study developed a scientifically justified and practically tested basis for geotechnical stabilization. This approach ensures the reliability of support design and offers effective solutions for maintaining gate road stability under geological and mining conditions.

Relying upon the stated, it is expedient for Donbas mines to increase height of gate roads at the expense of longer support legs to compensate the most intensive rock displacements from a floor which will help stabilize an equilibrium state of the rock periphery and provide the required effective section of a mine working.

Based on these findings, it is recommended that gate road heights in Donbas mines be increased through longer support legs, compensating for the most intensive floor displacements and stabilizing the rock periphery to maintain the effective mine working section. To determine the required support leg extension, an analytical boundary strain solution under pronounced rock loosening was applied:

$$U = kr_0 \tag{1}$$

where are:

U – a mine working periphery displacement,

k – the generalized proportionality factor demonstrating geomechanical interaction between conditionally radial mine working and rock mass,

 r_0 – an equivalent radius of the mine working.

The validity of this formula is supported by observed extreme displacements within the loosening zone and by empirical data indicating that support configuration and resistance have minimal influence on loosening zone dimensions. Formula (1) potential to be used for the problem solving is supported by following conditions:

- significant displacements within a gate road periphery result from a loosening zone impact (i.e. extreme deformations);
- configuration of support peripheries as well as resistance value does not impact practically loosening zone dimensions and displacements inside it defining meanwhile distribution of the displacements throughout the mine working boundary which is confirmed by numerous field data;
- within the rock mass under loosening, time factor influence is demonstrated the most accurately owing to full-scale measurements since the known solutions take into consideration rheological process in limit load.

In the context of the aforementioned conditions, data collected from more than twenty measuring stations installed in the gate roads were carefully processed and analyzed. These measurements captured the temporal evolution of roof heaving and the corresponding reductions in the gate road section area over time. By applying regression analysis to the observed displacements, semi-empirical relationships were established that reliably describe the connection between roof heaving and section area decrease. As a result, the following empirical ratios, with correlation coefficients ranging from 0.85 to 0.97, were derived:

$$\Delta S_i = 4.54h_i - 0.09h_i^2 + 0.38$$

$$h_i = (a_i \ln T + c_i) 10^{-3}$$
(2)

where are:

 S_i – decrease in a gate road section area, m^2 ,

 h_i – value of a gate road roof heaving, m,

T – time from the gate road construction start till to the moment under consideration, days,

 a_i , c_i – regression parameters.

Using geometric considerations, the equivalent radius of a mine working can be determined by relating the cross-sectional area of the gate road to a circular shape. This approach allows for the incorporation of both the initial operational area and the reductions in section area caused by instantaneous and time-dependent displacements. As a result, the equivalent radius, r_0 , can be calculated as::

$$r_0 = \left(\frac{S_p + \Delta S_0 + \Delta S_T}{\pi}\right)^{\frac{1}{2}} \tag{4}$$

$$\Delta S_0 = \pi U^2 \left(\frac{2}{k}\right) - 1 \tag{5}$$

where are:

 S_p – the required operational area of a gate road section,

 ΔS_0 , and ΔS_T – decrease in the section area corresponding to conditionally instantaneous displacements, and time interval T,

 r_0 – radius of S_0 section reduced to a circle.

For conditionally instantaneous displacements in the form of (1), and under further decrease of a gate road section (2, 3), following semi-empirical expression has been obtained during joint solution of formulas (1 and 5):

$$r_0 = \left[\frac{S_p + 10^{-3} a_i \ln T (4.54 - 9a_i \ln T)}{\pi (1 - 2k + k^2)} \right]^{\frac{1}{2}}$$
 (6)

Stable connection between α parameter and lithological and structural criterion has been defined for (3) ratios:

$$\Pi = \frac{\sum_{i=1}^{n} \frac{l_i + m_i}{m_i}}{n} \tag{7}$$

where are:

 l_i – distance to i^{th} sandstone seam roof over a mine working (or to a floor of a seam underlying the mine working), m_i – the i^{th} seam thickness,

n − the number of the seams being a_i − 93.5 if $\Pi \le 1.15$; a_i −63,5 within 1.15 < $\Pi < 1.30$ range; and a_i −38.7 if $\Pi \ge 1.30$.

It should be mentioned that while making practical calculations, values of C_i parameter in (7) formula can be ignored since $\alpha_i = h_i$ if T = 0, i.e. only elastic deformations operate in rock mass around the mine working.

The required extension of support legs is

$$l = \frac{\pi r_0^2 - S_{\min} - bA}{A} \tag{8}$$

where are:

 S_{min} and A – the specified standard gate road section and its width respectively,

b – a value of leg deepening into the loosened floor.

Comparison of the calculated support leg extensions with the measured field values showed a high degree of consistency, indicating the reliability of the proposed methodological framework. This agreement confirms that the combined analytical, numerical, and empirical approach can accurately predict the required support dimensions for gate roads. Consequently, the framework provides a robust and practical tool for ensuring the stability of mine workings under diverse geological conditions and over varying periods of time.

The methodological approach makes it possible to calculate the height of gate roads by extending support legs, which effectively compensates for intensive floor displacements and stabilizes the equilibrium state of the surrounding rock mass. The derived analytical and semi-empirical expressions, supported by field data, provide reliable tools for determining the required support leg extension under varying geological and temporal conditions.

3. Results and Discussions on Geotechnical Stabilization of Gate Road Floor Heaving

Gate road prop used in Western Donbas mines cannot provide maintain-free support of the mine workings under the conditions of intensive floor rock heaving; hence, adequate design selection should take into consideration regularities of rock pressure manifestation; characteristics and structure of wall rocks; and nature of their interaction with the support.

Mainly, rock pressure in gate roads is manifested as floor heaving. If soft wall rocks are available (i.e. when compression limit is 7-30 MPa) then floor heaving doesn't die away even mining depth exceeds 300 m becoming 0.5-1.0 m and more. In such a way, its blasting after gate roads are constructed of an extraction pillar length (i.e. 1200-1400 m) turns out to be the most essential part of the mine working total length. Practical studies and the research have helped understand that floor blasting activates rock heaving again. As a result, it becomes necessary to perform repetitive blasting before mining starts. In this regard, wall pressure makes the unrestrained support legs get inside a mine working provoking deformation of scarf joints. Figures 1 and 2 demonstrate characteristic of the indicator. In such a way, optimization of geotechnics to control the layered strata demonstrating significantly impact by interlayer loosening surfaces is currently the most problematic chain of efficient operation of gate roads in carboniferous rock mass. Geogenetic and geomechanical typing of loosening surfaces within Western Donbas layered rock mass becomes more and more important while using quantitative indicators.

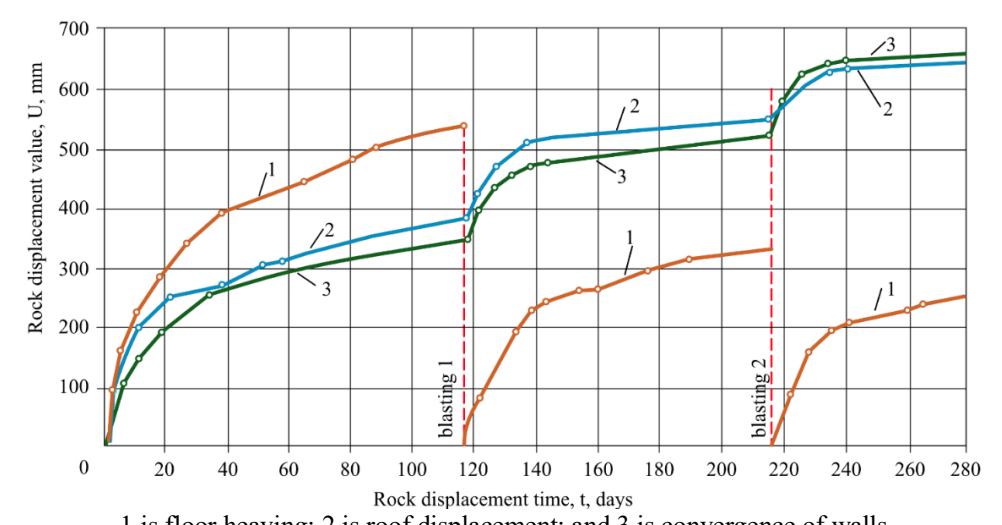
For the purpose, structural and genetic correlation procedure for carboniferous formations; probability-statistical analysis of rock strength data; and a method of combining correlation and analytical dependencies have been used to demonstrate geomechanical condition of the rock mass.

Approximate ratio between inrush height and sheet joints has been identified within $h_a \approx M \approx 2$ m. If M > 2 m then inrush height is quite less than a sheet joint contacting with a support.

 h_{ℓ} < M condition does not contradict the provision that within area of support-roof interaction, fracture rock loosening takes place with partial preservation of their bearing capacity; crack formation process continuation; and inelastic deformation zone progress when stopes stop.

Inelastic deformation zone formation depends heavily upon rheological changes in a rock strata. In addition, it is confirmed by the uncovered high dispersion of both factorial and resultative characteristics of the process with M > 2 m when influence of highspeed operation of stopes dominates. If M < 2 m then fracture loosening within an inelastic areas is compensated by rheological rock deformations.

Mass laboratory strength tests of core and mine samples with following petrographic analysis of the material forming layers have helped separate five types of loosening surfaces for Western Donbas conditions according to increase in their strength and decrease in textural anisotropy coefficient value. Wells for the sampling were drilled using short-cut runs to preserve the loosening surfaces. Figure 1 presents the dynamics of rock displacement in gate road 1019 of the Heroiv Kosmosu Mine.



1 is floor heaving; 2 is roof displacement; and 3 is convergence of walls

Figure 1. Rock displacement dynamics in a road gate 1019 (Heroiv Kosmosu mine)

Similar displacement dynamics of the enclosing rock mass have also been observed at the Bogdanka Mine in Poland. This similarity is explained by the presence of analogous mining and geological conditions of the coal deposits (Fig. 2). Comparative analysis of monitoring data from both mines indicates that floor heaving and peripheral displacements follow the same structural and temporal patterns. These findings highlight the broader relevance of the proposed geotechnical stabilization approach, as it can be effectively applied not only in the Western Donbas mines but also under comparable geological conditions abroad.

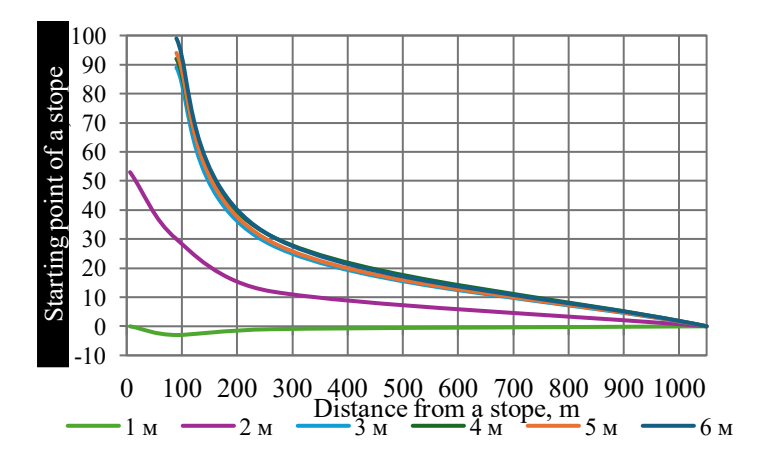


Figure 2. Rock foliation progress (measurement station 32 of a haulage gate 1/V1/385 in Bogdanka mine, Poland)

The attempts to strengthen support through floor arch increase its steel intensity as well as preparation period of an extraction pillar. It has also been proved in practice that the floor arch cannot prevent from bottom heaving within a zone of bearing longwall pressure; in turn, labour intensity and cost of the deformed element removal increases many times.

If rock displacement is more than 300 mm then regulations recommend to use five-chain support. Nevertheless, activities in Western Donbas mines show that flexibility in a lower scarf joint is applied very rarely. The matter is that if wall rocks are soft then support leg deepening into a mine working floor is 100-300 mm to 600-700 mm depending upon rock strength and pressure on the support. It is also known that while deepening, legs turn out to be pinched in a basement of the undisturbed floor rock which increases their resistance to shear movement of rocks. Consequently, taking into consideration the effect of leg deepening into a mine working floor, flexibility value of three-chain support achieves flexibility of a five-chain one (Figures 1, 2).

Using the proposed methodological approach and the mathematical mechanism expressed by formulas (1-8), a set of dependencies was obtained to describe the behavior of the gate road floor. The graphs presented in Figure 3 illustrate the dynamics of temporal changes in floor rock heaving beyond the retaining influence of the stope under varying

lithological and structural conditions. These results demonstrate the predictive capacity of the developed model and highlight its applicability for assessing gate road stability in diverse geological environments.

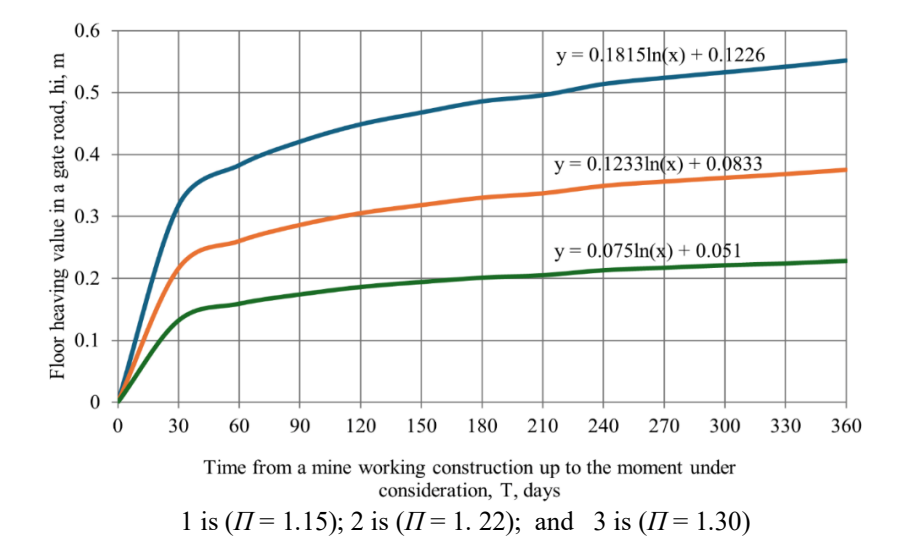


Figure 3. Dynamics of a gate road floor rock heaving in different values of lithological and structural criterion (Π)

The study demonstrates that conventional gate road support in Western Donbas mines cannot fully prevent floor heaving under intensive rock pressure, especially in soft wall rock conditions. Floor heaving and peripheral rock displacements are significantly influenced by lithological and structural properties, as well as rheological changes in the rock strata. Laboratory and field studies identified five types of loosening surfaces, providing a basis for geomechanical assessment and predictive modeling of gate road stability. Comparative analysis with the Bogdanka Mine confirms that the observed displacement patterns are consistent under similar geological conditions, supporting broader applicability of the stabilization approach. The developed methodological framework and mathematical model offer reliable predictions of floor heaving dynamics, informing optimized support design and operational strategies.

5. Conclusions

The present study demonstrates that conventional gate road support systems in Western Donbas mines are inadequate for fully controlling floor heaving under conditions of intensive rock pressure, particularly in zones with soft wall rocks. Floor heaving is the primary manifestation of rock pressure, and its magnitude and temporal evolution are strongly influenced by lithological and structural properties of the surrounding rock mass, as well as rheological changes in the strata over time. Laboratory and field investigations, including mass core testing, petrographic analysis, and drilling for sampling, enabled the identification of five types of loosening surfaces. These results provide a detailed geomechanical understanding of the rock mass, forming a reliable basis for predictive modeling of gate road stability.

Comparative analysis of displacement dynamics from the Western Donbas and Bogdanka mines shows that floor heaving and peripheral rock displacements follow consistent structural and temporal patterns under comparable geological conditions. This highlights the broader applicability of the proposed stabilization approach beyond the immediate study area. The study further demonstrates that conventional methods, such as increasing floor arch strength or employing rigid supports, are insufficient in addressing bottom heaving within the bearing zone of longwall pressure. In contrast, incorporating the effect of support leg deepening into the mine working floor provides substantial resistance to rock displacement while maintaining operational flexibility, effectively achieving the functional equivalence of more rigid support systems.

The integration of numerical simulations, analytical solutions, and full-scale field measurements resulted in a robust methodological framework for predicting gate road behavior under varying geological and temporal conditions. Empirical ratios derived from data collected at more than twenty measuring stations enabled accurate calculation of section area reductions and roof heaving over time. Stable relationships were established between non-linear regression parameters and lithological-structural indices, which were then applied to determine the required support leg extensions to compensate floor heaving. The developed approach provides a scientifically grounded and practically validated tool for optimizing support design, mitigating rock displacement, and maintaining equilibrium of the surrounding rock mass. Furthermore, the predictive capacity of the framework allows mining engineers to anticipate deformation zones, adjust operational strategies, and enhance safety and efficiency in gate road construction and maintenance.

Future research should focus on extending the proposed methodological framework to other mining regions with different geological and structural conditions to validate its broader applicability. Advanced numerical modeling incorporating coupled thermo-mechanical and hydro-mechanical processes could provide deeper insights into time-

dependent rock mass behavior and floor heaving dynamics. Investigating innovative support materials and adaptive support designs may further enhance gate road stability while optimizing operational efficiency and cost-effectiveness.

6. References

- Bondarenko, V., Kovalevska, I., Symanovych, H., Barabash, M., & Vivcharenko, O. (2018). Geomechanics of mine workings support systems. The Netherlands: *CRC Press/Balkema*, 231.
- Bondarenko, V., Kovalevska, I., Symanovych, H., Snihur, V. (2014). Experimental studies of floor rock heaving in development workings within flat Donbas seams. *D.: LizunovPres*, 224.
- Dychkovskyi, R. O., Lozynskyi, V. H., Saik, P. B., & Dubiei, Yu. V. (2019). Technological, lithological and economic aspects of data geometrization in coal mining. *Naukovyi Visnyk Natsionalnoho Hirnychoho Universytetu*, 5. https://doi.org/10.29202/nvngu/2019-5/4
- Dychkovskyi, R., Saik, P., Sala, D., & Cabana, E. C. (2024). The current state of the non-ore mineral deposits mining in the concept of the Ukraine reconstruction in the post-war period. *Mineral Economics*, 37(3), 589–599. https://doi.org/10.1007/s13563-024-00436-z
- Dychkovskyi, R.O., Tymoshenko, Y.V., Astafiev, D.O. (2014). Method of analytical investigation of wall advance speed and forms of line face influence on stress-strain state of a rock massif. *Naukovyi Visnyk Natsionalnoho Hirnychoho Universytetu*, (1), 11–16
- Haidai, O., Ruskykh, V., Ulanova, N., Prykhodko, V., Cabana, E. C., Dychkovskyi, R., Howaniec, N., & Smolinski, A. (2022). Mine Field Preparation and Coal Mining in Western Donbas: Energy Security of Ukraine A Case Study. *Energies*, 15(13), 4653. https://doi.org/10.3390/en15134653
- Małkowski, P., Niedbalski, Z., Majcherczyk, T., & Bednarek, Ł. (2016). Underground monitoring as the best way of roadways support design validation in a long time period. *Mining of Mineral Deposits*, no.14 (3), 1-14. https://doi.org/10.33271/mining14.03.001.
- Mondal, S., Mathew, A. S., Goswami, K., & Nair, V. C. (2024). Environmental Impact of Sediment Plumes in Deep-Sea Operations: Mitigation Strategies by Investigating the Efficacy of Flocculants. *Sustainable and Innovative Mining Practices*, 106–116. https://doi.org/10.1007/978-3-031-76614-5_9
- Muhammad, T., Ni, G., Chen, Z., Mallek, S., Dudek, M., & Mentel, G. (2024). Addressing resource curse: How mineral resources influence industrial structure dynamics of the BRI 57 oil-exporting countries. *Resources Policy*, 99, 105420. https://doi.org/10.1016/j.resourpol.2024.105420
- Namin, F. S., & Amou, A. (2024). Simultaneous evaluation of criteria and alternatives for mining method selection (Case studies: Gol-E-Gohar NO. 3 Iron Ore and Chahar-Gonbsd Copper Ore). *Rudarsko-Geološko-Naftni Zbornik*, 39 (2), 121–131. https://doi.org/10.17794/rgn.2024.2.10.
- Pivnyak, G., Bondarenko, V., & Kovalevska, I. (2015). New Developments in Mining Engineering. London, United Kingdom: CRC Press, Taylor & Francis Group, 32-39. https://doi.org/10.1201/b19901
- Rahimi, B., Sharifzadeh, M., Feng, X.T. (2020). Ground behaviour analysis, support system design and construction strategies in deep hard rock mining Justified in Western Australian's mines. *Journal of Rock Mechanics and Geotechnical Engineering*, №12(1), 1-20. https://doi.org/10.1016/j.jrmge.2019.01.006.
- Sahlabadi, S. M. R., Ahangari, K., & Eftekhari, M. (2025). Analysis of the impact of different blast energies on rock crushing using numerical modelling. *Rudarsko-Geološko-Naftni Zbornik*, 40 (2), 87–105. https://doi.org/10.17794/rgn.2025.2.7.
- Sakhno, I., & Sakhno, S., (2023). Numerical Studies of Floor Heave Control in Deep Mining Roadways with Soft Rocks by the Rock Bolts Reinforcement Technology. Advances in Civil Engineering, 1-23.https://doi.org/10.1155/ 2023/2756105.
- Shamganova, L. S., Syedina, S. A., & Berdinova, N. O. (2021). Geomechanical substantiation of the northeastern pit wall stability in Kurzhunkul mine. *Eurasian Mining*, 30–33. https://doi.org/10.17580/em.2021.01.06
- Snihur, V., Bondarenko, V., Kovalevska, I., Husiev, O., & Shaikhlislamova, I. (2022). Optimization solution substantiation for resource-saving maintenance of workings. *Mining of Mineral Deposits*, №16 (1), 9-18. https://doi.org/10.33271/mining16.01.009.
- Tsolas, I. E. (2021). Efficiency Analysis of Lignite Mining Operations Using Production Stochastic Frontier Modeling. *Mining*, 1(1), 100–111. https://doi.org/10.3390/mining1010007
- Vlasov S., Moldavanov Y., Dychkovskyi R., Cabana E., Howaniec N., Widera K., Andrzej B, Smoli'nski A. (2022). A Generalized View of Longwall Emergency Stop Prevention. *Processes*, 10,. P. 878 881. https://doi.org/10.3390/pr10050878 https://www.mdpi.com/journal/processes.

Author's contribution

Ivan Sadovenko (Professor): conceptualization, research, methodology, original draft, and writing. Serhii Vlasov (Professor): research, methodology, original draft, and writing. Vladyslav Vlasov: data processing and formal analysis. Stanislav Hroma: reviewing, and editing, Dmytro Tvilenov: experimental research at the Bogdanka mine.

All authors have read and agreed to the published version of the manuscript.



High-Precision 3D Scanning for the State and Stability Assessment of Underground Mining Facilities of Various Purposes

DIM-ESEE Conference



Serhii Pysmennyi^{1*} ^{□⊠}, Dmytro Brovko¹ ^{□⊠}, Mykhailo Fedko¹ ^{□⊠}, Svetlana Panova¹ ^{□⊠}

¹ Kryvyi Rih National University, Faculty of Mining and Metallurgy,11 Vitalii Matusevych Str., Kryvyi Rih, 50027, Ukraine

Abstract

To provide favorable working conditions, mining enterprises need to protect part of their industrial complex from damage. This can be achieved by relocating some facilities to a safer, underground location. This security method is feasible in the context of underground mining. When determining the underground location (at active or inactive levels), it is necessary to conduct a complex series of studies to ensure the stability of workings within the rock massif. To assess the current state of underground facilities, it is advisable to use 3D scanning. This method not only allows for the construction of a 3D model but also enables 3D modeling to evaluate the stability of the rock massif, taking existing facilities into account. The research conducted showed that the same working can have different dimensions, which is related to changes in the surrounding rock massif and stress field. 3D modeling enabled identification of unstable areas around underground workings. A methodology for the formation of a rockfall vault on the contour of the working was developed. It was established that for most mines in the Kryvyi Rih iron ore basin, workings fail in the vaulted area. Thus, in a homogeneous rock massif, the critical pressure acts on the contour of the working within the vaulted area at an angle of 55-65 degrees. It should also be noted that the results of 3D scanning can be used for various studies, depending on the specific task. A key advantage of 3D scanning is that it enables the subsequent analysis and comparison of how an underground facility changes during its operation.

Keywords: handheld scanner, 3D scanning, 3D modeling, working, stability, stresses, strains

1. Introduction

Since 2014, russia's aggression in Ukraine has caused significant damage to both surface and underground mining facilities, as well as dual-purpose infrastructure. Under martial law, a critical need has emerged for the rapid restoration and construction of damaged facilities of various purposes to ensure the effective operation of underground mining enterprises. Since the full-scale invasion in 2022, the annual productivity of mining enterprises has nearly halved. This decline is primarily due to a shortage of human resources and the inherent risks of storing the necessary quantities of explosives and equipment, which are essential for uninterrupted underground mineral extraction, on the surface.

This challenge can be addressed through two primary strategies: construction of artificial underground facilities for explosive storage and production, and for maintenance of mining equipment (Azaryan et al., 2018; Kuzmenko et al., 2023); and expanded employment of imported high-performance self-propelled machinery to partially compensate for human-related factors (Bazaluk et al., 2022a; Stupnik et al., 2021; Pysmennyi et al., 2020).

An analysis of operations at the Kiruna mines (Sweden) and Zaporizhzhia and Kryvyi Rih iron ore combines (Ukraine) reveals that employment of high-performance self-propelled equipment significantly enhances labor productivity. This enables a decrease in the overall workforce in underground mining and ensures the required annual mine output. However, most Ukrainian mines still rely on traditional domestic drilling equipment, with all development, preparation, and stoping projects specifically designed for this type of machinery.

Switching to high-performance self-propelled equipment in mining requires not only innovating mining systems, but also creating underground rooms for keeping and servicing this equipment (Bazaluk et al., 2021; Kosenko, 2023; Petlovanyi et al., 2019; Rudakov & Rudakov, 1999). The authors of the article present their own options of novel mining systems utilizing imported self-propelled equipment. These systems encompass both open stope mining and induced caving methods and are currently implemented at the Zhovtneva mine of Zaporizhzhia Iron Ore Combine and, to a limited extent, within Kryvyi Rih iron ore basin.

For effective implementation of advanced mining systems in the Kryvyi Rih iron ore basin, additional underground rooms are required at the haulage level to accommodate self-propelled equipment. Given the depth of operations (over 1,200 m) and geological conditions, such rooms are feasible only in stable formations like granites or amphibolites, typically near the shaft bottom. After five years at this depth, the surrounding rock mass has experienced partial disturbance from rock pressures exceeding 250 MPa in some areas.

2. Methods on High-Precision 3D Scanning

To accurately assess the stability of the rock massif surrounding underground workings, it is essential to develop a comprehensive model of the underground level. This model should precisely reflect the current condition of existing workings. Developing such a mathematical model necessitates significant underground data collection. The obtained data can then be processed in various computer modeling software, including but not limited to: *Tinkercad, SketchUp, Fusion 360, Blender, SolidWorks, AutoCAD*, and *K-Mine* (**Stupnik et al., 2022; Stupnik et al., 2023**). It should be noted that building this mathematical model demands not only an accurate spatial representation of all mining objects but also a thorough consideration of the technical condition of each individual working.

The application of the finite element method (**FEM**) to determine stress fields around the mined space offers several key advantages. It allows for the analysis of complex engineering structures and the study of three-dimensional problems, while also permitting the use of elastic-plastic elements to account for the rock massif plasticity.

The fundamental principles and applications of the FEM for a continuous elastic medium with an infinite number of degrees of freedom is well-established in the literature (**Dychkovskyi et al., 2019; Malanchuk et al., 2019; Khorolskyi et al., 2022**)This method discretizes the continuum into a finite number of structural elements, which are interconnected at nodal points. Forces are transmitted between these elements exclusively through the nodes. Within each element, displacements can be approximated by a simple function of coordinates. For a two-dimensional problem, the displacements are limited to the *u* and *v* components, and in the simplest cases, these can be represented by linear functions of the coordinates:

$$\begin{cases} u = a \cdot x + b \cdot y + c, \\ v = e \cdot x + f \cdot y + g \end{cases}$$
 (1)

where are:

u, v – displacement coordinates of the object under study,

x, y – initial coordinates of the object under study,

a, b, c, e, f, g – constants describing the object under study.

For the calculations, a combined scheme using both triangular and rectangular elements was chosen. The nodal displacements u_1 , u_2 , u_3 , u_4 , and v_1 , v_2 , v_3 , v_4 must satisfy **Equation (1)**, which describes the u and v displacements. Solving Equation (1) with its six unknowns a, b, c, e, f, g provides an expression for the constants and the nodal coordinates u and v. This solution defines the complete displacement field within each element as a function of its nodal displacements.

This equation must ensure continuity of the medium between adjacent elements: the displacements linearly varying on the boundary line between two elements will be the same for both elements, since the displacements of the two shared nodal points at the ends of the boundary line for both elements must be the same:

$$\begin{cases} \varepsilon_x = \partial u/\partial x, \\ \varepsilon_y = \partial v/\partial y \end{cases}$$
 (2)

Solving **Equation (1)** with six unknowns (a, b, c, e, f, g) provides an expression for the internal displacement field within the element. This expression is defined by the displacements at the nodal points (u, v). Since the displacements of the two shared nodal points at the ends of the boundary between two elements must be identical, the strain between adjacent elements is determined by the **Equation (3)**:

$$K = p \cdot \sqrt{\frac{E}{2 \cdot B} \cdot \frac{\partial C}{\partial a}} \tag{3}$$

where are:

E – Young's modulus,

B – linear parameter describing the object under study.

In a two-dimensional problem, the nodal forces have two components: one in the x-direction and the other in the y-direction. The forces acting at the nodal points of the boundary elements are equated to the external load or stresses, which are solved by the FEM (Bazaluk et al., 2022b; Kosenko et al., 2025):

$$\begin{cases}
\sigma_{ij} = \left(\frac{K}{\sqrt{2 \cdot \pi \cdot r}}\right) \cdot f_{ij}(\theta), \\
u_i = C \cdot K \cdot \sqrt{r} \cdot f_i(\theta)
\end{cases} \tag{4}$$

where are:

 σ_{ij} – equivalent stress (t/m²),

- K stress intensity factor,
- r distance from the center of the working to the point of analysis (m),
- θ angle at which the normal and tangential stresses are exerted by the rock massif on the contour of the working (degrees).
 - *C* − volumetric pressure modulus.

Knowing the stress and displacement of the object under study, the stress intensity factor value can be determined by **Equation (5) (Demin et al. 2023)**:

$$K = \left(\frac{\sigma_{ij}}{\sqrt{2 \cdot \pi \cdot r}}\right) \cdot f_{ij}\left(\theta\right) = C \cdot u_i \cdot \sqrt{r} \cdot f_i\left(\theta\right) \tag{5}$$

When studying ore deposits with complex geometries under tension or compression, the number of possible principal stress directions is infinite due to their varying limiting values. The FEM allows not only describing the object but also investigating the stress distribution around it for an elastic-plastic rock massif. Today, **Equation (3)** can be solved using software packages such as *SolidWorks*, *Lira*, and *Ansys*. These programs allow for the creation of an object and the determination of not only the stress field but also the deformation of the rock massif around a working. In this study, the stress and strain calculations around underground workings were performed specifically using the *Ansys* and *Lira* software packages. In design work, equivalent stress is used to represent any arbitrary three-dimensional stress state as a single positive value. To perform a strength analysis under complex conditions, it is necessary to first simplify the stress state to that of simple tension. This is achieved by finding the equivalent stress, using the most suitable strength or plasticity criterion for the given case and applying the generalized Hooke's law, **Figure 1**.

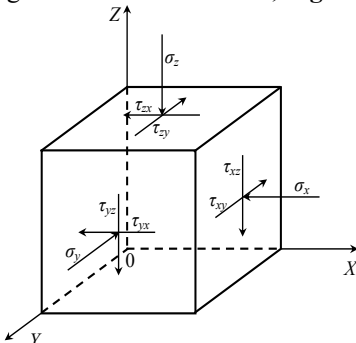


Figure 1. Stress vectors on the faces of the elementary parallelepiped

To model the object under study, a clear contour of the underground facility must be defined, accounting for changes during operation and the influence of the stress-strain state of the surrounding rock. However, determining the parameters of an underground working using traditional geodetic or mine surveying is complex and prone to a certain degree of error. This is because the reconstruction of the working from the measurement data is a manual process.

To ensure high-quality studies of the condition of underground facilities of various purposes, the authors propose utilizing high-precision 3D scanning and modeling. This advanced method enables identifying the geodynamic stabilization patterns of the rock massif during construction of underground facilities including safe underground refueling stations for mining equipment; underground service and repair facilities for self-propelled mining equipment; construction of technological workings, all while precisely taking into account the stress-strain state of the rock massif.

Currently, the study of underground objects is being significantly advanced through the use of a state-of-the-art handheld high-precision 3D scanner that enables rapid 3D scanning and modeling of underground structures, offering capabilities unparalleled in Ukraine. The results of the studies conducted using this innovative 3D scanning technology are presented in **Figure 2**.

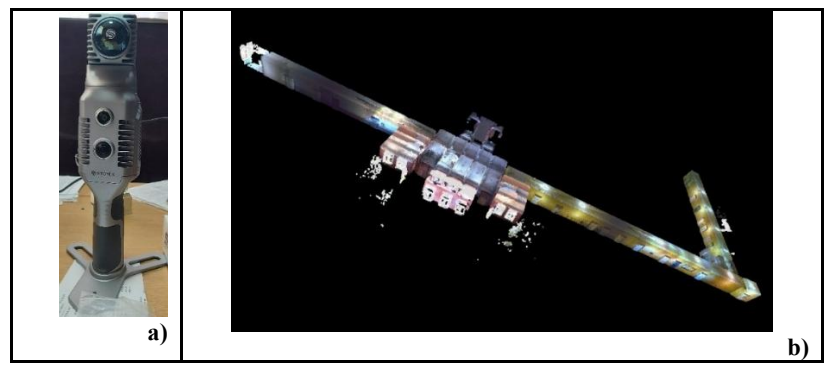


Figure 2. A fragment of the scanning results when using a handheld 3D scanner a) handheld 3D scanner b) 3D model

During the study conducted with the 3D scanner, a substantial data set is generated and securely stored in the cloud. This collected data then undergoes further processing using relevant software packages, selection of which depends on the specific research objectives. Furthermore, this data can also be utilized to track and analyze dynamic changes within the rock massif that occur over time as the deposit undergoes continued development.

3. Results of the Research on High-Precision 3D Scanning for State and Stability Assessment

To determine the stress field around a vault-shaped working using the FEM, the *Lira* 9.4 software package was chosen. This program is a multifunctional tool for the calculation, analysis, and design of various facilities. This software package was also used to perform a number of specific analyses, including: examining the overall stability of the model under study; checking the strength of element cross-sections according to various failure theories; performing calculations of objects taking into account physical, geometric, physico-geometric and constructive non-linearity; modeling changes in physical properties by creating appropriate finite-element and super-element models.

To determine the most hazardous combinations, the object can be subjected to a variety of conditions, including various connections (**Figure 3**), different static and dynamic loads, and the interactions between them.

This software package was used to determine the stress-strain state of the rock massif around the underground working. The analysis was conducted under several conditions: in a linear-elastic formulation, in the nonlinear theory of elasticity, and in an elastic-plastic medium. The calculations employed step-by-step and step-iterative methods, which handle a large number of unknowns and include automatic load step selection and consideration of the time factor.

By creating accurate computational models, which have virtually no limitations in describing the real properties of the analyzed objects, the research process yields key results. These include principal and equivalent stress values based on various failure theories, as well as the forces and stresses resulting from standard and arbitrary linear load combinations.

The calculation results allowed the authors to perform a detailed analysis of the model's stress-strain state using a variety of parameters, including: displacement and stress isofields; diagrams of forces and deflections; element failure mosaics; principal and equivalent stresses; instability modes; animation of structural vibrations, etc.

When forces are present in a given section, the system displays a distribution map of the principal and equivalent stresses corresponding to various failure theories, as well as diagrams of the sectorial characteristics.

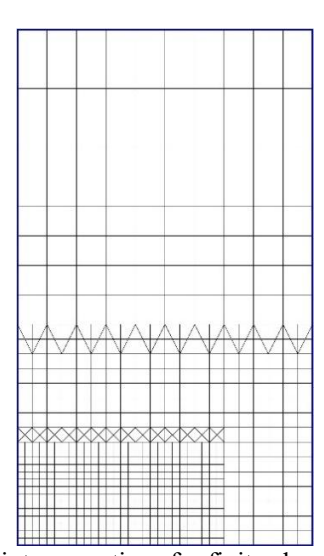


Figure 3. Principal diagram of nodal point connections for finite element analysis of stress fields around a working

Using the selected software package, the displacements of the objects were determined by **Equation (1)**, while the relative linear and shear deformations were determined by **Equation (2)**.

The analysis of principal and equivalent stresses was performed using the following initial conditions:

- dimensions of the rock massif under study 25 m x 25 m;
- nodal connections rectangular-triangular;
- element dimensions $-0.5 \text{ m} \times 0.5 \text{ m}$;
- nodal load: vertical 173 kPa, horizontal 76 kPa.
- Poisson's ratio -0.4;
- modulus of elasticity 1.96 kPa;
- volume weight -34 kN;
- shape of the working vaulted with a width of 5 m and heights of 5 m, 6 m and 7 m.

The results of the performed studies are presented in **Figure 4**.

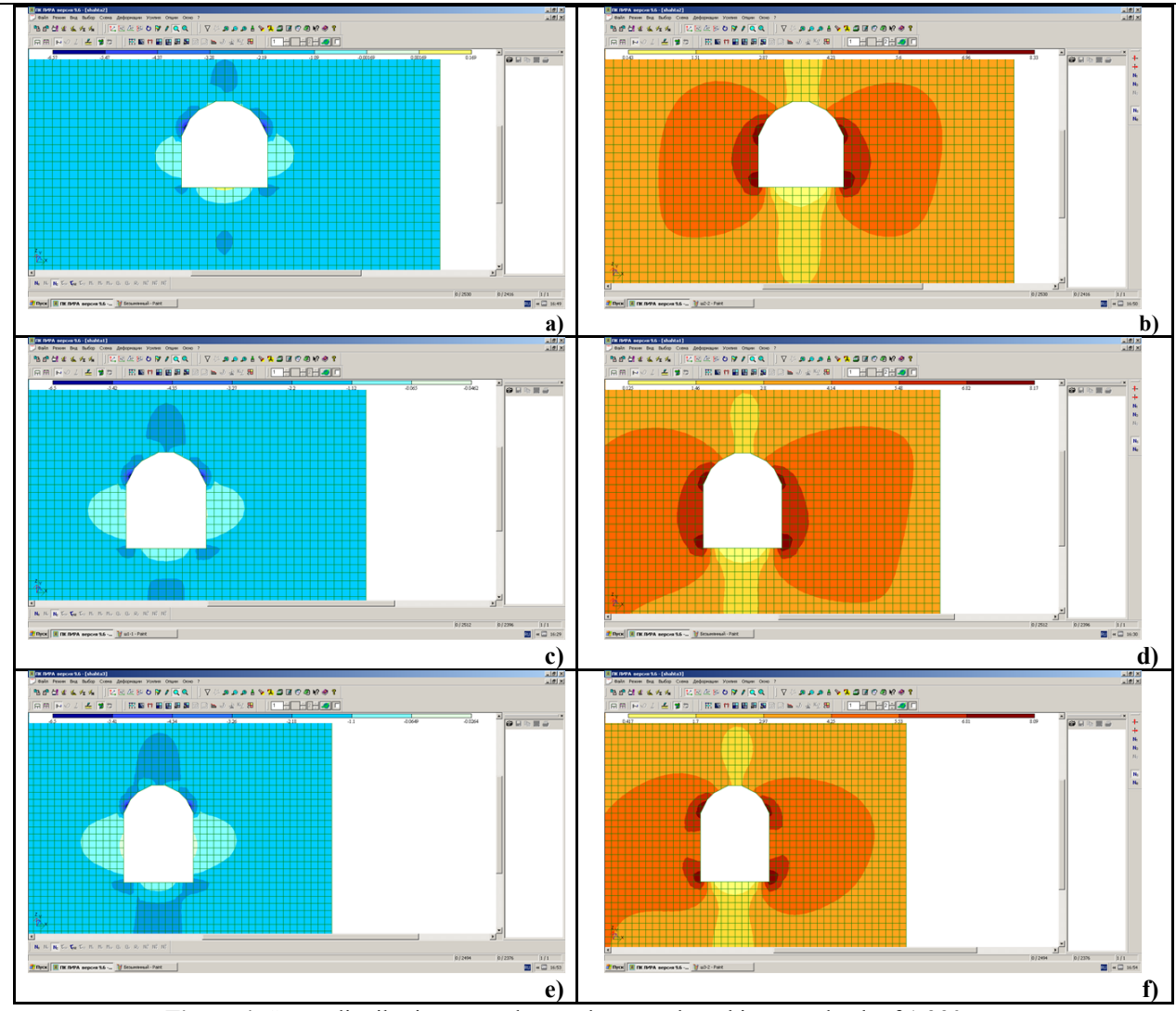


Figure 4. Stress distribution around an underground working at a depth of 1,390 m a), c), e) Vertical stresses at the heights of 5, 6, and 7 m, respectively b), d), f) Equivalent stresses at the heights of 5, 6, and 7 m, respectively

The calculation results provide a foundation for a detailed analysis of the stress-strain state of the model. This analysis is crucial for developing effective measures to stabilize geodynamic processes taking into account the stress-strain state of the massif, especially during rapid construction of underground facilities depending on mining, geological and technical conditions of their deployment.

From the diagrams of vertical and equivalent stresses shown in **Figure 4**, it is evident that the greatest stresses from the rock massif are concentrated on the contour of the underground working, specifically in its vaulted area. Furthermore, the angle of action of these stresses relative to the center of the vault's radius remains constant at 60 degrees under the specified geological conditions, even as the height of the working changes without altering the vault's radius. Based on prior research by (**Kyelgyenbai et al. 2021**) it was established that when the integrity of the contour of a working is disturbed, the rock massif experiences further failure, leading to the development of vault formation. Similarly, at the mines of the Kryvyi Rih iron ore basin, the formation of cavities is also observed along the contour of the working, **Figure 5**.

According to (Stupnik et al., 2018), cavity formation near the working occurs when a specific inequality is not satisfied:

$$P_{\Sigma} < \pm \frac{r \cdot \tau_0 \cdot \sin \delta}{\sin 2\delta - r^2 \cdot \cos \beta \cdot tg\varphi} \tag{6}$$

where are:

 τ_o – initial shear resistance (t/m²),

 δ – angle of load application to the contour of the working (degrees),

 β – shear angle of rocks (degrees),

 φ – angle of internal friction of rocks (degrees).

When a working is created at the *i*-th distance from the stoping area, Equation (6) takes the following form:

- if $0 < L \le 10 \cdot B$

$$P_{\Sigma} = P + \sqrt{P_{cav}^2 - L^2} \tag{7}$$

where are:

L – distance from the contour of the working to the ore body (m),

B – width of the mine working (m),

 P_{cav} – weight of rocks from the collapse zone (t/m²),

- if $L > 10 \cdot B$, the pressure created by the caved rocks during the stoping operations can be neglected:

$$P_{\Sigma} = P \tag{8}$$

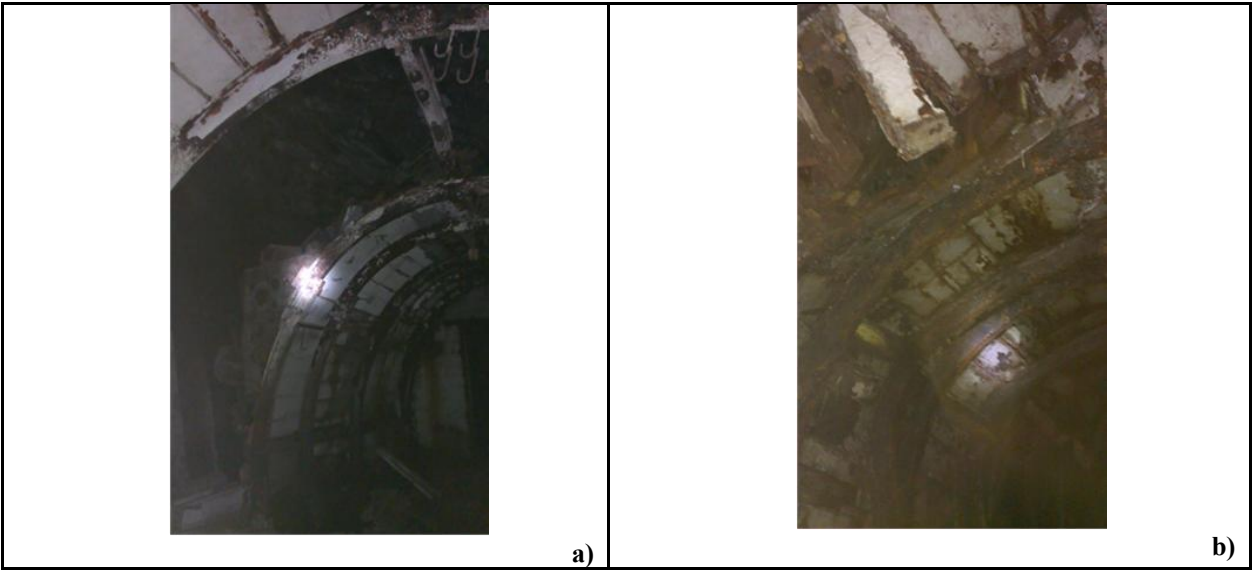


Figure 5. Current state of underground workings at a depth of 1,390 m, showing the effect of rock pressure

a) Without contour deformation

b) With sunsequent contour deformation

Based on the knowledge of the area of maximum confining forces on contour of the working, its stability can be ensured by implementing additional measures, which include: creating an additional loosening area around the working; securing the area of the working with bolts; drilling long holes with subsequent grouting using special mixtures (**Pysmennyi et al., 2018**).

According to the vault hypothesis (Pysmennyi et al., 2018; Matayev et al., 1924b), pressure is determined by the weight of the overlying rocks, which are contained within an unstable equilibrium vault or a dynamically unloaded vault (Kassymkanova et al., 2023; Salkynov et al., 2023). In this formation, particles move only under their own weight. With the high passing ability of the particles and a small internal friction angle, the displacement occurs very smoothly (Matayev et al., 1924a; Zhienbayev et al., 2023). However, when under the action of vertical forces, the vault fails; it results in microseismic events. The rate of particle fall-out in a dynamic vault is determined by the height of the pressure ellipsoid. The dynamic vault curve is then described by Equation (Kunin, 1964):

$$v^2 = 2 \cdot p \cdot x \tag{9}$$

where are:

p – height of the unloading (dynamic) vault figure (m),

x – current coordinate along the x-x axis.

According to research (Protod'yakonov, 1930), the height of the dynamic vault is determined by:

$$h_{v} = p = \frac{a}{2 \cdot tg\varphi} = \frac{a}{f} \tag{10}$$

where are:

 h_v – dynamic vault height (m),

a – width (span of exposure) of the vault in the lower part (m),

f – rock hardness coefficient (Protodyakonov scale).

According to research (**Protod'yakonov**, 1930), the height of the dynamic vault is calculated using the **Equation** (11):

$$h_{\nu} = \frac{a}{2 \cdot tg\alpha} \left(1 - \frac{R^2}{\left(0.5 \cdot a \right)^2} \right) \tag{11}$$

where are:

R – radius of the vault, m.

Based on S.V. Vetrov's hypothesis (Vetrov, 1975), the height of the dynamic vault of unstable equilibrium is generally determined by the Equation (12):

$$h_{v} = k_{hc} \cdot a \tag{12}$$

where are:

 k_{hc} – vault height coefficient.

Based on the research by Prof. V.A. Korzh (Korzh, 1996) on the rocks of the Kryvyi Rih basin, the vault height coefficient is determined by the Equation (13):

$$k_{hc} = exp\left(\frac{3\cdot\pi}{f} - 2\right) + 0.2\tag{13}$$

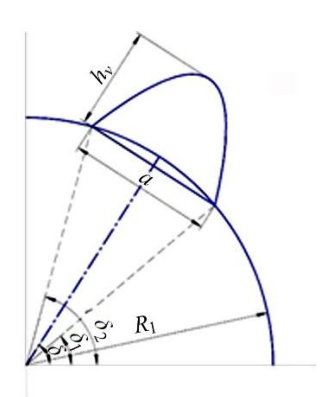


Figure 6. Diagram for determining vault formation parameters on the contour of the working

As shown in **Figure 6**, the span of the rockfall area beyond the contour of the working is determined by the **Equation** (14):

$$a = R_1 \cdot \sin\left(\frac{180 \cdot l}{2 \cdot \pi \cdot R_1}\right) \tag{14}$$

where:

 R_1 – radius of the arc of the vault height (m),

l – arc length (m.s).

The rockfall area is determined by the **Equation (15)**:

$$S = \frac{R_1}{6} \cdot \left(8 \cdot \left(1 - \frac{l}{2 \cdot R_1 \cdot f} \right) \cdot \sin \alpha - \frac{3 \cdot l}{R_1} - \sin 2\alpha \right)$$
 (15)

In layered rocks, the cause of local rockfalls is the reduced strength between layers. The strength characteristics at the contacts between the layers are substantially lower, so failure in the rock massif will occur precisely at these contacts. The stress-strain state around the workings is described by expressions for an elastic medium (Fedko et al., 2019). The boundary of the rockfall along the perimeter of the vault of the working, defined by the angles $\theta xz1$ and $\theta xz2$, is determined by the following Equation (16):

$$\begin{cases} sin \varphi + \frac{\tau_0}{P} cos \varphi \pm \varphi \\ 2 \cdot sin 2\delta \ge 0 \end{cases}, \tag{16}$$

where are:

 δ – angle of the vault (degree),

 h_{v}^{\prime} - height of the new vault contour (m),

The height of the newly formed vault corresponds to the new working contour, at which the tensile stresses reach the uniaxial tensile strength limit of the rocks. The height of the vault after deformation is then determined by the **Equation** (17):

$$\Delta h = h_{\nu}^{/} - h_{\nu} = \frac{a \cdot (1 - \mu)}{\mu} \cdot \left(\frac{1 - 2 \cdot \mu}{1 - \mu} - \frac{\sigma_{p}}{\sigma_{z}}\right) - h_{\nu}$$

$$\tag{17}$$

where are:

 Δh –deformation of the initial height of the unstable equilibrium vault due to tensile stresses (m);

 h_{v}^{\prime} – height of the new vault contour (m),

 σ_t – tensile strength limit of the rock (t/m²).

Based on the research conducted, it was established that if the critical pressure, as defined by **Equation (6)**, is greater than the normal stresses within the rock massif, the working will remain stable. Conversely, if the normal stresses in the rock massif exceed the critical pressure, deformations will occur on the working's contour, and an unstable equilibrium vault will form at an angle δ . Based on calculations using **Equation (6)** and considering **Equation (16)**, the relationship between the critical pressure on the contour of the working and the angle of the load from the surrounding rocks was plotted, **Figure 7**.

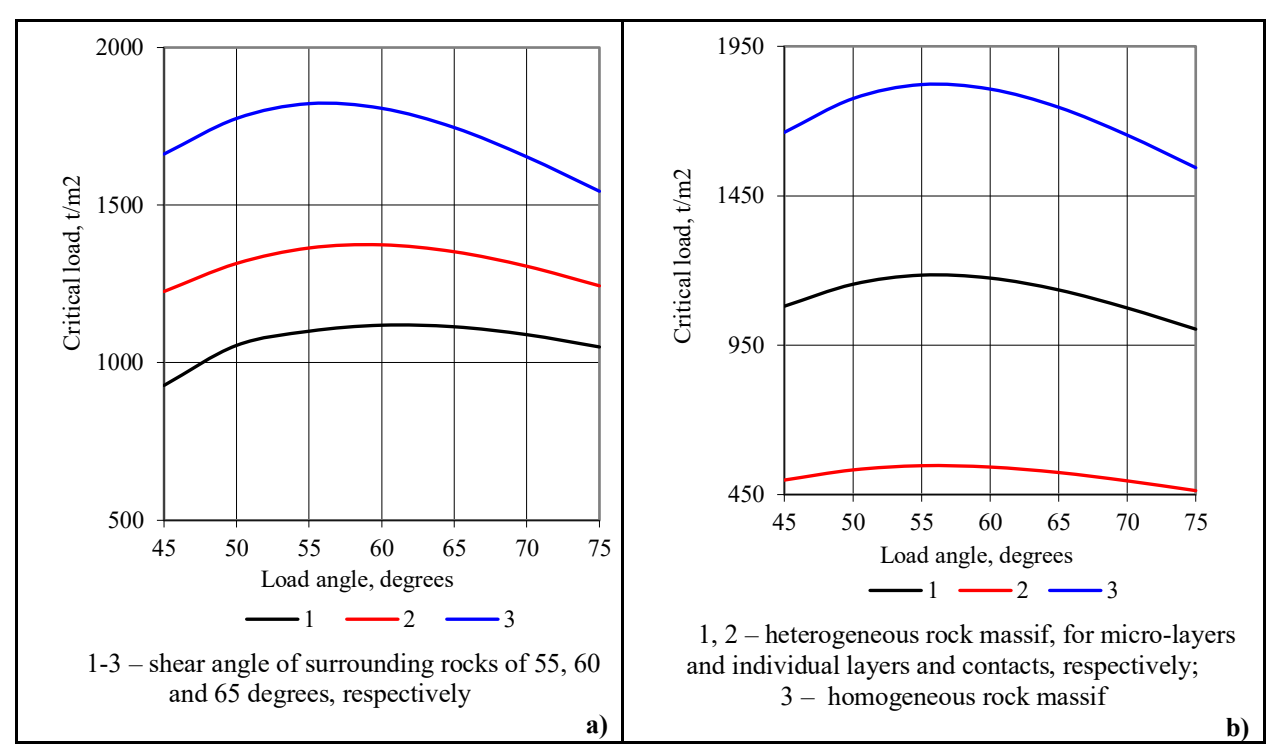


Figure 7. Relationships between the active load on the working contour and the applied load angle beyond the stoping influence area

a) In the homogeneous rock massif

b) In the heterogeneous rock massif

Based on the graphs in **Figure 7**, it is clear that the critical pressure on the working contour acts at an angle of 55 to 65 degrees, depending on the shear angle of the surrounding rocks. In the homogeneous rock massif, the critical pressure on the working contour forms within the range of 50 degrees to 60 degrees. As the rock shear angle increases from 55 degrees to 65 degrees, the critical pressure acting on the mine working contour increases from 1,100 t/m² to 1,830 t/m².

It should be noted that in a heterogeneous rock massif, the critical pressure acting on the working contour is reduced by a factor of nearly 1.5 to 2.0. For example, as the rock shear angle increases from 55 degrees to 65 degrees, the critical pressure acting on the mine working contour varies from 550 t/m² to 1,200 t/m².

4. Discussion

The research conducted proved that using 3D scanning and modeling for studing underground facilities significantly reduces the time required for research. Furthermore, depending on the software package used, the necessary results can be obtained for the specific task. The error between the analytical calculations and the mathematical modeling results is within 5-7%. The results of the study have significant and diverse applications, namely: rapid restoration and construction of underground technological facilities; construction of strategic underground plants for producing and storing explosives; construction of underground facilities for light and medium equipment repair and refueling stations for self-propelled mining equipment; restoration and construction of war-damaged industrial and technological facilities utilizing high-precision 3D scanning and modeling (Pysmennyi et al., 2018; Pysmennyi et al., 2020; Sakhno et al., 2025).

It should also be noted that while studying objects deployed underground or in hazardous areas, works are typically conducted by male personnel, the subsequent processing of data and 3D modeling can effectively involve female specialists. This helps to address the current shortage of human resources, a critical concern during the ongoing state of martial law in Ukraine.

The ability to repeatedly utilize the study results obtained through high-precision 3D scanning, coupled with their compatibility with various software packages for diverse applications, presents a highly promising outlook. This approach aligns perfectly with the guiding FAIR (Findability, Accessibility, Interoperability, Reusability) principles, ensuring that the valuable data generated can be readily discovered, accessed, integrated, and reused for future research and practical solutions.

5. Conclusions

Based on the research findings, it was established that at depths exceeding 1,200–1,390 m, local dynamic manifestations of rock pressure occur in the form of rock bumps and microseismic events. These phenomena lead to rockfalls along the contour of the working, particularly in the upper, vault-shaped section. The angle at which the critical pressure acts is influenced by several factors, including the vault radius, the physical and mechanical properties of the rocks, and the normal and tangential stresses along the contour of the working.

For the first time, the relationships between the critical load on the contour of the working, the angle of the acting load, and rock shear angles were established. It was demonstrated that, in a homogeneous rock massif, the critical pressure in the vaulted section acts at an angle of 55–65°. In phase-heterogeneous rock massifs, the angle of maximum load ranges from 55° to 60°, with the corresponding maximum critical load fluctuating between 550 and 1,190 t/m².

An improved methodology for determining the contour of the vaulting zone in local areas of workings, applicable to both homogeneous and heterogeneous rock massifs, was developed. The validity of this methodology is supported by the results of both mathematical modeling and high-precision 3D scanning. These findings provide a robust basis for assessing stability and designing safer underground workings.

6. References

- Azaryan, A.A., Batareyev, O.S., Karamanits, F.I., Kolosov, V.O., & Morkun, V.S. (2018). Ways to Reduce Ore Losses and Dilution in Iron Ore Underground Mining in Kryvbass. *Science and Innovation*, 14(4), 17-24. https://doi.org/10.15407/scine14.03.017
- Bazaluk, O., Ashcheulova, O., Mamaikin, O., Khorolskyi, A., Lozynskyi, V., & Saik, P. (2022a). Innovative activities in the sphere of mining process management. *Frontiers in Environmental Science*, (10), 878977. https://doi.org/10.3389/fenvs.2022.878977
- Bazaluk, O., Petlovanyi, M., Lozynskyi, V., Zubko, S., Sai, K., & Saik, P. (2021). Sustainable Underground Iron Ore Mining in Ukraine with Backfilling Worked-Out Area. *Sustainability*, 13(2), 834. https://doi.org/10.3390/su13020834
- Bazaluk, O., Rysbekov, K., Nurpeisova, M., Lozynskyi, V., Kyrgizbayeva, G., & Turumbetov, T. (2022b). Integrated monitoring for the rock mass state during large-scale subsoil development. *Frontiers in Environmental Science*, (10), 852591. https://doi.org/10.3389/fenvs.2022.852591
- Demin, V., Khalikova, E., Rabatuly, M., Amanzholov, Z., Zhumabekova, A., Syzdykbaeva, D., Bakhmagambetova, G & Yelzhanov, Y. (2023). Research into mine working fastening technology in the zones of increased rock pressure behind the longwall face to ensure safe mining operations. *Mining of Mineral Deposits*, 18(1), 27-36 https://doi.org/10.33271/mining18.01.027
- Dychkovskyi, R. O., Lozynskyi, V. H., Saik, P. B., Dubiei, Yu. V., Cabana, E.C. & Shavarskyi, I.T. (2019). Technological, lithological and economic aspects of data geometrization in coal mining. *Naukovyi Visnyk Natsionalnoho Hirnychoho Universytetu*, 5. https://doi.org/10.29202/nvngu/2019-5/4

- Fedko, M.B., Muzyka, I.O., Pysmennyi, S.V. & Kalinichenko, O.V. (2019). Determination of drilling and blasting parameters considering the stress-strain state of rock ores. *Naukovyi Visnyk Natsionalnoho Hirnychoho Universytetu*, (1), 37–41. https://doi.org/10.29202/nvngu/2019-1/20
- Kassymkanova, K.K., Istekova, S., Rysbekov, K., Amralinova, B., Kyrgizbayeva, G., Soltabayeva, S., & Dossetova, G. (2023). Improving a geophysical method to determine the boundaries of ore-bearing rocks considering certain tectonic disturbances. *Mining of Mineral Deposits*, 17(1), 17-27. https://doi.org/10.33271/mining17.01.017
- Khorolskyi, A., & Kosenko, A. (2022). Results of simulation modeling of the influence of technological parameters on the outburst hazard of coal seams. 5 th International Scientific and Technical Internet Conference "Innovative development of resource-saving technologies and sustainable use of natural resources". Book of Abstracts. Petroşani, Romania: Universitas Publishing, 157-160.
- Korzh, V.A. (1996) Equivalent Parameters of Broken Ore Pieces in a Block. Ore Deposit Development, 59, 52-59.
- Kosenko, A. (2023). Development of an efficient process scheme for breaking high-grade iron ores of low strength and stability during sublevel caving. *Science and innovation*, 19(3), 38-47. https://doi.org/10.15407/scine19.03.038.
- Kosenko, A., Khomenko, O., Kononenko, M., Polyanska, A., Buketov, V., Dychkovskyi, R., Polaski, J., Howaniec, N., & Smoliski, A. (2025). Sustainable Management of Iron Ore Extraction Processes using Methods of Borehole Hydro-Technology. *International Journal of Mining and Mineral Engineering*, 16(1), 92–112 https://doi.org/10.1504/ijmme.2025.10070190
- Kunin, I.K. (1964). Ore extraction and transport in underground mining, M.: Nedra, 357 p.
- Kuzmenko, O., Dychkovskyi, R., Petlovanyi, M., Buketov, V., Howaniec, N., & Smolinski, A. (2023). Mechanism of Interaction of Backfill Mixtures with Natural Rock Fractures within the Zone of Their Intense Manifestation while Developing Steep Ore Deposits. *Sustainability*, 15(6), 4889. https://doi.org/10.3390/su15064889.
- Kyelgyenbai K., Pysmennyi S., Chukharev S., Purev B., & Jambaa I. (2021). Modelling for degreasing the mining equipment downtime by optimizing blasting period at Erdenet surface mine. *E3S Web of Conferences*, (280), 08001. https://doi.org/10.1051/e3sconf/202128008001
- Malanchuk, Z.R., Moshynskyi, V.S., Korniienko, V.Y., Malanchuk, Y.Z., & Lozynskyi, V.H. (2019). Substantiating parameters of zeolite-smectite puff-stone washout and migration within an extraction chamber. *Naukovyi Visnyk Natsionalnoho Hirnychoho Universytetu*, (6), 11-18. https://doi.org/10.29202/nvngu/2019-6/2.
- Matayev, A., Uakhitova, B., Kaumetova, D., Imangazin, M., Sarkulova, Z., Issengaliyeva, G., & Orazbekova, R. (2024a). Substantiation and selection of parameters for supporting mine workings at deep levels. *Mining of Mineral Deposits*, 18(4), 125-138. https://doi.org/10.33271/mining18.04.125.
- Matayev, A., Zeitinova, S., Mussin, R., Doni, D., Shaike, N., Kuttybayev, A., & Iskakov, R. (2024b). Research into mechanical properties of ore and rocks in the ore deposits with assessment of the mass stress state natural field. *Mining of Mineral Deposits*, 18(2), 71-82. https://doi.org/10.33271/mining18.02.071.
- Petlovanyi, M., Kuzmenko, O., Lozynskyi, V., Popovych, V., Sai, K., & Saik, P. (2019). Review of man-made mineral formations accumulation and prospects of their developing in mining industrial regions in Ukraine. *Mining of Mineral Deposits*, 13(1), 24-38. https://doi.org/10.33271/mining13.01.024
- Protod'yakonov, M.M. (1930). Rock Pressure and Mine Support. M.: Gostekhizdat, 37p.
- Pysmennyi, S., Brovko, D., Shwager, N., Kasatkina, I., Paraniuk, D., & Serdiuk, O. (2018). Development of complex-structure ore deposits by means of chamber systems under conditions of the Kryvyi Rih iron ore field. *Eastern-European Journal of Enterprise Technologies*, 5(1(95)), 33–45. https://doi.org/10.15587/1729-4061.2018.142483
- Pysmennyi, S., Chukharev, S., Peremetchy, A., Fedorenko, S., & Matsui, A. (2023). Study of Stress Concentration on the Contour of Underground Mine Workings. *Inżynieria Mineralna Journal of the Polish Mineral Engineering Society*, 1(1). 69–78. http://doi.org/10.29227/IM-2023-01-08
- Pysmennyi, S., Fedko, M., Shvaher, N., & Chukharev, S. (2020). Mining of rich iron ore deposits of complex structure under the conditions of rock pressure development. *E3S Web of Conferences*, (201), 01022. https://doi.org/10.1051/e3sconf/202020101022.
- Rudakov, D. V. & Rudakov, V. C., 1999. Analytical modeling of aquifer pollution caused by solid waste depositories. Ground Water, 37 (3), 352-357. https://doi.org/10.1111/j.1745-6584.1999.tb01111.x
- Sakhno, I., Sakhno, S., & Vovna, O. (2025). Surface Subsidence Response to Safety Pillar Width Between Reactor Cavities in the Underground Gasification of Thin Coal Seams. Sustainability, 17(6), 2533. https://doi.org/10.3390/su17062533
- Salkynov, A., Rymkulova, A., Suimbayeva, A., & Zeitinova, S. (2023). Research into deformation processes in the rock mass surrounding the stoping face when mining sloping ore deposits. *Mining of Mineral Deposits*, 17(2), 82-90. https://doi.org/10.33271/mining17.02.082.
- Stupnik, M., Fedko, M., Hryshchenko, M., Kalinichenko, O., & Kalinichenko, V. (2023). Study of Compensation Room Impacts on the Massif Stability and Mined Ore Mass Quality. *Inżynieria Mineralna Journal of the Polish Mineral Engineering Society, 1*(1), 137-144. https://doi.org/10.29227/IM-2023-01-16
- Stupnik, M., Kalinichenko, V., Kalinichenko, O., & Pochtarev, A. (2022). Improvement of extracted iron ore grade in underground mining. *IOP Conference Series: Earth and Environmental Science*, 970(1), 012048. https://doi.org/10.1088/1755-1315/970/1/012048

- Stupnik, M.I., Kalinichenko, V.O., Kalinichenko, O.V, & Pochtarev, A. (2021). Technological measures to enhance efficiency of mining ore from stopes applying self-propelled equipment. *E3S Web of Conferences*, (280), 08010. https://doi.org/10.1051/e3sconf/202128008010.
- Stupnik, M.I., Kalinichenko, V.O., Pysmennyi, S.V., & Kalinichenko, O.V. (2018). Determining the qualitative composition of the equivalent material for simulation of Kryvyi Rih iron ore basin rocks. *Naukovyi Visnyk Natsionalnoho Hirnychoho Universytetu*, (4), 21–27. https://doi.org/10.29202/nvngu/2018-4/4
- Vetrov, S.V. (1975). Allowable dimensions of rock exposures in underground ore mining. M: Nedra, 221 p.
- Zhienbayev, A., Balpanova, M., Asanova, Z., Zharaspaev, M., Nurkasyn, R., & Zhakupov, B. (2023). Analysis of the roof span stability in terms of room-and-pillar system of ore deposit mining. *Mining of Mineral Deposits*, 17(1), 129-137. https://doi.org/10.33271/mining17.01.129

Acknowledgment

The authors extend their sincere gratitude to the management and engineering staff of the State Enterprise "Skhidnyi Mining and Processing Plant". Their assistance in providing materials concerning the plant's operations during the martial law period was invaluable to this research.

Funding

This research was supported by the Ministry of Education and Science of Ukraine during 2024-2025, as part of the following state research projects: "30-122-25 Creation of a methodology and development of a technology for the restoration of dual-purpose underground facilities using high-precision 3D scanning (State registration 0125U001757)", "30-118-24 Research and development of the advanced strategy for the technological development of the uranium mining industry during wartime and post-war periods (State registration 0124U000876)", and "30-120-24 Research and stabilization of the stress-strain state of the rock massif for the rapid construction of safe underground military engineering facilities with a high level of protection against air strikes (State registration 0121U111709)".

Author's contribution

Serhii Pysmennyi (associate professor): conceptualization, funding acquisition, supervision, and investigation. **Dmytro Brovko** (professor): data curation, project administration and resources. **Mykhailo Fedko** (associate professor): methodology, validation and writing — original draft. **Svetlana Panova** (Associate Professor): formal analysis, visualization and software.

All authors have read and agreed to the published version of the manuscript.



The variation of safety pillar's width with depth under the influence of thermo-mechanical stresses in Underground Coal Gasification

DIM-ESEE Conference



Svitlana Sakhno¹ ®⊠, Ivan Sakhno¹* ®⊠, Serhii Bashynskyi² ®⊠, Munkhtsetseg Oidov³ ®⊠

- ¹ Technical University "Metinvest Polytechnic" LLC, Pivdenne Shose 80, Zaporizhzhia, 69008, Ukraine
- ² Zhytomyr Polytechnic State University, Chudnivska Str. 103, Zhytomyr, 10005, Ukraine
- ³ Mongolian University of Science and Technology, Baga Toiruu 34, Ulaanbaatar, 14191, Mongolia

Abstract

Underground coal gasification is one of the main trends of green mining. The basic principles of underground gasification have been long known. However, the practical implementation of this technology is unfortunately still not widespread. Recently, the Parallel Controlled Retraction Injection Points method has been actively developed, which is the subject of research in this article. An open problem of this technology is the determination of the pillar's width between reactor cavities taking into account the influence of thermo-mechanical destruction of coal. In this study, numerical simulation by ANSYS 17.2 software was used to solve it. The distribution of thermo-mechanical stresses in a coal pillar was studied. Mohr's theory was proposed to predict the destruction of a coal pillar at different depths. It was found that the coal seam failure near the production well and injection well leads to a reduction in the functional width of the safety pillar. Although, contrary to expectations, this effect is not particularly significant. The greater the depth of the seam, the greater the width of the zone of thermo-mechanical destruction of coal in the pillar. In this case, the main reason for the destruction of the coal pillar is the abutment pressure, increased as a result of the collapse of rocks above the gasification cavity in the post-gasification period.

Keywords: "underground coal gasification", "pillars stability", "safety pillar width", "thin coal seam gasification", "thermal stress"

1. Introduction

The most important component of sustainable development in recent years is the reduction of carbon emissions. The implementation of global commitments involves a planned reduction of greenhouse gas emissions and decarbonization (UNFCCC: 2021). In the energy sector this can be achived primarily due to a decrease of fossil coal dependence, which is considered the main source of environmental pollution. The energy crisis caused by the war in Ukraine has shown the world's unwillingness to abandon coal (Allam et al., 2022). However, an analysis of trends in global coal production shows that, contrary to expectations, the world is gradually increasing coal production, with its transfer to developing countries (URL 1). According to various experts, if current trends in global energy will stay, coal will remain one of the key energy sources for at least the next ten years. In such conditions, along with the development of alternative "green" energy sources, technologies for reducing carbon emissions based on fossil coal usage as an energy resource are becoming increasingly relevant. In a global context, this is reflected in the increased scientific and engineering interest in underground coal gasification technologies (UCG).

Energy independence is one of the key factors for the survival of the economy during the war and development during the post-war reconstruction of Ukraine. Significant explored coal reserves of destroyed mines and promising areas which are, according to various estimates, guarantee the provision of the domestic market with this energy resource for a period of 100 to 250 years. At the same time, the integration of Ukraine into the European space includes reducing greenhouse gas emissions, which creates a contradiction between the necessity to increase generation, which can be realized by burning fossil coal, and obligations to reduce the carbon footprint. The solution to this contradiction is possible through the widespread implementation of UCG, which reveals the regional context of the relevance of this technology.

Nowadays experimental research is being conducted in underground gas generators and in laboratory conditions. Significant progress has been made in controlling the front of the UCG face; the optimal ranges of changes in the pressure rate of the blast mixture and the influence of the concentration of gases and steam on the gasification process have been determined; new methods of underground gasification have been introduced (Dychkovskyi et al., 2025; Kostúr et al., 2018; Laouafa et al., 2016; Lozynskyi et al., 2024; Saik et al., 2016). Among the problematic issues limiting the use of UCG are the environmental hazards. First of all, there is a high risk of subsidence of the Earth's

surface, flooding and water pollution due to the evolution of fractures in the overlying strata and the displacement of rocks above the UCG reactor cavities (Sakhno et al., 2025).

Parallel Controlled Retraction Injection Points (CRIP) method was investigated in this research. This method is more promising as it has higher efficiency of synthesis gas production, more stable gas production levels and increased coal utilization rates (Lozynskyi et al., 2024; Seifi al., 2015). The stability of overburden rock over gasification panels with the CRIP method largely depends on the stability of the safety pillars.

Many scientists have studied the parameters of safety pillars in the case of using of the CRIP method (Li et al., 2015; Najafi et al., 2014; Jiang et al., 2024). However, the influence of thermo-mechanical destruction of coal near production wells and injection wells on the width of the pillar between reactor cavities has not been sufficiently studied. Coal near the UCG panel are subjected to high temperatures which may be more then 1000 °C. This causes irreversible changes in the properties of coal, increased fracturing and a decrease in bearing capacity in the heat-affected zone. As a result of heating, the coal expands, creating additional thermal stress in the pillar. Thus, the functional pillar width becomes less than the geometrically designed width. The specified problem forms the explored surface of the study.

2. Methods

In this study finite element method in Ansys software was used. The three-dimentional coupled thermal-mechanical numerical model was used. The model was 100 m wide, 130 m high, and 50 m long (Figure 1). The model included two goaf cavities and one UCG reactor. The length of the reactor was 30 m. In this study, the coal pillar's width was also 30 m. A caved zone was modeled above the gasification panel during the post-gasification period. This zone in goaf had the arch shape. The height of the caved zone was 8 times higher than the thickness of the coal seam (**Zhang et al., 2019; Sakhno, et al., 2025**). The goaf was filled with combustion material and self-collapsed rocks. The lateral boundaries of the model were fixed against the corresponding horizontal displacements, and the bottom boundaries were fixed against the corresponding vertical displacements. The vertical pressure was equal to the weight of the rock strata at the corresponding depth. The coal seam's depth varied from 200 m to 600 m.

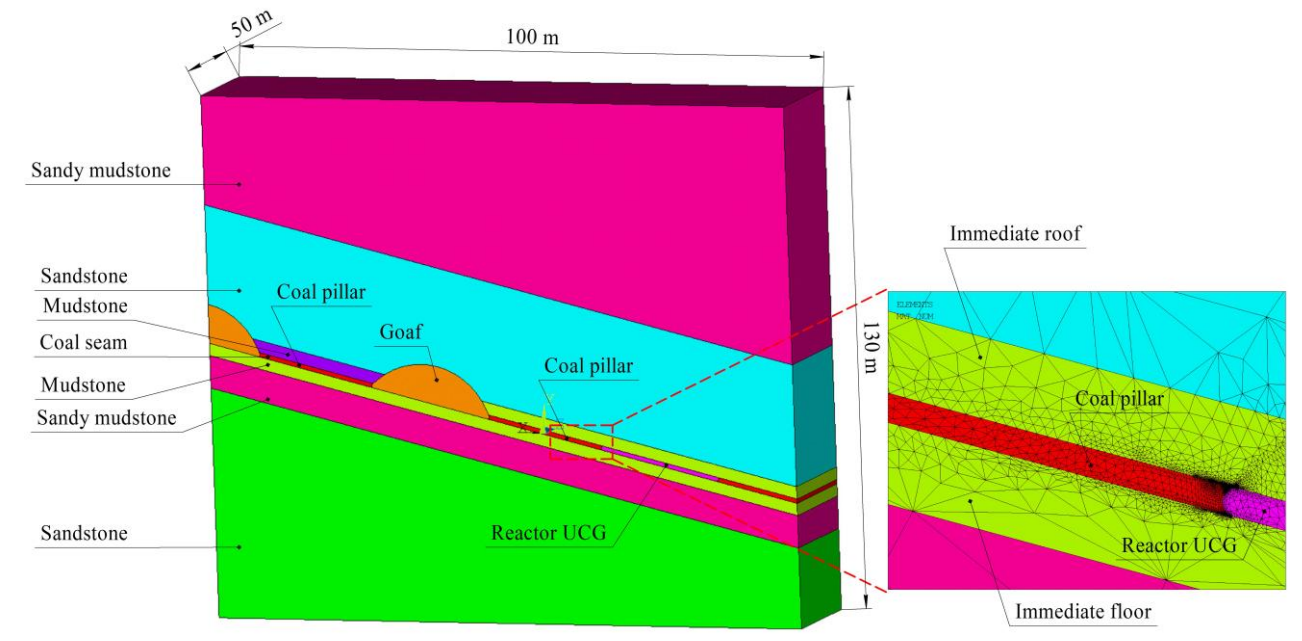


Figure 1. Numerical model

The Drucker-Prager model was used to simulate the behavior of rock mass outside the thermal influence of UCG reactor. The Hoek-Brown Failure Criterion was used to calculate the properties of rock mass (Hoek et al., 2002). The method for calculating rock mass parameters is described in the work (Sakhno, et al., 2024).

The temperature of the rock mass was adopted as 27 °C. The temperature in the UCG face was 1000 °C. The behavior of rocks in the zone of influence of the UCG reactor was simulated temperature-independent for reasons described in more detail in the article (Sakhno et al., 2025). The properties of coal in the heat-affected zone were adopted on the basis of research (Song et al., 2024, Wang et al., 2023). The properties of the mudstone in the immediate roof and floor within the thermal impact of the UCG reactor were calculated taking into account studies (Otto et al., 2015, Zhang et al., 2014) (Table 1).

3. Results

Stress-strain analysis and analysis of temperature distribution have created the basis for understanding the mechanism of loss of pillar's bearing capacity and studying the laws of reduction of the functional width of the coal pillar depending on the depth.

Linear thermal expansion coefficient (α) (K ⁻¹)	Specific heat capacity (CP) (J/(kg K))	Thermal conductivity (\lambda) (W/(mK))	Tensile strength (MPa)	Deformation modulus (GPa)	Poisson's ratio	Cohesion value, (MPa)	Angle of internal friction (deg)	
		Immedia	te roof/floor ((mudstone)				
3.0 10 ⁻⁵	800	1.67	0.36	1.17	0.3	2.7	27	
	Coal seam							
1 10-5	620	0.16	0.27	0.5	0.4	1.13	20	

Table 1. Rock mass parameters in the zone of thermal influence of UCG.

Figure 2a shows the temperature distribution in the model. It should be noted that the model takes into account the thermal destruction of coal in the sides of the production and injection wells, which leads to the formation of non-rectangular reactor walls. The thermal impact zone of the reactor, which is limited by a 250 Celsius degree in the reactor walls, according to the simulation results does not exceed 30 cm. In this case, the maximum width of the temperature increase zone in the sides of the reactor is concentrated in the middle part of the coal seam thickness.

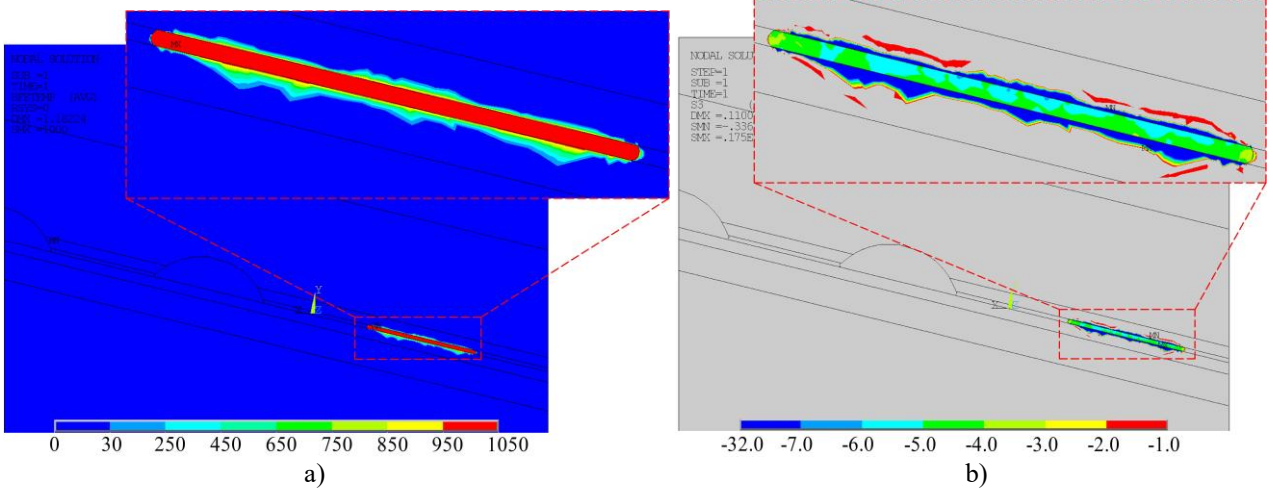


Figure 2. Distribution of temperature in Celsius degree (a) and thermal stress (b) in the model.

Figure 2b shows the distribution of thermal stresses around the reactor cavity. Thermal stresses caused by rock expansion in the temperature-influenced zone have a minus sign. This means that these stresses are compressive. Thus, thermal stresses increase the minimum principal mechanical stresses in the surrounding rocks. Since thermal stresses do not depend on depth, the share of their influence on sum of thermo-mechanical stresses decreases with depth. The value of maximum thermal stresses in the walls of the reactor cavity is 3,6 MPa. At a depth of 200 m, this is an additional 72% to geostatic stresses, and at a depth of 600 m, only 24%. Thus, coal pillars located at a shallow depth are more sensitive to thermal stresses according to the principle of superposition.

Coal pillars are fractured in the result of compression, therefore the critical stresses for them are the principle minimum stresses. The distribution of coupled mechanical and thermal stresses in the surrounding rocks of the UCG reactor at a depth of 200 and 600 m is shown in **Figure 3**. Stress field at different depths vary significantly both on the face of the UCG reactor and in its walls.

Figure 4 shows the change of the coupled compressive stress in a coal pillar with depth. The monitoring line is located in the center of the coal seam and extends from the wall of the reactor cavity to the wall of the previously gasified cavity. The increase of stresses in the pillar (relative to lithological stresses) from the side of the previously worked out cavity is caused by the abutment pressure increased as a result of the collapse of rocks above the gasification cavity in the post-gasification period. This process is well studied and does not cause interest. The increase in stresses from the side of the UCG reactor is caused by thermal stresses. There, a sharp increase in compressive stresses is observed with a peak value on the surface of the reactor wall. The depth of the thermal influence of the reactor on the distribution of minimum principal stresses does not exceed 50 cm for the geological conditions of this study.

It is evident from **Figure 4a** that the increase in stress near the reactor is not constant and is 3.07 MPa, 3.09 MPa, 3.20 MPa, 3.32 MPa, 3.44 MPa for depths of 200 m, 300 m, 400 m, 500 m, 600 m, respectively. This is explained by the combined effect of thermal and mechanical stresses in the UCG cavity wall. Moreover, since the cavity has an arched shape and the coal properties are simulated nonlinearly, an indirect relationship is observed between the increase in depth and the stresses in the UCG cavity wall at a constant value of thermal stresses. Since the arched shape allows to reduce compressive stresses on the contour, the sum of increase in thermo-mechanical stresses in the studied range is less than thermal stresses. However, in the skewbacks of the arch from the roof and floor sides, increased compressive stresses arise. However, they do not have a significant effect on the fracturing of the coal pillar.

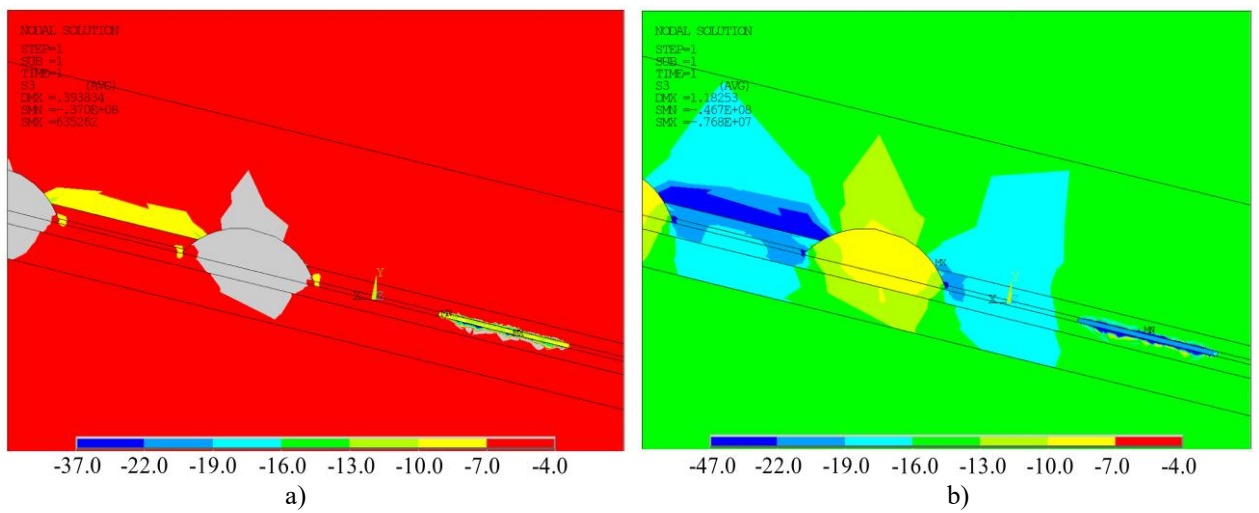


Figure 3. Distribution of minimum principal stresses (MPa) in the model at a depth of 200m (a) and 600 m (b).

Figure 4b shows the change in the stress concentration coefficient in the pillar at different depths of the coal seam. The compressive stress factor (k_{cs}) is:

$$k_{cs} = \frac{\sigma_{sum}}{\sigma_0},\tag{1}$$

where are:

 σ_{sum} – coupled thermo-mechanical stress, MPa,

 σ_0 – lithological stress, MPa.

As anticipated, the share of thermal stress influence decreases with depth. Thus, the compressive stress factor on the surface of reactor wall is 1.62 for a depth of 200 m and 1.23 for a depth of 600 m.

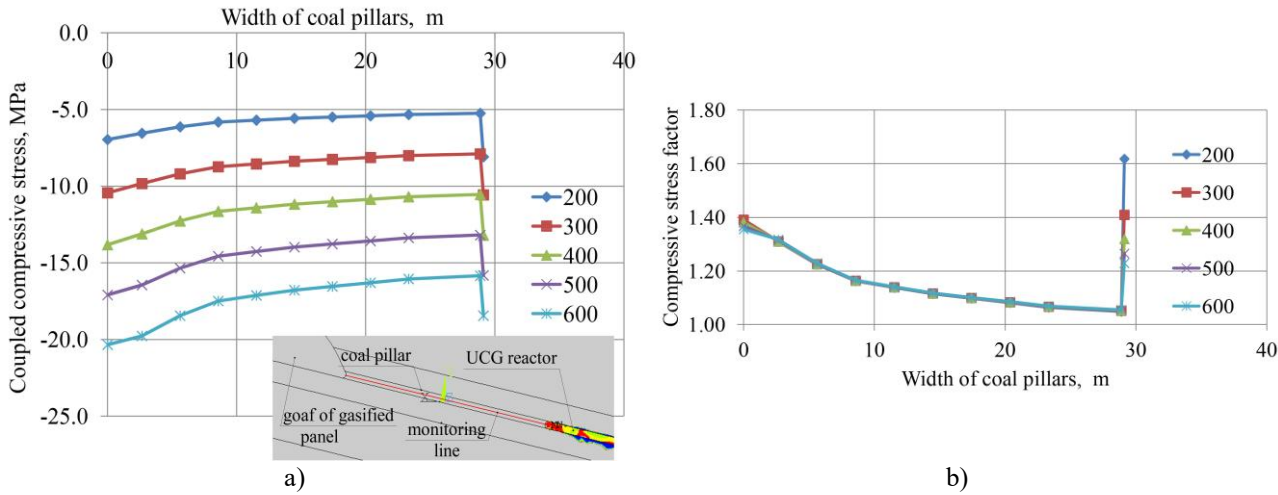


Figure 4. Variation of thermo-mechanical stresses (a) and stress concentration factor (b) in a coal pillar at depth of 200m - 600 m.

4. Discussion

In this study is proposed to use the Mohr criterion to determine the depth of the coal pillar fracturing near the reactor cavity. It is known that the strength of rock in the volumetric stress field increases. With a certain degree of

simplification, the increase in depth can be interpreted as an increase in confined stresses. Thus, the results of coal testing in a volumetric stress field can provide data for assessing the pillar failure at different depths. As an example, the results of coal specimens testing in a triaxial compression machine are used in this article; the experimental technique was described in detail in the previous study (Sakhno, et al., 2018).

During laboratory tests, an increase in the coal seam depth was simulated by increasing the confined stress. Thus, a depth of 200 m, 300 m, 400 m, 500 m, 600 m corresponded to a lateral pressure of 5.0 MPa, 7.5 MPa, 10.0 MPa, 12.5 MPa, 15.0 MPa. At the initial stage of the specimens loading, the vertical and lateral pressures had been being increased simultaneously. After reaching the required level of confined stress, the vertical pressure had been increased until the specimens were destroyed. The Mohr circles for long-flame coal are shown in **Figure 5a**.

Triaxial peak stress at depth of 200 m, 300 m, 400 m, 500 m, 600 m is 7.20 MPa, 1.10 MPa, 13.72 MPa, 16.00 MPa, 18.25 MPa respectively. The angle of internal friction (φ) of coal is 31 degrees. **Figure 5b** combines the results of laboratory tests and numerical simulation. The part of the pillar in which the stress is higher than the triaxial peak stress (according to Mohr's theory) will be failured. Thus, the intersection points of the peak stress and coupled compressive stress lines at the corresponding depth characterize the peak states.

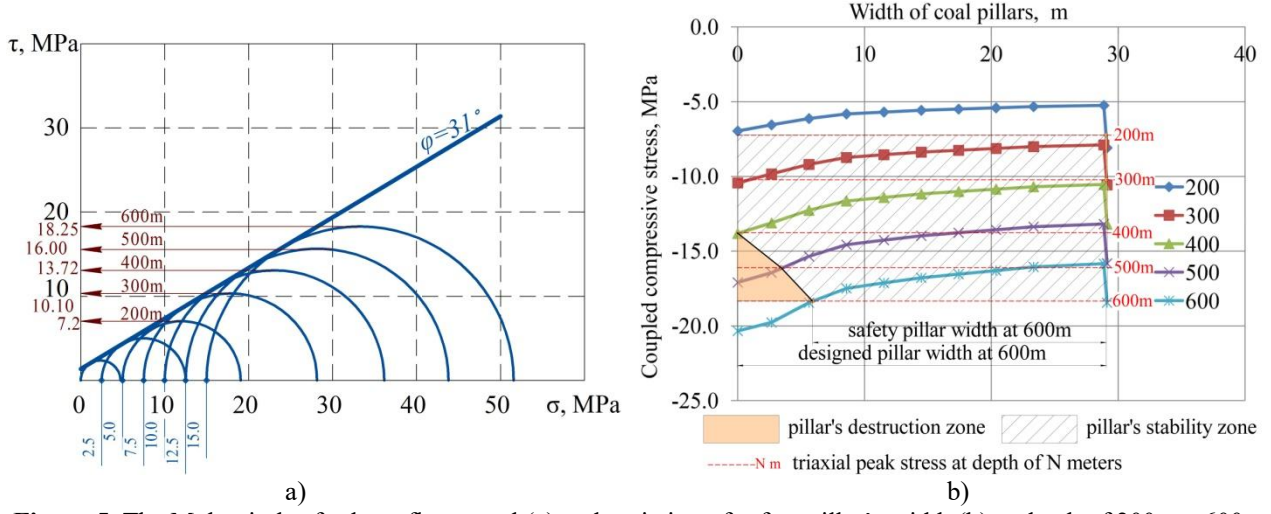


Figure 5. The Mohr circles for long-flame coal (a) and variation of safety pillar's width (b) at depth of 200m – 600 m.

For the case illustrated in **Figure 5 b**, it can be concluded that thermal stresses will lead to the destruction of the pillar on the side of the UCG reactor only at a depths of 200 mand 300 m, since for these depths the peak stress line cuts off part of the coupled compressive stress curve. The fracturing zone is only a few centimeters. On the side of the worked out cavity, at depths of 500 m and 600 m, coal fracturing is observed, which leads to a decrease in the safety of the pillar's width. The width of the fracturing zone at a depth of 500 m is 3.4 m, and at a depth of 600 m - 6.1 m. The safety pillar's width is reduced on the mentioned values, which should be taken into account during designing of the pillars. However, the main reason for this is mechanical stress. Thus, it can be concluded that for the conditions considered in the article, thermal destruction of coal in the walls of the UCG reactor does not significantly reduce the safety pillar's width.

5. Conclusions

This study was focused on the issue of the calculation of safety pillar's width in Underground Coal Gasification. Thermo-mechanical stresses in the coal pillar were studied. Specific attention is paid to the area of the coal pillar near the UCG reactor. Mohr's theory is proposed to predict the failure of a coal pillar at different depths. Based on the results of this investigation, the following conclusions can be drawn:

- (1) In the coal pillar from the UCG reactor side, two processes causing destruction are observed. The first one is thermal destruction as the result of temperature increase. The second one is mechanical fracturing of coal caused by its expansion in a result of heating, i.e. thermal stress. The depth of the thermal destruction zone does not exceed 30 cm. The depth of the destruction zone caused by thermal stress is about 10 cm. Thus, it can be concluded that for the conditions considered in the paper, thermal destruction of coal in the walls of the UCG reactor does not significantly reduce the safety pillar's width.
- (2) In the coal pillar on the side of the worked out cavity, the fracturing of the pillar was caused by the abutment pressure increased as a result of the collapse of rocks above the gasification cavity in the post-gasification period. When calculating the safety pillar's width, it should be taken into account that mechanical stress increases with depth. The results of the study showed that with a designed width of 30 m, at depths of 500 and 600 m, the safety pillar's width decreases to 26.6 and 23.9 m, respectively. The reason for this is the fracturing of coal in the zone of increased stresses.

6. References

- Allam, Z., Bibri, S.E., & Sharpe, S.A. (2022). The Rising Impacts of the COVID-19 Pandemic and the Russia–Ukraine War: Energy Transition, Climate Justice, Global Inequality, and Supply Chain Disruption. *Resources*, 11, 99. https://doi.org/10.3390/resources11110099.
- Dychkovskyi, R., Falshtynskyi, V., Saik, P. Lozynskyi, V., Sala, D., Hankus, Ł., Magdziarczyk M. & Smoliński, A. (2025). Control of contour evolution, burn rate variation, and reaction channel formation in coal gasification. *Sci Rep 15*, 9075. https://doi.org/10.1038/s41598-025-93611-3.
- Jiang, Y., Chen, B., Teng, L., Wang, Y., Xiong, F. (2024). Surface Subsidence Modelling Induced by Formation of Cavities in Underground Coal Gasification. *Applied Sciences*, 14, 5733. https://doi.org/10.3390/app14135733.
- Hoek, E., Carranza-Torres, C., Corkum, B. (2002). Hoek-Brown failure criterion—2002 edition. In Proceedings of the 5th North American Rock Mechanics Symposium and the 17th Tunnelling Association of Canada Conference, NARMS-TAC, Toronto, ON, Canada, 7–10 July 2002, 267–271.
- Kostúr, K., Łaciak, M. & Durdan, M. (2018). Some influences of underground coal gasification on the environment. *Sustainability 10*, 1512. https://doi.org/10.3390/su10051512.
- Laouafa, F., Farret, R., Vidal-Gilbert, S. & J-B. Kazmierczak (2016). Overview and modeling of mechanical and thermomechanical impact of underground coal gasification exploitation. *Mitigation and Adaptation Strategies for Global Change 21*, 547–576. https://doi.org/10.1007/s11027-014-9542-y.
- Li, H., Guo, G., Zha, J., Yuan, Y., Zhao, B. (2015). Research on the surface movement rules and prediction method of underground coal gasification. *Bulletin of Engineering Geology and the Environment*, 75(3), 1133-1142. https://doi.org/10.1007/s10064-015-0809-7.Lozynskyi, V., Falshtynskyi, V., Kozhantov, A., Kieush, L., & Saik, P. (2024). Increasing the underground coal gasification efficiency using preliminary electromagnetic coal mass heating. *IOP Conf. Ser.: Earth Environ. Sci. 1348*, 012045. https://doi.org/10.1088/1755-1315/1348/1/012045/.
- Najafi, M., Jalali, S.M.E., KhaloKakaie, R. (2014). Thermal–mechanical–numerical analysis of stress distribution in the vicinity of underground coal gasification (UCG) panels. *International Journal of Coal Geology*, 2014,134–135, 1–16. https://doi.org/10.1016/j.coal.2014.09.014.
- Otto, C., & Kempka, T. (2015). Thermo-Mechanical Simulations of Rock Behavior in Underground Coal Gasification Show Negligible Impact of Temperature-Dependent Parameters on Permeability Changes. *Energies*, 8(6), 5800-5827. https://doi.org/10.3390/en8065800.
- Saik, P.B., Dychkovskyi, R.O., Lozynskyi, V.H., Malanchuk, Z.R., & Malanchuk, Ye. Z. (2016). Revisiting the underground gasification of coal reserves from contiguous seams. *Nauk. Visn. NHU*, *6*, 60–66.
- Sakhno, I.G., Molodetskyi, A.V. & Sakhno, S.V. (2018) Identification of material parameters for numerical simulation of the behavior of rocks under true triaxial conditions. Naukovyi Visnyk NHU, № 5, pp. 48-53.
- Sakhno, I., Sakhno, S., Skrzypkowski, K., Isaienkov, O., Zagórski, K., & Zagórska, A. (2024). Floor Heave Control in Gob-Side Entry Retaining by Pillarless Coal Mining with Anti-Shear Pile Technology. *Applied Sciences*, 14(12), 4992. https://doi.org/10.3390/app14124992.
- Sakhno, I., Sakhno, S., & Vovna, O. (2025). Surface Subsidence Response to Safety Pillar Width Between Reactor Cavities in the Underground Gasification of Thin Coal Seams. *Sustainability*, 17(6), 2533. https://doi.org/10.3390/su17062533.
- Seifi, M., Chen, Z., Abedi, J. (2015). Large scale simulation of UCG process applying porous medium approach. *Can. J. Chem. Eng.* 93, 1311–1325. https://doi.org/10.1002/cjce.22218.
- Song, J., Sun, Y., & Liu, Y. (2024). Study on the Thermal Expansion Characteristics of Coal during CO2 Adsorption. *Processes*, 12(6), 1229. https://doi.org/10.3390/pr12061229.
- UNFCCC. Glasgow Climate Pact; UNFCCC: 2021; pp. 1–10. Available online: https://unfccc.int/sites/default/files/resource/cma2021_10_add1_adv.pdf (accessed on 10 June 2025).
- URL 1. https://www.iea.org/energy-system/fossil-fuels/coal (accessed on 10 June 2025).
- Wang, R., Su, X., Yu, S., Su, L., Hou, J., & Wang, Q. (2023). Experimental Investigation of the Thermal Expansion Characteristics of Anthracite Coal Induced by Gas Adsorption. *Adsorption Science & Technology*. 2023. https://doi.org/10.1155/2023/5201794.
- Zhang, L., Mao, X., Liu, R. Guo, X., Ma, D. (2014). The Mechanical Properties of Mudstone at High Temperatures: an Experimental Study. *Rock Mechanics and Rock Engineering*, 47, 1479–1484. https://doi.org/10.1007/s00603-013-0435-2.
- Zhang, C., Tu, S., Zhao, Y. (2019). Compaction characteristics of the caving zone in a longwall goaf: A review. Environ. Earth Sci., 78, 27. https://doi.org/10.1007/s12665-018-8037-7.

Acknowledgment

The authors are grateful to the administration of Technical University "Metinvest Polytechnic" LLC for supporting this research.

Funding

This research received no external funding.

Author's contribution

Svitlana Sakhno (associate professor): conceptualization, investigation, methodology, software and writing – review. **Ivan Sakhno** (professor): project administration, resources, software, supervision and writing – original draft. **Serhii Bashynskyi** (associate professor): formal analysis, visualization and editing. **Munkhtsetseg Oidov** (associate professor) methodology, validation and editing.



Examples of comparative measurements of active concentration of radon (Rn) in air in Croatia

DIM-ESEE Conference 15th – 17th October 2025, Dubrovnik, Croatia



Hrvoje Vukosic¹* [®]⊠, Željko Ban² [®]⊠, Dalibor Kuhinek¹ [®]⊠, Želimir Veinović¹ [®]⊠

¹ University of Zagreb, Faculty of Mining, Geology and Petroleum Engineering, Pierottijeva 6, 10000 Zagreb, Croatia

² University of Zagreb Faculty of Electrical Engineering and Computing, Department of Control and Computer Engineering, Unska 3, 10000 Zagreb, Croatia

Abstract

Radon (²²²Rn) is a chemically inert (noble) gas, present in soil, water, and air, a natural radionuclide, with generation and decay through radioactive decay chain of radium ²²⁶Ra in the uranium (²³⁸U) series. As alpha emiter radon gas poses a significant health risk and is included in the parameters of air quality in enclosed spaces. Therefore, it is necessary to identify locations and objects with elevated levels (parts of buildings and mines where people reside or work), which can only be achieved by the measurement of the active concentration of radon. Goal of this research was to compare example results from different measurement instrements. In this paper examples of several measurement results are presented. Measurements were performed at several micro-locations, including faculty building rooms and Santa Barbara mine in Croatia. Several different instruments were used in measurements, and the results were analyzed with basic statistical methods.

Keywords: air quality in mines, Rn radon in air, comparative measurements, statistical methods.

1. Introduction

Radon (Rn) occurs as a chemically inert (noble) gas, the heaviest gas by molar mass in nature, present in soil, water, and air. Rn is a natural radionuclide, with generation and decay through radioactive decay of radium 226 Ra in the uranium, 238 U, series, with a half-life of $T_{1/2}$ =3.823 days and a decay constant λ_{Rn} = 2.0984·10⁻⁶ s⁻¹. During this process, ionizing radiation is emitted as α - (alpha) particles (the nucleus of a helium atom with an electric charge of +2e), and this can be detected electrically (**George, 2008; 'Nuclear Data** – **Table', n.d.).** In the following text, prevailing radon isotope 222 Rn will be simply referred to as 'Rn'.

Under normal conditions, Rn represents the largest source of the total dose of ionizing radiation that a person receives over the year, and is a significant parameter of air quality (eng. Indoor air quality/IAQ) (Joshi, Aswal, & Chandra, 2024). Rn poses a significant health risk since it can be inhaled as a gas and the chain of radioactive decay of Rn atoms ends with lead (206Pb) ('Health Physics', n.d.). For this reason, Rn is included in the parameters of air quality in enclosed spaces, as concentrations in open spaces are very low. Measurements of Rn active concentrations are conducted at microlocations and are most reliable and accurate in the long term (1 year), which requires a large number of measurements and a long time for conducting the measurements. (Font et al., 1999; Tsapalov & Kovler, 2024) The active concentration of Rn is measured in Bq/m³ or pCi/l (1 Bq/m³ = 0.027 pCi/l). Reference level for the annual average active concentration in the air is 300 Bq/m³, which is the highest allowed annual average value of active concentration in indoor air. ('Directive 2013/59/Euratom - EU-OSHA', n.d.). Measuring radon is also applied in predicting earthquakes or volcanic activity, exploring uranium ores, locating underground tectonic faults, monitoring the migration of underground gases over large distances, groundwater, and monitoring atmospheric circulation (Röttger et al., 2022).

Rn in buildings comes from soil gas, groundwater, outdoor air, and water and gas installations, and is transported/migrates over greater distances. The concentrations of Rn in the air (within a closed building) are variable as they depend on several influences, such as atmospheric conditions, geological composition of the soil, construction properties, seismic activity of the area/location, and ventilation. (Carslaw, 2007; Hess, 1953)

The (active) concentration of Rn is measured passively (for long-term) and actively (for short-term measurements) in several ways by detecting alpha particles (Bayrak et al., 2013; Elísio & Peralta, 2020; Gutiérrez et al., 2004; Sofia Clareu Elísio & Luís Peralta, 2019):

- 1. Passive: e.g., solid state nuclear track detectors (SSNTD),
- Active e.g.:
 - with a semiconductor Si photodiode / Si semiconductor surface barrier detector,
 - pulse ionization chamber,
 - electrostatic charge accumulation,
 - Lucas scintillation cells.

Activity concentration of Rn can be expressed through the mass balance law of conservation of mass in the system.

Rn radiation decay is described by a cumulative sum according to ideal decay model Equation (1):

$$N_{\text{active}}(t) = N_0 * (1 - e^{-\lambda_{Rn} * t})$$
 (1)

where are:

t - time interval θ - t

 $N_{\text{active}}(t)$ - number of decayed Rn atoms in time interval t

 N_0 - number of Rn atoms at t=0

 λ_{Rn} - Rn decay constant 2.0984·10⁻⁶/s = 0.1813/day with half-life $T_{1/2 Rn}$ = 3.8232 days.

Accumulated active concentration in a closed system is stable and constant after time period dependent on $\lambda(T_{1/2})$ and is called saturation concentration. According to mass balance/conservation of mass law and then rate of generation of Rn atoms is equal to rate of decay which is active concentration in volume of space according to **Equation (2)**:

$$N_{0-1\text{day}} = N_{\text{active-n.day}} \tag{2}$$

where are:

 $N_{0-1\text{day}}$ - number of Rn atoms generated from Ra source material in 1 day,

 $N_{\text{active-n.day}}$ - number of decayed/active Rn atoms in 1 day after n days in saturation.

Goal of this paper is to show results of some Rn measurements indoor and in mines with different instruments, which are conducted to develop model which aims to reduce the number and time of measurements needed to determine the long-term level of active concentration and to improve and innovate at least one part of the existing research that deals with determining and predicting changes in the indoor active concentration of Rn (buildings and mines). (Health -Kirkby et al., 2006; Janik et al., 2012; Mphaga et al., 2024; Nunes & Curado, 2023)

2. Methods

Over the past 2 years, around 30 measurements of Rn active concentration in air have been performed:

- indoors at RGN faculty buildings rooms,
- at St. Barbara mine, a remote corridor in the tunnel,
- saturation measurement inside enclosed boxes with different volumes of about 0.005 m³ to 0.02 m³ (5 l to 20 l) with source of Ra.

Rooms where measurements have been performed were:

- less closed with very little ventilation or more open/well-ventilated,
- mining tunnel in Sv. Barbara mine with natural geological walls with very little ventilation and very stable atmospheric/meteorological conditions,
- completely enclosed without ventilation or air exchange (saturation box).

The duration of the measurements ranged from 2 days to 3 months.

The aims of the measurements have been:

- get acquainted with the form of time change of Rn concentration,
- try to determine the specific pattern of change in Rn and the density distribution of the number of counts occurrence probability, and the magnitude/amplitude of the concentration,
- determine the mean values and maximum of Rn concentration,
- determine the correlations with atmospheric/meteorological parameters: pressure, temperature and humidity inside and outside the room, by height inside the room and different geological or building materials, day/night, seasons, rain/dry, frozen ground/thaw at a temperature above 0 °C,
- attempt to determine/quantify the legality of the change in Rn in relation to: atmospheric/meteorological parameters, by height inside the room and different geological or building materials, day/night, seasons, rain/dry, frozen ground/thaw at a temperature above 0 °C,
- clarify whether it is possible to determine the long-term mean value of Rn concentration with measurements of a few days (48 hours),
- study different methods/technologies for detecting and measuring Rn concentration and try to develop a new device for measuring Rn concentration,
- study the literature and the approach and problems that arise in measuring and determining the dose of Rn radiation,
- measure the deviations of the results of different types of instruments and the scattering of the results when measuring under the same conditions.

- 7	Fable 1. Instruments for the	e measurement of Rn	active concentration in	air
DEVICE MODEL:	1.Bertin AlphaE	2. RadonEye RD200	3. Sarad Home Scout	4. Radonova Robin ² sensor
Application	indoor (low concentration in buildings), outdoor (underground environment)	Internal, short-term	long-term monitoring of radon indoors, concentration in the air (homes)	Indoor and outdoor (underground environment)
Duration of measurement	Long-term, short-term, continuous	short-term, continuous	Long term	Long-term, short-term, continuous (converts concentration into proportional output analog voltage signal)
Detection Mode	Silicon Semiconductor Diode Diffusion Chamber	Dual pulsed ionization chamber	Semiconductor Silicon Detector	Filtered diffusion in high-voltage Comoros - alpha spectrometry
MEASUREMENT RANGE (Bq/m³)	20 - 10·10 ⁶ (10 MBq/m³)	7 - 3,700	1 - 1·10 ⁶ (1 MBq/m ³)	0 - 4000

3. Results

3.1. Measurement results No. 1.

Measurement No. 1 was conducted to determine saturation inside enclosed boxes with volume of around 0.005 m³ (5 l) with source of Ra - completely enclosed without ventilation or air exchange. All three instruments were recording measurements simultaneously and each measurement lasted 473.5 hours. Basic parameters and results are presented in **Table 2.** and **Figure 1.**

Table 2. Parameters for measurement No. 1.

Measurement ID	250607_36							
Location	RGNf building, room 207, 2	RGNf building, room 207, 2 nd floor, enclosed box 51						
Instruments	1. Bertin AlphaE (AE2)	2. RadonEye RD200	3. Radonova Robin ² sensor					
Start of measurement	12.6.2025 16:15:00							
(dd.mm.yyyy hh:mm)								
End of measurement	2.7.2025 9:45:00							
(dd.mm.yyyy hh:mm)								
Duration of measurement	19.43 days	473.5 hours						

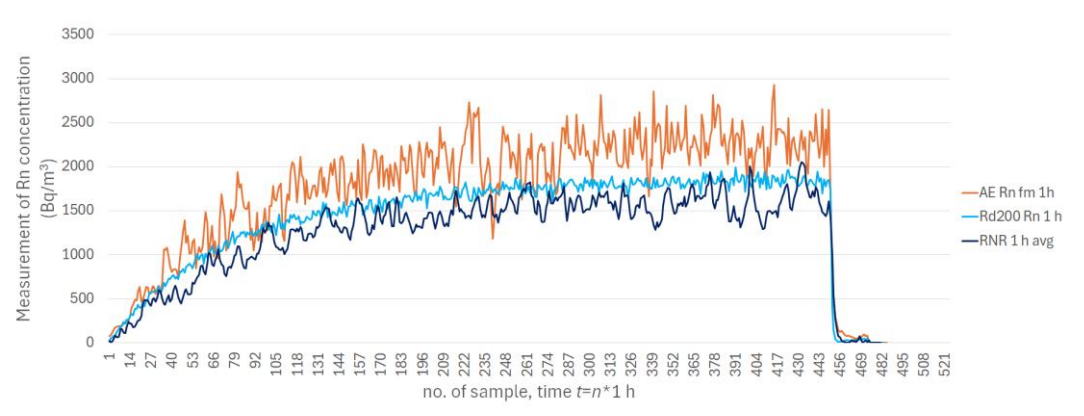


Figure 1. Measurements of Rn concentration No. 1.

Legend for Figure 1. shows Rn floating mean or Rn average value for each 1 hour of measurement for the three used instruments:1. Bertin AlphaE (AE), 2. RadonEye RD200 (Rd200) and 3. Radonova Robin² (RNR).

3.2. Measurement results No. 2. and No. 3.

Measurement No. 2. and No. 3. were performed in rooms with natural ventilation (window partially open part or all day, opening doors, multiple glass surfaces with slightly permeable sealing – PVC windows), lower concentration values were generally measured, examples in 2 rooms.

Measurement No. 2. parameters and results are presented in **Table 3.** and **Figure 2.** Measurement No. 3. parameters and results are presented in **Table 4.** and **Figure 3.** Measurement No. 2. was performed in RGNf building, room 207, 2nd floor and measurement No. 3. was performed in RGNf building basement, spectroscopy lab.

Table 3. Parameters for measurement No. 2

Measurement ID	240304 015					
Location	RGNf building, room 20	RGNf building, room 207, 2 nd floor				
Instrument	Bertin AlphaE AE1					
Start of measurement	18.3.2024 15:10	dd.mm.yyyy hh:mm				
End of measurement	12.4.2024 8:20	dd.mm.yyyy hh:mm				
Duration of measurement	24.7 days	593.2 hours				

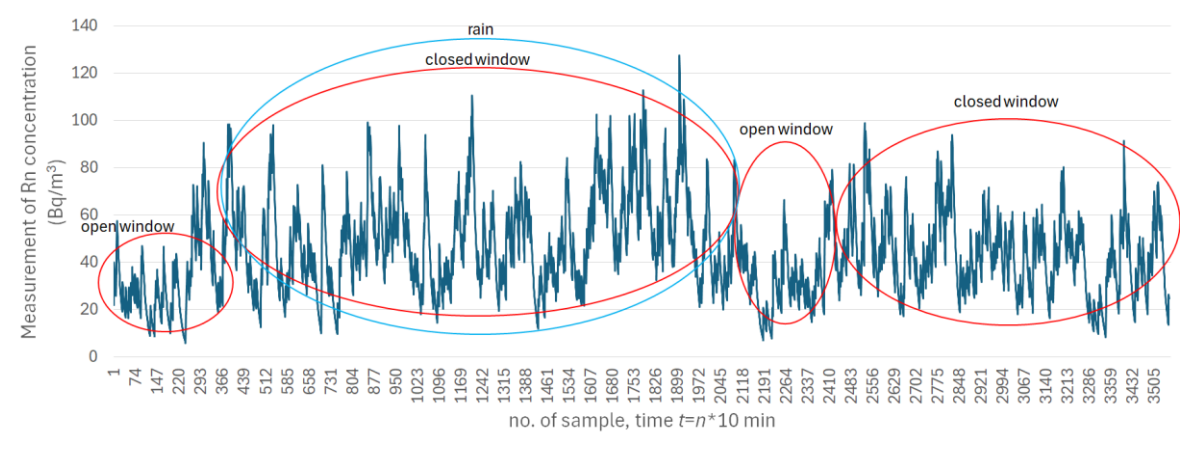


Figure 2. Measurement of Rn concentration for measurement No. 2.

Table 4. Parameters for measurement No. 3.

Measurement ID	250304_25_5					
Location	RGNf building, basement, s	RGNf building, basement, spectroscopy lab				
Instrument	Bertin AlphaE (AE1)					
Start of measurement	21.3.2025 10:40	dd.mm.yyyy hh:mm				
End of measurement	10.4.2025 8:00	dd.mm.yyyy hh:mm				
Duration of measurement	19.9 days	478.5hours				

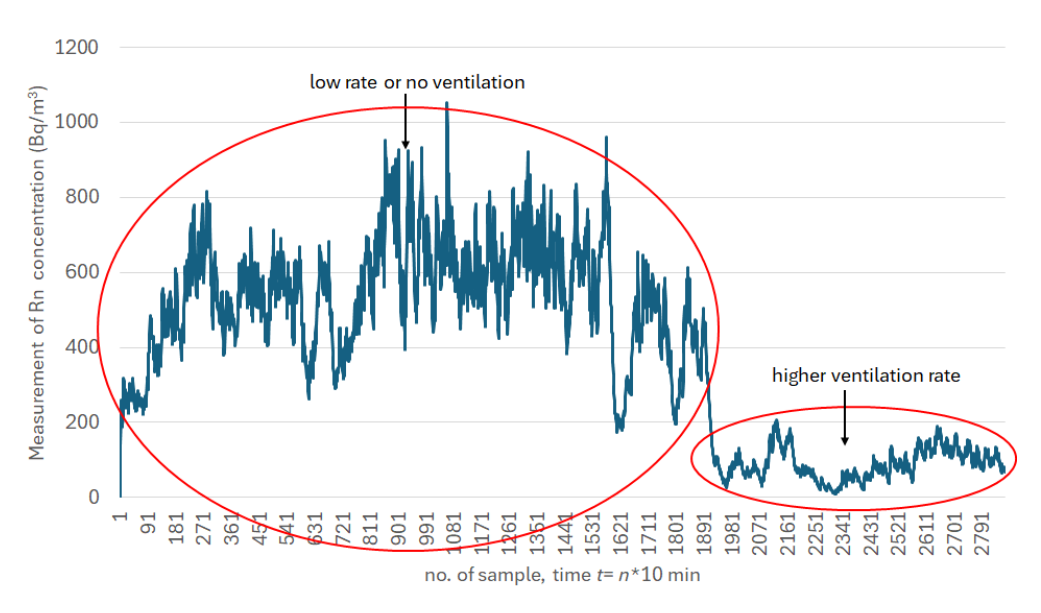


Figure 3. Measurement of Rn concentration for measurement No. 3.

Descriptive statistics parameters for measurement No. 2. and No. 3 are presented in **Table 5**. Measurement No. 3. is divided into two parts/data sets: No. 3.1. and No. 3.2., because of significant change in ventilation rate. Coefficient of variation (CV) is the ratio of the standard deviation to the mean/average value as percentage.

Table 5. Descriptive statistics for measurements No. 2. And No. 3.

Measurement	No. 2.	No. 3.1 (sample no. 1-1912)	No. 3.2 (sample no. 1913-2865)
Mean	44.69 Bq/m^3	535.23 Bq/m ³	89.83 Bq/m ³
Standard Deviation	19.15 Bq/m^3	154.70 Bq/m^3	40.87 Bq/m^3
Coefficient of Variation	42.85 %	28.95 %	45.50 %
Range	121.5 Bq/m ³	1052 Bq/m^3	199.5 Bq/m ³
Minimum	6 Bq/m ³	143.5 Bq/m^3	8.5 Bq/m ³
Maximum	127.5 Bq/m ³	1052 Bq/m^3	208 Bq/m ³
Count	3555	1912	953
Confidence Level (95.0 %)	0.63	6.94	2.60

3.3 Measurement result No. 4.

Measurement No. 4. was performed inside mining tunnel in Sv. Barbara mine with natural geological walls with some ventilation and very stable atmospheric/meteorological conditions. Basic parameters and results are presented in **Table 6** and **Figure 4**.

Table 6. Parameters for measurement No. 4.

	14010 00 1 0101111000	TO TOT INCOME ON CONTROL TO CO.				
Measurement ID	240709_024					
Location	Corridor of mining tunnel i	Corridor of mining tunnel in Sv. Barbara mine				
Instrument	Bertin AlphaE (AE1)					
Start of measurement	10.7.2024 16:10	dd.mm.yyyy hh:mm				
End of measurement	12.9.2024 20:30	dd.mm.yyyy hh:mm				
Duration of measurement	64.2 days	1540 hours				

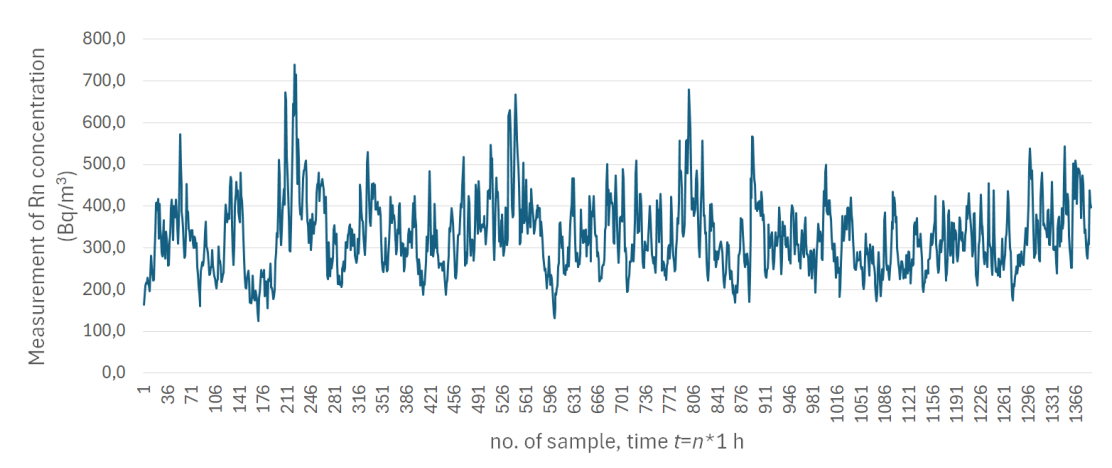


Figure 4. Measurement of Rn concentration for measurement No. 4.

Descriptive statistics parameters for measurement No. 4. re presented in **Table** 7.

Table 7. Descriptive statistics for measurement No. 4.

Mean	327.3 Bq/m ³
Standard Deviation	87.32 Bq/m^3
Coefficient of Variation	26.68 %
Range	613.2 Bq/m ³
Minimum	125.4 Bq/m^3
Maximum	738.7 Bq/m ³
Count	1388
Confidence Level (95.0%)	4.60

4. Discussion

Presented results of measurements of Rn saturation concentration in model of closed system from measurement No. 1. shows that all three instruments are approaching to some final concentration. The final concentration is calculated and presented in **Table 8**. The result is obtained as mean/average of measurements from last 24 hours (24 averages of 1 hour

measurements) before opening the box. Mean/average for all three instruments saturation concentration is equal to 1938 Bg/m^3 .

Table 8. Comparison	of the measured	I saturation concents	rations by instrum	ents in meas	urement No. 1
Table 6. Companson	or the ineasured	i Saturanon Concenti	lauons ov msuun	ichis ili ilicas	outement no. 1.

Instrument	Calculated saturation	Relative difference to
	concentration (Bq/m ³)	mean/average value (%)
1. Bertin AlphaE (AE2)	2293	18.3
2. RadonEye RD200	1830	-5.57
3. Radonova Robin² sensor	1691	-12.8
Mean/average value of measurements	1938	

Variations exist even in completely enclosed boxes (saturation measurement) without any ventilation and without external migration of Rn atoms, which is due to changes in meteo/atmospheric parameters outside and inside the box and non-linearity of microlocation migration and radiation decay.

Table 9. Comparison of descriptive statistics parameters by instruments in measurement No. 1.

Instrument	Mean (Bq/m ³)	Standard Deviation (Bq/m³)	Coefficient of Variation	Minimum (Bg/m³)	Maximum (Bq/m³)
1. Bertin AlphaE (AE2)	2293	254.5	11.1 %	1704	3096
2. RadonEye RD200	1830	52.7	2.9 %	1694	1942
3. Radonova Robin² sensor	1691	189.8	11.2 %	1426	2049

Graphical comparison of descriptive statistical parameters for measured saturation concentrations by instruments is presented in **Figure 5.** Graphical comparisonwhere red line is the average and black line is plus, minus two times standard deviation.



Figure 5. Graphical comparison of descriptive statistics parameters in measurement No. 1.

In interpretation of result in measurement No. 1. which lasted for around 473.5 hours (around 20 days), instrument Bertin AlphaE (AE2) had positive difference to mean/average from all three instruments equal to 18.32 % and Radonova Robin² sensor had negative difference equal to -12.7 5%. Standard deviation (SD) for instrument RadonEye RD200 is smallest and equal to 52.7 Bq/m³. SD for instrument Bertin AlphaE AE2 was around 4.8 times larger and for instrument Radonova Robin² sensor and was around 3.6 times larger than the smallest SD for instrument RadonEye RD200. Coefficient of variation (CV) for instrument RadonEye RD200 was equal to 2.88 which is around 4 times less than two other instruments.

In interpretation of the results in measurement No. 2. and No. 3. which lasted around 600 and 480 hours (around 25 and 20 days) were performed with only one instrument Bertin AlphaE (AE1), it can be seen that measurements have high variation (range) from lowest to highest level. Lower levels were measured in rooms with higher ventilation rate or when windows or doors had been opened. Higher levels were measured in rooms with low ventilation rates.

In measurement No. 3 there are two very different parts of concentrations measurement, first with no ventilation (No. 3.1.) and second with higher ventilation (No. 3.2.). This resulted in very different mean/average values, where mean value for No. 3.1. is equal to 535.23 Bq/m³ and standard deviation is equal to 154.70 Bq/m³ (CV equal to 28.95 %) and for No.

3.2. mean value is equal to 89.83 Bq/m³ and standard deviation is equal to 40.87 Bq/m³ (CV equal to 45.50 %). We can compare measurement No. 3.2 to measurement No. 2 which has smaller variations with mean value equal to 44.69 Bq/m³, standard deviation is equal to 19.15 Bq/m³ (CV equal to 42.85 %).

In measurement No. 4. inside mining tunnel in Sv. Barbara mine with natural geological walls with some ventilation and very stable atmospheric/meteorological conditions, which lasted around 1540 hours (around 64 days), mean/average value is equal to 327.31 Bq/m³ and standard deviation is equal to 87.33 Bq/m³ (CV equal to 26.68).

Significant variations between low and high levels (large SD and CV values) seem to be dependent on ventilation rate and rain as precipitation which cause significant changes in concentrations. In closed system (as in measurement No.1) CV has a few times lesser values, as these external processes are blocked out. In open system with more stable atmospheric conditions such as the Sv.Barbara mine in measurement No. 4. (almost constant temperature and relative humidity at 100 % with only air pressure variations) and measurement No. 3.1., SD and CV had smaller values compared to more open systems (higher ventilation rate) such as in measurements No. 2 and No. 3.2.

5. Conclusions

Data analysis leads to a conclusion that in measurement No. 1 of saturation in a closed system, different instruments show similar but different values for saturation concentration. The rate of change is similar.

Variations of concentrations are statistically described by standard deviation and coefficient of variation and are dependent on how each instrument integrates floating mean/average values with changing/increasing reference concentration values plus variations due to changes in meteo/atmospheric parameters outside and inside the box and non-linearity of microlocation migration and radiation decay. Instrument RD200 has the least standard deviation and coefficient of variation, and also its measurement is closest to the average of all three instruments (CV equal to 2.88 % and relative difference to mean/average value -5.57 %), making it suitable for preliminary assessments.

From other measurements (No. 2., No. 3. and No. 4.) of open systems it seems that the more open system is (more changing parameters and ventilation rate), larger standard deviation and coefficient of variation can be expected. CV in measurements No.2 and No.3.2. were 42.85 % and 45.50 %. In open system with no or low ventilation such as in measurement No. 3.1., CV was equal to 28.95 %, or more stable atmospheric conditions such as the Sv.Barbara mine (almost constant temperature and relative humidity at 100% with only air pressure variations), CV was equal to 26.68 %.

Larger mean/average values can be expected in rooms closer to the ground or underground and with low ventilation rates (such as in basements and in mines). In basement room measurement No. 3.1 mean/average value was equal to 535.2 Bq/m³, and within Sv. Barbara mine corridor in measurement No. 4 mean/average value was equal to 327.3 Bq/m³.

Lower mean/average values can be expected in rooms with higher ventilation rates (rooms with more frequent opening of windows or doors), such as in room in measurement No. 2 with mean/average value equal to 44.7 Bq/m³.

In measurement No. 3 there were two very different parts of the measurement where mean concentration dropped from 535.2 Bq/m³ for part No 3.1. to 89.83 Bq/m³ for part No. 3.2. within around 4.5 hours (approx. from sample no. 1912 to sample no. 1939, sample time was equal to 10 min.).

6. References

- Bayrak, A., Barlas, E., Emirhan, E., Kutlu, Ç., & Ozben, C. S. (2013). A complete low cost radon detection system. *Applied Radiation and Isotopes*, 78, 1–9. doi:10.1016/j.apradiso.2013.03.054
- Carslaw, N. (2007). A new detailed chemical model for indoor air pollution. *Atmospheric Environment*, 41(6), 1164–1179. doi:10.1016/J.ATMOSENV.2006.09.038
- Directive 2013/59/Euratom protection against ionising radiation | Safety and health at work EU-OSHA. (n.d.). Retrieved 28 May 2025, from https://osha.europa.eu/en/legislation/directives/directive-2013-59-euratom-protection-against-ionising-radiation
- Font, L. L., Baixeras, C., Domingo, C., & Fernandez, F. (1999). Experimental and theoretical study of radon levels and entry mechanisms in a mediterranean climate house. *Radiation Measurements*, 31(1–6), 277–282. doi:10.1016/S1350-4487(99)00110-9
- George, A. C. (2008). World History Of Radon Research And Measurement From The Early 1900's To Today. *AIP Conference Proceedings*, 1034(1), 20–33. doi:10.1063/1.2991210

- Groves-Kirkby, C. J., Denman, A. R., Crockett, R. G. M., Phillips, P. S., Woolridge, A. C., & Gillmore, G. K. (2006). Time-integrating radon gas measurements in domestic premises: Comparison of short-, medium- and long-term exposures. *Journal of Environmental Radioactivity*, 86(1), 92–109. doi:10.1016/J.JENVRAD.2005.07.008
- Gutiérrez, J. L., García-Talavera, M., Peña, V., Nalda, J. C., Voytchev, M., & López, R. (2004). Radon emanation measurements using silicon photodiode detectors. *Applied Radiation and Isotopes*, 60(2–4), 583–587. doi:10.1016/J.APRADISO.2003.11.080
- Health Physics. (n.d.). Retrieved 17 March 2025, from https://journals.lww.com/health-physics/abstract/1996/12000/Bayesian Prediction of Mean Indoor Radon.9.aspx
- Hess, V. F. (1953). Radon, Thoron, and their decay products in the atmosphere. *Journal of Atmospheric and Terrestrial Physics*, 3(3), 172–177. doi:10.1016/0021-9169(53)90103-2
- Janik, M., Łoskiewicz, J., Tokonami, S., Kozak, K., Mazur, J., & Ishikawa, T. (2012). Determination of the minimum measurement time for estimating long-term mean radon concentration. *Radiation Protection Dosimetry*, 152(1–3), 168–173. doi:10.1093/RPD/NCS217
- Joshi, M., Aswal, D. K., & Chandra, A. (2024). Radiation Protection Policies: Safeguarding Health and the Environment. *Handbook on Radiation Environment, Volume 1*, 385–415. doi:10.1007/978-981-97-2795-7_13
- Mphaga, K. V., Mbonane, T. P., Utembe, W., & Rathebe, P. C. (2024). Short-Term vs. Long-Term: A Critical Review of Indoor Radon Measurement Techniques. Sensors 2024, Vol. 24, Page 4575, 24(14), 4575. doi:10.3390/S24144575
- Nuclear Data Table Laboratoire National Henri Becquerel. (n.d.). Retrieved 25 June 2025, from http://www.lnhb.fr/home/nuclear-data/nuclear-data-table/
- Nunes, L. J. R., & Curado, A. (2023). Long-term vs. short-term measurements in indoor Rn concentration monitoring: Establishing a procedure for assessing exposure potential (RnEP). Results in Engineering, 17. doi:10.1016/J.RINENG.2023.100966
- Röttger, S., Röttger, A., Grossi, C., Vargas, A., Karstens, U., Cinelli, G., ... Radulescu, I. (2022). Radon metrology for use in climate change observation and radiation protection at the environmental level. *Advances in Geosciences*, 57, 37–47. doi:10.5194/ADGEO-57-37-2022
- Sofia Clareu Elísio, S., orientada por, D., & Luís Peralta, D. (2019). Development of an active detector for radon detection in air. Retrieved from https://repositorio.ulisboa.pt/handle/10451/39062
- Tsapalov, A., & Kovler, K. (2024). Metrology for Indoor Radon Measurements and Requirements for Different Types of Devices. *Sensors*, 24(2). doi:10.3390/S24020504

Author's contribution

Hrvoje Vukošić (assistant): conceptualization, data curation, formal analysis, investigation, writing – original draft, Željko Ban (professor): supervision, conceptualization, writing – review & editing, Želimir Veinović (assistant professor): supervision, conceptualization, methodology, writing – review & editing, Želimir Veinović (assistant professor): supervision, conceptualization, methodology, writing – review & editing,.

All authors have read and agreed to the published version of the manuscript.



Analysis of Drilling Parameters for Construction Pit Excavation

DIM-ESEE Conference

Siniša Stanković¹* ^{□⊠}, Vinko Škrlec¹, Mario Dobrilović¹, Mihaela Fajdetić¹



¹ University of Zagreb, Faculty of Mining, Geology and Petroleum Engineering, Pierottijeva 6, Zagreb, Croatia

Abstract

Drilling accuracy and geometry govern blasting outcomes in construction pits where perimeter control and vibration limits are strict. This study proposes a simple predictor that links drill pattern geometry to borehole diameter, allowing rapid first-pass design without explicitly specifying explosive type and quantity. A dataset from Croatian construction pits (Povlja, TC Koromačno, Kvarner Palace–Crikvenica, Dubrovnik, Vis, Visoka–Split) was cleaned using a two-sigma outlier rule and de-duplication, minimum/maximum depths were combined and depth normalized to 1 m in line with common powder-factor practice. For each blast, the burden–spacing product (Bs, m²) and borehole diameter (Φ , mm) were extracted. Linear regression yielded the predictor Bs = $0.0825 \cdot \Phi - 2.4859$ with R² = 0.7598 (n = 7 unique Φ –Bs pairs). Validation against measured Bs showed good agreement for most cases: five of seven predictions were within $0.78-1.10\times$ of measured values, with two outliers (Φ = 52 mm and 32 mm) at $3.68\times$ and $0.31\times$, respectively. The equation provides a transparent estimate of Bs that can be split into burden and spacing using customary B:s = 1:1-1:2 ratios, helping to seed designs for urban construction pits where drill quality and wall control dominate performance. While site-specific calibration, monitoring, and powder-factor adjustment remain essential, the predictor offers a practical starting point that can shorten early design cycles and support selection of drill diameter and pattern within excavation constraints.

Keywords: drilling, construction pit, excavation, predictor equation

Introduction

Drilling forms the backbone of all blasting operations and is the crucial link between explosive energy and controlled rock demolition. The accuracy, geometry and quality of drill holes determine not only the efficiency of rock crushing, but also the success of subsequent blasting operations, including wall stability, vibration control and excavation precision. Advances in top hammer, down-the-hole and rotary drilling systems, as well as improvements in bit design, automation and borehole deviation monitoring, have significantly improved the ability of engineers and contractors to match drilling patterns to geological conditions and project constraints (Epiroc, 2019). Effective drilling is therefore the key design variable through which the blasting engineer controls the burden, spacing, charge concentration and ultimately the degree of control over the excavation.

Drilling plays an even more important role in connection with construction pits. Excavations for foundations, shafts and underground infrastructure often require tight control of excavation walls, minimizing overbreak and reducing damage caused by blasting to protect adjacent structures and utilities. Federal and local specifications such as FHWA Rock Blasting and Overbreak Control and USACE EM 1110-2-3800 Blasting for Rock Excavations emphasize that drilling precision largely determine whether perimeter control methods as pre-splitting, smooth blasting, line drilling or buffer blasting, can achieve the intended performance. By combining detailed site characterization with tailored drilling patterns, practitioners are able to integrate vibration management, air pressure control, and safety considerations into blasting practices ((U.S.) & Administration, 1993; US Army Corps of Engineers, 2018).

While drilling and geometry provide the framework for successful blasting, the powder factor provides the energetic benchmark for matching explosive energy to rock volume. Defined as the ratio between the weight of the explosive and the rock volume or tonnage, the powder factor provides a link between drill design and fragmentation efficiency. The literature repeatedly shows that the powder factor must be adapted not only to the strength and structure of the rock, but also to the drilling accuracy and the sensitivity of the excavation environment (**Dyno**, 2017; **ISEE**, 1998; **USBM**, 1980). In excavation pits, the powder factor is often intentionally lowered in the contour holes to reduce damage, while adequate energy is maintained in the production holes to ensure fragmentation and displacement.

Taken together, these three dimensions, drilling accuracy, excavation geometry and control, and powder factor calibration, form the basis of modern blast design. By emphasizing drill quality, placing the design in the context of excavation constraints, and fine-tuning blast energy, engineers can achieve the twin goals of operational efficiency and excavation stability. To accelerate the determination of drilling parameters for newly acquired projects, we present a prediction equation based on previously performed drilling and blasting operations in construction pit excavations.

The role of drilling for blasting performance

Drilling is the most influential factor in determining the success of a blast. The geometry, accuracy and condition of the boreholes determine the burden, spacing and charge concentration, parameters that determine how the explosive energy interacts with the rock mass. Even the most carefully selected explosive cannot compensate for poorly drilled holes. Excessive deviation, inconsistent depth or spacing will directly lead to uneven fragmentation, risk of flyrock, overbreak and increased ground vibration. In contrast, precise drilling leads to predictable blasting results, optimal fragmentation and stable excavation walls.

Context and limitations of the construction pit

Construction pits are common in civil engineering projects such as basements and underground infrastructure. Unlike opencast mining, where space and vibration tolerances can be more flexible, excavation pits are often located in urban or infrastructure-rich environments. This proximity to sensitive structures, utilities and the public requires strict limits on vibration (Croatian Standards Institute, 2011), air blast and flying rock. In addition, the pit walls must remain stable and only break out minimally in order to maintain the geometry of the excavation and avoid costly support measures.

In this context, drilling accuracy and blasting design are not only technical considerations, but also contractual and legal obligations. Federal and local specifications such as the FHWA Rock Blasting and Overbreak Control, the USACE Blasting for Rock Excavations emphasize that excavation blasting must ensure both excavation progress and excavation quality.

Powder factor

The powder factor (PF) is the ratio of the explosive mass to the volume of the blasted rock. It is expressed in kilograms of explosive per cubic meter of rock, **Equation (1)**.

$$PF = \frac{Total\ explosive\ mass\ (kg)}{Rock\ volume\ (m^3)} \tag{1}$$

Powder factor can be calculated as PF per hole via **Equation (2)**. The Total explosive mass is replaced with explosive mass in the hole and rock volume is product of burden (B) Spacing (s) and depth (D) of the borehole.

$$PF = \frac{Explosive \ mass \ in \ the \ hole}{B \cdot s \cdot D} \ (kg/m^3)$$
 (2)

The powder factor is more than just a calculation and serves as a practical measure of how efficiently drilling and explosives are used to achieve the desired breakage. An optimal powder factor ensures adequate fragmentation, stable walls and cost-effective handling of the blasted material. In the literature, the powder factor is presented as a guideline, but not as an absolute design tool. In the classic studies of the U.S. Bureau of Mines (e.g. USBM RI 8507), guide values for the powder factor and relationships to vibrations were defined. The International Society of Explosives Engineers (ISEE) Explosives Handbook emphasizes field adjustment and points out that actual performance depends on variations in rock mass, drilling accuracy, and explosive type. FHWA guidelines reinforce the view that the powder factor should be calibrated through monitoring and field testing and not applied as a rigid design value. Sanchidrian et. al. described influence of Powder Factor vs. Delay on fragment size distribution curves (Sanchidrian et al., 2022). Ultimately, the powder factor is best understood as a mechanism for calibrating energy within the broader system of drilling accuracy and excavation control. It is not the primary driver of blasting success, but a refinement tool to balance fragmentation, excavation efficiency and wall integrity.

Predictor equation idea

The idea behind the research is to develop a predictor equation for calculating the drilling parameters for construction pit excavation without directly including the explosives. It was done in a similar way to the development of predictors for the blast-induced seismic effects. This would reduce the time required to perform the initial calculations with sufficient precision. The input data was taken from previously completed excavation projects throughout Croatia.

Input data

The data was collected at various locations in Croatia, including Povlja, TC Koromačno, Kvarner Palace in Crikvenica, Dubrovnik, Vis and Visoka (near Split). The complete dataset includes the number of blasts in a given project, borehole diameter Φ , minimum and maximum borehole depth for each blast, burden and spacing (Table 1).

Table 1. Complete dataset							
Construction pit	Blast area	Φ (mm)	Depth, min (m)	Depth max (m)	Burden (m)	Spacing (m)	
Povlja	MP-1	52	1.65	4.8	0.7	0.7	
TC Koromačno	MP-1	64	3	8.5	1.8	2.0	
TC Koromačno	MP-2	64	3	6	1.7	1.7	
TC Koromačno	MP-3	64	3	5.5	1.7	1.7	
TC Koromačno	MP-4	64	3	4.5	1.5	1.7	
Kvarner Palace Crikvenica	MP-1	82	4	4	2.0	2.0	
Kvarner Palace Crikvenica	MP-2	82	5	5	2.0	2.0	
Kvarner Palace Crikvenica	MP-3	82	5	5	2.0	2.0	
Kvarner Palace Crikvenica	MP-4	82	6	6	2.0	2.0	
Dubrovnik	MP-2	76	3.5	3.5	1.2	1.2	
Vis	MP-11	32	0.8	3.15	0.7	0.7	
Vis	MP-12	32	0.8	3.15	0.7	0.7	
Vis	MP-13	32	0.8	3.15	0.7	0.7	
Vis	MP-14	32	0.8	3.15	0.7	0.7	
Vis	MP-15	32	0.8	3.15	0.7	0.7	
Vis	MP-16	32	0.8	3.15	0.7	0.7	
Vis	MP-17	32	0.8	3.15	0.7	0.7	
Vis	MP-18	32	0.8	3.15	0.7	0.7	
Vis	MP-21	32	0.8	3.15	0.7	0.7	
Vis	MP-22	32	0.8	3.15	0.7	0.7	
Vis	MP-23	32	0.8	3.15	0.7	0.7	
Vis	MP-24	32	0.8	3.15	0.7	0.7	
Vis	MP-25	32	0.8	3.15	0.7	0.7	
Visoka,Split	MP-1	64	3	3	2.0	1.7	
Visoka,Split	MP-2	64	3	3	2.0	1.7	
Visoka,Split	MP-3	64	3	3	2.0	1.7	

The input data was cleaned in two steps. First, we excluded atypical values (outliers) using the sigma 2 rule (confidence interval 0.9545). Second, we removed all data with duplicate values within a given project and then from all remaining data in the table and combine minimum and maximum depth. The resulting values are shown in Table 2.

Construction pit	Blast area	Φ (mm)	Depth (m)	Burden (m)	Spacing (m)
Povlja	MP-1	52	1.65	0.7	0.7
Povlja	MP-1	52	4.8	0.7	0.7
TC Koromačno	MP-1	64	3	1.8	2.0
TC Koromačno	MP-2	64	3	1.7	1.7
TC Koromačno	MP-4	64	3	1.5	1.7
TC Koromačno	MP-4	64	8.5	1.5	1.7
TC Koromačno	MP-4	64	6	1.5	1.7
TC Koromačno	MP-4	64	5.5	1.5	1.7
TC Koromačno	MP-4	64	4.5	1.5	1.7
Kvarner Palace Crikvenica	MP-1	82	4	2.0	2.0

Kvarner Palace Crikvenica	MP-2	82	5	2.0	2.0
Kvarner Palace Crikvenica	MP-4	82	6	2.0	2.0
Dubrovnik	MP-2	76	3.5	1.2	1.2
Vis	MP-11	32	0.8	0.7	0.7
Vis	MP-11	32	3.15	0.7	0.7
Visoka,Split	MP-1	64	3	2.0	1.7

Since the value 1 m is generally used for the calculation of the powder factor for the depth of the borehole according to **Equation (2)**, it was excluded from the further procedure as the parameter that has the least influence on the result, thus final input values are shown in **Table 3**.

Table 3. Final input data

Table 3. Piliai input data								
Construction pit	Blast area	$\Phi \ (mm)$	Burden (m)	Spacing (m)				
Povlja	MP-1	52	0.7	0.7				
Povlja	MP-1	52	0.7	0.7				
TC Koromačno	MP-1	64	1.8	2.0				
TC Koromačno	MP-2	64	1.7	1.7				
TC Koromačno	MP-4	64	1.5	1.7				
TC Koromačno	MP-4	64	1.5	1.7				
TC Koromačno	MP-4	64	1.5	1.7				
TC Koromačno	MP-4	64	1.5	1.7				
TC Koromačno	MP-4	64	1.5	1.7				
Kvarner Palace Crikvenica	MP-1	82	2.0	2.0				
Kvarner Palace Crikvenica	MP-2	82	2.0	2.0				
Kvarner Palace Crikvenica	MP-4	82	2.0	2.0				
Dubrovnik	MP-2	76	1.2	1.2				
Vis	MP-11	32	0.7	0.7				
Vis	MP-11	32	0.7	0.7				
Visoka,Split	MP-1	64	2.0	1.7				

Development of the model

Model is presented as predictor equation for the dependence of the product of B and s (burden x spacing) on the borehole diameter Φ . The quantity of explosive is indirectly included in the drilling diameter.

The form of the equation we are looking for is:

$$B \cdot s = k \cdot \emptyset - b \tag{3}$$

where are:

B – burden (m),

s – spacing (m),

k and b - koeficients,

 Φ – Borehole diameter (mm).

To simplify the equation, the expression $B \times s$ is replaced by the single value of the product Bs (m²), so the above expression reads:

$$Bs = k \cdot \emptyset - b \tag{4}$$

The values of Φ and Bs were taken from the measurement study for excavation of construction pits. Than again duplicate values were removed. The values are listed in the **Table 4**:

Table 4. Values of Φ and Bs							
<i>Bs</i> (m ²)	0.49	3.6	2.89	2.55	4	0.49	3.4
Φ (mm)	52	64	64	64	82	32	64

The values from **Table 4** are entered into a scatter diagram in which the dependence of Bs on Φ is graphically represented (**Figure 1**). The dependency equation (predictor) and R^2 are also displayed.

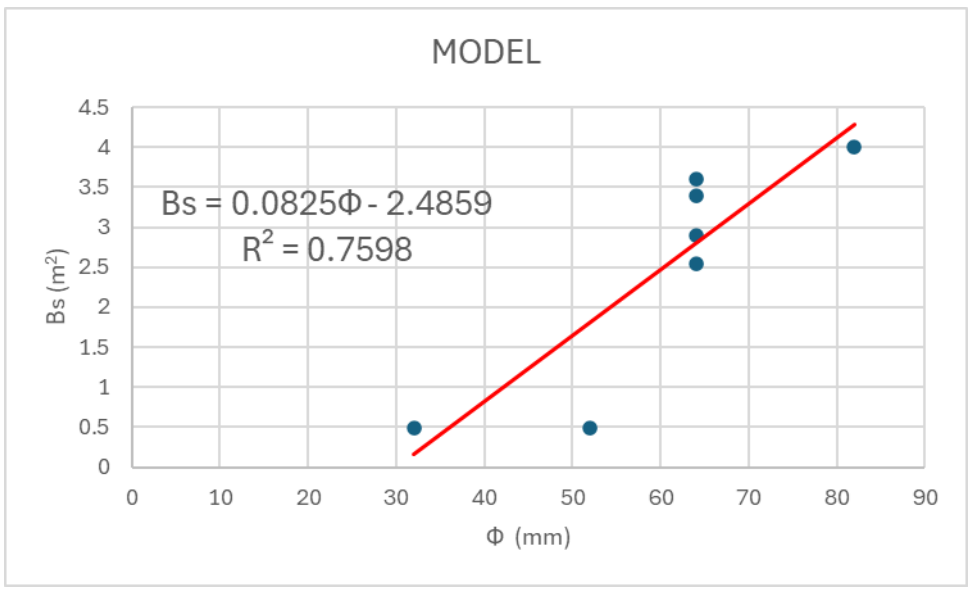


Figure 1. Dependence model

The developed equation (predictor) is:

Diff. (%)

368.18

77.61

$$Bs = 0.0825 \cdot \emptyset - 2.4859 \tag{5}$$

The R²=0.7598 which is relatively good value of coefficient of determination.

Results and discussion

From the single value *Bs*, as the final result we can calculate separate values due to the rule that the usual ratio of *B:s* can be between 1:1 and 1:2. However, for a clearer presentation, we will continue to use the single value. To validate result, the comparison between measured values and calculated values is done. We will expand Table 4 by filling the newly calculated values.

Table 5. Comparison of measured and calculated values							
<i>Bs</i> (m ²)	0.49	3.6	2.89	2.55	4	0.49	3.4
Φ (mm)	52	64	64	64	82	32	64
<i>Bs</i> ' (m ²)	1.80	2.79	2.79	2.79	4.28	0.15	2.79

109.57

106.98

31.45

82.18

From the **Table 5** it is visible that except calculated value in the first column (1.8 m²) which is 3.68 times larger than measured value and in sixth (0.15 m²) which is a third of the measured value, all the rest are between 0.77 and 1.09.

96.68

Using the linear predictor $Bs = 0.0825 \cdot \Phi - 2.4859$, we compared calculated values (Bs') with measured Bs from seven field cases (Table 5). Overall, the model captures the central tendency well but shows sensitivity at the extremes of borehole diameter

The predictor is a first-pass tool to seed patterns from a chosen Φ . Designers can then resolve B and s from Bs using a ratio r = B/s in the typical 1:1 to 1:2 range:

Conclusion

Drilling accuracy and geometry are the primary levers for controlled blasting in construction pits, where excavation quality and vibration limits dominate design. Using field data from multiple Croatian projects, we proposed a compact

predictor that links the burden–spacing product to borehole diameter, $Bs = 0.0825 \cdot \Phi - 2.4859$. Despite its simplicity, the model explained a substantial coefficient of determination ($R^2 = 0.7598$) and reproduced most measured cases in the common construction range (≈ 64 mm -82 mm) to within about ± 20 %, with two deviations at smaller diameters of 32 mm and 52 mm.

Practically, the predictor provides a rapid, transparent first-pass estimate of Bs that practitioners can split into B and s using customary ratios (B:s = 1:1-1:2), then refine through routine monitoring and site-specific adjustments. This shortens early design cycles, supports disciplined perimeter control, and offers a consistent starting point when project constraints or available drill bits diameter.

The main limitations are the modest sample size, clustering around 64 mm holes, and omission of covariates known to influence pattern design (rock mass quality, hole deviation, etc.). Future work should expand the dataset across lithologies.

Overall, the proposed relation is not a replacement for field calibration, but a useful basic model that improves design efficiency while maintaining the excavation stability and safety standards required in urban construction pits.

References

(U.S.), N. H. I., & Administration, U. S. F. H. (1993). Rock blasting and overbreak control. In *TA - TT -*. U.S. Dept. of Transportation, Federal Highway Administration. https://doi.org/ LK - https://worldcat.org/title/31163835 Croatian Standards Institute. (2011). *DIN 4150 Vibracije u građevinama – 3. dio: Djelovanje na konstrukcije*. Croatian Standards Institute.

Dyno. (2017). Explosives Engineers Guide, Dyno Consult, Dyno Nobel Asia Pacific Pty Ltd., 52.

Epiroc. (2019). Drilling in surface mining, quarrying and construction.

ISEE. (1998). Blasters' Handbook.

Sanchidrián, J. A., Segarra, P., Ouchterlony, F., & Gómez, S. (2022). The Influential Role of Powder Factor vs. Delay in Full-Scale Blasting: A Perspective Through the Fragment Size-Energy Fan. *Rock Mechanics and Rock Engineering*, 55(7), 4209–4236. https://doi.org/10.1007/s00603-022-02856-1

US Army Corps of Engineers. (2018). Blasting For Rock Excavations. 352.

USBM. (1980). RI-8507 (pp. 1-84).

Author's contribution

Siniša Stanković (associate professor): conceptualization, methodology and supervision. Vinko Škrlec (associate professor): data curation and formal analysis. Mario Dobrilović (professor): investigation and validation. Mihaela Fajdetić (student): investigation, visualization and writing – original draft.

All authors have read and agreed to the published version of the manuscript.



Waste organic materials in emulsion explosivesproperties and possibilities

DIM-ESEE Conference

Mario Dobrilović^{1*}, Ivana Dobrilović¹, Muhamed Sućeska¹, Vinko Škrlec¹, Romano Cardinale¹

¹ University of Zagreb, Faculty of Mining, Geology and Petroleum Engineering, Pierottijeva 6, 10000 Zagreb, Croatia



Abstract

As part of the project Verification of the technical concept for an emulsion matrix with the addition of organic waste, experimental and numerical studies were conducted on the incorporation of waste plastic into emulsion explosives. The research objective was to replace diesel fuel with waste organic materials, thereby achieving fuel savings while simultaneously addressing the issue of plastic waste management. Preliminary results demonstrated that up to 10 wt.% of ground PET plastic can be incorporated into the emulsion matrix without negatively affecting detonation parameters. Under typical blasting conditions in Croatia, between 100 kg and 1,000 kg of waste plastic could be utilized per blast, offering both environmental and economic advantages.

Keywords: waste organic materials, emulsion explosives, PET plastic, EXPLO5, detonation parameters

1. Introduction

In recent years, global efforts have intensified toward developing strategies for the management and disposal of plastic waste. In the field of commercial explosives, several studies have examined the potential application of waste plastics in combination with ANFO-type explosives (**Bieganska et al., 2022**). The present paper focuses on emulsion explosives and the use of waste organic materials in the production of commercial blasting agents.

Special attention was given to polyethylene terephthalate (PET), widely used in the manufacture of synthetic fibers and packaging for beverages, food, and liquids. PET's degradation period in the natural environment extends over several hundred years. According to the **ESTAT-2020-PA8-E-ENVACC** Report on plastic waste generation and management, a large proportion of sorted plastics ultimately ends up in landfills rather than being recycled, due primarily to the complexity of sorting different plastic types. Analyses have shown that Croatia demonstrates insufficient progress toward a circular economy, requiring more effective waste-prevention measures. While the average circularity rate in the EU-27 was 12.5 % in 2019 and 11.7 % in 2021, Croatia's rate was significantly lower, at 5.2 % and 5.7 %, respectively. (**ESTAT**, **2022**).

This growing need for effective plastic waste management has also been recognized in the production of civil explosives. The application of waste organic materials could contribute to improved safety, reduced environmental impact, and lower dependence on petroleum-based fuels during blasting operations.

As part of the project Verification of the technical concept for an emulsion matrix with the addition of organic waste (NPOO.C3.2.R3-I1.05.0103), both experimental and numerical studies were conducted. The initial analysis involved addition of plastic in emulsion explosive, while the second phase involved replacing fuel components in explosives with plastics.

Currently used emulsion energetic mixtures, like other types of civil explosives, exhibit an unbalanced ratio between released energy and the energy required for rock fragmentation. This imbalance results in unfavourable grain size distribution of fragmented rock and energy losses, primarily in the form of seismic effects during blasting. In the proposed emulsion energetic mixtures for civil blasting, waste recycled organic materials will replace fuel oils. The role of ammonium nitrate—as the oxygen carrier necessary for thermal chemical reactions—will be partially assumed by aerated organic materials. The project's goal is to achieve mixture stability by optimizing the types and proportions of ingredients at the laboratory scale.

Before starting the experimental work, a market analysis of commercial explosives was performed, yielding the following results: in Croatia alone, annual consumption of commercial explosives is approximately 3×10^3 tons -4×10^3 tons, the majority of which are non-explosive mixtures based on ammonium nitrate. Globally, the commercial explosives market is valued at around USD 10 billion, with emulsion energetic mixtures accounting for roughly USD 3 billion and projected to grow to USD 4.5 billion by 2033.

2. Methods

Emulsion explosive used in this study is a standard AN & SN base. The detonation parameters for emulsion explosives are shown in **Table 1**.

meters (Ester, 2005)

Parameter	Unit	Value Range
Density	g/cm ³	1.10-1.30
Detonation velocity	m/s	4000–6000
Gas volume	dm³/kg	900-1100
Heat of explosion	kJ/kg	2100-2800
Specific energy	kJ/kg	600-800
Energy density	kJ/dm³	700–1000
Oxygen balance	%	-10.0 to +10.0

For this study, three samples were prepared for each of three different mass fractions of waste plastic. The waste plastic, in the form of PET beverage containers (**Figure 1**), was finely ground using a Pulverisette 11 mill (**Figure 2**).



Figure 1. Finely ground PET

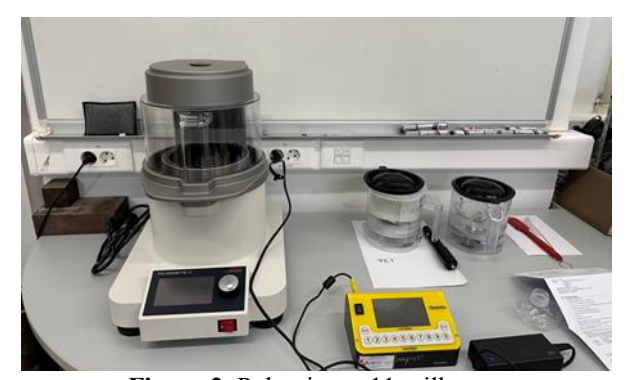


Figure 2. Pulverisette 11 mill

The ground plastic was was sieved, and the fraction < 0.5 mm was used and then incorporated into the sensitized emulsion explosive by manual mixing. The emulsion matrix used in this test comprised an aqueous solution of ammonium nitrate as the dispersed phase and diesel fuel as the continuous phase, and it was sensitized with glass microballoons.

The detonation velocity was measured on samples that have diameter approximatly 23 mm and length 100 mm, using an electro-optical (discontinuous) method with an "Explomet 2" device. Results of detonation velocity measurements under laboratory conditions are shown in **Table 2**.

Table 2. Results of detonation velocity measurements under laboratory conditions

PET mass fraction	Sample No.	Explosive density pe, (g/cm³)	Distance between measuring points (mm)	Measured time (μs)	Measured detonation velocity (m/s)	Average velocity (m/s)
	1	1.17	26.00	5.04	5159	
1 %	2	1.20	27.20	5.93	4587	4691
	3	1.19	28.60	6.61	4327	_
	7	1.16	26.85	7.71	4702	<u></u>
5 %	8	1.22	27.45	5.90	4653	4702
	9	1.19	29.70	6.25	4752	_
-	A	1.16	28.05	5.44	5156	
10 %	В	1.18	27.80	6.76	4112	4702
	С	1.20	28.35	5.86	4838	_

Alongside the experimental work, numerical simulations were performed using the thermochemical code EXPLO5 to provide a rough framework for the results. The emphasis is on a rough framework because the simulation assumes an ideal detonation, whereas commercial explosives — including this formulation with added plastic — are characterized by non-ideal detonation behavior.

2.1. Numerical simulations

The detonation properties of the studied mixtures are calculated using the EXPLO5 thermochemical code (Sućeska, 2025). The code predicts detonation properties (such are detonation velocity, detonation pressure, energy, heat, temperature, etc.) of an explosive, knowing only the chemical formula (elemental composition) of the explosive (or explosive mixtures), enthalpy of formation, and density. The calculation is done applying the chemical equilibrium steady-state Chapman-Jouguet (C-J) detonation model. It should be noted that in the case of non-ideal explosives, such a calculation gives the so-called ideal detonation velocity, i.e. the detonation velocity that would be achieved with an infinitely large charge diameter. Reactant properties are shown in Table 3.

Table 3. Reactant properties

Reactant name	Bruto formula	Mol. mas	Oxygen balance (%)	TMD (g/cm3)	Gravimetric density (g/cm3)	Enthalpy of formation (kJ/kg)
Polyetileneterephtalate (PET)	$C_{5.20}H_{4.27}O_{2.078}$	100	-167.26	1.38	0.55	-3737.38
Emulsion explosive, AN/SN+2.4% GMB	$\begin{array}{c} C_{0.22}H_{3.13}N_{0.97} \\ O_{2.05}Si_{0.02}Na_{0.07} \end{array}$	54.26	-0.81	1.326	1.26	-6488.62

During the calculation, the mass fraction of ground PET varied from 0 % to 20 %, with a step increase of 2 %. Results of numerical simulation are shown in **Table 4**.

Table 4. Numerical simulation results

Table 4. Numerical simulation results						
Reactant names and weight fractions (wt %)	PET (wt %)	Bruto formula	Density (g/cm ³)	D (m/s)	р _{СЈ} (GPa)	Q (kJ/kg)
Emulsion + 2.4% GMB 100,0 %	0	C(0,215) H(3,131) N(0,967) O(2,047) Si(0,022) Na(0,070)	1.26	6094	10.73	-2849.34
Emulsion + 2.4% GMB 98,0 %	2	C(0,271) H(3,160) N(0,961) O(2,058) Si(0,022) Na(0,070)	1.23	5923	10.03	-2719.46
Emulsion + 2.4% GMB 96,0 %	4	C(0,329) H(3,190) N(0,956) O(2,070) Si(0,022) Na(0,069)	1.20	5770	9.45	-2624.73
Emulsion + 2.4% GMB 94,0 %	6	C(0,388) H(3,221) N(0,950) O(2,081) Si(0,022) Na(0,069)	1.17	5625	8.74	-2550.36
Emulsion + 2.4% GMB 92,0 %	8	C(0,449) H(3,253) N(0,944) O(2,094) Si(0,021) Na(0,068)	1.14	5490	8.23	-2484.47
Emulsion + 2.4% GMB 90,0 %	10	C(0,512) H(3,285) N(0,938) O(2,106) Si(0,021) Na(0,068)	1.12	5360	7.7	-2424.32
Emulsion + 2.4% GMB 88,0 %	12	C(0,578) H(3,319) N(0,931) O(2,119) Si(0,021) Na(0,067)	1.09	5235	7.14	-2368.4
Emulsion + 2.4% GMB 86,0 %	14	C(0,645) H(3,354) N(0,925) O(2,133) Si(0,021) Na(0,067)	1.07	5114	6.7	-2314.2
Emulsion + 2.4% GMB 84,0 %	16	C(0,714) H(3,390) N(0,918) O(2,146) Si(0,021) Na(0,066)	1.04	4997	6.25	-2262.48
Emulsion + 2.4% GMB 82,0 %	18	C(0,786) H(3,427) N(0,911) O(2,161) Si(0,021) Na(0,066)	1.02	4884	5.88	-2211.74
Emulsion + 2.4% GMB 80,0 %	20	C(0,860) H(3,465) N(0,903) O(2,175) Si(0,021) Na(0,065)	1.00	4775	5.6	-2161.22

Furder resulta of numerical simulation of detonation parameters related to weight percentage of grouted PET are shown on **Figures 3, 4, 5, 6** i 7.

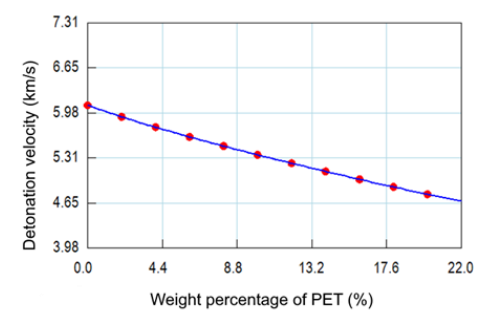


Figure 3. Detonation velocity vs weight percentage of PET

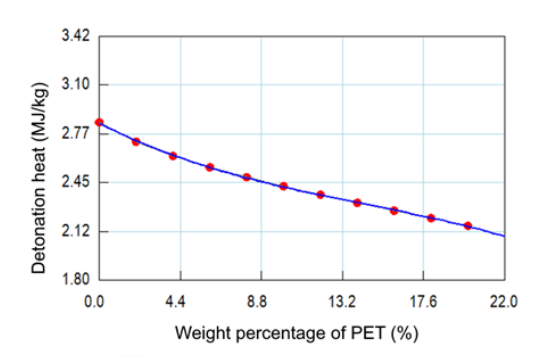


Figure 5. Detonation heat vs weight percentage of PET

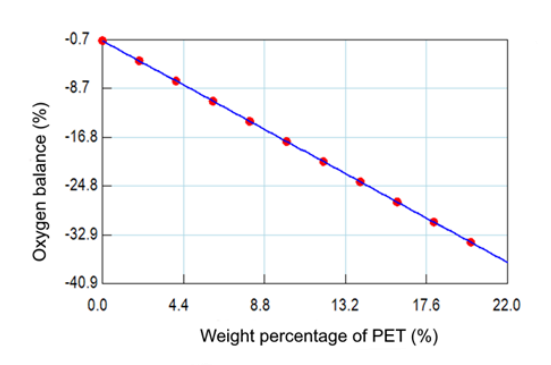


Figure 7. Oxygen balance vs weight percentage of PET

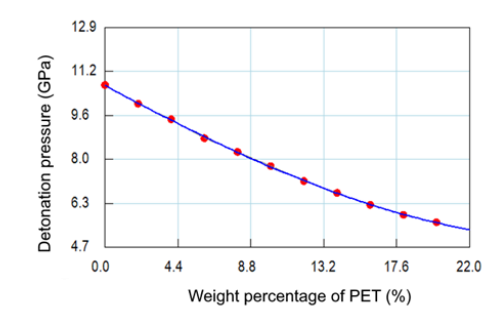


Figure 4. Detonation pressure vs weight percentage of PET

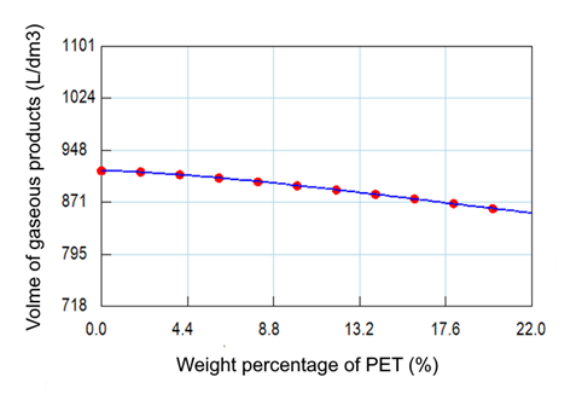


Figure 6. Volume of detonation products vs weight percentage of PET

3. Results

Preliminary results of experimental researches shown that with the addition of up to 10 % PET plastic, in fractions smaller than 0.5 mm, the experimental detonation velocity varied from 4691 m/s to 4702 m/s. The experimental detonation velocity variation can be considered as result without varation since the mesaurement uncertainty ranges approximately ± 100 m/s.

On the other hand, the numerical simulation indicated somewhat higher values, which, with the addition of 2 % plastic increments, ranged from 5923 m/s to 5360 m/s.

As noted above, the numerical simulations used an ideal detonation model that is not representative of the emulsion explosive; therefore, the observed discrepancies were expected. More relevant data will be obtained from tests with larger-diameter charges. Nevertheless, the numerical model remains useful because it provides a relative scale for the mixture ratios.

4. Discussion

In a typical blasting operation in Croatia, between 1,000 kg and 10,000 kg of explosive can be consumed. Based on preliminary research, a single blast could incorporate between 100 and 1,000 kg of waste plastic. If plastic were to replace diesel fuel, approximately 1,000 liters of diesel could be saved per blasting operation.

Further research is currently underway to ensure the repeatability and reproducibility of the experimental results on laboratory scale. The study will also be expanded to include other types of plastics as well as additional waste materials such as textiles, waste oils, and similar substances.

And finaly, focus will be on optimizing the emulsion formulation, assessing long-term storage stability, and conducting field-scale testing to evaluate performance under real mining conditions.

5. Conclusions

The experimental and numerical researches demonstrate the feasibility of incorporating waste PET plastic into emulsion explosives. The addition of up to 10 wt. % PET did not produce a significant change in detonation velocity or other detonation parameters. These findings indicate that PET can be incorporated without materially affecting explosive performance. Potential benefits include improved plastic waste management through repurposing, reduced landfill burden and carbon footprint, and partial substitution of diesel fuel in explosive formulations — all of which could yield notable cost and resource savings.

6. Reference

Biegańska, J.; Barański, K.; Hebda, K.; Pytlik, M. Thermodynamic Assessment of the Impact of Selected Plastics on the Energy Parameters of Explosives. Energies 2022, 15, 9583. https://doi.org/10.3390/en15249583

ESTAT-2020-PA8-E-ENVACC Izvještaj o nastanku i gospodarenju otpadom od plastike. Project HRPWD Deliverable D2.2 (in Croatian).

ESTER, Z. 2005. Miniranje 1. Eksplozivne tvari, svojstva i metode ispitivanja. Zagreb: Sveučilište u Zagrebu, Rudarsko-geološko-naftni fakultet. (in Croatian).

M. Sućeska, EXPLO5 – Users Guide, OZM Research, Pardubice, 2025.

Funding

"This research was funded by [Next Generation EU (NGEU)], grant number [NPOO.C3.2.R3-I1.05.0103]."

Author's contribution

Mario Dobrilović (professor): funding acquisition, conceptualization, methodology, investigation, writing – original draft and writing – review & editing. Ivana Dobrilović (PhD): visualization, investigation and writing – original draft. Muhamed Sućeska (professor): formal analysis, software and supervision. Vinko Škrlec (associate professor): investigation and data curation. Romano Cardinale (bacc.ing.min): investigation.

All authors have read and agreed to the published version of the manuscript.



Geomechanical studies of the rock mass during underground block leaching of uranium

DIM-ESEE Conference



Mykola Stupnik¹ $\bigcirc \boxtimes$, Olena Kalinichenko¹ $\bigcirc \boxtimes$, Vsevolod Kalinichenko^{1*} $\bigcirc \boxtimes$, Volodymyr Pilchyk² $\bigcirc \boxtimes$

- ¹ Kryvyi Rih National University, Faculty of Mining and Metallurgy,11 Vitalii Matusevych Str., Kryvyi Rih, 50027, Ukraine
- ² «Eastern Mining and Processing Plant» State Enterprise, Gorkogo Str., 2, Zhovti Vody, Dnipropetrovsk region, 52210, Ukraine

Abstract

The presented work proves that, from an economic standpoint, it is advisable to apply the underground block leaching technology when mining deposits of low-grade uranium ores. To implement this technology, the authors propose using strip mining with vertically arranged rooms. Adjacent vertical rooms can be separated by a temporary inter-level pillar (crown). To study the stress-strain state of the surrounding rock massif and determine the stability of the pillar-crown when using strip leaching technology for uranium extraction, the authors employ a mathematical modeling technique utilizing the finite element method. To determine the degree of influence of the acid solution's contact time on the strength of uranium ores and host rocks, a group of acid-treated cubes was examined. The strength of uranium ore samples was tested using a hydraulic press connected to a computer. This setup recorded the load diagram for each sample and automatically registered the current stress and maximum load at the moment of its destruction. Based on their research, the project authors develop fundamental theoretical foundations and establish new patterns of geodynamic stabilization of the rock massif. This work specifically considers the stress-strain state of the massif when employing underground block leaching technology for uranium ore extraction. The authors determine the influence of the main acidic reagents on geotechnical factors and the overall geodynamic stability of the rock massif. The stability of technological elements is determined through mathematical modeling. Highly efficient underground vertical strip leaching technologies for shrinked uranium ores are developed.

Keywords: "uranium ores", "underground mining", "pillar-crown", "underground vertical strip leaching technology", "shrinked uranium ores"

1. Introduction

Underground block leaching (UBL) of uranium is a relatively advanced and economically viable technology that allows extraction of uranium directly from ore-bearing formations without the need for extensive conventional mining. This method is based on the injection of leaching solutions into ore-bearing blocks, followed by recovery of the uranium-rich fluid (Yussupov et al., 2024). While the technique minimizes surface disturbance and reduces waste generation, it also creates complex geomechanical challenges (Lyashenko et al., 2024). The infiltration of chemical solutions and their prolonged interaction with host rocks alter the structural integrity, permeability, and stability of the rock mass, making geomechanical research a crucial foundation for the safe and efficient application of UBL (Vladyko et al., 2022).

The rock mass in uranium-bearing formations consists of heterogeneous lithological layers, including sandstones, shales, and fractured zones (Vladyko et al., 2022; Dodge & Powell, 1975). The injection and migration of leaching solutions can weaken intergranular bonds, increase pore pressure, and lead to subsidence or deformation of overlying strata. Geomechanical studies aim to predict these changes by analyzing stress distribution, deformation mechanisms, and fluid—rock interactions (Lyashenko et al., 2024; Vladyko et al., 2025). This ensures that solution pathways are maintained for effective uranium recovery while preventing uncontrolled collapse and surface subsidence.

Research in this area employs a combination of laboratory testing, numerical modeling, and field monitoring. Laboratory studies assess changes in rock strength and permeability under leaching conditions, while numerical simulations help forecast stress—strain evolution within the leaching block. Field monitoring provides feedback on real-time deformation, fracture propagation, and subsidence risks. By integrating these approaches, researchers can develop predictive models that guide the optimization of leaching parameters, block design, and solution control strategies.

An analysis of current global uranium extraction technologies reveals several key aspects. The world's major uranium deposits, such as Coles Hill in Virginia and the Colorado Plateau, are classified according to the International Atomic Energy Agency (IAEA) system (Roehrlich, 2025). However, this classification does not consider changes in the stress-strain state of the host rock mass, nor does it address the behavior of inter-room and inter-level pillars exposed to acidic solutions during block leaching of uranium. The technology proposed by the authors, termed "underground vertical strip leaching of shrinked uranium ores", is being applied in Ukraine for the first time (Stupnik et al., 2018a).

The actuality of this research stems from both energy security and environmental perspectives. Uranium remains a strategic resource for nuclear energy, which is central to low-carbon power generation. However, public concerns about ecological safety demand strict control over leaching operations. Geomechanical studies directly contribute to minimizing risks of ground instability, aquifer contamination, and long-term subsidence. They also provide the basis for developing regulatory frameworks and technical standards that balance resource extraction with environmental stewardship.

In practical terms, geomechanical insights support the sustainable scaling of underground uranium leaching projects. They enable engineers to determine safe injection pressures, predict deformation boundaries, and implement monitoring systems that prevent geotechnical accidents. Moreover, findings from these studies can be transferred to other fields of in-situ mining, such as copper or rare earth element extraction. Thus, geomechanical research not only ensures the efficiency and safety of uranium block leaching but also strengthens the technological foundation for a broader transition toward environmentally conscious mining methods.

2. Methods

Current methodologies do not account for changes in the stress-strain state of the rock massif, the influence of the deposit dip, or the degree to which existing workings disturb the pillar-crown. Consequently, they are not designed to determine the safe thickness of the pillar-crown, and thus cannot establish the parameters for the proposed underground vertical strip leaching technology for shrinked uranium ores.

To analyze the stress-strain state of the surrounding rock mass and evaluate the stability of the pillar crown during the application of strip leaching technology for uranium extraction, the authors employed mathematical modeling based on the finite element method (**Figure 1a**). The mechanical behavior of uranium ore samples was investigated using a computer-assisted hydraulic press. This experimental setup generated load-displacement diagrams for each specimen and automatically recorded the evolution of stress, as well as the ultimate load at the point of structural failure (**Figure 1b**).

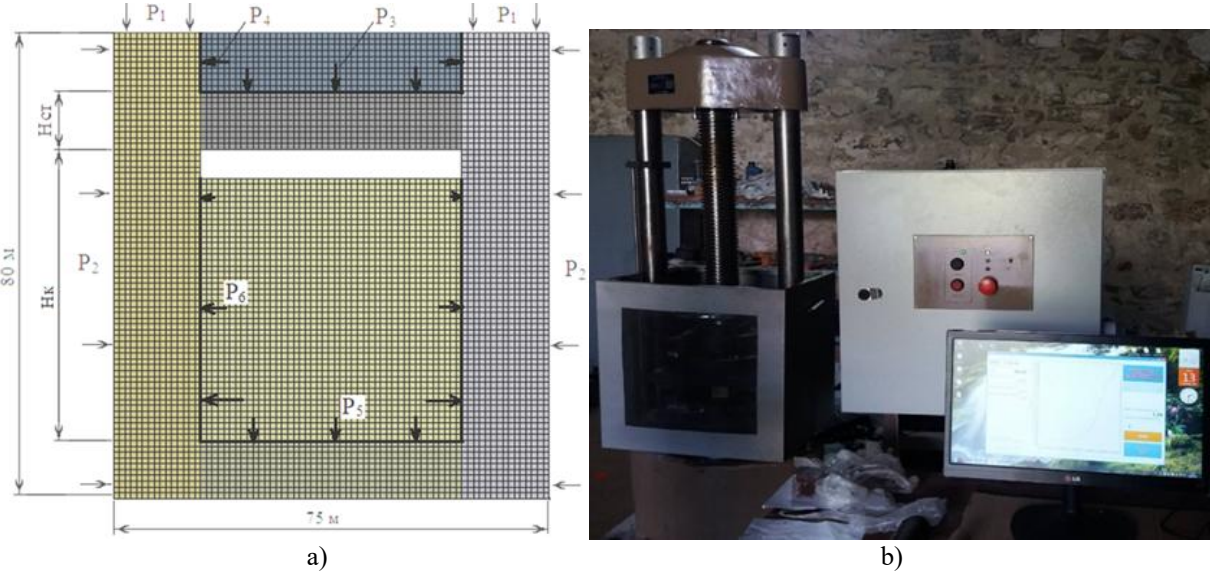


Figure 1. Schematic of the mathematical modeling technique using the finite element method: a) rock mass under study with a finite element mesh; b) photofixation of uranium ore strength testing using a hydraulic press.

Figure 2 illustrates the results of one of the variants of modeling the stress-strain state of the rock massif and the crown during the mining of uranium deposits using rooms filled with broken ore. The parameters of the presented variant are as follows: ore density -2650 kg/m^3 ; ultimate compressive strength of the ore -164 MPa; ultimate tensile strength -11 MPa; Poisson's ratio -0.24; crown height -10 m; $\alpha = 90^{\circ}$.

To evaluate the influence of acid solution contact time on the strength of uranium ores and host rocks, a series of acid-treated cubic specimens was tested. The mechanical strength of uranium ore samples was measured using a computer-assisted hydraulic press. This setup generated load—displacement diagrams for each specimen and automatically recorded both the current stress and the maximum load at the point of failure (**Figure 1b**). The objective of the study is to identify the regularities governing changes in the stress—strain state of the rock mass during the implementation of underground vertical strip leaching of shrinked uranium ores.

The stated goal of the research was achieved through a sequence of interrelated tasks. First, both global and domestic experience in the leaching of shrinked uranium ores was analyzed. Experimental studies were conducted to assess the effect of acid solutions, used in underground block leaching, on the strength of uranium ores. Based on these findings, the fundamental principles of underground vertical strip leaching of shrinked uranium ores were developed and refined. An algorithm was then proposed to determine the stable parameters of loaded pillars under block leaching conditions, and the main regularities in the evolution of modern technologies for underground vertical strip leaching were substantiated.

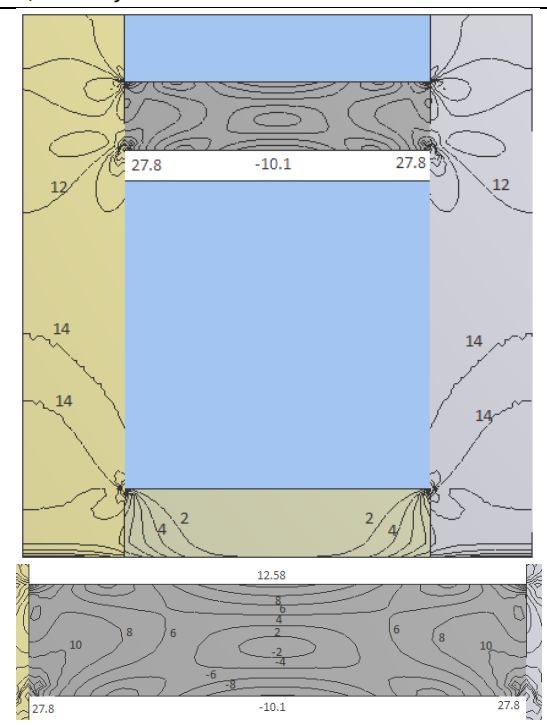


Figure 2. Results of one of the variants of modeling the stress-strain state of the rock massif and the crown

The core concept of this work is to apply established patterns of geotechnical factor influence on rock pressure manifestations and the stability of artificial underground structures. This involves accounting for dependencies of the stress–strain state of the rock mass on the structural elements of mine workings and further developing advanced technologies for underground vertical strip leaching of shrinked uranium ores. The working hypothesis suggests that state-of-the-art measures for stabilizing geodynamic processes associated with the stress–strain state of the rock mass can be achieved through the implementation of a high-tech strategy of underground vertical strip leaching of shrinked uranium ores.

3. Geomechanical Study Results of the Rock Mass

Underground block leaching is a recommended technology for the efficient extraction of low-grade uranium ore. In this approach, stoping blocks are arranged vertically, one above the other, to minimize the costs associated with technology implementation. Initially, the reserve in the upper block is blasted, forming a room filled with broken ore. This ore remains in the room while a sulfuric acid solution is introduced to initiate the uranium leaching process. Simultaneously, the ore reserve in the lower, second-stage block is blasted to create a similar room, separated from the upper block by a temporary inter-level pillar (crown) while leaching continues above. Once blasting in the second-stage block is complete, the inter-level pillar is removed, allowing simultaneous leaching in both rooms. The process is repeated in the third-stage lower block, with a temporary crown separating it from the upper rooms until drilling and blasting are completed, after which leaching occurs simultaneously in all three rooms. This approach, termed "underground vertical strip leaching of shrinked uranium ores", allows the number and dimensions of rooms to vary depending on the technological requirements of the deposit.

This technology differs significantly from traditional mining methods, particularly in how the stress field develops within the main structural elements and the surrounding rock mass. Temporary crowns are compromised both by the excavation of workings and by the chemical action of leaching reagents. Current methodologies for determining permissible dimensions of structural elements in room-and-pillar mining systems either neglect the effects of dip angle and the degree of pillar compromise on stability or are not designed to establish the safe thickness of inter-level crowns. Therefore, understanding the stress–strain behavior of the rock mass under these conditions is essential for ensuring operational safety and optimizing the leaching process.

The stress-strain state of the rock massif and the stability of the crowns were investigated using mathematical modeling with the finite element method. The analysis was performed for the conditions of the Mychurinske deposit of the State Enterprise "Eastern Mining and Processing Enterprise" (SE "SkhidGZK"), where the "underground vertical strip leaching technology for shrinked uranium ores" can be applied. The hardness of uranium ores is 14–16 (Protodyakonov scale), while that of the host rocks is 13–15. The ore deposit dip angles vary from 60° to 90° in 10° increments. The stress field was calculated using the Ansys 18 software package.

The studies conducted established that the most dangerous area is the zone of tensile stress, which is located in the central lower part of the crown. Under the same conditions, as the ore strength decreases, the absolute stress values within the crown also slightly decrease (by 0.1 MPa – 0.5 MPa, representing a change of 1 % - 2 % to 6 % - 7%).

This phenomenon can be attributed to the fact that rock of lower strength is less prone to stress accumulation, as it can more effectively relieve stress through larger strains toward a free surface (e.g., a room). Conversely, rocks of greater strength exhibit a higher capacity for stress accumulation due to their smaller strain capabilities. Despite this, the stability of crowns composed of lower-strength ores is compromised by a more substantial reduction in their ultimate strength.

At a deposit dip angle of $\alpha = 90^{\circ}$, ores with hardness of 14–16 points exhibit a tensile stress level of up to 10 MPa in the lower part of the crown. However, since the ultimate strength of these ores is approximately 11 MPa, such stresses will not cause rock failure. In ores with hardness of 10–11 points, the tensile stress level is 9.9 MPa. Given that their tensile strength limit is 7.7 MPa, this will lead to rockfalls with a volume of 80 m³ – 100 m³ to 150 m³. It is important to note that rockfalls exceeding 250 m³ – 300 m³ are considered critical.

At a dip angle of $\alpha = 70^{\circ}$ in ores with hardness of 14–16 points, there is practically no crown failure. However, at a dip angle of $\alpha = 60^{\circ}$, even in the crown of these same ores, small rockfalls of 4 m³ – 5 m³ will occur. In ores with hardness of 10–11 points, the volume of rockfalls at dip angles of $\alpha = 70^{\circ}$ and $\alpha = 60^{\circ}$ will be approximately 150 m³ – 220 m³ and 400 m³ – 450 m³ respectively. This indicates a near-critical state of the crown at $\alpha = 70^{\circ}$, and complete failure at $\alpha = 60^{\circ}$. Thus, the results obtained confirm the significant influence of the deposit's dip angle on the stress-strain state and stability of the crowns. To account for this, the authors propose using a correction factor K_{α} , whose numerical values are shown in **Figure 3**. The influence of pre-existing workings on the stress-strain state of the crown is defined by a fundamental principle: any working within a rock massif disrupts the initial stress field for up to three times the working's dimensions.

Consequently, it is proposed that the thickness of the crown, h_{cr}^{n} , which is compromised by the workings, be adjusted using the following expression:

$$H_{cr}^{n} = h_{cr} \cdot K_{dis}$$
,

where are:

 h_{cr} – the thickness of the undisturbed crown (m),

 K_{dis} – the coefficient accounting for the degree of crown disturbance by the workings created in it, unit fraction.

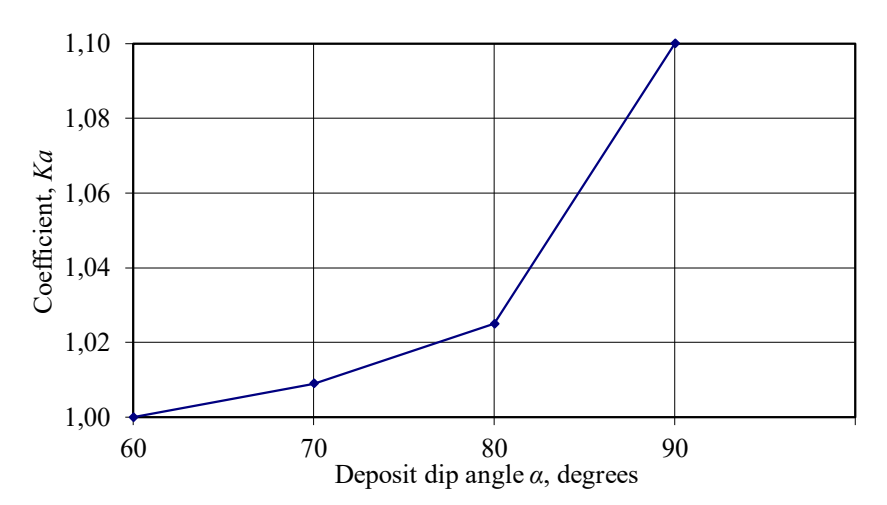


Figure 3. Values of K_{α} depending on the dip angle α

Based on these studies, the authors established the relationship between the dip angle of the ore deposit, the crown thickness, and the degree of disturbance from mine workings on the stress-strain state and stability of the crowns. This was done for the block leaching of uranium ores using the "underground vertical strip leaching technology for shrinked uranium ores". It has been established that these relationships must be considered when determining the safe dimensions of crowns and exposures using the proposed correction coefficients. Consequently, the thickness of the crown must be adjusted to account for the reduction in its stability caused by adverse factors, thereby preventing its failure and ensuring the safety of operations.

The effect of sulfuric acid on the strength of uranium ores was investigated to assess the impact of underground block leaching on inter-level pillars. Forty cubic samples (5 cm edges) were prepared, with 10 samples tested in their natural state (Group 1) and 30 samples (Group 2) exposed to acid on a single face, the remaining faces coated with paraffin to simulate field conditions. Samples were immersed for 2.5 months, 4 months and 6 months, reflecting operational reagent contact times.

Strength measurements were performed using a 50-tonne hydraulic press with computer-assisted load control, which recorded load—displacement diagrams and automatically determined stress and maximum load at failure. Group 1 samples exhibited an average ultimate strength of 128 MPa. Immersion in acid reduced strength progressively: after 2.5 months, the average strength was 82 MPa (–36 %), after 4 months 78.5 MPa – 79 MPa (–38.5 %), and after 6 months 76.5 MPa –77 MPa (–40 %). These results demonstrate a significant, time-dependent reduction in ore strength due to acid exposure, highlighting the importance of accounting for chemical weakening in the stability assessment of temporary crowns and surrounding rock mass during underground block leaching.

The research conducted confirms that the acid solution used in the underground block leaching of uranium ores significantly influences their strength. The authors propose using the coefficient K_{as} to account for the degree of this influence. This coefficient is defined as the ratio of the ultimate strength of uranium ores exposed to the acid solution to the ultimate strength of the initial, unexposed samples. The dependence of the coefficient K_{as} on the duration of the action of the acid solution on uranium ores during underground block leaching is shown in **Figure 4**.

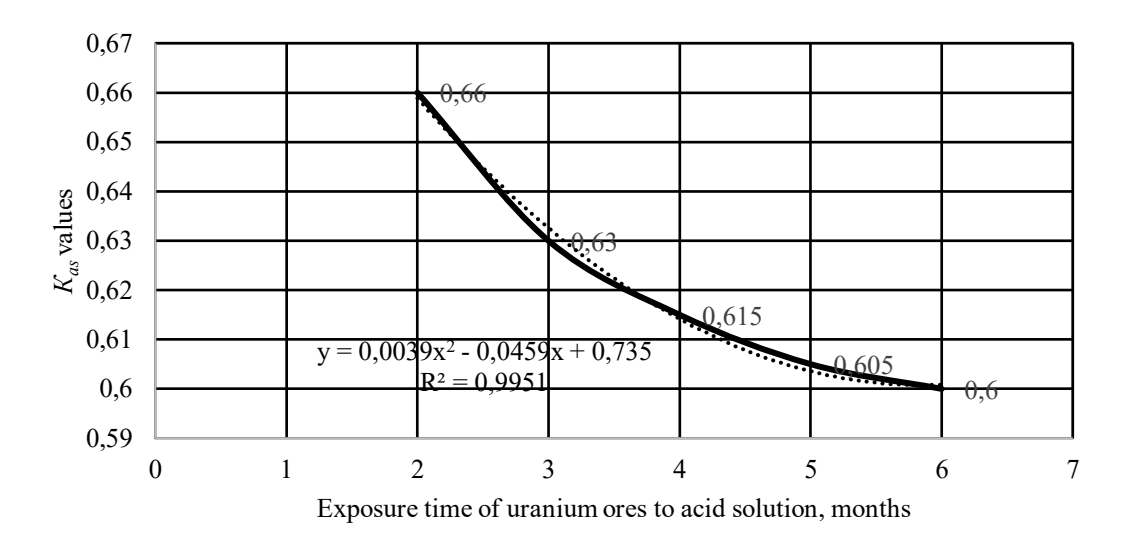


Figure 4. The dependence of the coefficient K_{as} on the time of exposure of uranium ores to the acid solution

So, the established relationship is accurately described by a polynomial function of the form:

```
K_{as} = 0.0039t^2 - 0.0459t + 0.735,
R^2 = 0.9951,
```

where are:

t – the exposure time of uranium ores to the acid solution (months),

 R^2 – the coefficient of determination.

Thus, when determining the stable dimensions of the inter-level pillar (crown), it is necessary to take into account the reduction of the ultimate strength of the crown rocks caused by the action of the acid solution in accordance with the approximate term of its existence.

4. Discussion of the Results

An analysis of current global uranium extraction technologies reveals the following (Stupnik et al., 2022; Petlovanyi et al., 2019; Pysmennyi et al., 2020). The world's leading uranium deposits, such as Coles Hill, Virginia, and the Colorado Plateau, are covered by the International Atomic Energy Agency (IAEA) classification. However, this classification does not account for changes in the stress-strain state of the host rock massif or the inter-room and interlevel pillars that meet acid solutions during uranium block leaching (Stupnik et al., 2018a; Bazaluk et al., 2022; Kosenko et al., 2024).

Mathematical modeling using the finite element method was employed to study the stress-strain state of the rock massif and the stability of the crowns, depending on the dip angle of the ore deposit (Stupnik et al., 2018b; Beridze et al., 2024). The studies were carried out for the geological conditions of the Mychurinske deposit (SE "SkhidGZK"), where the "underground vertical strip leaching technology for shrinked uranium ores" is considered for application (Stupnik et al., 2018b; Stupnik et al., 2019].

5. Conclusions

Based on their research, the authors have developed fundamental theoretical foundations and identified new patterns of geodynamic stabilization of the rock mass. This study specifically addresses the stress—strain behavior of the rock mass under underground block leaching technology for uranium ore extraction. The influence of the primary acid reagents on geotechnical parameters and the overall geodynamic stability of the rock mass has been determined. Theoretical frameworks have been established for managing the state of the massif during the underground application of block leaching technology.

The stability of technological elements is assessed through advanced mathematical modeling. Furthermore, highly efficient underground vertical strip leaching technologies for shrinked uranium ores have been developed. Based on the conducted research, the study establishes the effects of ore deposit dip angle, crown thickness, and the degree of disturbance caused by mining workings on the stress—strain state of the rock mass and the stability of the crowns. These findings provide a comprehensive basis for the implementation of the "underground vertical strip leaching technology for shrinked uranium ores" in uranium block leaching operations.

The dependence of the coefficient K_{as} on the time of exposure of uranium ores to the acid solution was established. It was proven that when determining the stable dimensions of the inter-level pillar (crown), it is necessary to account for the reduction in the ultimate strength of the crown's rocks due to the action of the acid solution, in accordance with the approximate service life of the crown.

6. References

Bazaluk, O., Rysbekov, K., Nurpeisova, M., Lozynskyi, V., Kyrgizbayeva, G., & Turumbetov, T. (2022). Integrated monitoring for the rock mass state during large-scale subsoil development. *Frontiers in Environmental Science*, (10), 852591. https://doi.org/10.3389/fenvs.2022.852591

Dodge, H. W., & Powell, J. D. (1975). Stratigraphic and paleoenvironment data for the Uranium-bearing Lance and Fox Hills formations, Crook and northern Weston Counties, northeastern Wyoming. *Open-File Report*. 112 p. https://doi.org/10.3133/ofr75502

Kosenko, A., Khomenko, O., Kononenko, M., Myronova, I., and Pazynich, Y. (2024) Raises advance using borehole hydraulic technology. *E3S Web of Conferences*, *567*, 01008. https://doi.org/10.1051/e3sconf/202456701008

Lyashenko, V. I., Dudar, T. V., Stus, V. P., & Shapovalov, V. A. (2024). Improvement of combined technologies of underground block leaching of metals from out of balance and unconditioned ores. *Environmental Safety and Natural Resources*, 52(4), 5–27. https://doi.org/10.32347/2411-4049.2024.4.5-27

Petlovanyi, M., Lozynskyi, V., Zubko, S., Saik, P., & Sai, K. (2019). The infuence of geology and ore deposit occurrence conditions on dilution indicators of extracted reserves. *Rudarsko Geolosko Naftni Zbornik*, 34(1), 83-91. https://doi.org/10.17794/rgn.2019.1.8

Pysmennyi, S., Fedko, M., Shvaher, N., & Chukharev, S. (2020). Mining of rich iron ore deposits of complex structure under the conditions of rock pressure development. *E3S Web of Conferences*, (201), 01022. https://doi.org/10.1051/e3sconf/202020101022

Roehrlich, E. (2025). International Atomic Energy Agency (IAEA). *Routledge*. 1-19. https://doi.org/10.4324/9780367199838-RECW8-1

Stupnik, M. I., Kalinichenko, V. I., Fedko, M. B., & Kalinichenko, O. V. (2018b). Investigation into crown stability at underground leaching of uranium ores. *Naukovyi Visnyk Natsionalnoho Hirnychoho Universytetu*, 6, 20–25. https://doi.org/10.29202/nvngu/2018-6/5

Stupnik, M., Kalinichenko, O., Kalinichenko, V., Pysmennyi, S., & Morhun, O. (2018a). Choice and substantiation of stable crown shapes in deep-level iron ore mining. *Mining of Mineral Deposits*, 12(4), 56-62. https://doi.org/10.15407/mining12.04.056

Stupnik, M., Kalinichenko, V., Fedko, M., Kalinichenko, O., Pukhalskyi, V., & Kryvokhin, B. (2019). Investigation of the dust formation process when hoisting the uranium ores with a bucket. *Mining of Mineral Deposits*, *13*(3) 96-103. https://doi.org/10.33271/mining13.03.096.

Stupnik, M., Kalinichenko, V., Fedko, M., Pysmennyi, S., Kalinichenko, O., & Pochtarev, A. (2022). Methodology enhancement for determining parameters of room systems when mining uranium ore in the SE "SkhidGZK" underground mines, Ukraine *Mining of Mineral Deposits*, 16(2), 33-41. https://doi.org/10.33271/mining16.02.033.

Vladyko, O., Maltsev, D., Gliwiński, Ł., Dychkovskyi, R., Stecuła, K., & Dyczko, A. (2025). Enhancing Mining Enterprise Energy Resource Extraction Efficiency Through Technology Synthesis and Performance Indicator Development. Energies, 18(7), 1641. https://doi.org/10.3390/en18071641

Vladyko, O., Maltsev, D., Sala, D., Cichoń, D., Buketov, V., & Dychkovskyi, R. (2022). Simulation of leaching processes of polymetallic ores using the similarity theorem. Rudarsko-Geološko-Naftni Zbornik, 37(5), 169–180. https://doi.org/10.17794/rgn.2022.5.14

Yussupov, K., Aben, E., Myrzakhmetov, S., Akhmetkanov, D., & Sarybayev, N. (2024). Increasing the Efficiency of Underground Block Leaching of Metal. Civil Engineering Journal, 10(10), 3339–3349. https://doi.org/10.28991/cej-2024-010-10-014

Acknowledgment

The authors extend their sincere gratitude to the management and engineering staff of the State Enterprise "Skhidnyi Mining and Processing Plant". Their assistance in providing materials concerning the plant's operations during the martial law period was invaluable to this research.

Funding

This research was supported by the Ministry of Education and Science of Ukraine during 2024-2025, as part of the following state research projects: "30-118-24 Research and development of the advanced strategy for the technological development of the uranium mining industry during wartime and post-war periods (State registration 0124U000876)", "30-120-24 Research and stabilization of the stress-strain state of the rock massif for the rapid construction of safe underground military engineering facilities with a high level of protection against air strikes (State registration 0121U111709)" and "30-122-25 Creation of a methodology and development of a technology for the restoration of dual-purpose underground facilities using high-precision 3D scanning (State registration 0125U001757)".

Author's contribution

Mykola Stupnik (professor): methodology, validation and writing – original draft. Olena Kalinichenko (professor): data curation, project administration and resources. Vsevolod Kalinichenko (professor): conceptualization, funding acquisition, supervision, and investigation. Volodymyr Pilchyk (postgraduate): formal analysis, visualization and software.

All authors have read and agreed to the published version of the manuscript.



Economic Assessment of Geothermal System Installation in Abandoned Mines

DIM-ESEE Conference



Dmytro Rudakov¹*[©]

Oleksandr Inkin¹ [©]

Rolf Schiffer²

¹ Dnipro University of Technology, Department of Hydrogeology and Engineering Geology, 19 Yavornytskoho Ave., 49005 Dnipro, Ukraine

¹ Schiffer Consult − GEO Services (SC-SGS), Treibweg 1, 45772 Marl, Germany

Abstract

In this study, the authors developed and tested a methodology for assessing the economic efficiency of geothermal systems in closed mines, depending on thermal capacity, operational costs, and design features, using the relevant statistical data on electricity and heating tariffs. The proposed approach includes calculations of the cost of electricity consumed and heat generated, the costs of the main and associated equipment, the number of heat consumers, the net present value (NPV), and the payback period, depending on the discount rate and actual tariffs. The calculations revealed that the critical indicator for economic efficiency is the ratio between the electricity and heating tariffs. When this ratio is above 3.5 (Great Britain, 2023), the NPV becomes negative, at 3.1 (Ukraine, 2023) the potential NPV was estimated positive only for open non-circulating systems with a distance to the heat consumer of less than 2 km, at \leq 2.2 (Germany, Ukraine in 2021), the NPV can be positive regardless of the system type. The NPV of non-circulating systems under favorable conditions is estimated at several million of ϵ , and for circulating and closed-type systems, hundreds and tens of thousands of ϵ . In the pre-war period in Ukraine, the NPV reached positive values, but now it is negative due to a sharp increase in electricity costs, with almost fixed tariffs on heating. Among the countries considered, the calculated payback period was estimated to be the shortest in Germany and the longest in the UK.

Keywords: closed mine, mine water, heat recovery, geothermal system, net present value

1. Introduction

In line with the modern trends of the power sector transition to "green energy", recovery of residual energy resources from closed coal mines is getting active development in the world (Banks et al., 2019; Timoshuk et al., 2012; Walls et al., 2021; Lapshin et al., 2025). Notably, using the geothermal potential of closed mines allows for reducing emissions of harmful substances, including CO₂, SO₂, and NO_x, into the atmosphere by decreasing the consumption of fossil fuels (Kovrov et al., 2022). The projects focusing on mine water heat recovery are being implemented in Germany, the UK, Spain, the Netherlands, and other countries (Ramos et al., 2015; Rudakov & Inkin, 2023).

Thermal energy from mine water is extracted at geothermal systems of open type with discharge of thermally spent water to surface watercourses or water bodies (non-circulating systems) or back to the mine (open-loop or circulating systems), and at the closed-loop systems (geothermal probes called also borehole heat exchangers) with a heat transfer fluid that extracts heat without hydraulic contact with mine water (Banks et al., 2019).

Environmental benefits and prospects of energy extraction from closed mines depend on multiple factors, and primarily the mine water temperature, the cost of electricity spent on system operation, for water lifting and running heat pumps, and heat transportation to consumers (Walls et al., 2021; Vladyko et al., 2025). This requires adapting the operating mode to variations of heat consumption throughout the year, considering mine water level rebound (Rudakov & Westermann, 2021), and performance efficiency of systems under operation (Rudakov & Inkin, 2022). So, the purpose of this study is to develop and test a robust methodology for assessing the economic efficiency of geothermal systems of various designs in closed mines, comparing the tariff conditions in different countries.

2. Method

The total volume of premises that geothermal systems can heat depends on the ratio of their average thermal capacity P_{th} to the amount of thermal energy q_r required for heating 1 m³ of indoor spaces (**Gavrysya**, 2015)

$$q_r = q_{r0} \, k_h \, V \, (T_l - T_{av}) \tag{1}$$

where are:

 q_{r0} – the average specific heating factor of the building, assigned 1254 J/(m³.°C) in calculations,

 k_h – the factor depending on the heating system type, and it is set to 1.15 for the calculations,

V – the volume of premises (m³);

 T_l – the room temperature (°C),

 T_{av} – the average monthly air temperature (°C).

The number of potential consumers of heat produced by geothermal systems can be estimated as the ratio of the total volume of premises to the standard indoor volume per person. According to the Ukrainian documents for residential buildings and offices (**DBN**, **2020**), these standards are set to 45 m³ and 13.5 m³, respectively. The most favorable indoor temperature for inhabitants is deemed to be 22 °C.

The heating period duration depends on the outdoor air temperature. According to regulatory documents (**Rules for the provision, 2019**), heating of civil and industrial facilities in Ukraine should begin after three days with a stable average daily air temperature below 8 °C. The heating period ends when the mean air temperature exceeds this threshold for three days. Therefore, based on the climatic data for eastern and central Ukraine, the heating period should last on average from the end of October to the beginning of April, on average 165 days.

In addition to indoor space heating, the thermal energy from geothermal systems can be used for hot water supply throughout the year. The maximum possible hot water flow rate Q_{hw} that a geothermal system with a thermal capacity P_{th} (W) can provide is calculated as follows.

$$Q_{hw} = P_{th} / [C_w' (T_h - T_c)]$$
 (2)

where are:

 C_w' – the volumetric heat capacity of water (4.18 MJ/(m³ ·°C)),

 T_h – the temperature of hot water, which is taken to be 50 °C,

 T_c – the temperature of cooled water, which can be taken for preliminary calculations, to be on average 6 °C in the period from October to April and 15 °C in the period from May to September (°C).

The number of consumers of the hot water supply is calculated by dividing the hot water consumption (**Equation 2**) by the standard rates of consumption per person. The national standard of Ukraine (**DBN, 2013**) sets these rates for apartments and offices at 0.14 m³/d and 0.01 m³/d, respectively.

Due to maintaining active drainage in closed mines and the need to keep a hydrodynamically safe mine water level, electricity costs for drainage in open non-circulating systems are mandatory, so they may not be included in the cost balance of heat recovery. In this case, most of the electricity is consumed by heat pumps, which can be calculated as the ratio of thermal capacity P_{th} to the Coefficient of Performance (COP). In the case of open circulating and closed-loop systems, the costs of electricity consumed when lifting water to the surface or circulating the fluid in tubes are additionally taken into account. For all systems, the electricity costs for transporting heat to consumers must also be accounted for.

As the economic indicator of geothermal system performance, operating income (OI) can be used. OI is calculated by subtracting operating expenses (OE), depreciation (D), and amortization (A) from gross profit (GP). In a first approximation, GP can be defined as the cost of thermal energy generated and delivered to consumers, taking into account its losses during transportation, S_{th} . The cost of electricity spent on system operation, S_{el} , can be considered as OE. D and A can be accounted through the cost of work and materials associated with the maintenance of the systems, adjustment, depreciation, and malfunction prevention, S_{mn} . Note that the cost of electricity spent by the systems of different types should be accounted for differently.

Given these assumptions, the OI of the geothermal system can be estimated by the following formulae.

$$OI = S_{th} - S_{el} - S_{mn} \tag{3}$$

$$S_{th} = C_{th} \Delta t_{on} P_{th} (1 - n_l) \tag{4}$$

$$S_{el,nc} = C_{el} \frac{P_{th,nc}}{COP} \Delta t_{op}, \quad S_{el,cr} = C_{el} \left(\frac{P_{th,cr}}{COP} + P_{pw} \right) \Delta t_{op}, \quad S_{el,cl} = C_{el} \left(\frac{P_{th,cl}}{COP} + P_{pw} \right) \Delta t_{op}, \tag{5}$$

where are:

 S_{th} – thermal energy cost (\in),

 $S_{el,nc}$, $S_{el,cr}$, $S_{el,cr}$ – cost of electrical energy consumed during operation of open non-circulating and circulating systems, and closed-loop systems (\mathfrak{E}),

 $P_{th,nc}$, $P_{th,cr}$, $P_{th,cl}$ – average thermal capacity of these systems, respectively (kW),

 S_{mn} – costs of system maintenance (\in),

 C_{th} , C_{el} – tariffs for thermal and electrical energy (\notin /kWh),

 Δt_{op} – period of system operation (h),

 P_{pw} – pump power for lifting water to the surface or circulating the heat transfer fluid (kW),

COP – heat pump Coefficient of Performance (–),

 n_l – the share of thermal energy losses during its transportation (–).

The parameter n_l can be evaluated according to the Ukrainian standards (**Dubrovska & Shklyar, 2021**). Heat losses with a heating pipeline length L_p of up to 300 m are estimated at 1 % for every 100 m of the route; for L_p up to 500 m at 2.9 % for the entire route length; for L_p up to 1000 m at 4.8 % for the entire route length; for L_p over 1000 m plus 0.6 % for every 100 m of the route exceeding 1000 m.

The maintenance costs of the systems S_{mn} can be estimated in a first approximation by the share of the cost of electricity consumed during the operation of the systems. The annual costs of electricity and maintenance of geothermal systems S_{as} (\mathcal{E}/a) at the mine, can be calculated by the correlation (Matas-Escamilla et al., 2023)

$$S_{gs} = 65792 P_{th} + 6334 \tag{6}$$

where is:

 P_{th} – thermal capacity of the system (MW).

Using **Equation 6**, the operating costs for a geothermal system are estimated at \in 72,000 per 1 MW. According to **Equation 3**, the cost of electricity consumed when operating a system of this capacity can be evaluated at \in 66,000, taking into account the electricity tariff in Spain for very large consumers of \in 0.067/kWh for the reported period (**Quarterly energy, 2025**). Comparing these figures allows us to roughly estimate the annual maintenance costs for the system at \in 5,800, which is 8.7 % of the electricity costs.

To calculate the *NPV* from geothermal systems of different types using **Equations 1–6**, it is necessary to apply the tariffs for electricity and thermal energy in the locations where these systems are planned to be installed, namely, in postmining regions. These tariffs change over time due to economic development and the calculation principles accepted in different countries. So, the assessment of geothermal system economic efficiency should include the tariff conditions being in effect in a specific period and the trends of tariff evolution.

A comprehensive assessment of the economic profitability of geothermal systems at closed mines, including indicators of profit, capital and operating costs, can be performed using the generally accepted criterion of net present value (NPV), discussed in (Chen, 2025). It quantifies the amount of net profit that an investor can gain from a geothermal system after the profit covers the investment costs associated with installation and operation. The NPV of different systems depends on the share of additional costs associated with auxiliary equipment (circulation pumps, probes, heat exchangers, tanks, connectors, pipelines between the shaft and the heating system), the discount rate, and the distance to the consumer of thermal energy. The amount of additional costs can be estimated at 20 % – 40 % of the heat pump cost and should be refined in further studies with the known case studies.

3. Results

In calculations, we compared the tariff conditions in Ukraine with those in Great Britain and Germany, where geothermal systems have already been installed at many sites. To perform a comprehensive analysis, the authors collated the period of development under favorable and unfavorable tariff ratios in Europe (2013 and 2023). As for Ukraine, we compared the pre-war period (2021) with the martial law time (2023).

The electricity tariff in Great Britain depends on the consumer capacity (**Quarterly energy, 2025**). The customers are classified as small at an annual consumption E_a of up to 500 MWh, medium at E_a up to 20,000 MWh, large at E_a up to 70,000 MWh, and very large at E_a up to 150,000 MWh. Based on the calculated total amount of electricity consumed by geothermal systems during the off-peak period using **Equation 5**, it is possible to attribute an open non-circulating system with an annual consumption of 990 MWh to an average consumer, an open circulating system (252 MWh), and a closed-loop system (55 MWh) to a small consumer. Based on these classifications, heat tariffs and fuel costs, proportions between tariffs on electricity and heating can be identified (**Table 1**).

In Ukraine, the electricity tariff paid by industrial companies covers the services of the transmission system operator, the distribution system operator, the supplier, the dispatcher, and the actual cost of electricity. The tariff significantly changes from a minimum at night (23:00–07:00) to average values during daytime and partly in the evening (07:00–19:00), and reaches a maximum in the late evening (19:00–23:00). So, the total electricity tariff for geothermal systems is calculated by the weighted sum of tariffs acting within 24 hours. This variation provides a space to optimize system performance with the most intensive heat recovery at night.

Table 1. Discount rate and proportions between electricity and heat tariffs for industrial consumers in the UK, Germany, and Ukraine (**Entwicklung des Zinssatzes, 2025; Guidance, 2023;** the data of the National Bank of Ukraine)

		n	C_{el}/C_{th}		
Country	Year	R, %	Non-circulation systems	Circulating and closed- loop systems	
The LUZ	2013	1	2.3	2.9	
The UK	2023	3.5	3.5	3.7	
C	2013	1	1.7	2.2	
Germany	2023	2	1.7	2.1	
Ukraine	2021	7	1.	2	
Okraine	2023	15	3.	1	

The heating tariffs for Great Britain and Germany in 2013 and 2023 were determined according to **Warner (2016)** and **Quarterly Energy (2025)**, respectively. Remarkable that there is no centralized heat supply in Great Britain; therefore, the heating tariff in this country was calculated by the cost of natural gas and oil products.

Based on the reviews of current practices in mine water heat recovery and actual thermal capacities of running geothermal systems around the globe (Banks et al., 2019; Walls et al., 2021), the authors took the following average figures for calculations: the thermal capacity of non-circulating systems $P_{th,nc}$ as 1000 kW, open-loop systems $P_{th,cr}$, as 200 kW, and closed-loop systems $P_{th,cl}$ as 50 kW; COP=4; $\Delta t_{op}=3960$ h (165 days). The share of thermal energy losses, n_l , was estimated depending on the distance to the heat consumer, L. The pump power P_{pw} for mine water pumping and fluid circulation was calculated following the recommendations of Larock et al. (2000), with the flow rate that differs for the considered types of geothermal systems. Following the numerical analysis using Equations (3) and (6), the maintenance costs, S_{mn} , were taken to be equal to 10 % of electricity costs. The tariffs for thermal and electric energy were set considering the annual consumption.

Depending on the month of the heating period, an open non-circulating system of 1 MW capacity is capable of heating 88 thousand m³ to 198 thousand m³ of premises, an open circulating system of 200 kW capacity 17 thousand m³ to 39 thousand m³, and a closed-loop system of 50 kW capacity 4 thousand m³ to 10 thousand m³. The area of heated premises, and the number of heating consumers (**Figure 1**), depend on the outdoor temperature in colder months, so the average specific amount of thermal energy spent on heating q_r in January (0.011 kW/m³) is more than double that in April (0.005 kW/m³).

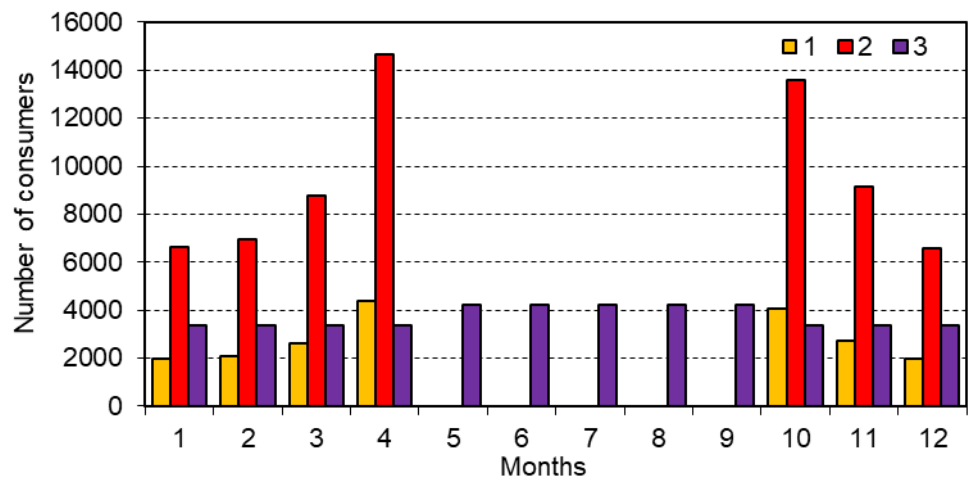


Figure 1. Number of consumers whose heat demand can be met by an open non-circulating geothermal system with a thermal capacity of 1000 kW: 1) heating residential buildings, 2) offices, 3) hot water supply for residential buildings

The calculations made by Equations 1–6 revealed that the ratio of the electricity tariff to the heat tariff, C_{el}/C_{th} , is the critical indicator that significantly affects the *NPV* of geothermal systems (Tables 1 and 2).

Table 2. Estimated NPV of geothermal systems for a period of 25 years, thousand €

		10	nae, L, – km	Geothermal system		
Counrty	Year	nae,		Open		Closed-
		_	KIII	Non-circulating	Circulating	loop
		0.2	1	943.6	-99.7	1.2
The UK	2013 -	0.2	3	470.3	-194.4	-22.4
The UK	2013	0.4	1	900.7	-108.3	-0.9
		0.4	3	427.3	-203.0	-24.5
		0.2	1	2961	187.0	79.7
	2013 -	0.2	3	2179	30.6	40.6
	2013	0.4	1	2918	178.4	77.5
Commons		0.4	3	2136	22.0	38.4
Germany		2023 - 0.2	1	4110	353.4	132.1
	2022		3	3015	134.5	77.4
	2023		1	4067	344.8	130.0
		0.4	3	2972	125.9	75.2
		0.2	1	1020	166.3	47.2
T 711 .	2021 -	0.2	3	774.5	117.3	35.0
Ukraine	2021 -	0.4	1	976.5	157.7	45.1
		0.4	3	731.5	108.7	32.8

 n_{ae} is the ratio of additional equipment cost to the heat pump cost.

For example, with a tariff ratio of $C_{el}/C_{th} \ge 3.5$, which was typical for the UK in 2023, the calculated *NPV* was negative. With $C_{el}/C_{th} = 3.1$ for Ukrainian tariff conditions in 2023, the *NPV* could be positive only for non-circulating systems at a distance of up to 2 km from the heat consumer. With $C_{el}/C_{th} \le 2.2$, which was in Germany in 2013 and 2023, and Ukraine in 2021, the calculated *NPV* was positive regardless of the system type and the distance to the heat consumer nearer than 3 km (**Table 2**). The most significant *NPV* is expected for non-circulating systems due to significant water discharges and the non-inclusion of drainage costs in the efficiency of heat recovery. Increasing the distance to a heat consumer reduces the profit, which is most sensitive for closed-loop systems of low capacity. The expected *NPV* falls significantly when the electricity cost increases over the thermal energy cost.

The payback periods calculated for all systems, mostly between 3 and 9 years, are close to the real values of this parameter reported for operating geothermal systems in closed mines (Walls et al., 2021).

4. Discussion

At present, the installation of geothermal systems at closed and decommissioned mines in Germany looks most attractive in terms of investment among the three countries, considering the martial law declared in Ukraine in 2022. In this case, the NPV of non-circulating systems is estimated at several million \in , and open-loop and closed-loop systems at hundreds and tens of thousands \in . The high expected profitability indicators of geothermal systems in mines in Germany are linked with a lower tariff ratio of 1.7 - 2.2 and the discount rate R of 1% - 2% compared to other countries.

In the pre-war period (2021), Ukraine had quite favorable tariff conditions with a low tariff ratio of 1.2, which ensured positive NPV for geothermal systems of all types for the considered data ranges. The NPV could reach \in 1 million depending on the share of additional costs, discount rate, and distance to the heat consumer. Due to a sharp increase in electricity tariffs against the background of almost fixed tariffs for district heating services, the tariff ratio exceeded 3.0 in 2023, which caused a decrease in the NPV to negative values in the country.

The tariff ratio in the UK rose to 3.5–3.7 in 2022–2023, so the *NPV* of mine-water-based geothermal systems in the UK in 2023 temporary became negative due to a sharp increase in electricity cost. At the time being, due to a certain stabilization of electricity prices in the country, the tariff ratio may become acceptable again for investments in geothermal system installation.

Currently, within the transition to the "green" economy, there are specific tools to reduce the electricity tariffs for companies that use renewable energy sources in different countries. This could potentially reduce the cost of electricity required to operate geothermal systems. After their closure, powerful transmission lines are still connected to the mines, which are not used to a significant extent. In this context, the installation and operation of geothermal systems enable a more complete use of the existing mining infrastructure, which significantly reduces the required costs. To fully assess their economic efficiency, it is also necessary to calculate the capital costs, as well as the modern profitability indicators of the power generation units.

In general, for geothermal systems of all types in the three countries, the NPV decreases with an increase in the share of additional costs, discount rate, and distance to the heat consumer. The NPV of open non-circulating geothermal systems is generally higher compared to other systems due to significant volumes of water withdrawn, in case the electricity costs to maintain a hydrodynamically safe mine water level are covered from other sources. At the same time, the NPV of open-loop systems often becomes negative due to the high costs of electricity spent on mine water circulation. Closed-loop systems, compared to others, have the lowest NPV due to insignificant thermal capacity. However, combining such systems within the same mining field would enable significantly increasing total capacity and the NPV.

5. Conclusions

In this study, a method has been developed to assess the economic efficiency of mine-water-based geothermal systems on the grounds of analysing the state-of-the-art and applied technologies. It accounts for the cost of electrical and thermal energy consumed and produced during the operation, maintenance costs, and capital and technological costs associated with the installation and operation. By applying the general criteria of net present value and payback period, it becomes possible to compare promising sites for installation under changing economic conditions.

The proposed methodology was tested for the tariffs on electricity and thermal energy in the UK, Germany, and Ukraine in 2013, 2021, and 2023. The critical indicator for the profitability of geothermal systems was found to be the ratio between the electricity and heating tariffs, which varies depending on local economic and political development. Heat recovery from mine waters can be profitable if this ratio is below 2–2.5 at a distance to the heat consumer of up to 2 km. If this ratio exceeds 3, the operation of the systems becomes unprofitable primarily. The most significant potential *NPV* can be anticipated for open non-circulating systems if drainage costs are not included in the heat generation efficiency calculations.

The NPV of these systems under favorable conditions may reach several million \in , and for open-loop and closed-loop systems hundreds and tens of thousands of \in . High expected profitability is achievable in the case of a lower tariff ratio of 1.7–2.2 and discount rate R of 1 % – 2%. The NPV decreases if additional costs and the discount rate increase. At the current tariffs, the shortest payback period for mine-water-based geothermal systems is expected in Germany, and longer ones in the UK. As the input parameters for NPV calculation depend on domestic economic conditions, refining the obtained estimates and forecasting with detailed analysis by countries could be the subject of future studies.

6. References

- Banks, D., Athresh, A., Al-Habaibeh, A., & Burnside, N. (2019). Water from abandoned mines as a heat source: practical experiences of open- and closed-loop strategies, United Kingdom. *Sustainable Water Resources Management*, 5, 29-50. https://doi.org/10.1007/s40899-017-0094-7
- Chen, S. (2025). Net Present Value (NPV) sensitivity analysis: understanding risk in investment projects. *Advances in Economics Management and Political Sciences*, 150(1), 186-194. https://doi.org/10.54254/2754-1169/2024.19301
- DBN V.2.2-18:2007. (2020). Buildings and structures. Social protection institutions. Kyiv, 73 p.
- DBN V.2.5-74:2013. (2013). Water supply, external networks, and structures. Basic design provisions. Kyiv, 301 p.
- Dubrovska, V., Shklyar, V. (2021). Heat engineering and power machines. Calculation of the air conditioning system. Kyiv, 56 p.
- Entwicklung des Zinssatzes der Europäischen Zentralbank für das Hauptrefinanzierungsgeschäft von 1999 bis 2025. (2025). https://de.statista.com/statistik/daten/studie/201216/umfrage/ezb-zinssatz-fuer-das-hauptrefinanzierungsgeschaeft-seit-1999/
- Gavrysya, O. (2015). Optimization of heat supply systems using economic and mathematical modeling: monograph. Kyiv, 209 p.
- Guidance. DHSC group accounting manual 2022 to 2023: additional guidance, version 3. (2023). https://doi.org/10.33271/nvngu/20232/011
- Kovrov, O., Dereviahina, N., & Sherstiuk, Ye. (2022). Ecological estimation of installing geothermal systems on the territories of closed coal mines. *Naukovyi Visnyk Natsionalnoho Hirnychoho Universytetu*, 4, 84-90. https://doi.org/10.33271/nvngu/2022-4/084
- Lapshyn, Y., Shevchenko, O., Dybrin, S., & Dychkovskyi, R. (2025). Feasibility of Fine Classification in Processing Watered Coal Sludge from Storage: A Case Study of the Dnipro Coke Chemical Plant. Acta Montanistica Slovaca, 100. https://doi.org/10.46544/ams.v30i1.07
- Larock, B., Jeppson, R., & Watters, G. (2000). Hydraulics of pipeline systems. Direct all inquiries to CRC Press LLC, N.W. Corporate Blvd., Boca Raton, Florida. 33431, 533 p.
- Matas-Escamilla, A., Álvarez, R., García-Carro, F., & Álvarez-Alonso, L. (2023). Mine water as a source of energy: an application in a coalfield in Laciana Valley (León, NW Spain). *Clean Technologies and Environmental Policy*, 25, 2747-2760. https://doi.org/10.1007/s10098-023-02526-y
- Quarterly energy prices. Collection of Department for Energy Security and Net Zero. (2025) https://www.gov.uk/government/collections/quarterly-energy-prices
- Ramos, E., Breede, K., & Falcone, G. (2015). Geothermal heat recovery from abandoned mines: a systematic review of projects implemented worldwide and a methodology for screening new projects. *Environmental Earth Sciences*, 73, 6783-6795. https://doi.org/10.1007/s12665-015-4285-y
- Rudakov, D., Inkin, O. (2022). Evaluation of vertical closed loop system performance by modeling heat transfer in geothermal probes. *Geothermics*, 106, 102567. https://doi.org/10.1016/j.geothermics.2022.102567
- Rudakov, D., Inkin, O. (2023). An approach for ranking abandoned mines by the efficient use of their geothermal potential. *Naukovyi Visnyk Natsionalnoho Hirnychoho Universytetu*, 2, 11-18. https://doi.org/10.33271/nvngu/2023-2/011
- Rudakov, D., Westermann, S. (2021). Analytical modeling of mine water rebound: Three case studies in closed hard-coal mines in Germany. *Mining of Mineral Deposits*. 15(3), 22-30. https://doi.org/10.33271/mining15.03.022
- Rules for the provision of thermal energy supply services, approved by Resolution of the Cabinet of Ministers of Ukraine No. 830 of August 21, 2019. https://zakon.rada.gov.ua/laws/show/830-2019-%D0%BF
- Timoshuk, V., Tishkov, V., Inkin, O., & Sherstiuk, E. (2012). Influence of coal layers gasification on bearing rocks. Geomechanical Processes During Underground Mining - Proceedings of the School of Underground Mining, 109-113. https://doi.org/10.1201/b13157-20
- Vladyko, O., Maltsev, D., Gliwiński, Ł., Dychkovskyi, R., Stecuła, K., & Dyczko, A. (2025). Enhancing Mining Enterprise Energy Resource Extraction Efficiency Through Technology Synthesis and Performance Indicator Development. Energies, 18(7), 1641. https://doi.org/10.3390/en18071641
- Walls, D., Banks, D., Boyce, A., & Burnside, N. (2021). A review of the performance of minewater heating and cooling systems. *Energies*, 14, 6215. https://doi.org/10.3390/en14196215
- Warner, S. (2016). European District Heating Price Series. 58 p.

Author's contribution

Dmytro Rudakov (doctor of technical sciences, full professor): conceptualization, investigation, validation, and writing – review & editing. **Oleksandr Inkin** (doctor of technical sciences, full professor): methodology, data curation, methodology, visualization, writing – original draft. **Rolf Schiffer** (Dr. rer. nat.): investigation, data curation, formal analysis.

All authors have read and agreed to the published version of the manuscript.



Hydrogen Recovery from Coal Industry Waste Using Pyrolysis: Experimental Analysis and Perspectives

DIM-ESEE Conference



Eduard Kliuiev¹* [©]⊠, Ruslan Ahaiev ¹ [©]⊠, Vasyl Zberovskyi¹ [©]⊠ Kateryna Dudlia¹ [©]⊠

¹ M.S. Poliakov Institute of Geotechnical Mechanics of the National Academy of Sciences of Ukraine (IGTM of the NAS of Ukraine), Ukraine, Dnipro, Simferopol'ska street 2A, 49005

Abstract

The article investigates the relevance of hydrogen recovery as a key element of decarbonization of the energy sector of Ukraine, taking into account its significant volumes of coal waste. The aim of the work is to analyze the potential of pyrolysis of carbonaceous raw materials, in particular a mixture of slime and coal, to produce hydrogen. The methodology included laboratory studies, where key parameters such as fraction size (0.1 mm, 0.5 mm, 1.5 mm) and heating duration (20, 25, 40 minutes) were varied, at a fixed final temperature of 750 °C. The obtained results confirmed that the dynamics and total amount of hydrogen release significantly depend on these parameters. In particular, it was found that larger fractions demonstrate faster and higher peaks of hydrogen release, while smaller particles require prolonged heating to achieve maximum yield. The proposed technology of pyrolysis of carbon-contained raw material not only allows to obtain hydrogen, but also provides utilization of industrial waste, turning an environmental problem into an economic opportunity. The general conclusions indicate the high potential of this method for achieving the strategic goals of the Hydrogen Strategy of Ukraine, improving the environmental situation and strengthening the energy independence of the country. Further research will be aimed at optimizing the process and its integrating into coal conversion technologies.

Keywords: "hydrogen", "coal waste", "pyrolysis", "decarbonization".

1. Introduction

Hydrogen is recognized as a key element in formation of the future low-carbon economy and plays a crucial role in the decarbonization of the energy sector, transport and industry. Its potential as a clean energy carrier and feedstock for the chemical industry is significant, as its use produces only water or water vapor, minimizing carbon emissions. The International Energy Agency predicts that hydrogen could provide up to 24 % of global energy needs by 2050, contributing to a significant reduction in greenhouse gas emissions from fossil fuels (URL 1). Global demand for hydrogen exceeded 97 millions tons in 2023 and is expected to reach more than 100 millions tons in 2025 (URL 2).

Ukraine is actively integrating into global hydrogen initiatives, as confirmed by the publication by the Ministry of Energy of the draft Hydrogen Strategy until 2050. This document provides for ambitious goals for hydrogen recovery in Ukraine: up to 1.3 million tons in 2035 and up to 3 million tons in 2050 (URL 3). Hydrogen is also used in is a unique technology for large-scale long-term energy storage, which significantly improves the flexibility of the energy system and contributes to the integration of renewable energy sources (URL 4). Its high energy content per unit mass, where 1 kg of hydrogen is equivalent to 2.8 kg of oil or 2.1 kg of natural gas, makes it an attractive alternative to traditional fuels (Yuzbasioglu & Olgun, 2024). In addition, hydrogen can play an important role in sectors that are difficult to decarbonize by other means, such as freight transport, shipping and air transport, where progress is still at an early stage (Hossain Bhuiyan, M.M. & Siddique, Z., 2025).

The current dominance of "grey" hydrogen, which is produced mainly from fossil fuels such as methane and coal, is accompanied by significant carbon dioxide emissions (URL 5). This creates an urgent need to develop and implement technologies that minimize the carbon footprint, which is critical to achieving global and national decarbonization goals (Lewicka, 2010). The use of coal waste as a carbon-contained raw materials for hydrogen recovery through pyrolysis could be an important step towards obtaining "blue" hydrogen, provided that carbon capture and storage technologies are integrated. This will allow for the efficient use of available resources while reducing the environmental impact associated with carbon-contained waste (Zberovskyi et al., 2024).

Hydrogen recovery from coal industry waste via pyrolysis represents a promising pathway for both energy recovery and waste utilization. The process is based on the thermal decomposition of carbonaceous residues in an oxygen-limited environment, which not only yields gaseous hydrogen but also reduces the volume of hazardous by-products (Dychkovskyi et al., 2019). Compared with conventional coal gasification, pyrolysis requires less energy input and allows greater flexibility in integrating catalysts to enhance hydrogen selectivity. Laboratory studies confirm that

temperature, heating duration, and feedstock composition significantly influence hydrogen yield, with higher temperatures generally favoring gas production (**Dychkovskyi et al., 2025**). By contrast, hydrogen generation during coal gasification occurs through high-temperature reactions of coal with steam, oxygen, or air, producing syngas rich in H₂ and CO. While this method can achieve large-scale hydrogen supply, its efficiency depends on parameters such as temperature, pressure, and steam-to-coal ratio, and it remains limited by high CO₂ emissions, process complexity, and the need for carbon capture technologies (**Falshtynskyi et al., 2011**). In both pyrolysis and gasification, the cogeneration of value-added by-products such as syngas components, tar, and char improves overall economic feasibility, though scaling laboratory results to industrial applications still requires overcoming challenges in reactor design, feedstock heterogeneity, and process optimization (**Fedoreiko, 2024**).

Effective ecological management of hydrogen recovery from coal industry waste requires minimizing emissions and ensuring safe handling of by-products (Golovchenko et al., 2018). Pyrolysis has an environmental advantage over gasification, as it operates without direct combustion and generates fewer greenhouse gases. However, both processes demand strict control of tar, char, and particulate emissions to prevent secondary pollution. Integration of carbon capture, utilization, and storage (CCUS) technologies is essential, particularly for gasification, to mitigate CO₂ release and align with decarbonization goals (Myronova, et al., 2025). Sustainable waste management strategies should include recycling of char for use in construction materials or soil amendments, thereby reducing disposal challenges (Bondarenko et al., 2007; Kurt Yuzbasioglu & Olgun et al., 2024)). Overall, applying a circular economy approach, where energy recovery is combined with by-product valorization, can significantly improve the ecological footprint and environmental sustainability of these technologies.

The Ukrainian National Hydrogen Strategy and global trends highlight the growing need for hydrogen as a key element of the energy transition. At the same time, Ukraine is one of the leaders among European countries in terms of the volume of industrial waste generation, a significant part of which is coal waste (URL 6).

Ukraine generates about 450 million tons of such waste annually, of which over 250 million tons are coal waste, including slimes and tailings. Approximately 25 billion tons of this waste are stored in Ukrainian landfills, covering an area of 1,600 square kilometers, equivalent to about 4 % - 7% of the total territory of Ukraine. According to other estimates, there are about 1,500 tailings dumps in Ukraine, covering about 165,000 hectares (URL 7). Projections indicate that within the next 3 years to 5 years, a significant number of these dumps will exhaust their storage capacity, posing a threat of a large-scale environmental disaster. The main coal-mining basins of Ukraine, where this waste is concentrated, include the Donetsk (Donbas) and Lviv-Volyn coal basins.

The development and implementation of technologies for obtaining hydrogen from these waste allows not only to contribute to energy security and decarbonization, but also to solve the acute problem of disposing of huge volumes of industrial waste. This approach turns an environmental problem into an economic opportunity, creating a multifaceted positive effect for sustainable development.

2. Methodology, Methods and Materials for Hydrogen Recovery from Coal Industry Waste

The research methodology is designed to analyze hydrogen recovery from coal industry waste through pyrolysis, emphasizing both experimental validation and reaction pathway assessment. The process is investigated under controlled thermal decomposition in an inert atmosphere, focusing on the influence of temperature, residence time, heating duration, and catalytic enhancement on hydrogen yield (Dychkovskyi et al., 2019). Particular attention is given to the fundamental reactions, including primary devolatilization of carbonaceous matter, secondary cracking of volatiles, and catalytic steam reforming of hydrocarbons. The water-gas shift reaction ($CO + H_2O \rightarrow CO_2 + H_2$) is also considered, as it plays a critical role in enriching the hydrogen fraction. Comparative evaluation with conventional coal gasification is incorporated to highlight advantages in energy efficiency and emission reduction (Falshtynskyi et al., 2011; Dychkovskyi et al., 2025). Data analysis includes hydrogen yield quantification, syngas composition, and byproduct characterization, supported by statistical treatment to ensure reproducibility and process optimization.

Hydrogen recovery from fossil fuels is currently the dominant method worldwide, despite its significant environmental impact. The main thermochemical methods used for this purpose include steam reforming of methane, which accounts for about 95 % of global hydrogen recovery, coal gasification, partial oxidation of hydrocarbons, autothermal reforming and hydrocarbon pyrolysis (URL 8). This process occurs at high temperatures (750 °C -1000 °C) in the presence of catalysts such as nickel. Coal gasification involves the conversion of coal into gas, consisting of carbon monoxide (CO), hydrogen (H₂), carbon dioxide (CO₂), methane (CH₄) and water vapor (H₂O), which can then be processed to extract hydrogen in different conditions (Kurt Yuzbasioglu & Olgun et al., 2024; Pivnyak et al., 2020).

Pyrolysis is the thermal decomposition of carbon-contained materials in the absence of oxygen, resulting in the formation of volatile products and a solid carbonaceous residue. Fast pyrolysis is the most common variant of this method in both scientific researches and practical application. The gas formed during this process contains hydrogen, methane and carbon oxides. Scientific studies show that pyrolysis and gasification of biomass, which is an analogue of carbon-contained waste, have significant potential for sustainable hydrogen recovery.

Although pyrolysis is not always mentioned as a primary method for direct hydrogen recovery, it is an effective form of thermal destruction of carbon-contained raw materials, which generates a hydrogen. This process allows not only to obtain hydrogen, but also other valuable products, such as tar and solid residue, which increases the overall

economic attractiveness of waste processing. Thus, pyrolysis can be considered as an effective intermediate step in the complex processing of coal waste.

Coal industry waste samples, including coal tailings, slurry, and fine residues, are pretreated by drying at 105 °C, homogenization, and sieving to achieve a uniform particle size distribution. Pyrolysis experiments are performed in a fixed-bed quartz reactor under nitrogen flow, with reaction temperatures ranging from 400 °C to 900 °C and heating duration of 10 °C/min – 20 °C/min. Catalytic tests are conducted using nickel-based, iron-supported, and zeolite catalysts to promote hydrogen selectivity via steam reforming and tar cracking reactions. During experiments, steam is introduced in controlled amounts to enhance hydrogen recovery through steam reforming of hydrocarbons ($C_nH_m + nH_2O \rightarrow nCO + (n+m/2)H_2$) and subsequent water–gas shift conversion (Falshtynskyi et al., 2011). The gaseous products are collected in gas sampling bags and analyzed using gas chromatography equipped detectors, while solid residues (char) are examined by proximate and ultimate analysis, surface area, and calorific value testing. Tar and condensable liquids are described to assess potential for by-product valorization. All procedures follow laboratory safety standards and environmental protocols to ensure accuracy, reproducibility, and sustainability of the experimental framework.

The success of hydrogen extraction from hydrocarbons, especially from coal waste, depends largely on precise control over the technological parameters of the process. Such parameters include temperature, holding time, feedstock particle size and heating duration. The data obtained in laboratory studies allow to study in detail the relationships between these parameters and hydrogen yield, which is critical for further scaling and commercialization of the technology. This approach allows to move from a general understanding to the development of specific engineering solutions that optimize the process.

Laboratory studies were performed using a mixture of coal slime and coal in a ratio of 2:1, sourced from the Lviv-Volyn basin, to investigate the potential for hydrogen recovery via pyrolysis. Each experimental sample had a mass of 10 g, and the pyrolysis process was conducted at a final temperature of 750 °C. To assess the effect of particle size on hydrogen evolution, the feedstock was prepared in three different fractions: fine (<0.1 mm), medium (<0.5 mm), and coarse (<1.5 mm). This variation allowed for the analysis of how grain size influences heat transfer, devolatilization rates, and the overall dynamics of gas release during pyrolysis.

Apart from particle size, the influence of heating duration to the target temperature was investigated, with heating cycles set at 20 minutes, 25 minutes, and 40 minutes. The holding time at the final temperature was consistently maintained at 20 minutes for all experiments to ensure uniform conditions for the secondary reactions and hydrogen release. By systematically varying both the particle size and heating duration, the study aimed to identify the optimal combination of operational parameters that maximizes hydrogen yield while providing insights into the kinetics of the pyrolysis process. These controlled laboratory conditions provide a reliable basis for interpreting the effects of feedstock characteristics and thermal management on hydrogen recovery potential.

3. Laboratory Research Results Analysis

For a visual presentation and analysis of the obtained results, graphs were constructed in Figure 1. The figure illustrates the dynamics of gas release during the pyrolysis process under varying degrees of feedstock dispersion and different heating durations. Such graphical representation makes it possible to track the evolution of gas formation in real time and compare the influence of operational parameters on hydrogen yield. The observed trends highlight the role of particle size reduction and heating intensity in accelerating devolatilization and secondary cracking reactions. Overall, the figure provides a clear basis for interpreting experimental outcomes and supports the identification of optimal conditions for maximizing hydrogen recovery.

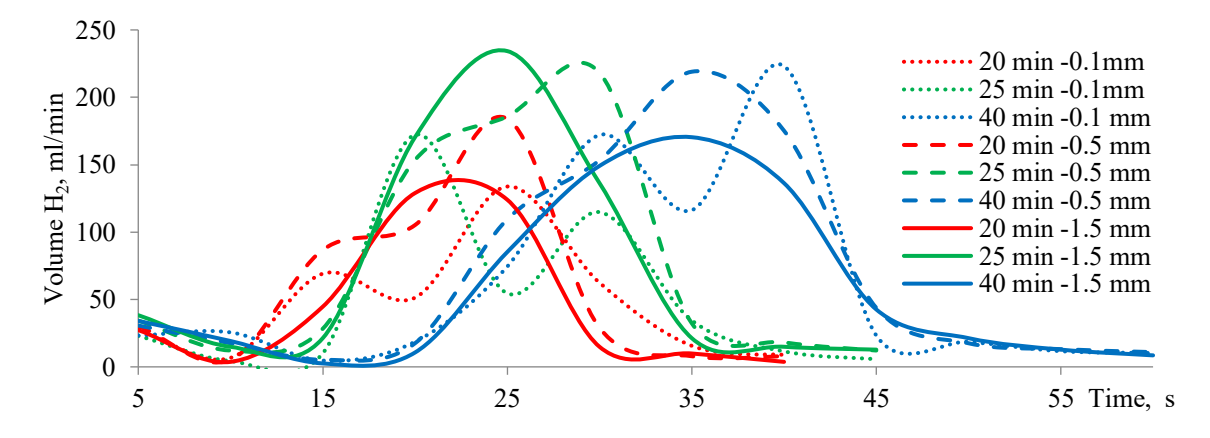


Figure 1. Dynamic of hydrogen release during pyrolysis for different dispersion degree (0.1 mm, 0.5 mm, 1.5 mm) and heating duration (20 min, 25 min, 40 min) of carbon-contained raw material

These graphs illustrate the dynamics of differential hydrogen release (gas volume in ml/min) during the pyrolysis of a sludge-coal mixture (ratio 2:1) under varying particle sizes (0.1, 0.5, and 1.5 mm) and heating durations (20

minutes, 25 minutes, or 40 minutes, with an additional 20-minute holding time). Across all experiments, hydrogen evolution was uneven, with relatively low gas flow observed at the initial stage (5 minutes – 10 minutes), followed by sharp spikes indicating rapid gas formation. For the fine fraction (0.1 mm) under a short heating cycle of 20+20 minutes, two distinct local maxima were recorded: approximately 69 ml/min at the 15th minute and 134 ml/min at the 25th minute, immediately after reaching the final temperature. Extending the heating time to 40 minutes shifted the main peak to the end of the process, with the highest hydrogen release reaching about 223 ml/min at the 40th minute.

The observed peak widths provide valuable insight into the optimal periods for maximum hydrogen evolution and reflect the interplay between particle size, thermal conductivity, and reaction kinetics. Fine particles exhibited a gradual accumulation of internal energy, resulting in delayed but higher cumulative hydrogen release under prolonged heating. In contrast, shorter cycles produced earlier, smaller peaks, demonstrating that heating duration directly influences both the timing and intensity of gas release. These patterns indicate that the dynamics of hydrogen evolution are strongly dependent on feedstock characteristics and thermal conditions, emphasizing the importance of carefully selecting particle size and heating strategy to optimize the efficiency of hydrogen recovery during pyrolysis.

Consistent with previously observed trends, the intensity and timing of maximum hydrogen release are strongly influenced by the heating duration. Shorter heating cycles (20+20 minutes) generally produce smaller peaks that occur earlier in the process, whereas longer cycles (40+20 minutes) lead to higher peaks appearing later. This indicates that extended heating allows for more complete devolatilization and secondary cracking reactions, resulting in a larger cumulative hydrogen output. The temporal shift of the peaks also reflects the progressive penetration of heat into the particle mass, which governs the release of hydrogen from internal layers.

The effect of particle size on hydrogen dynamics is equally pronounced. Larger particles (1.5 mm) exhibit earlier and higher peaks under moderate heating cycles; for instance, at 25+20 minutes, the peak hydrogen release reaches approximately 234 ml/min at the 25th minute. Medium-sized particles (0.5 mm) achieve a maximum of about 219 ml/min at the 35th minute under the 40+20-minute cycle. In contrast, smaller particles (<0.1 mm) demonstrate a more gradual hydrogen evolution, with the peak shifting to the end of longer heating periods. These observations highlight the interplay between thermal inertia and particle dispersion, emphasizing the need to optimize both heating duration and particle size to maximize hydrogen yield and control the release dynamics.

In the conducted experiments, the following data were obtained:

- heating cycle 20+20 minutes, particle size 0.1-1.5 mm the total hydrogen yield is 37.6- 45.6 m³ per 1 ton of feedstock;
- heating cycle 25+20 minutes, particle size 0.1-1.5 mm the total hydrogen yield is 43.1- 69.5 m³ per 1 ton of feedstock;
- heating cycle 40+20 minutes, particle size 0.1-1.5 mm the total hydrogen yield is 69.3- 81.3 m³ per 1 ton of feedstock.

All curves show that after the peak, the hydrogen yield decreases sharply. Thus, larger components are prone to rapid and significant hydrogen release in the middle of the process, while small ones accumulate reaction potential and give a higher yield at long heating. This indicates that large particles, despite their greater thermal inertia, accumulate more hydrogen in the deep layers and sharply release it when reaching a critical temperature. Therefore, the balance between grain size and heating time is key to optimizing the dynamics and volumes of hydrogen release in the pyrolysis process.

4. Discussion of the Results

The obtained results demonstrate that both feedstock dispersion and heating duration play a decisive role in the dynamics and volume of hydrogen release during pyrolysis of coal—sludge mixtures. The observed multi-peak character of hydrogen emission indicates that the process is governed not only by surface devolatilization but also by secondary cracking reactions and diffusion-controlled release from deeper layers of the material. Fine particles (<0.1 mm) showed a gradual hydrogen evolution with delayed maximum peaks under extended heating, which can be explained by uniform heat transfer and slower accumulation of internal reaction products before their final release (Falshtynskyi et al., 2011; Ahaiev et al., 2025). Conversely, larger particles (1.5 mm) exhibited sharper and earlier peaks, suggesting that hydrogen accumulates in the inner porous structure and is released suddenly once the critical temperature zone penetrates the particle core. This effect highlights the role of thermal inertia, which accelerates peak formation in coarser fractions but limits total gas yield over prolonged exposure.

The heating duration further influenced hydrogen dynamics, as shorter heating cycles resulted in earlier and smaller peaks, while longer heating durations shifted the maximum release toward the end of the cycle, producing significantly higher peak intensities. These findings emphasize that the synergy between particle size and heating duration determines the efficiency of hydrogen recovery: larger particles favor high-intensity, rapid release, whereas fine particles under prolonged heating enable extended and higher cumulative output. The post-peak decline across all experimental curves indicates depletion of reactive hydrogen precursors, marking the end of effective pyrolysis activity. From an environmental and technological standpoint, the results suggest that optimizing hydrogen recovery requires balancing feedstock dispersion with heating time to ensure both high peak efficiency and sustainable gas yield. Overall, the study confirms that tailored thermal management can significantly enhance hydrogen recovery from coal industry waste, providing a scientific basis for scaling pyrolysis technologies toward industrial application.

In order to optimize hydrogen yield, ecological and environmental considerations are critical for the sustainable implementation of pyrolysis processes. The generation of gaseous, liquid, and solid by-products requires careful management to prevent emissions of harmful compounds such as polycyclic aromatic hydrocarbons, tars, and particulate matter (Zberovskyi et al., 2024; Bieda. et al., 2017). Incorporating gas cleaning systems and adopting closed-loop processes can minimize the release of pollutants into the atmosphere, while valorization of char and condensable liquids as secondary materials supports a circular economy approach (Bieda et al., 2017; Pan et al., 2025). Moreover, controlling operational parameters such as temperature and heating duration not only enhances hydrogen recovery but also reduces the risk of incomplete pyrolysis and associated environmental hazards. Integration of carbon capture, utilization, and storage (CCUS) technologies can further mitigate CO₂ emissions, ensuring that the process aligns with decarbonization goals (Bieda. et al., 2017; Pan et al., 2025). Overall, environmentally responsible design and operation of pyrolysis reactors are essential to balance energy recovery with protection of air, soil, and water resources.

Based on the laboratory results, several practical conclusions can be drawn for process optimization. Fine fractions (<0.1 mm) are best suited for long heating cycles (40 min + 20 min), as they maximize cumulative hydrogen yield due to uniform devolatilization. Medium fractions (~0.5 mm) demonstrate stable release with moderate heating durations, making them a balanced option for continuous hydrogen recovery systems. Coarser particles (1.5 mm) provide the highest instantaneous hydrogen release at shorter cycles (25 min + 20 min), which may be advantageous for rapid gas generation but less efficient for total yield. Therefore, an industrial-scale process should consider blending different fractions to combine rapid hydrogen spikes with extended release phases. Such an integrated strategy would not only maximize recovery efficiency but also improve the stability and controllability of pyrolysis reactors.

4. Conclusions

The conducted laboratory studies confirmed that both particle size and heating duration have a significant effect on the dynamics and efficiency of hydrogen release during pyrolysis of coal–sludge mixtures. The experiments revealed that hydrogen evolution occurs unevenly, with characteristic peak formations influenced by both thermal conditions and feedstock dispersion. Fine particles (<0.1 mm) showed delayed but higher cumulative hydrogen yields under prolonged heating, while coarse particles (1.5 mm) released hydrogen more rapidly, reaching peak values earlier in the process. These differences reflect the roles of thermal inertia, devolatilization, and secondary cracking in governing hydrogen recovery potential.

The results also demonstrated that heating duration is a critical factor for optimizing the process. Shorter heating cycles led to lower and earlier peaks, whereas extended heating durations shifted the maximum hydrogen release to later stages and increased peak intensity. The combination of dispersion degree and heating duration thus defines the balance between rapid hydrogen output and total cumulative yield. This indicates that pyrolysis conditions must be carefully tailored depending on whether the goal is to maximize immediate hydrogen flow or ensure sustained gas production over time.

From a practical standpoint, the findings suggest specific optimization strategies for industrial application. Fine fractions are most effective for long heating cycles, medium fractions provide stable performance under moderate conditions, and coarse fractions are optimal for achieving high-intensity hydrogen spikes within shorter cycles. An integrated approach that blends different particle sizes could deliver both stable hydrogen recovery and peak intensification, thereby enhancing reactor efficiency and operational flexibility. These insights form the basis for developing scalable pyrolysis technologies aimed at converting coal industry waste into a valuable hydrogen resource while reducing environmental impacts.

The results of this study demonstrate the high potential of coal waste pyrolysis as an effective and environmentally friendly method of hydrogen recovery in Ukraine. Further scientific and engineering researches should be aimed at comprehensive optimization of the process to achieve maximum hydrogen yield, development of effective technologies for purification and separation of gas products, as well as integration with carbon capture technologies to ensure the recovery of "blue" hydrogen. The implementation of such innovative technologies will contribute to achieving the strategic goals of the Hydrogen Strategy of Ukraine, improving the environmental situation in coal-mining regions through the utilization of accumulated coal-contained waste, as well as strengthening the country's energy independence.

5. References

- Ahaiev, R., Prytula, D., Zberovskyi, V., Kliuiev, E., Antoniuk, O., & Pererva, A. (2025). Environmental aspects and statistical analysis of geological data of gas recovery in surface degassing wells. IOP Conference Series: Earth and Environmental Science, 1457(1), 012019. https://doi.org/10.1088/1755-1315/1457/1/012019
- Bieda, B., Skalna, I., Gaweł, B., Grzesik, K., Henclik, A., & Sala, D. (2017). Life cycle inventory processes of the integrated steel plant (ISP) in Krakow, Poland-continuous casting of steel (CCS): a case study. The International Journal of Life Cycle Assessment, 23(6), 1274–1285. https://doi.org/10.1007/s11367-017-1365-0
- Bondarenko, V., Buzylo, V., Falshtynskiy, V. & Dychkovskiy, R. (2007). Parameters of Injection Fill Above an Underground Gas Generator. Technical, Technological and Economical Aspects of Thin-Seams Coal Mining,

- International Mining Forum, 2007, 89–95. https://doi.org/10.1201/noe0415436700.ch11
- Dychkovskyi, R., Shavarskyi, J., Cabana, E. C., & Smoliński, A. (2019). Characteristic of Possible Obtained Products during the well Underground Coal Gasification. Solid State Phenomena, 291, 52–62. https://doi.org/10.4028/www.scientific.net/ssp.291.52
- Dychkovskyi, R., Falshtynskyi, V., Saik, P., & Lozynskyi, V. (2025). Aspects of co-utilization of solid waste and coal through underground gasification. IOP Conference Series: Earth and Environmental Science, 1457(1), 012002. https://doi.org/10.1088/1755-1315/1457/1/012002
- Golovchenko, A., Pazynich, Y., & Potempa, M. (2018). Automated Monitoring of Physical Processes of Formation of Burden Material Surface and Gas Flow in Blast Furnace. Solid State Phenomena, 277, 54–65. https://doi.org/10.4028/www.scientific.net/ssp.277.54
- Fedoreiko, V. (2024). Distributed energy generation based on jet-vortex bioheat generators. E3S Web of Conferences, 567, 01001. https://doi.org/10.1051/e3sconf/202456701001
- Falshtynskyi, V., Dychkovskyi, R., & Zasedatelev, O. (2011). Economic indicators of BUCG on an experimental station in the OJSC Pavlogradvugillia conditions. Technical and Geoinformational Systems in Mining, 201–206. https://doi.org/10.1201/b11586-33
- Kurt Yuzbasioglu, S., & Olgun, H. (2024). Hydrogen Production via Waste Pyrolysis: A Review of A Study. Erzincan University Journal of Science and Technology(SUIC), 129-141. https://doi.org/10.18185/erzifbed.1524216
- Lewicka, D. (2010). The impact of HRM on creating proinnovative work environment. International Journal of Innovation and Learning, 7(4), 430. https://doi.org/10.1504/ijil.2010.032932
- Md Monjur Hossain Bhuiyan & Zahed Siddique (2025). Hydrogen as an alternative fuel: A comprehensive review of challenges and opportunities in production, storage, and transportation. International Journal of Hydrogen Energy, 102, 1026-1044. https://doi.org/10.1016/j.ijhydene.2025.01.033
- Myronova, I., Kovrov, O., Dudek, M., Voronkova, Y., & Kononenko, M. (2025). Environmental assessment of the impact of iron ore mine emissions on biological indicators of winter wheat. IOP Conference Series: Earth and Environmental Science, 1457(1), 012004. https://doi.org/10.1088/1755-1315/1457/1/012004
- Pan, F., Zhao, X., Dudek, M., Rehman, M. Z., & Shahzad, U. (2025). Ecological Impacts of Cultivated Land Conversion and Urban Eco-Resilience in the COP29 Era. Land Degradation and Development, Portico. https://doi.org/10.1002/ldr.70080
- Pivnyak, G., Falshtynskyi, V., Dychkovskyi, R., Saik, P., Lozynskyi, V., Cabana, E., & Koshka, O. (2020). Conditions of Suitability of Coal Seams for Underground Coal Gasification. Key Engineering Materials, 844, 38–48. https://doi.org/10.4028/www.scientific.net/kem.844.38
- Zberovskyi, V., Ahaiev, R., Vlasenko, V., & Prytula, D. (2024). Hydrodynamic impact as a way of controlling the state of the coal-gas system: analysis and data processing. IOP Conference Series: Earth and Environmental Science, 1348(1), 012039. https://doi.org/10.1088/1755-1315/1348/1/012039
- URL 1. https://glavcom.ua/new_energy/news/zeleniy-voden-mozhe-zrivnyatis-u-cini-z-prirodnim-gazom-do-2050-roku-671696.html (accessed 26th June 2025).
- URL 2. https://www.iea.org/reports/global-hydrogen-review-2024 (accessed 25th June 2025).
- URL 3. https://www.mev.gov.ua/sites/default/files/field/file/vodneva-strategiya17.05.2024.pdf (accessed 29th June 2025)
- URL 4. https://mindscope.biz.ua/vodneva-energetyka-v-ukrayini-zelene-majbutnie-na-krok-blyzhche/ (accessed 29th June 2025)
- URL 5. https://energy-cities.eu/50-shades-of-grey-and-blue-and-green-hydrogen/ (accessed 29th June 2025)
- URL 6. https://zn.ua/ukr/ECOLOGY/zasillja-promislovikh-vidkhodiv-chi-vdastsja-ukrajini-perejti-do-tsirkuljarnoji-ekonomiki.html (accessed 29th June 2025)
- URL 7. https://ecoaction.org.ua/wp-content/uploads/2024/12/analit-zvit-rekultyvacia-terykoniv2024s.pdf (accessed 29th June 2025)
- URL 8. https://www.maximizemarketresearch.com/market-report/steam-methane-reforming-hydrogen-generation-market/220453/ (accessed 29th June 2025)

Funding

The authors declare that this research was conducted without any external funding.

Author's contribution

Eduard Kliuiev (Senior Researcher): methodology, supervision, writing – review & editing. **Ruslan Ahaiev** (Senior Researcher): data curation, formal analysis, project administration. **Vasyl Zberovskyi** (Senior Researcher): conceptualization, investigation, writing – original draft. **Kateryna Dudlia** (Researcher)- literature review and search, visualization.

All authors have read and agreed to the published version of the manuscript.



Hybrid Approach of Neural Networks and Analog-Based Methods for Industrial Assessment of Technogenic Deposits

DIM-ESEE Conference



Artem Pavlychenko¹ ©⊠, Dagmara Lewicka² ©⊠, Ivan Miroshnykov¹ ⊠, Serhii Dybrin¹ ©⊠, Andrii Pererva³ ©⊠, Roman Dychkovskyi¹,2* ©⊠

- ¹ Dnipro University of Technology, Dmytra Yavornytskoho Ave., 19, Dnipro, 49005, Ukraine
- ² AGH University of Krakow, Al. Mickiewicza 30, 30059, Krakow, Poland
- ³ Public Joint Stock Company "Lviv Coal Company", Lviv Region, Ukraine

Abstract

Technogenic deposits, originating from mining and industrial activities, are increasingly recognized as valuable secondary sources of critical raw materials. Traditional analog-based assessment methods offer practical tools for evaluating their industrial potential but often struggle with the complexity and heterogeneity of such formations. This study proposes a hybrid methodology that integrates analog-based approaches with artificial neural networks (ANNs) to enhance the accuracy and reliability of technogenic deposit assessments. Analog methods are first employed to establish baseline parameters from historical data, which then serve as training inputs for a multilayer perceptron (MLP) neural network. The model demonstrated strong predictive performance, achieving classification accuracies above 90% on validation datasets. Sensitivity analysis identified pollutant concentration, mineral composition, and particle size distribution as the most influential factors in determining industrial suitability. By combining empirical knowledge with machine learning, the hybrid approach enables robust, adaptive, and scalable evaluations, even under conditions of incomplete or uncertain data. The results confirm its potential to improve decision-making in resource recovery, environmental remediation, and sustainable development. This framework contributes to the digital transformation of resource management and supports the responsible exploitation of technogenic deposits within circular economy principles.

Keywords: "AI in mining", "neural networks" "technogenic deposit" "decision making", "physical-chemical extraction"

1. Introduction

Technogenic deposits, formed as a result of mining, mineral processing, and related industrial activities, are increasingly recognized as a significant category of secondary mineral resources (Hutniczak et al., 2025; Pavlychenko et al., 2025). Traditionally perceived as waste, these formations are now receiving renewed attention due to the rising demand for critical raw materials and the urgent need to reduce the environmental impacts of extractive industries. In this study, the term technogenic deposit is understood as an anthropogenic accumulation of mineral matter formed because of industrial activity. Specifically, we focus on deposits generated during the coal beneficiation process, which contain a significant number of valuable components. These materials, although initially classified as waste, represent an important secondary resource base that can be further utilized in various sectors of the national economy. Their valorization represents not only an economic opportunity but also an ecological necessity, supporting sustainable resource management and the principles of the circular economy.

Analog-based methods, relying on comparative analyses with previously studied or exploited sites, have long provided a practical framework for assessing the industrial potential of technogenic deposits (Polyanska et al., 2025a; Vladyko et al., 2025). However, the inherent complexity, heterogeneity, and spatial variability of these formations often limit the accuracy of conventional approaches. As a result, decision-making processes based solely on analogies remain prone to uncertainty and may fail to reflect the multifactorial nature of technogenic systems.

The environmental consequences of technogenic waste further complicate assessment and management. Large-scale contamination, involving diverse hazardous pollutants, extends across significant land areas and poses serious risks to ecosystems and human health (Miroshnykov et al., 2025). As shown in Figure 1, the mass of contaminated land varies substantially by pollutant type and concentration, underscoring the need for analytical tools that can integrate both environmental risks and resource recovery potential. Such data provide a foundation for prioritizing remediation efforts, designing recovery strategies, and identifying deposits with the industrial value.

In our previous research, we conducted a comprehensive assessment of the environmental degradation resulting from technogenic waste (Miroshnykov et al., 2025). Figure 1 illustrates this impact by presenting the mass of contaminated land categorized by pollutant type, expressed in millions of tons. The figure offers a detailed breakdown of the total volume of affected soil for each identified hazardous substance, highlighting notable variations in contamination levels according to the type and concentration of pollutants. Such visual representation is essential for accurately evaluating the extent of environmental damage and for guiding the prioritization of remediation actions and strategies for resource recovery.

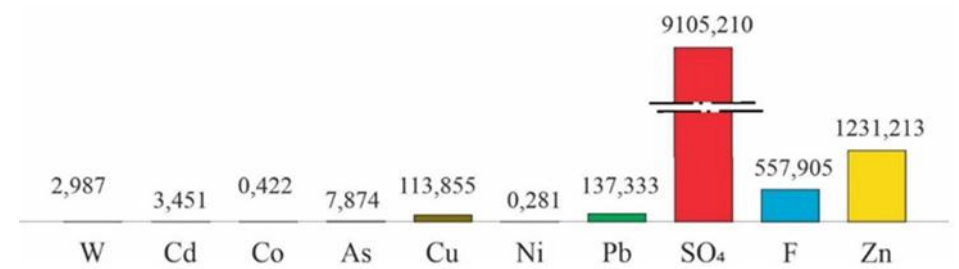


Figure 1. Extent of Soil Contamination by Pollutant Type (millions of tons) (Miroshnykov et al., 2025).

At the same time, global trends in resource governance increasingly emphasize sustainable exploitation, digital transformation, and the adoption of advanced computational tools. Artificial intelligence (AI), particularly artificial neural networks (ANNs), has shown remarkable capabilities in addressing nonlinear, multidimensional, and uncertain problems in engineering and environmental studies (Polyanska et al., 2023b). Their ability to learn from data, detect hidden patterns, and generate reliable predictions makes them particularly suitable for modeling technogenic deposits, where incomplete datasets and high uncertainty are common challenges (Dychkovskyi et al., 2025).

Integrating neural networks into analog-based assessment frameworks offers a promising pathway toward improving precision, adaptability, and scalability. This hybrid approach combines the empirical robustness of analog reasoning with the predictive power of machine learning, thereby reducing reliance on subjective expert judgment and supporting more data-driven decision-making (Wang et al., 2018; Bas, 2016). Importantly, such integration aligns with broader sustainability goals by facilitating resource recovery, minimizing environmental damage, and enhancing planning strategies for post-industrial territories.

This research addresses the need for intelligent and resilient assessment methodologies by proposing a hybrid framework that unites analog-based techniques with neural network modeling. The approach is designed to enhance the reliability of evaluating technogenic deposits for industrial exploitation while simultaneously supporting environmental remediation and sustainable development. Beyond its immediate application, the framework may serve as a prototype for broader use in mineral resource management, adaptive land-use planning, and the development of digital tools for the circular economy.

2. Methodology, Methods and Materials of the Research

This research employs a hybrid methodological framework that integrates analog-based assessment techniques with artificial neural networks (ANNs) to evaluate the industrial suitability of technogenic deposits. The methodology is designed to leverage the empirical strengths of analog-based approaches while enhancing predictive accuracy through machine learning (Ghayoumi et al., 2021).

Initially, analogy-based methods are used to identify reference cases from historical data, geological surveys, and mining records (Bas, 2016; Gallego & Corchuelo, 2019). These reference cases serve as the foundation for establishing baseline parameters, including mineral composition, granulometry, contamination levels, and past recovery efficiency. Such parameters are essential for the preliminary classification of technogenic waste. Selected deposits are then characterized according to spatial, environmental, and material attributes, which are compiled into a structured dataset to support subsequent neural network training and validation.

The machine learning component is implemented as a multilayer perception (MLP) neural network, capable of capturing complex, non-linear relationships between input and output variables (Dyczko, 2023). The network architecture comprises an input layer, multiple hidden layers with non-linear activation functions, and an output layer that generates predictions or classification results. The general formulation of the network is expressed as:

$$h(1) = \varphi(1)(W(1)xi + b(1)), \tag{1}$$

$$h(2) = \varphi(2)(W(2)xi + b(2)),$$

$$h(n) = \varphi(k)(W(k)xi + b(k)),$$
(2)

$$yi = \sigma(W(k)h(k-1) + b(k))$$

where are:

 $\varphi^{(k)}$ – the non-linear activation function (e.g., ReLU),

 σ – the sigmoid function,

 $W^{(k)}$, $b^{(k)}$ – the weight coefficients and biases corresponding to each studied parameter.

Elemental composition of the samples was determined by arc spectral analysis performed at the laboratories of the Dnipro University of technology and our partner laboratory of KP "Pivdenukrgeologiya" using a STE-1 spectrograph with a USI-10 attachment and the "powder dispersion" technique. This method allowed semi-quantitative identification of a wide range of elements, including Ba, Be, P, Cr, Pb, Sn, Ga, Ni, Y, Yb, Zn, Zr, Co, Ti, Cu, V, Ge, Mo, Li, La, Sr, Mn, W, Bi, Nb, Sc, Ce, Ag, and As. The detection limits varied from 0.05% to 5% depending on the element, whereas Os, Sb, Cd, U, Nf, Hg, Ta, and Au were below the instrument's sensitivity. The procedure ensured reliable differentiation between magnetic, strongly magnetic, and non-magnetic fractions of the investigated waste products.

In parallel, X-ray fluorescence spectrophotometry (XRF) was applied in the Central Plant Laboratory of "Krymskiy Titan" to obtain quantitative oxide compositions. The analysis provided mass fractions of MgO, Al₂O₃, SiO₂, CaO, TiO₂, Fe₂O₃, SO₃, K₂O, ZrO₂, and BaO, which were validated against chemical assays of iron content to confirm accuracy. These complementary methods enabled both semi-quantitative and quantitative assessment of the elemental distribution, highlighting the enrichment of Al₂O₃ in non-magnetic fractions and ZrO₂ in magnetic products, and allowed us to investigate the correlations between molybdenum content and these chemical compounds and products, thereby providing a comprehensive picture of the geochemical characteristics of the studied materials.

Supervised learning algorithms are applied to train the MLP on labeled datasets derived from known deposit cases. The model is optimized to predict the industrial potential of unexplored or poorly documented technogenic sites using input features obtained from the analog assessment. Cross-validation techniques are employed to ensure generalizability and prevent overfitting. Additionally, sensitivity analysis identifies the most influential input parameters, such as mineral composition, particle size distribution, and contaminant concentration, thereby improving interpretability and supporting data-driven decision-making (Kumaraswamy, 2021).

The study relies on a combination of historical mining records, geological surveys, and environmental monitoring datasets to construct the input features for both analog-based and neural network analyses. The integration of empirical analog knowledge with machine learning allows for robust, adaptive, and scalable assessment of technogenic deposits, even under conditions of incomplete or uncertain data (Bas, 2016).

By combining analog-based reasoning with neural network modeling, the proposed methodology enables accurate, interpretable, and efficient evaluation of technogenic deposits for industrial exploitation, while simultaneously accounting for environmental and material variability. This hybrid approach represents a flexible tool for resource management, remediation planning, and sustainable development in post-industrial territories.

3. Neural Network and Analog-Based Modeling Results

For the purpose of this study, one of the industrial companies located in the Western Ukraine was selected as a case study site. The enterprise operates in a post-mining region where approximately 80 million tons of mine waste have accumulated over several decades of extraction and processing activities. These technogenic deposits, largely untreated and stored in waste dumps and tailings, represent both an ecological challenge and a potential secondary resource base. Their presence has resulted in the significant environmental pressure on the surrounding landscapes, including soil degradation, air polution, water contamination, and altered land use patterns. Therefore, the site provides a representative example for testing hybrid assessment methodologies that integrate analog-based approaches with neural network modeling in order to evaluate both industrial potential and environmental management strategies.

To support the development of a neural network for analog-based modeling in the industrial assessment of technogenic deposits, a flowchart was designed and is presented in Fig. 1. The scheme outlines a hybrid methodology that starts with *Analog-Based Assessment*, where reference cases are analyzed to define baseline parameters. This is followed by *Dataset Preparation*, which organizes spatial, environmental, and material data into a structured form suitable for model training. In the *Neural Network Training* stage, the system learns complex, non-linear dependencies between input variables and output results. The subsequent step, *Prediction & Sensitivity Analysis*, produces evaluation outcomes while identifying the influence of critical parameters on model accuracy. The process concludes with *Decision Support*, where the integrated results are applied to optimize industrial exploitation strategies and to prioritize remediation and resource recovery.

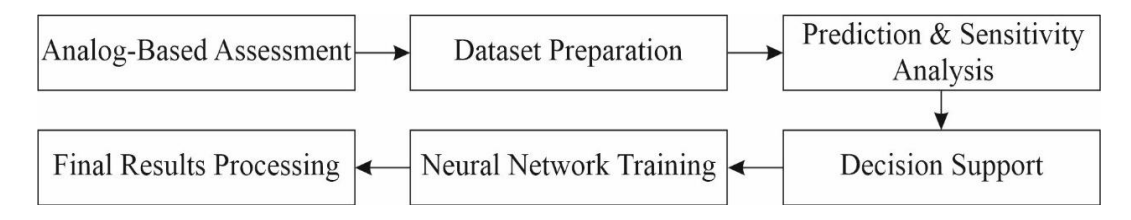


Figure 1. Hybrid methodology for assessing technogenic deposits using analog-based analysis and neural networks

By industrial assessment we refer to the evaluation of technogenic deposits based on industrial criteria such as processing feasibility, technological applicability, and potential for large-scale utilization. The term analog-based assessment is used to describe the method of comparing the studied deposits with already explored or utilized analogs, to estimate their potential value and applicability.

The hybrid analog-ANN framework was applied to evaluate the industrial potential of technogenic deposits with a specific focus on molybdenum (Mo) as the primary target element. The model incorporated analog-based reference data for baseline characterization, while the multilayer perceptron (MLP) neural network captured nonlinear relationships between compositional and environmental parameters. A priority index (*PIMo*) was introduced to rank the different magnetic fractions according to normalized Mo content, enrichment factor, and technological compatibility with associated elements. Separate investigations were carried out for the magnetic, strongly magnetic, and non-magnetic fractions, ensuring a more comprehensive assessment of element distribution and recovery potential.

The predictive model was implemented as a feed-forward multilayer perceptron (MLP) trained using a supervised learning approach. The input layer consisted of five parameters, namely particle size distribution, ash content, moisture, density, and processing conditions. The network architecture included three hidden layers with 64, 32, and 16 neurons, respectively, each employing the Rectified Linear Unit (ReLU) activation function to ensure nonlinearity and effective feature extraction. The output layer contained a single neuron with a sigmoid activation function, which produced the predicted recovery of valuable components. Model training was performed using the backpropagation algorithm with the Adam optimizer, applying a learning rate of 0.001 to achieve stable convergence and minimize prediction error. The structure of the developed feed-forward multilayer perceptron (MLP) designed for predicting the recovery of valuable components is summarized in **Table 1**.

Layer Number of neurons Activation function Functional description

Particle size, ash, moisture, density,

Table 1. Architecture of the developed feed-forward multilayer perceptron (MLP) model for predicting the recovery of valuable components

Input layer 5 processing conditions Hidden layer 1 64 ReLU Feature extraction 32 Hidden layer 2 ReLU Non-linear mapping Hidden layer 3 16 ReLU Dimensionality reduction Predicted recovery of valuable components Output Layer 1 Sigmoid

The dataset used for the supervised learning algorithm consisted of nearly 1,200 samples, each containing 10 input features representing sensor measurements of material properties, and a corresponding output label representing the predicted material strength. The dataset was split into a training set of 840 samples (70% of total) and a validation set of 180 samples (15% of total). The remaining 180 samples (15%) were reserved as a test set for final evaluation. Feature preprocessing included min-max normalization, and the split was performed using stratified random sampling to ensure an even distribution of output values across the sets.

The neural network used was a feedforward multilayer perception (MLP) consisting of three hidden layers with 64, 32, and 16 neurons, respectively. The input layer consisted of 10 neurons, corresponding to the number of features in each sample, while the output layer contained 1 neuron representing the predicted material strength. The activation function for the hidden layers was ReLU, and for the output layer linear. The network was trained using the mean squared error loss function and the Adam optimizer with a learning rate of 0.001.

The analysis demonstrated that the strongly magnetic fraction contained the highest concentration of Mo (0.5 ppm) compared with both the magnetic and non-magnetic fractions (0.3 ppm each). Consequently, this fraction was selected as the primary target for the industrial assessment. Within the same fraction, three co-priority phases were identified on the basis of concentration and technological value: TiO₂ (1.71 %), ZrO₂ (1.09 %), and Mn (100 ppm). From an economic perspective, however, Cu (15 ppm) may also serve as an alternative co-priority element due to its higher market demand and compatibility with established recovery processes. This prioritization highlights the advantage of the hybrid approach, which not only quantifies the relative enrichment of critical elements but also supports the strategic selection of co-recovery targets. The results provide a practical basis for designing recovery schemes that integrate Mo with other valuable elements, thereby enhancing both the economic efficiency and sustainability of technogenic deposit utilization.

The multilayer perceptron (MLP) model developed in this study demonstrated high predictive capability in assessing the industrial potential of technogenic deposits. Trained on a dataset incorporating a wide range of reference sites with diverse mineralogical and environmental characteristics, the neural network successfully identified complex non-linear patterns that conventional analog-based methods were unable to capture (Bas, 2016; Dyczko, 2023; Psyuk & Polyanska, 2024). Validation results confirmed its robustness and transferability, with the classification accuracy exceeding 90 % across different deposit types. When combined with analog-based assessments, neural network predictions provided more refined and data-driven evaluations of poorly studied or undocumented technogenic sites. This hybrid methodology leveraged the complementary strengths of empirical knowledge and machine learning,

enabling more comprehensive interpretations of complex datasets. Several deposits previously considered of limited value were identified as promising for industrial exploitation, and subsequent field sampling together with laboratory tests confirmed the predictive reliability of the model.

A sensitivity analysis of the MLP further highlighted the parameters exerting the strongest influence on assessment results, namely pollutant concentration, mineral composition, and particle size distribution. These findings not only validate the model's explanatory capacity but also provide practical guidance for directing future sampling programs and monitoring efforts. Overall, the integration of neural networks with analog-based reasoning offers a scalable and adaptable approach to resource evaluation, enhancing both the accuracy and efficiency of technogenic deposit assessments while supporting sustainable resource management strategies.

The proposed algorithm for selecting three co-priority elements, in addition to molybdenum, begins with the systematic preparation of input data. Concentrations of elements within the chosen fraction are collected and expressed either in percentages or parts per million (ppm). To ensure comparability, all values are converted into ppm and normalized relative to the maximum observed concentration across fractions. This normalization step provides a consistent basis for evaluating elements of differing magnitudes and geological origins.

Once normalized, the dataset undergoes a filtering stage designed to eliminate major gangue oxides, such as SiO₂, Al₂O₃, CaO, MgO, K₂O, and SO₃. These components, while present in significant amounts, are not considered recovery targets due to their limited economic value and lack of technological significance in co-extraction processes. This reduction step ensures that the focus of the algorithm remains on elements with industrial potential and environmental relevance.

The evaluation of candidate elements is then carried out using a weighted scoring system. Four main weighting criteria are considered: relative concentration (w_1) , technological compatibility with molybdenum circuits (w_2) , economic value based on criticality and market demand (w_3) , and environmental significance (w_4) , where removal may help reduce contamination. A Priority Index (PI) is calculated for each element as:

$$PI_e = w_1 \cdot G_{norm} + w_2 \cdot T + w_3 \cdot E + w_4 \cdot E_{nv}$$

where $w_1 + w_2 + w_3 + w_4 = 1$.

In the proposed Priority Index (PI) framework, four parameters are used to evaluate each candidate element. G_{norm} (Normalized Grade) represents the relative concentration of the element within the selected fraction. It is obtained by converting concentrations into a uniform unit (ppm) and scaling them against the maximum observed value, which enables comparison across elements of different magnitudes. T (Technological Compatibility) is expressed on a scale from 0 to 1 and reflects the feasibility of recovering the element within the same processing circuit as molybdenum. A higher value indicates stronger synergy with existing technologies, whereas lower values suggest the need for separate or more complex processing. E (Economic Value) refers to the market significance of the element, determined by factors such as global demand, criticality indices, and current economic assessments. Finally, E_{nv} (Environmental Factor) captures the ecological importance of recovering the element. Positive values are assigned when extraction reduces environmental risks, for example in the case of toxic metals such as Pb or Cr, while neutral or zero values indicate limited environmental impact. Together, these parameters ensure that the Priority Index accounts for geological, technological, economic, and ecological dimensions of decision-making.

This formulation enables a balanced assessment that integrates geological, technological, economic, and environmental dimensions. Finally, the algorithm ranks all candidate elements according to their Priority Index values. The two highest-scoring elements are automatically selected as co-priorities. For the third position, a tie-breaking rule is applied: if two candidates have Priority Index values within 10% of each other, the element with the greater economic value is chosen. This rule ensures that the final selection not only reflects quantitative grades but also accounts for industrial demand and market relevance, providing a structured and adaptable approach to multi-criteria decision-making in technogenic deposit assessment.

Table 2. Ranking of co-priority elements for Mo recovery (strongly magnetic fraction)

Scenario	Mo (ppm)	Co-element 1	Co-element 2	Co-element 3
Base Case (concentration only)	0.5	TiO ₂ (1.71%)	ZrO ₂ (1.09%)	Mn (100 ppm)
Alternative (economic weight ↑)	0.5	TiO ₂ (1.71%)	ZrO ₂ (1.09%)	Cu (15 ppm)

While the absolute concentrations of many elements in the waste fractions are below typical smelter feed grades, the results gain significance when interpreted through relative enrichment and co-occurrence patterns. For instance, in the strongly magnetic fraction, Mo was detected at \sim 0.5 ppm, a level too low for direct metallurgical recovery. However, when normalized against associated elements, the analysis indicates a consistent co-enrichment of Mo with TiO₂ (1.71 %), ZrO₂ (1.09 %), and Mn (100 ppm). These associations suggest that Mo is preferentially concentrated in mineral phases that also host Ti and Zr, thus opening perspectives for co-recovery strategies in processing scenarios targeting Ti- or Zr-bearing materials.

This approach allows the results to be presented in a ranking framework (Table 2), where co-priority elements are

identified based on concentration and potential economic relevance. In the base case, Mo clustering with TiO₂, ZrO₂, and Mn highlights a mineralogical linkage; in an alternative weighting scenario, Cu (15 ppm) becomes a more relevant co-priority element due to its economic value despite its lower concentration. Such comparative ranking provides a clearer interpretation of the data, emphasizing enrichment factors and recovery synergies rather than absolute grades, thereby making the findings more relevant for evaluating resource potential in industrial practice.

The analysis confirms that the strongly magnetic fraction, containing the highest concentration of molybdenum (0.5 ppm), represents the most suitable target for recovery. In both scenarios considered, titanium dioxide (TiO₂, 1.71 %) and zirconium dioxide (ZrO₂, 1.09 %) consistently emerge as priority co-elements. Their selection is driven not only by their elevated concentrations but also by their significant technological value, which enhances the potential economic and industrial benefits of their recovery. These findings underscore the importance of identifying both primary and secondary targets when planning extraction processes, ensuring that resource utilization is both efficient and strategically informed.

The choice of the third co-element, however, varies depending on the applied weighting criteria, highlighting the flexibility of the evaluation framework. When a concentration-driven approach is used, manganese (Mn, 100 ppm) is prioritized, whereas copper (Cu, 15 ppm) becomes the preferred target under an economically focused model. This comparison illustrates how the hybrid analog-artificial neural network (ANN) methodology can adapt to different objectives by balancing elemental grade, technological compatibility, and market demand. Overall, the results emphasize the value of multi-criteria decision-making as a tool for optimizing the sustainable recovery of valuable elements from technogenic deposits, providing a structured approach to resource management in complex industrial contexts.

4. Discussion of the Results

The results of this study demonstrate the effectiveness of combining analog-based assessments with neural network modeling for evaluating the industrial potential of technogenic deposits. The case study from Western Ukraine, where approximately 80 million tons of mine waste are accumulated, illustrates how such deposits simultaneously present ecological risks and opportunities for secondary resource recovery. The hybrid approach allowed for more precise identification of priority fractions and valuable co-elements, thereby addressing both environmental management needs and industrial exploitation strategies (Bas, 2016; Dyczko, 2023; Blinov et al., 2025; Vladyko et al., 2025)

The multilayer perceptron model proved capable of capturing complex non-linear relationships between geological, environmental, and compositional parameters that traditional analog-based methods often overlook(Vladyko et al., 2025; Dyczko, 2023; Pan et al., 2025). Its high classification accuracy, exceeding 90% on validation datasets, underlines its robustness and transferability across deposit types. The integration of neural network outputs with analog reasoning not only improved predictive reliability but also enhanced interpretability, supporting more confident decision-making in poorly documented or heterogeneous technogenic sites.

The prioritization of the strongly magnetic fraction for molybdenum recovery, along with TiO₂ and ZrO₂ as consistent co-elements, highlights the potential of oxide-based recovery pathways. The variable selection of Mn or Cu as the third co-priority element, depending on whether concentration or economic value is emphasized, demonstrates the adaptability of the hybrid framework (**Vladyko et al., Miroshnykov et al., 2025; Bashynska, 2025**). This flexibility is particularly important in real-world contexts where technological compatibility, market demand, and sustainability considerations must be balanced.

Finally, the proposed Priority Index algorithm offers a structured and transparent decision-making tool. By integrating normalized grade, technological compatibility, economic value, and environmental factors, it ensures that resource assessments reflect multiple dimensions of sustainability. The tie-breaker mechanism further refines element selection in borderline cases, prioritizing industrial and market relevance. Overall, the study confirms that hybrid analog-ANN approaches provide a scalable and ecologically informed pathway for optimizing the recovery of valuable elements from technogenic deposits while mitigating environmental impacts.

4. Conclusions

This study demonstrates that a hybrid methodology combining analog-based assessment with neural network modeling provides an effective and scalable approach for evaluating the industrial potential of technogenic deposits. The integration of multilayer perceptron (MLP) neural networks with analog reasoning captures complex non-linear relationships between compositional, geological, and environmental parameters, enhancing predictive accuracy and supporting informed decision-making.

The results identified the strongly magnetic fraction as the most suitable target for molybdenum (Mo) recovery, with titanium dioxide (TiO₂) and zirconium dioxide (ZrO₂) consistently emerging as key co-priority elements. The choice of a third co-element, either manganese (Mn) or copper (Cu), depends on the applied weighting criteria, highlighting the flexibility of the evaluation framework to balance concentration, technological feasibility, and economic value.

Overall, the hybrid analog-ANN methodology proves to be a powerful tool for optimizing both industrial exploitation and environmental management of technogenic deposits. The combination of empirical analog data with

neural network predictions enables identification of previously undervalued resources and supports the development of co-recovery strategies that maximize economic benefits while minimizing ecological impacts. The proposed approach offers a transparent, adaptable, and reproducible framework for resource evaluation, which can be applied to similar post-mining regions worldwide, advancing sustainable utilization of secondary mineral resources.

5. References

- Bas, E. (2016). The Training of Multiplicative Neuron Model Based Artificial Neural Networks with Differential Evolution Algorithm for Forecasting. Journal of Artificial Intelligence and Soft Computing Research, 6(1), 5–11. https://doi.org/10.1515/jaiscr-2016-000
- Bashynska, I. (2025). Ethical aspects of AI use in the circular economy. AI and Society, 1-19. https://doi.org/10.1007/s00146-025-02436-1
- Blinov, I., Radziukynas, V., Shymaniuk, P., Dyczko, A., Stecuła, K., Sychova, V., Miroshnyk, V., & Dychkovskyi, R. (2025). Smart Management of Energy Losses in Distribution Networks Using Deep Neural Networks. Energies, 18(12), 3156. https://doi.org/10.3390/en18123156
- Dychkovskyi, R., Dyczko, A., & Borojević Šoštarić, S. (2024). Foreword: Physical and Chemical Geotechnologies Innovations in Mining and Energy. E3S Web of Conferences, 567, 00001. https://doi.org/10.1051/e3sconf/202456700001
- Dyczko, A. (2023). Real-time forecasting of key coking coal quality parameters using neural networks and artificial intelligence. Rudarsko-Geološko-Naftni Zbornik, 38(3), 105–117. https://doi.org/10.17794/rgn.2023.3.9
- Gallego, F., & Corchuelo, R. (2019). On Mining Conditions using Encoder-decoder Networks. Proceedings of the 11th International Conference on Agents and Artificial Intelligence, 624–630. https://doi.org/10.5220/0007379506240630
- Ghayoumi, M. (2021). Artificial Neural Networks (ANNs) Fundamentals and Architectures. Deep Learning in Practice, 51–75. https://doi.org/10.1201/9781003025818-4
- Hutniczak, A. K., Bryś, W., Dychkovskyi, R., Gaj, R., Dyczko, A., Błońska, A., Bierza, K., Bacler-Żbikowska, B., & Woźniak, G. (2025). Identifying and understanding novel ecosystem functions: a scientific approach to nature restoration law. Journal of Water and Land Development, 203–203. https://doi.org/10.24425/jwld.2025.153532
- Kumaraswamy, B. (2021). Neural networks for data classification. Artificial Intelligence in Data Mining, 109–131. https://doi.org/10.1016/b978-0-12-820601-0.00011-2
- Miroshnykov, I., Cichoń, D., Shyrin, L., Dybrin, S., & Dychkovskyi, R. (2025). Ensuring the environmental sustainability of molybdenum ore mining. IOP Conference Series: Earth and Environmental Science, 1457(1), 012014. https://doi.org/10.1088/1755-1315/1457/1/012014
- Pan, F., Zhao, X., Dudek, M., Rehman, M. Z., & Shahzad, U. (2025). Ecological Impacts of Cultivated Land Conversion and Urban Eco-Resilience in the COP29 Era. Land Degradation and Development, Portico. https://doi.org/10.1002/ldr.70080
- Pavlychenko, A., Sala, D., Pyzalski, M., Dybrin, S., Antoniuk, O., & Dychkovskyi, R. (2025). Utilizing Fuel and Energy Sector Waste as Thermal Insulation Materials for Technical Buildings. Energies, 18(9), 2339. https://doi.org/10.3390/en18092339
- Polyanska, A., Pazynich, Y., Mykhailyshyn, K., & Buketov, V. (2023a). Energy transition: the future of energy on the base of smart specialization. Naukovyi Visnyk Natsionalnoho Hirnychoho Universytetu, 4, 89–95. https://doi.org/10.33271/nvngu/2023-4/089
- Polyanska, A., Pazynich, Y., Sabyrova, M., & Verbovska, L. (2023b). Directions and prospects of the development of educational services in conditions of energy transformation: the aspect of the coal industry. Polityka Energetyczna Energy Policy Journal, 26(2), 195–216. https://doi.org/10.33223/epj/162054
- Psyuk, V., & Polyanska, A. (2024). The usege of artificial intelligence in the activities of mining enterprises. E3S Web of Conferences, 526, 01016. https://doi.org/10.1051/e3sconf/202452601016
- Vladyko, O., Maltsev, D., Gliwiński, Ł., Dychkovskyi, R., Stecuła, K., & Dyczko, A. (2025). Enhancing Mining Enterprise Energy Resource Extraction Efficiency Through Technology Synthesis and Performance Indicator Development. Energies, 18(7), 1641. https://doi.org/10.3390/en18071641
- Wang, W., Pan, S. J., & Dahlmeier, D. (2018). Memory networks for fine-grained opinion mining. Artificial Intelligence, 265, 1–17. https://doi.org/10.1016/j.artint.2018.09.002

Funding

The present study reports findings obtained within the framework of project GP-516, funded by the Ministry of Education and Science of Ukraine, as well as the international EMREI project # 03C1069, supported through the European cooperation program INTERREG.

Author's contribution

Artem Pavlychenko (professor): scientific supervision, methodology design. Dagmara Lewicka (professor): critical review, funding acquisition, English language support. Ivan Miroshnykov (post graduate student): data

curation & preprocessing. **Serhii Dybrin** (post graduate student): model development and testing. **Andrii Pererva** (post graduate student): formal analysis, validating results. **Roman Dychkovskyi**: (professor): conceptualization, supervising the scientific and technical aspects.

All authors have read and agreed to the published version of the manuscript.



Laboratory Investigation of Cement Kiln Dust (CKD) for Stabilization of Clay Soil from Cegléd, Hungary

DIM-ESEE Conference



Sirine Trabelsi^{1*} , Andrea Tóth¹, Tamás Kántor¹ Institute of Water Resources and Environmental Management, University of Miskolc, 3515 Miskolc, Egyetem út 1.

Abstract

Soil stabilization is essential in construction projects by improving the engineering properties of soil, such as strength, durability, and load-bearing capacity.). Traditional stabilization technologies typically involve the use of conventional materials, such as cement and lime. However, as environmental awareness grows and we are in transition into the world of sustainable practices, awareness of using industrial waste materials has come to the attention. By-products of the industry, such as cement kiln dust (CKD), fly ash, ground granulated blast furnace slag (GGBFS), or other by-products based on pozzolanic materials, can improve soil properties and are an integral part of many sustainable approaches for soil stabilization. By utilizing waste materials in stabilization, they can divert materials from the landfill, as well as limit the amount of greenhouse gases produced in the manufacturing of traditional binders. In this study, the aim is to evaluate the effect of CKD on the engineering behaviour of medium clay. The research used a detailed geotechnical testing program, including Atterberg limits, particle size distribution, water uptake capacity, and cone penetrometer, to investigate the influence of the CKD addition in different percentages on the clay soil studied. This is an important step towards acceptance of low-carbon, cost-effective alternatives in geotechnical engineering practice, while also providing helpful information about the practical application of green stabilizing methods. Finally, the goal is to prove the potential to convert fine-grained soils with poor engineering properties into durable ground layers by using industrial waste to stimulate strong and sustainable infrastructure development.

Keywords: Soil stabilization, cement kiln dust, waste materials, clay, laboratory testing.

1. Introduction

To advance more sustainable policies, the construction industry is facing a dual challenge: responding to the high demand for reliable building products amidst rapid urbanization and limiting the environmental impact of its by-products.

In this context, Cement Kiln dust (CKD), an abundant by-product of the cement production process, has increased in parallel with the speeding growth of cement manufacturing and has resulted in its accumulation. The considerable amount of CKD has drawn the interest of many researchers to explore its utilization. The cement production by-product has pozzolanic properties, can be cost-effective, and has the potential to reduce environmental impacts by redirecting it from landfill (Adevanju & Okeke, 2019; Alhassani et al., 2021; Rahman et al., 2011).

Traditional stabilization technologies typically involve the use of conventional materials, such as cement and lime. However, as environmental awareness grows and we transition into the world of sustainable practices, awareness of using industrial waste materials has come to attention (Mohanty et al., 2017; Arulrajah et al., 2014). The interest in reusing CKD began in the early 1970s and increased in the early 2000s with the development of laboratory and field measurements (Miller et al., 1999; Parsons & Kneebone, 2004). This progression is shown in Figure 1, which illustrates the scientific research trends related to the use of CKD as an alternative stabilizer. A review conducted by the authors considers 60 open-source studies that focused mainly on geotechnical investigation.

Consequently, CKD has emerged as a promising material that can be used in soil stabilization. In this study, the term "soil" refers to the natural ground material composed of mineral particles, organic matter, water and air, and it is used in the geotechnical sense. It can be an alternative stabilizer, particularly for problematic soils like clay, known for their high plasticity, low shear strength, and volume instability (Adeyanju & Okeke, 2019; Mohanty et al., 2017; Alhassani et al., 2021; Hossain & Khandaker, 2011).

e-mail address: trabelsi.sirine@student.uni-miskolc.hu

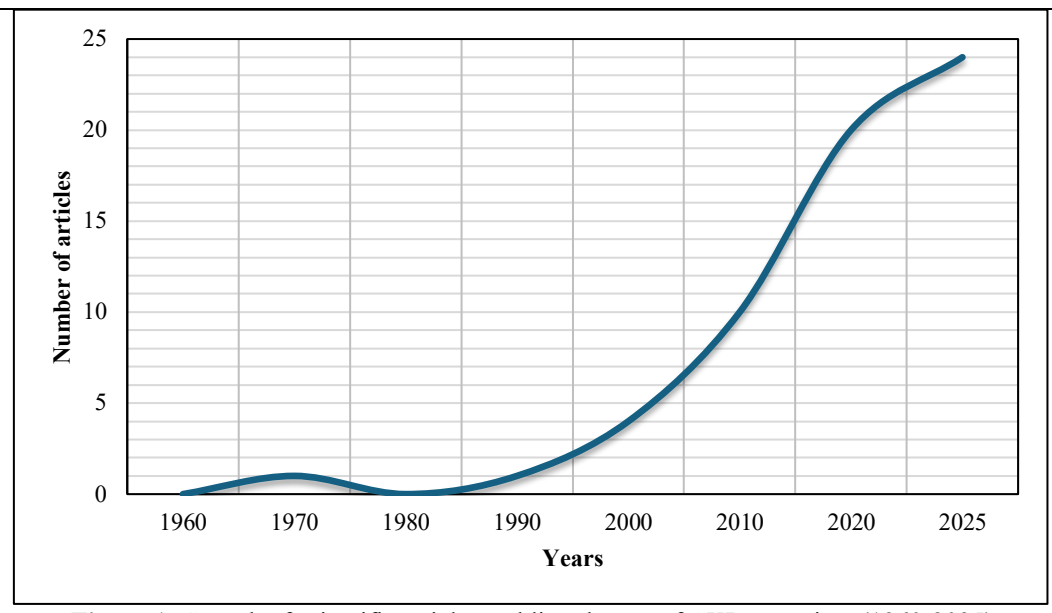


Figure 1. Growth of scientific articles tackling the use of CKD over time (1960-2025)

Recent articles have examined and reviewed the use of various industrial waste for soil stabilization techniques, which can provide useful references on the applicability and usage of CKD material as an alternative stabilizer (Basha et al., 2005; Arulrajah et al., 2014; Sariosseiri & Muhunthan, 2009). Particularly, several studies have shown that CKD can improve the geotechnical properties of soils. They have demonstrated that soils treated with CKD can have increased unconfined compressive strength, reduced plasticity index and improved compaction characteristics (Alhassani et al., 2021; Miller et al., 1999; Hossain & Khandaker, 2011; Jala & Janewoo, 2016). The idea of reusing such industrial byproducts was also supported by the global push to sustainability.

In geotechnical engineering, laboratory tests are a vital aspect of evaluating and predicting soil behaviour under various circumstances. In the overall study, the research used a detailed geotechnical testing program, including Atterberg limits, particle size distribution, water uptake capacity, ring shear testing, cone penetration resistance,... The goal is to show that CKD may have a stabilizing effect on the physical and mechanical properties of clay. These improved performance results may be justified by the pozzolanic and cementitious reactions of reactive oxides in CKD (CaO, SiO₂, Al₂O₃) with minerals in the clayey soil to develop cementitious compounds that enhance the bonding and interlocking of the particles (Harichane et al., 2011; Al-Mukhtar et al., 2012; Singh et al., 2024; Zali et al., 2018).

The study aligns sustainable engineering goals by promoting the reuse of industrial by-products and lowering reliance on energy-intensive, greenhouse gas-emitting traditional binders like cement and lime (Arulrajah et al., 2014; Basha et al., 2005; Kaniraj & Havanagi, 2001).

2. Methods and materials

Through an examination of important geotechnical soil identification tests, this research aims to clarify the complex interactions between soil properties and stabilization techniques, which will be useful in developing innovative and successful stabilization plans. This approach is based on an important but often overlooked mechanism in geotechnical and geoenvironmental engineering: Pozzolanization. Pozzolanic materials are high-silica (SiO₂), alumina (Al₂O₃), and ferric oxide (Fe₂O₃) materials consisting of not less than 70% of the combined silica, alumina, and ferric oxide contents, that react with calcium hydroxide, in the presence of water, to produce binding cementitious substances that may hold soil particles together (Kasaniya et al., 2019). Pozzolans may be either natural (like volcanic ash, pumice, diatomaceous earth) or artificial, typically manufactured using industrial by-products (Juenger et al., 2012).

In this study, CKD is provided by Duna-Dráva Cement Kft company to be used as the stabilizing binder, and the soil treated is sourced from a clayey soil deposit mined in Cegléd, Hungary. To assess the effect of CKD, incremental additions of 2 %, 5 %, 8 %, and 15 % dry weight of CKD were chosen. These percentages represent an incremental increase in the stabilization intensity, allowing the observation of both low-dosage and high-dosage behaviors. The effectiveness of CKD depends on factors such as soil type, CKD chemical composition, and dosage. Based on the literature, optimal improvement is often observed with CKD-treated soils ranging from 5 % to 15 % by dry weight, which further justifies the percentage choice (Adeyanju & Okeke, 2019; Alhassani et al., 2021; Jala & Janewoo, 2016).

2.2 Properties of the materials studied

Table 1 shows the analysis of the clayey soil studies. The soil is a fine-grained, cohesive soil type, composed mainly of silt and clay. These soil characteristics dictate a plastic behavior, which is one of the primary concerns in geotechnical

engineering. The CI-CH classification denotes that this soil has both the properties of CI (clay of intermediate plasticity) and CH (clay of high plasticity). This classification occurs when a soil's data point is very close to the boundary line separating the CI and CH regions in the plasticity chart. The dual classification is important because it shows that the soil can be sensitive to changes in moisture (**Knappett & Craig, 2012**). The soil can behave like a high-plasticity clay that may undergo significant volume changes, such as swelling and shrinking, which can create challenges for engineering and construction.

The tests were conducted in accordance with MSZE CEN ISO/TS 17892-12:2006 standards.

Table 1. Geotechnical characteristics of the studied soil

Properties		Results		
Color		gray		
Particle size distribution	cle size distribution Gravel (%)			
	Sand (%)	8.6		
	Silt (%)	59.4		
	Clay (%)	31.3		
Atterberg limits	Liquid limit (%)	48.5		
	Plastic limit (%)	24.9		
	Shrinkage limit (%)	11.2		
	Plasticity index	23.6		
Soil classification	•	CI–CH		

Table 2 shows the physical properties of a cement kiln dust (CKD) sample, including its particle size distribution and specific surface area. The data was derived using a HORIBA laser scattering particle size distribution analyzer (Levoguer ,2013).

Table 2. Physical properties of cement kiln dust

Tuble 2.1 hybreat properties of coment kinn as			
Parameter	Value		
Median size (d50)	12.91 μm		
Mean size	23.33 μm		
Mode size	12.36 μm		
Specific surface area	9247.5 cm ² /cm ²		
Particle size range	$\sim 1-300 \ \mu m$		

The cement kiln dust (CKD) sample was also tested to know its chemical and mineralogical composition. Chemically, it is a calcium-rich material, primarily calcium oxide (CaO) with 37.06 %, and showing significant levels of silicon dioxide (SiO2) at 10.67 % and potassium oxide (K2O) at 9.62 %. For chemical analysis, the CKD sample was first crushed to a grain size below 65 µm using a ceramic mortar, then dried at 120 °C for 2 hours. From the dried powder, 4.000 g was weighed and mixed with ultra-pure fine polyethylene (Cereox binder) in a 4:1 ratio and homogenized in an agate mortar. The mixture was pressed into a 32 mm diameter pellet under a pressure of 25 tons. Both main and trace elements were analyzed using a Supermini 200 WDXRF (Rigaku) equipped with an air-cooled 200 W X-ray tube with Pd target, operated at 50 kV and 4.00 mA. Calibration and measurements for each element were performed at 1.2 Pa - 1.6 Pa pressure using the ZSX driver and evaluation program. Peak angle positions and backgrounds were measured using LiF200, PET, and XR25 crystals. On the other hand, mineralogically, lime is the most prevalent crystalline material at 41.5 %, followed by larnite at 18.7 %, and the sylvite component at 8.3 %, which directly relates to the high amount of potassium oxide. The mineralogical composition was determined using X-ray diffraction (XRD) with Cu-Kα radiation, scanning from 5° to 70° 20 with a step size of 0.02° and a counting time of 1 s per step. Rietveld refinement was applied to quantify the crystalline phases, and approximately 15.5 % of the material was identified as amorphous, representing non-crystalline silicates and aluminates. There is a significant amorphous portion, at 15.5 %, indicating that it is not composed of arranged crystal phases. The CKD is then a reactive material with features that are crucial for its possible usage in a variety of applications because of its alkaline, calcium-rich chemistry and mixture of crystalline and non-crystalline phases.

2.2 Experimental testing procedures

In this study, the liquid limit (LL) and plastic limit (PL) of soil and soil—CKD mixes were determined to evaluate consistency for comparison across mixes. To determine the liquid limit (LL), the cone penetration method is used, where the LL is defined as the water content at which a standard cone penetrates 20 mm in 5 seconds. Approximately 150 g of

soil (sieved at 425 µm) is mixed into a paste. The samples are tested at several water contents, and the penetration depth (displacement) is recorded. A graph of water content (W) vs. penetration (P) is plotted, and the W corresponding to 20 mm penetration will be the liquid limit according to the IS 2720 (Part 5). The testing choice was made due to the soil-CKD mixtures' excessive slickness on the Casagrande bowl; the conventional Casagrande procedure was not applicable in this situation because of excessive slickness on the Casagrande bowl.

The plastic limit (PL), which represents the moisture content at which the soil transitions from plastic to a semi-solid state, and the shrinkage limit (SL), which represents the water content at which the soil changes from a semi-solid to a solid state, were determined following MSZE CEN ISO/TS 17892-12:2006 standard. Eventually, the plasticity index (PI = LL - PL) is calculated, and it indicates the soil's workability and proneness to deformation when mixed with Cement Kiln Dust (CKD).

Another test performed is the water uptake capacity test, also known as the Enslin-Neff method (Kaufhold & Dohrmann, 2008). This test measures a soil's ability to absorb and retain water, providing insight into its hydraulic characteristics and water behavior. It is especially useful for soils with high clay content (Kaufhold & Dohrmann, 2008).

Comparing these values across different mixes allows us to determine which formulations offer optimal stability, limitations on shrinkage, and better bearing capacity characteristics, thereby enhancing their overall suitability for future engineering applications.

3. Results and Discussion

The results obtained from the testing programs are presented below. All consistency data is combined in Figure 2 for clearer representation and easier interpretation.

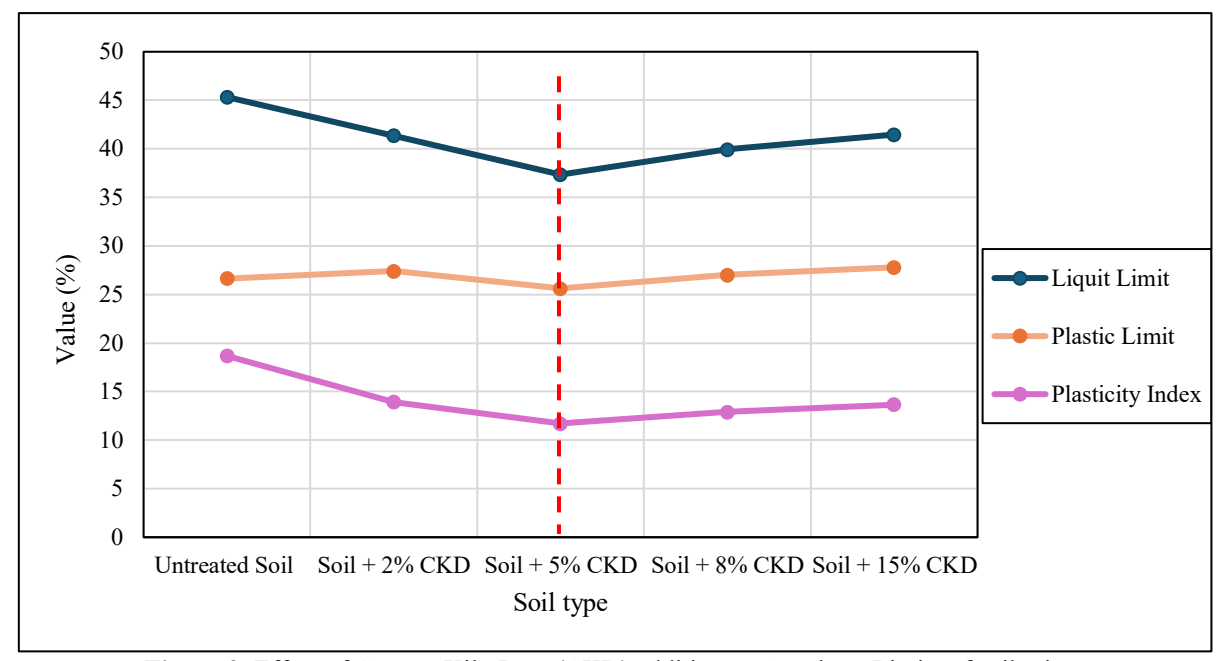


Figure 2. Effect of Cement Kiln Dust (CKD) addition on Atterberg Limits of soil mixes

Figure 2 shows that CKD acts as a chemical stabilizer and mechanical filler, achieving optimal stabilization at 5 % addition. Even though there was a slight increase in plasticity index at higher CKD amounts (8 % – 15 %), the values were still less than those of untreated soil.

Parameter	Virgin Soil	5% CKD	Improvement
Liquid Limit (%)	45.33	37.35	-17.60 %
Plastic Limit (%)	26.65	25.63	-3.80 %
Plasticity Index	18.68	11.72	-37.20 %
Classification	High Plasticity	Medium Plasticity	✓ Improved

The use of 5 % Cement Kiln Dust shows better potential for soil stabilization, maximizing the decrease in plasticity compared with the least amount of plasticity in soil with workable behavior characteristics. This treatment turns a highplasticity soil into a medium-plasticity soil, as stated in **Table 3**, significantly increasing its geotechnical use.

For the water uptake capacity results, the untreated clay exhibited a moderate water retention capacity (60.5 %). With CKD addition, the amount of water the clay absorbed showed a progressive increase until 15 % CKD was added (87 %) (**Figure 3**).

The progressive increase in water uptake capacity with higher additions of CKD can be explained both microstructurally and chemically. Microstructurally, CKD promotes flocculation/aggregation of clay particles, which reconstitutes the soil fabric into a more open structure with larger pore spaces. The additional voids are reservoirs for retaining water. Chemically, CKD is reactive because it contains reactive oxide species such as CaO, SiO₂, and K₂O, which react in a pozzolanic and cementitious capacity when moisture is included. These reactions consume water as a reactant and produce other hydration products, including calcium silicate hydrate (C-S-H) and calcium aluminate hydrate (C-A-H). Such waterproofing products include material-cementitious chemical species, which initially enhance the affinity for moisture during stabilization.

At greater dosages and especially at the 15 % CKD dosage, the sharp increase in water uptake could be as high as 87 %. It could suggest increased porosity of the soil, thus the potential for greater water entrapment.

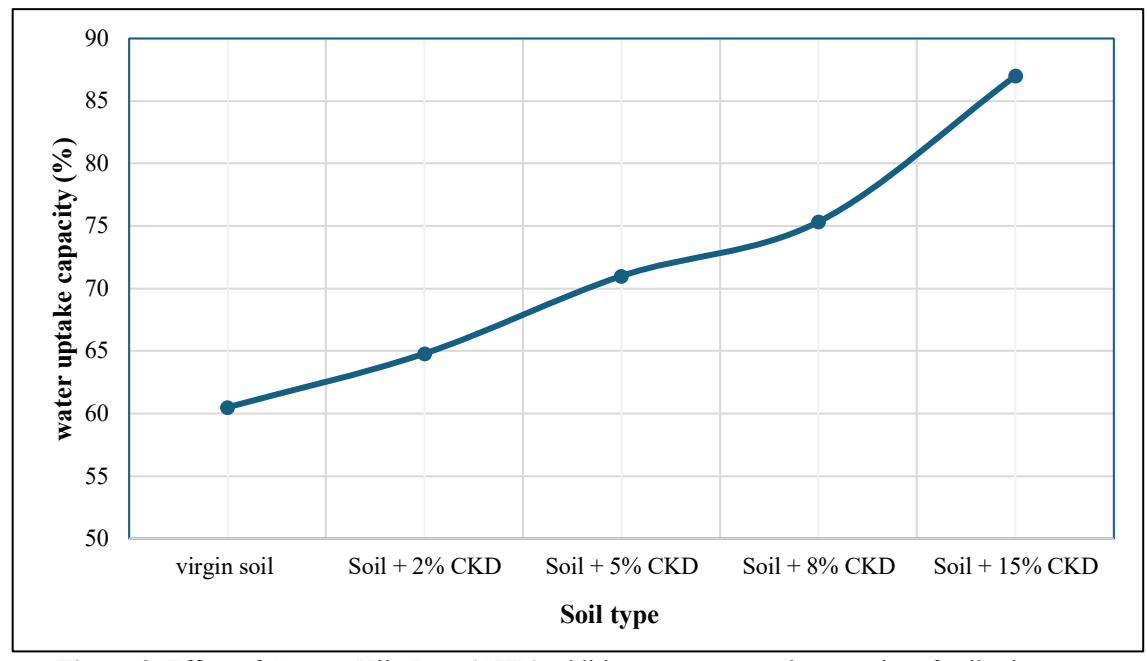


Figure 3. Effect of Cement Kiln Dust (CKD) addition on water uptake capacity of soil mixes

While increased moisture affinity can assist in compaction procedures and enhance chemical reactivity, this could also result in volumetric instability, as prolonged or excessive moisture content can contribute to swelling and shrinkswell cycles in field conditions.

While the soil, in this study, is classified and studied in terms of particle size and Atterberg limits, we acknowledge that X-ray Diffraction (XRD) and Scanning Electron Microscopy (SEM) analysis would greatly contribute to exploring the specific stabilization mechanisms, particularly with respect to the formation of the C-S-H and C-A-H products and the water affinity produced. This mineralogical characterization will be the focus of our longer-term future research.

4. Conclusions

The study indicated that Cement Kiln Dust (CKD) has the potential to be an effective stabilizer of clayey soils. Based on the findings, the addition of CKD was proven to improve some of the important geotechnical properties by reducing the plasticity index and changing the consistency of the soil, along with increasing the soil's water absorption capacity. The changes can be explained by the pozzolanic and cementitious reactions between the reactive oxides of CKD and soil minerals that contribute to the improved structure and performance of engineering applications.

By promoting the valorization of industrial by-products, particularly CKD, within geotechnical soil stabilization, this research contributes to the mineral raw materials industry. It supports resource efficiency, waste minimization, and the circular use of raw materials. Such applications decrease the reliance on primary natural resources and support the wider perspective of sustainable raw material management and industrial integration in the construction supply chain.

The next phase in this research will involve using CKD in conjunction with fly ash as a stabilizing agent. Fly ash is a pozzolanic material that is known for its high silica (SiO₂) and alumina (Al₂O₃) content and, as such, can react with the calcium hydroxide leached from the CKD to create additional cementitious compounds. This combined potential may induce further increases in soil strength, durability, and volumetric changes while enabling a sustainable approach to stabilize soil using two industrial by-products. Various curing times, in addition to the mineralogical analyses (XRD and SEM), be examined to help evaluate the evolving time-dependent quadrupole effects of strength and stability, which will

assist in offering a more cohesive understanding of CKD-fly ash-treated soils in geotechnical applications. These approaches aim to create a more robust, sustainable, and practical strategy for problematic soils.

5. References

- Adeyanju, A., & Okeke, C. (2019). Exposure effect to cement dust pollution: A mini review. Environmental Challenges, 1, 100005. https://doi.org/10.1016/j.envc.2019.100005
- Alhassani, A. M. J., Kadhim, S. M., & Fattah, A. A. (2021). Stabilization of clayey soil using cement kiln dust as sustainable material. IOP Conference Series: Earth and Environmental Science, 856(1), 012038. https://doi.org/10.1088/1755-1315/856/1/012038
- Al-Mukhtar, M., Lasledj, A., & Alcover, J. F. (2012). Behaviour and mineralogy changes in lime-treated expansive soil at 20 °C. Applied Clay Science, 50(2), 191–198. https://doi.org/10.1016/j.clay.2010.07.023
- Arulrajah, A., Mohammadinia, A., Phummiphan, I., & Samingthong, W. (2016). Stabilization of recycled demolition aggregates by geopolymers comprising calcium carbide residue, fly ash and slag precursors. Construction and Building Materials, 114, 864–873. https://doi.org/10.1016/j.conbuildmat.2016.03.150
- Basha, E. A., Hashim, R., Mahmud, H. B., & Muntohar, A. (2005). Stabilization of residual soil with rice husk ash and cement. Construction and Building Materials, 19(6), 448–453. https://doi.org/10.1016/j.conbuildmat.2004.08.001
- Jala, S., & Janewoo, U. (2016). Stabilization of expansive soil with cement kiln dust and RBI Grade 81 at subgrade level. Geotechnical and Geological Engineering, 34(5), 1465–1476. https://doi.org/10.1007/s10706-016-0024-8
- Juenger, Maria & Provis, John & Elsen, Jan & Matthes, Winnie & Hooton, Doug & Duchesne, J. & Courard, Luc & He, Huan & Michel, Frédéric & Snellings, Ruben & De Belie, Nele. (2012). Supplementary Cementitious Materials for Concrete: Characterization Needs. MRS Proceedings. 1488. https://doi.org/10.1557/opl.2012.1536.
- Hossain, M. A., & Khandaker, M. (2011). Stabilization of black cotton soil by using cement kiln dust. International Journal of Scientific & Technology Research, 7(2), 1–6.
- Kasaniya, M., Thomas, M., & Moffatt, E. (2019). Development of a rapid and reliable pozzolanic reactivity test method. ACI Materials Journal, 116(4), 145–154. https://doi.org/10.14359/51716718
- Kaufhold, S., & Dohrmann, R. (2008). Comparison of the traditional Enslin–Neff method and the modified Dieng method for measuring water-uptake capacity. Clays and Clay Minerals, 56(5), 686–692. https://doi.org/10.1346/CCMN.2008.0560609
- Knappett, J., & Craig, R. F. (2012). Craig's soil mechanics (8th ed.). CRC Press. https://doi.org/10.1201/b12841
- Levoguer, C. (2013). Using laser diffraction to measure particle size and distribution. *Metal Powder Report*, 68(1), 15–18. https://doi.org/10.1016/S0026-0657(13)70090-0
- Miller, G. A., Zaman, M. M., Rahman, J., & Tan, N. K. (1999). Laboratory and field evaluation of soil stabilization using cement kiln dust (Report No. ODOT-2144). Oklahoma Department of Transportation.
- Mohanty, S., Pradhan, P., & Mohanty, C. (2017). Stabilization of expansive soil using industrial wastes. Geomechanics and Engineering, 12(1), 111–125. https://doi.org/10.12989/gae.2017.12.1.111
- Rahman, M. K., Rehman, S., & Al-Amoudi, O. S. B. (2011). Literature review on cement kiln dust usage in soil and waste stabilization and experimental investigation. International Journal of Civil Engineering, 9(1), 1–10.
- Sariosseiri, F., & Muhunthan, B. (2009). Effect of cement treatment on geotechnical properties of some Washington State soils. Engineering Geology, 104(1–2), 119–125. https://doi.org/10.1016/j.enggeo.2008.09.003
- Singh, S., Kumar, V., & Tiwari, R. (2024). Stabilization of expansive soil: A review. In Advances in geotechnical and transportation engineering (pp. xxx–xxx). Springer. https://doi.org/10.1007/978-981-99-3557-4 20

Internet sources

URL1: https://hdl.handle.net/11244/320272 (accessed 16th August 2025)

URL2: https://www.ijste.org (accessed 15th August 2025)

Funding

"The research presented in the article was carried out within the framework of the Széchenyi Plan Plus program with the support of the RRF 2.3.1 21 2022 00008 project."

Author's contribution

Sirine Trabelsi (Ph.D. student): conceptualization, investigation, methodology, writing – original draft. **Andrea Tóth** (associate professor): supervision, resources, – review & editing. **Tamás Kántor** (associate professor): supervision, resources, – review & editing. All authors have read and agreed to the published version of the abstract.



Red mud as geotechnical composite

DIM-ESEE Conference

Primož Pavšič¹* [©]⊠, Marija Đurić¹ [©]⊠, Mateja Košir¹ [©]⊠, Primož Oprčkal¹ [©]⊠, Vesna Zalar Serjun¹ [©]⊠

¹ Slovenian National Building and Civil Engineering Institute, (Dimičeva ulica 12, SI-1000 Ljubljana, Slovenia)



Abstract

Red mud (RM), a by-product of the Bayer process, is produced in large quantities worldwide. It is mainly disposed of in settling ponds or through dry stacking, both of which pose environmental risks due to instability, alkaline emissions, and leaching of potentially toxic elements (PTEs). Several efforts have been made to utilize RM as an additive in soil remediation or in the production of construction materials. However, due to its fine-grained texture, poor mechanical properties, and tendency to leach harmful substances, RM alone is unsuitable for direct use in construction. Nevertheless, its mechanical properties and workability can be significantly improved by mixing it with hydraulic or pozzolanic binders, such as calcareous ashes.

In the present study the use of calcareous paper mill ash (PA) as an additive to RM, for production of geotechnical RM/PA composite was studied. The results demonstrate that mixing RM slurry with PA produces a soil-like geotechnical composite with suitable workability and mechanical properties for use in earthworks, comparable to natural soils. Moreover, the RM/PA composite exhibits lower leaching of PTEs, in comparison to the RM, improving the environmental acceptability of RM for its use in construction.

This study confirms that RM composites, with addition of alternative binders, can be a viable construction material, which not only meet the geotechnical performance requirements for earthworks but also comply with Slovenian environmental standards. This approach offers a dual benefit: it reduces the environmental and economical burden associated with RM disposal while simultaneously decreasing the demand for natural construction materials.

Keywords: red mud; recycling; geotechnical composites; environment

1. Introduction

Aluminium (Al) is one of the most produced metals in the world (Svobodova-Sedlackova et al. 2024). Its global consumption is expected to increase at a compound annual growth rate (CAGR) of 3.33 %, increasing from 101 million tonnes in 2024 to 119 million tonnes by 2030 (URL 1). Primary aluminium production is performed in two stages, via Bayer and Hall-Héroult processes. During the first stage, under Bayer process, alumina is extracted from the bauxite ore and RM is generated as a waste residue (Svobodova-Sedlackova et al. 2024; URL 2). The process is based on the digestion of the bauxite ore in a hot concentrated sodium hydroxide (NaOH) solution. The alumina-rich solution is then separated from the solid residue, which consists predominately of iron (Fe) and Al (hydr)oxides and is referred to as RM. The global production of RM amounts to more than 160 million tonnes per year (Zalar Serjun et al., 2018; Pavšič et al., 2024; URL 2).

Red mud has hazardous properties, which mostly result from its high pH (Nayak et al., 2024), as well as from the total content and leaching of potentially toxic elements (PTEs), and alkaline airborne dust emissions (Jha et al., 2020; Samal, 2021). Due to its colloidal structure, the containment and handling of RM pose a significant environmental problem (Jha et al., 2020; Nayak et al., 2024; Pavšič et al., 2024).

Therefore, potential applications for the use of RM need to be explored in order to minimise the associated negative environmental impacts (Zalar Serjun et al., 2018; Jha et al., 2020). However, the chemical and physical - mechanical properties of RM vary considerably and reflect the different sources - differences in the Bauxite composition and processing plant operation (Jha et al., 2020; Oprčkal et al., 2020). This means that from the scope of recycling each RM deposit must be considered case-by-case (Oprčkal et al., 2020). Various studies have shown that RM is a potential secondary source for the recovery of metals, such as iron (Fe), titanium (Ti), manganese (Mn), sodium (Na), potassium (K) and also various rare earth elements (REE) (Samal, 2021), but residual RM, after extraction of theses raw materials can also be regarded as a source of construction material (Jha et al., 2020; Samal, 2021; Pavšič et al., 2024). Due to its fine-grained nature and poor mechanical properties, as well as environmental concerns, RM cannot be used as a construction material by itself. The properties of RM residues can be significantly improved, when mixed with hydraulic or pozzolanic binders, such as calcareous ashes, to produce mechanically stable and environmentally acceptable composites for earthworks (Jha et al., 2020; Pavšič et al., 2024).

Based on the results of laboratory tests, this study presents a useful utilisation of RM slurry by producing a geotechnical composite with addition of calcareous paper mill ash (PA), which is also an industrial residue, and offers dual benefits: It reduces the environmental impact associated with RM and PA disposal while reducing the demand for natural construction materials.

2. Materials and methods

Since PA and RM can be environmentally problematic (Jha et al., 2020; Oprčkal et al., 2020), the leaching of the PTEs, was investigated. The mineralogical composition of the PA and RM used in preparation of the RM/PA composite was also determined, since it defines the nature and behaviour of both materials in composite. Leaching of PTEs, mineralogical changes and basic geotechnical properties of the RM/PA composite were determined in order to evaluate the properties of the composite from the scope of potential use in earthworks and to investigate the influence of the PA addition on environmental and mechanical properties of the RM/PA composite in comparison to the RM itself.

2.1. Materials

In this study the sample of red mud (RM) from the old pond in Podgorica (Montenegro) after gravitational and magnetic large-scale separation of raw materials (metals, REE) was used. Residues were first left undisturbed for a longer period of time so that particles were able to settle. This was followed by decantation of the supernatant liquid. The residues used for investigations were in the form of slurry with a moisture content of 139 wt.%, which represents a 42 wt.% of solids in the slurry.

Fly ash from paper mill (PA) is a recycled material with hydraulic and pozzolanic properties that can be used as an alternative binder for soil remediation, solidification and stabilization. It is a highly alkaline material that contains a (latent) hydraulically active phase. The composition and properties of PA are highly dependent on the type of fuel burned, the combustion technology used, and the combustion conditions, which could affect the properties of the geotechnical composite material produced from it. In this study, a PA from the paper mill Lenzing AG, produced from burning of deinking sludge and waste cellulose fibre from recycling of paper was used.

2.2. Methods

A geotechnical composite, designated as RM/PA was prepared by mixing RM slurry with PA. The amount of PA required to produce the geotechnical composite was determined on basis of laboratory trials. Quantity of added PA with which the appropriate consistency of the RM/PA for the compaction was achieved was selected. The RM/PA mixture was prepared by homogenizing RM and a selected amount of PA, with a hand-held screw-mixer. For the preparation of RM/PA geotechnical composite, 0.75 kg of PA was added to each 1 kg of RM slurry.

Prior to the RM/PA specimen preparation, the mellowing period of 24 hours was required to allow the chemical reactions to take place and to achieve suitable consistency - workability of the mixture. During the mellowing period, the mix was stored in an airtight plastic container at ambient temperature. After the mellowing period, the mixture was homogenized again and the test specimens were prepared by compaction in the molds according to SIST EN 13286-50 (2005) using the standard Proctor compaction effort (SIST EN 13286-2, 2013). The specimens were removed from the mold by a press and then cured at 22 °C and 98 % humidity for the selected period of time. The prepared specimens were used to determine the geotechnical, mineralogical and chemical properties of the investigated geotechnical composite at selected curing times.

Bulk mineralogical composition of the PA, RM and RM/PA composite was determined by using X-Ray Powder Diffraction (XRD) using an EMPERYAN (PANalytical) X-ray diffractometer equipped with Cu K α radiation. Data were collected at 45 kV and 40 mA in the range 5–70° 2 θ , with a 0.013° 2 θ step size and measuring time per step of 148.9 s. Interpretation of the results was carried out by means of Highscore v.4.x LTU software, involving PDF 4 database. Prior to the XRD analysis, the subsamples were dried up to a constant mass and pulverised in an agate mortar.

The leaching tests on PA, RM and RM/PA composite after 7 days of curing, were performed according to **SIST EN 1744-3** (2002), at the liquid to solid ratio of 10:1. The preparation of the eluates was carried out in high density polyethylene (HDPE) beaker.

Concentrations of chromium, cobalt, nickel, copper, zinc, arsenic, selenium, molybdenum, cadmium, antimony, barium, mercury and lead in eluates, were measured by inductively coupled plasma mass spectrometry (ICP-MS), according to SIST EN ISO 17294-2 (2017). The content of chloride and sulphate was defined by spectrophotometry according to ISO 15923-1 (2013), while the fluoride content was defined according to the 4500-FD – colorimetric SPADNS method (SMWW, 2017).

Limiting values of the PTEs in RM/PA eluates were taken from the Slovenian national legislation according to the Waste decree – Annex 5: Permissible levels for pollutants in their leachates for processed substances or objects that will be used in the external environment and exposed to atmospheric influences and have the property of leaching with permeability $\leq 10^{-9}$ m/s (URL 3).

Geotechnical properties of RM/PA composite, such as the unconfined compressive strength (Rc) (SIST EN 13286-41, 2022), the consolidation properties (SIST EN ISO 17892-5, 2017), permeability (SIST EN ISO 17892-11, 2019),

and shear strength (SIST EN ISO 17892-10:2019) were determined after the selected time of curing (2 days, 7 days and 14 days for Rc, and 2 days for the others), while the moisture content (SIST EN ISO 17892-1, 2015) was determined at preparation.

3. Results

For the preparation of the RM/PA a RM from Podgorica pond after extraction of raw materials, with moisture content of 139 % wt. (42 % wt. solids) and PA from paper mill Lenzing AG were used. The mineralogical compositions of RM, PA and RM/PA composite after 7 days of curing are presented in **Table 1** and in **Figures 1 - 3**, while eluates quality for both materials, and the composite after 7 days of curing, alongside the legislative limits (URL 3) are presented in **Table 2**.

Table 1. Mineralogical composition of RM and PA

	Mineral phases	
RM	PA	RM/PA
Hematite (Fe ₂ O ₃)	Anhydrite (CaSO ₄)	Gypsum (CaSO ₄ x2H ₂ O)
Gibbsite (Al(OH) ₃)	Lime (CaO)	Hematite
		(Fe_2O_3)
Cancrinite (Na,Ca) ₈ (Al ₆ Si ₆ O ₂₄)(CO ₃ ,SO ₄) ₂ x2H ₂ O)	Quartz (SiO ₂)	Calcite (CaCO ₃)
Calcite (CaCO ₃)	Calcite (CaCO ₃)	Quartz (SiO ₂)
Boehmite (AlO(OH))	Magnetite (Fe ₃ O ₄)	Gibbsite (Al(OH) ₃)
Aluminium fluoride (AlF ₃)	Portlandite (Ca(OH) ₂)	Cancrinite (Na,Ca) ₈ (Al ₆ Si ₆ O ₂₄)(CO ₃ ,SO ₄) ₂ x2H ₂ O)
	Periclase (MgO)	Portlandite Ca(OH) ₂)
	Gehlenite (Ca ₂ Al(AlSiO ₇))	Gehlenite Ca ₂ Al(AlSiO ₇))
		Ettringite (Ca ₆ Al ₂ (SO ₄) ₃ (OH) ₁₂
		$x26H_2O$)

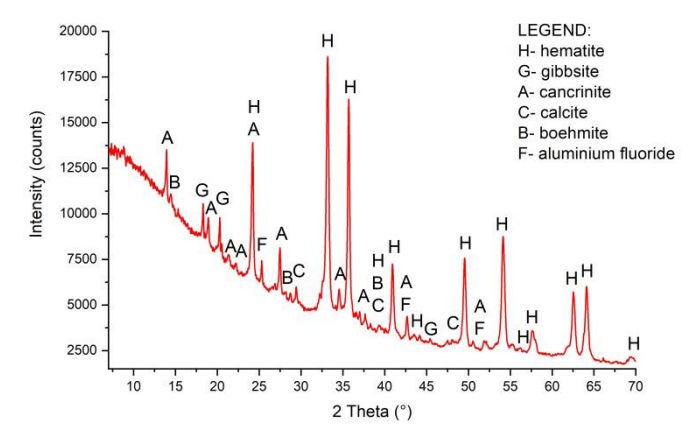


Figure 1. XRD spectrum of RM

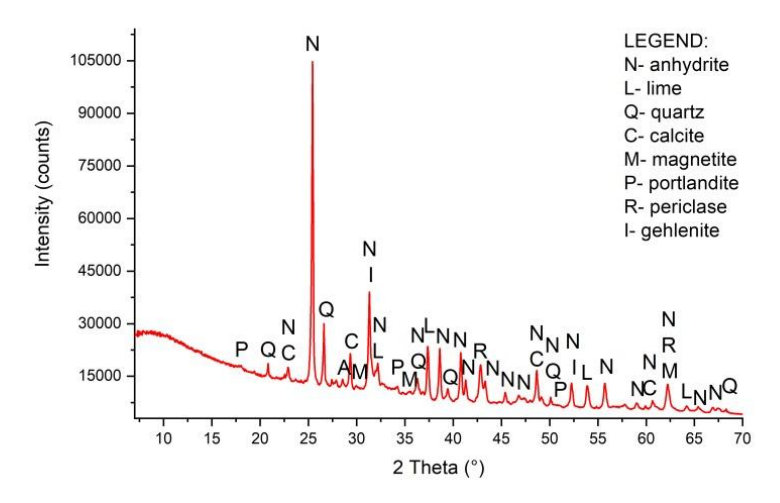


Figure 2. XRD spectrum of PA

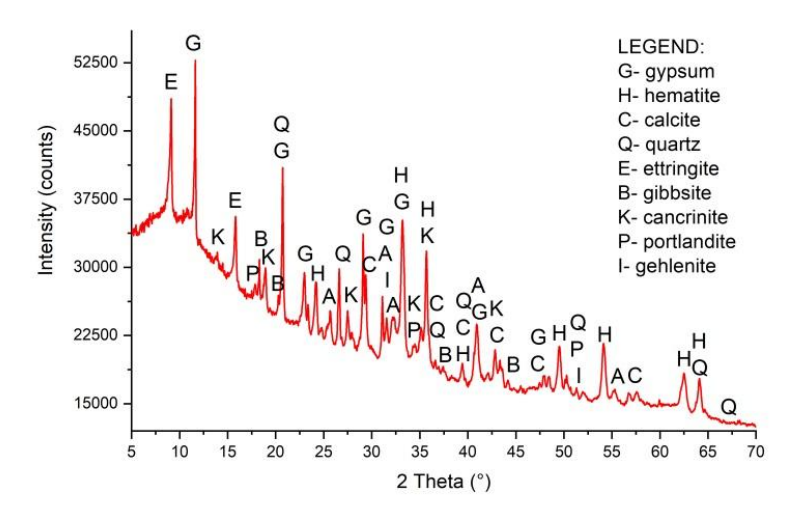


Figure 3. XRD spectrum of RM/PA

Table 2. Chemical analyses of eluates from RM, PA and RM/PA

Parameters	Concentration (mg/kg _{d.m.})					
	RM	PA	RM/PA	Limit values (URL3)		
Chromium (Cr)	0.03	0.03	0.02	0.6		
Cobalt (Co)	0.003	0.006	0.002	0.05		
Nickel (Ni)	0.02	0.01	< 0.01	0.5		
Copper (Cu)	0.03	0.113	0.106	2		
Zinc (Zn)	< 0.002	22.2	< 0.002	3.5		
Arsenic (As)	0.87	0.01	0.01	0.4		
Selenium (Se)	0.02	< 0.002	< 0.002	1		
Molybdenum (Mo)	0.02	1.14	0.09	1		
Cadmium (Cd)	< 0.001	0.002	< 0.002	0.04		
Antimony (Sb)	0.004	< 0.002	0.014	0.5		
Barium (Ba)	0.01	1.83	0.52	20		
Mercury (Hg)	< 0.001	0.001	0.001	0.01		
Lead (Pb)	0.009	0.115	0.003	0.6		
Fluoride (F-)	16	520	<5	10		
Chloride (Cl ⁻)	62	3720	210	1000		
Sulphate (SO ₄ ²⁻)	131	22860	3480	10000		

The geotechnical properties of the compacted RM/PA composite are presented in Table 3.

Table 3. Geotech	nical properties of RM/PA composite	
Parameter	Method	Result
Moisture content	SIST EN ISO 17892-1:2015	39.7 %
Dry density of compacted sample	SIST EN 13286-	1 14 May/2003
ρ_d	2:2010/AC:2013	$1.14~\mathrm{Mg/m^3}$
Unconfined compressive strength,		
tested after curing time:		
- 2 days	SIST EN 13286-41:2022	144 kPa
- 7 days		3548 kPa
- 14 days		4939 kPa
Consolidation properties – Oedometer test		
Vertical stress:	SIST EN ISO 17892-5:2017	
- 50 kPa	SIST EN ISO 17692-3.2017	3560 kPa
- 100 kPa		79400 kPa
Permeability k ₂₀	SIST EN ISO 17892-11:2019	
at 200 kPa	5151 EN 150 1/892-11:2019	$5.5 \times 10^{-11} \text{ m/s}$
Shear strength		_
- Friction angle φ'	SIST EN ISO 17892-10:2019	51.5 °
- Cohesion c'		0.0 kPa

4. Discussion

The major mineral phases of the RM used are hematite, gibbsite and cancrinite, while calcite, boehmite and aluminium fluoride are in the minority. The leaching tests have shown that the concentrations of As and F⁻ in the eluate of RM exceed the limits specified in the Slovenian environmental legislation (URL 3). The mineralogical analysis of the PA used in preparation of the composite shows that, it contains, among other minerals, anhydrite, which could affect the mechanical stability of the RM/PA composite due to the volumetric changes during the transformation into gypsum and also causes high concentrations of sulphate in the PA eluate. Lime (CaO) and periclase (MgO) are present in the PA as active phases that can form hydration products. The leaching test shows an access concentrations of Zn, Mo, F⁻, Cl⁻ and SO₄²⁻ (URL 3) in the PA eluate.

The mineralogical composition of the RM/PA composite shows that a new mineral phase - ettringite - was formed during the curing of the investigated geotechnical composite, which is associated with the immobilisation of various PTEs (**Kumarathasan et al., 1997**). The immobilization effect, which could be at least partially contributed to ettringite formation, is confirmed by the RM/PA eluate, in which the concentrations of As and F⁻ from RM and of Mo, Zn, F⁻, Cl⁻ and SO₄²⁻ from PA were reduced below the Slovenian legislative limits (**URL 3**), which is also partly due to the formation of insoluble species, thus ensuring the environmental acceptability of RM/PA. However, despite the favourable results of RM/PA eluate quality, the long-term environmental acceptability of RM/PA could be affected by exposure to various environmental factors. Although the possibility of environmental degradation of the RM/PA composite is very low due to its high alkalinity, assumed high buffering capacity and low permeability, which reduces the potential migration of PTEs, its long-term and pH-dependent behaviour should be further investigated.

The geotechnical composite RM/PA exhibits high shear strength and low compressibility and permeability. The uniaxial compressive strength increases with the age. After 7 days of curing, the increase in strength slows down, indicating that most of the hydration process has been completed. The early Rc value of RM/PA is relatively low, but after 7 days of curing the minimum Rc value of 0.4 MPa is exceeded (SCS, 1989). From the point of view of evaluated geotechnical properties, the investigated composite material shows even better properties than most natural soils, which confirms its applicability as a construction material.

5. Conclusions

In this study, the utilization of RM with addition of PA as a geotechnical composite material was investigated. Since the RM residue is in the form of slurry, it cannot be used as a geotechnical material by itself, but must be treated with binders to obtain a geotechnical composite material with appropriate geotechnical properties. An alternative recycled material, PA, containing (latent) hydraulically active phases was selected as an additive to the RM slurry in a geotechnical composite RM/PA. A material with the desired properties for use in earthworks was obtained, with even better geotechnical properties than most natural soils used in earthworks. During the production of the samples, a mellowing period was needed to gain proper workability of the investigated composite. The composition of the binder also affects the leaching of potentially hazardous substances and thus the environmental acceptability of the composites. Therefore, the alternative binder should be carefully selected according to the properties that must be suitable for the composite production and should be carefully investigated in advance.

The results of this study show that RM after extraction of raw materials (metals, REE) could be used as an alternative construction material in earthworks, if it is treated with appropriate additives or binders, such as paper mill

ash, to produce geotechnical composites. Such a composite could be manufactured and marketed as a construction product after obtaining technical approval at European or national level, depending on its intended use and properties.

Nevertheless, red mud composites need to be further investigated, especially with regard to the evaluation of long-term stability under changing climatic conditions.

6. References

- ISO 15923-1:2013 (2013): Water quality Determination of selected parameters by discrete analysis systems Part 1: Ammonium, nitrate, nitrite, chloride, orthophosphate, sulfate and silicate with photometric detection, International Organization for Standardization, Switzerland.
- Jha, A. K., Kumar, D., & Sivapullaiah, P. V. (2020). Influence of fly ash on geotechnical behaviour of red mud: a micro-mechanistic study. *Geotechnical and Geological Engineering*, 38(6), 6157–6176. https://doi.org/10.1007/s10706-020-01425-z
- Kumarathasan, P., McCarthy, G. J., Hassett, D. J., & Pflughoeft-Hassett, D. F. (1989). Oxyanion Substituted Ettringites: Synthesis and Characterization; and their Potential Role In Immobilization of As, B, Cr, Se and V. *MRS Proceedings*, 178. https://doi.org/10.1557/proc-178-83
- Nayak, K. C., Pathania, A., & Pathania, A. R. (2024). Red mud: Characteristics, utilization, and environmental remediation strategies in the aluminium industry. Materials Today Proceedings. https://doi.org/10.1016/j.matpr.2024.05.026
- Pavšič, P., Đurić, M., Košir, M., Pranjić Mauko, A., Mladenovič, A., Oprčkal, P., Seršen, S., & Zalar Serjun, V. (2024). Recycled red mud as an useful geotechnical material. In *Proceedings of the XVIII European Conference on Soil Mechanics and Geotechnical Engineering*, Guerra, Nuno (ed.), 3224–3227. https://doi.org/10.1201/9781003431749-634
- Samal, S. (2021). Utilization of red mud as a source for metal Ions—A review. *Materials*, 14(9), 2211. https://doi.org/10.3390/ma14092211
- SCS Skupnost za ceste Slovenije (1989). Popis del in posebni tehnični pogoji za zemeljska dela in temeljenje, knjiga 3, Skupnost za ceste Slovenije. (in Slovenian).
- SIST EN 13286-2:2010/AC:2013 (2013): Unbound and hydraulically bound mixtures Part 2: Test methods for laboratory reference density and water content Proctor compaction, SIST Slovenski inštitut za standardizacijo, Slovenija.
- SIST EN 13286-41:2022 (2022): Unbound and hydraulically bound mixtures Part 41: Test method for the determination of the compressive strength of hydraulically bound mixtures, SIST Slovenski inštitut za standardizacijo, Slovenija.
- SIST EN 13286-50:2005 (2005): Unbound and hydraulically bound mixtures Part 50: Method for the manufacture of test specimens of hydraulically bound mixtures using Proctor equipment or vibrating table compaction, SIST Slovenski inštitut za standardizacijo, Slovenija.
- SIST EN 1744-3:2002 (2002): Tests for chemical properties of aggregates Part 3: Preparation of eluates by leaching of aggregates, SIST Slovenski inštitut za standardizacijo, Slovenija.
- SIST EN ISO 17294-2:2017(2017): Water quality Application of inductively coupled plasma mass spectrometry (ICP-MS) Part 2: Determination of selected elements including uranium isotopes, SIST Slovenski inštitut za standardizacijo, Slovenija.
- SIST EN ISO 17892-1:2015 (2015): Geotechnical investigation and testing Laboratory testing of soil Part 1: Determination of water content, SIST Slovenski inštitut za standardizacijo, Slovenija.
- SIST EN ISO 17892-10:2019 (2019): Geotechnical investigation and testing Laboratory testing of soil Part 10: Direct shear tests, SIST Slovenski inštitut za standardizacijo, Slovenija.
- SIST EN ISO 17892-11:2019 (2019): Geotechnical investigation and testing Laboratory testing of soil Part 11: Permeability tests, SIST Slovenski inštitut za standardizacijo, Slovenija.
- SIST EN ISO 17892-5:2017 (2017): Geotechnical investigation and testing Laboratory testing of soil Part 5: Incremental loading oedometer test, SIST Slovenski inštitut za standardizacijo, Slovenija.
- SMWW (2017): Standard Methods for the examination of water and wastewater-SMWW. 4500 F-Fluoride -SPADNS Method 4500 F-D, 23 rd edition, American PublicHealth Association, American Water Works Association, Water Environment Federation: Washington, DC.
- Svobodova-Sedlackova, A., Calderón, A., Fernandez, A. I., Chimenos, J. M., Berlanga, C., Yücel, O., Barreneche, C., & Rodriguez, R. (2024). Mapping the research landscape of bauxite by-products (red mud): An evolutionary perspective from 1995 to 2022. *Heliyon*, 10(3), e24943. https://doi.org/10.1016/j.heliyon.2024.e24943
- URL 1. https://www.alcircle.com/news/aluminium-consumption-climbs-steadily-indicating-sustained-market-strength-113646?srsltid=AfmBOoqwr8TAh7NSFhxTQWiNTyJgVPTOq6quI8uZQ6xdjPpjmFk5b2bB (accessed 21 st August 2025)
- URL 2. https://international-aluminium.org/wp-content/uploads/2022/04/BRManagementGuidance.pdf (accessed 21 st August 2025)
- URL 3. https://pisrs.si/pregledPredpisa?id=URED8482 (accessed 21 st August 2025)

Zalar Serjun, V.; Mladenovič, A.; Milačič, R.; Ščančar, J.; Ašler, A.; Zupančič, N.; Nikolić, I.; Oprčkal, P. (2018). Red mud as an alternative material for the production of a geotechnical composite. In *Proceedings of the 2nd International Bauxite Residue Valorisation and Best Practices Conference : BR 2018*, Pontikes, Yiannis (ed.), 143-149. ISBN 9789082825923.

Acknowledgment

The authors acknowledge the Slovenian Research and Innovation Agency core funding P2-0273 and project J1 - 4413.

Funding

This research was funded by EIT RawMaterials project, RIS-RESTORE, project no. 19269, co-funded by the European Union.

Author's contribution

Primož Pavšič (PhD): investigation, writing – review & editing. Marija Đurić (PhD): investigation, writing – review & editing. Mateja Košir (PhD): conceptualization, funding acquisition, investigation, writing – review & editing. Primož Oprčkal (PhD): conceptualization, funding acquisition, investigation, writing – review & editing. Vesna Zalar Serjun (PhD): conceptualization, investigation, writing – review & editing.

All authors have read and agreed to the published version of the manuscript.



Development of Porous Foam Glass from Endof-Life PV Panels Using Secondary Raw Materials

DIM-ESEE Conference



Busra Karakas^{1*}, Ildikó Fóris², Gábor Mucsi¹

¹Institute of Raw Material Preparation and Environmental Technology 3515 Miskolc, University of Miskolc

Abstract

The growing accumulation of end-of-life photovoltaic (PV) modules presents a critical environmental issue, particularly due to the substantial volume of non-biodegradable glass components. This study investigates the recycling of PV panel glass waste into porous glass foam using thermal treatment methods, aiming to create lightweight materials suitable for heat insulation. The research on industrial waste products was investigated as additional additives. Nabentonite was added (2 wt%) as a binder. Specimens were formed into cylindrical pellets (10 g each) using a hydraulic piston press at 30 MPa.

Thermal treatment was performed in a Nabertherm static laboratory furnace across temperatures of 750 °C to 900 °C, at different heating rates and holding times. Physical properties, including density and volume expansion, were determined using the geometric method, while a standardized falling test assessed mechanical integrity. Microstructural changes and foaming efficiency were evaluated through comparative image analysis.

The lowest density (0.17 g/cm³) was achieved at 900 °C and 10 °C/min with red mud and eggshell powder. Increasing the foaming temperature and heating rate enhanced gas entrapment and porosity, whereas extended holding times sometimes resulted in densification due to the escape of generated gases. Fly ash-containing samples exhibited limited foaming behavior and higher densities (>0,37 g/cm³), likely due to reduced viscosity control.

Mechanical resistance, as evaluated through repeated falling tests, showed no direct correlation with specimen density but was instead influenced by pore morphology and distribution. In contrast, slower heating rates and extended holding times resulted in thicker cell walls and structural heterogeneity, which negatively impacted the mechanical integrity of the foams.

The results confirm the practical potential of repurposing photovoltaic panel glass waste into lightweight, porous foam glass through the use of environmentally friendly additives. This research supports the broader adoption of secondary raw materials in circular economy models and contributes to lowering the environmental impact associated with both PV panel disposal and construction materials.

Keywords: PV panel, glass foam, recycling, secondary raw materials

1. Introduction

Solar photovoltaic (PV) panels are increasingly important for renewable energy, but their limited lifespan (20–25 years) will result in an estimated 8 million tons of waste by 2030 and up to 80 million tons by 2050 (Rodríguez et al., 2023). Since glass accounts for over 80 wt% of a PV module's weight, it is the principal recyclable fraction (Weckend et al., 2016). PV glass waste has been explored in applications such as glass substrates (Rodríguez et al., 2023), construction materials (Thang et al., 2024), ceramics (Savvilotidou et al., 2019), and zeolites (Lee et al., 2023). More recently, attention has shifted to glass foams produced by heat-treating waste glass powders with foaming agents and additives (Scheffler & Colombo, 2005). These materials combine high porosity (>80 %), low density (0.1 g/cm-1.2 g/cm³), low thermal conductivity (<0.1 W/(m·K)), and moderate compressive strength (0.4 MPa-12 MPa), making them suitable for insulation, filtration, biomedical, optical, and electromagnetic applications (Barbosa et al., 2016; 2021; Hassan et al., 2024).

Recent studies confirm that PV glass can generate foams with properties comparable to commercial products. For example, Thach et al. achieved porosities of ~77 % – 81% and densities of 0.25 g/cm³ – 0.43 g/cm³ using CaCO₃ (**Thach et al., 2022**), while **Brykalski et al. (2025**) produced foams from PV glass with eggshells and clay, reaching densities of ~0.20 g/cm³ – 0.47 g/cm³, compressive strengths up to 5.7 MPa, and thermal conductivities as low as 0.046 W/(m·K) (**Brykalski et al., 2025**). Similarly, Bui et al. reported 91 % porosity at 870 °C using CaCO₃ (**Bui et al., 2025**). These values are close to or within the ranges of commercial foams (**König et al., 2020**).

² University of Miskolc, 3515 Miskolc-Egyetemváros

The present study advances this research by producing glass foams from PV panel waste combined with red mud (RM), fly ash (FA), and eggshell (ES) as a CaCO₃-rich foaming agent. RM, a by-product of alumina production, may either promote crystallization and large pores or reduce viscosity at low levels (Guo et al., 2014; Bai et al., 2024), while FA, improves mechanical strength but can limit porosity at high contents (Chen et al., 2012). Since foam glass properties depend on multiple factors, including foaming agent, additives, heating rate, and temperature (Smiljanić et al., 2021), this study systematically examines how red mud and fly ash affect the structure, density, and mechanical performance of PV panel-based foams under varied thermal conditions.

2. Methods

The raw materials used in the experiments included photovoltaic (PV) panel waste, Na-bentonite as a binder, eggshell as a foaming agent, and two additives: red mud sourced from Ajka, Hungary, and lignite-based fly ash obtained from Mátra, Hungary.

2.1. Raw material preparation

PV panels were initially pre-crushed using a roll crusher equipped with a 1 mm screen, followed by dry milling for 15 minutes in a planetary mill with stainless steel grinding balls (Ø 30 mm). This process aimed to achieve an optimal particle size of less than 100 µm for the glass powder (Fóris and Mucsi, 2022), as larger particles have been shown to limit effective foaming (Chen et al., 2012; König et al 2020).

The eggshell foaming agent, owing to its plate-like morphology, required extended preparation. It was boiled for 30 min to remove organics, then dry-milled for 120 min in a ball mill with ceramic media (Ø 30 mm). In contrast, Nabentonite, fly ash, and red mud required no additional grinding, but unsieved powders formed aggregates that reduced efficiency. To avoid this, all materials were wet-sieved through a 32 µm mesh and dried at 105 °C to constant weight.

In the methods and results sections, glass powder is referred to as GP, eggshell as ES, red mud as RM and fl ash as FA.

2.2. Particle size distribution

The particle size distribution of the ground raw materials was measured under wet conditions using a HORIBA LA-950V2 laser diffraction particle size analyzer. Distilled water served as the dispersing medium, and the measurements were evaluated based on Mie scattering theory. The particle size analysis of the raw materials is presented in **Table 1**.

Table 1: Particle size of the raw materials							
	GP (µm)	ES (µm)	FA (µm)	RM (µm)			
X_{10}	13.43	7.48	15.56	6.56			
X50	45.54	18.65	62.50	10.14			
X90	50.67	43.77	92.43	20.23			

Table 1: Particle size of the raw materials

Among the samples, FA exhibited the coarsest distribution, with median (X_{50}) and upper percentile (X_{90}) values of 62.50 µm and 92.43 µm, respectively. GP showed intermediate fineness ($X_{50} = 45.54$ µm), while ES and RM were considerably finer, with X_{50} values of 18.65 µm and 10.14 µm. RM demonstrated the narrowest distribution, while FA displayed the broadest spread. These results indicate that FA has a relatively coarse and heterogeneous particle size, whereas RM and ES are finer and more uniform, which may influence their dispersion and reactivity in glass foam production.

2.3. Chemical composition

Chemical compositions of raw materials were measured by X-ray fluorescence (XRF) analysis. The loss of ignition (LOI) was measured at 950 °C with 90 min heating time, and 60 min holding time in a static furnace. **Table 2** shows the results of the chemical composition analysis of raw materials (XRF).

XRF analysis (**Table 2**) shows that eggshells are CaO-rich (54.4%) with a high LOI (45.7%) from carbonate decomposition. Glass powder is dominated by SiO₂ (72.1%) with Na₂O and CaO, typical of soda-lime glass. Red mud contains high Fe₂O₃ (35.1%) and Al₂O₃ (17.9%), while fly ash is silico-aluminous (SiO₂ 39.8%, Al₂O₃ 14%) with moderate CaO and Fe₂O₃. These compositions indicate GP as the main glass former, ES as a foaming agent, RM as a viscosity modifier, and FA as a reinforcing additive.

			Ta	ble 2: C	hemica	I compo	osition o	of ES, G	P, KM,	and FA			
	SiO ₂	Al ₂ O ₃	MgO	CaO	Na ₂ O	K ₂ O	Fe ₂ O ₃	MnO	TiO ₂	P ₂ O ₅	S	F	LOI
Unit	m/ _m 0/ ₀	m/ _m %	m/ _m %	m/ _m 0/ ₀	m/ _m %	m/ _m %	m/ _m 0/ ₀	m/ _m %	m/ _m %	m/ _m %	m/ _m 0/ ₀	m/ _m %	m/ _m %
ES	0.3	0.0	0.62	54.4	0.13	0.13	0.03	0.001	0.002	0.499	0.21	< 0.3	45.71
GP	72,1	0,9	3,06	8,71	12,65	0,06	0,06	<0,005	0,009	0,011	0,145	<0,3	i
RM	16.10	17.90	1.66	8.50	9.98	0.08	35.10	0,31	4.08	1.39	1.59	< 0.3	12.8
FA	39.8	14	3.41	12.1	0.54	1.61	11.2	0.176	0.495	0.346	6.5	< 0.3	4.28

2.4. Systematic foaming experiments

Tables 3 present the composition of the tablets. Green tablets with a diameter of 25 mm were generated with a laboratory hydraulic piston press under 30 MPa using a hydraulic piston press. Each tablet weighed 10 g. The green tablets were then heat-treated in a Nabertherm L(T) 3 laboratory static furnace at various heat-treatment profiles. These variations include four different peak temperatures (750 °C, 800 °C, 850 °C, and 900 °C), holding times (15 min, 30 min and 60 min), and heating rates (2°C/min, 5 °C/min and 10 °C/min), as specified in **Table 3**. One series was produced without FA, while the other included FA, however, the temperature ranges, foaming agent, and RM ratios were kept identical in both series under the same conditions. After heat treatment, the samples were left to cool to room temperature.

Table 3: Sample abbreviations in this study without fly ash

7 D 4			E			T1 1
Target	Heating Rate	Holding Time	Foaming Agent	Red mud	Fly ash	Fly ash
Temp. (°C)	(°C/min)	(min)	(wt.%)	(wt.%)	(wt.%)	(wt.%)
750	10	15	1% ES	5% RM	0% FA	5% FA
750	5	30	1% ES	5% RM	0% FA	5% FA
750	2	60	1% ES	5% RM	0% FA	5% FA
800	10	15	1% ES	5% RM	0% FA	5% FA
800	5	30	1% ES	5% RM	0% FA	5% FA
800	2	60	1% ES	5% RM	0% FA	5% FA
850	10	15	1% ES	5% RM	0% FA	5% FA
850	5	30	1% ES	5% RM	0% FA	5% FA
850	2	60	1% ES	5% RM	0% FA	5% FA
900	10	15	1% ES	5% RM	0% FA	5% FA
900	5	30	1% ES	5% RM	0% FA	5% FA
900	2	60	1% ES	5% RM	0% FA	5% FA

2.5. Measurements of the properties of finished glass foam tablets

Since glass foams are lightweight materials, it is essential to determine their density both before and after heat treatment. The specimen density (ρs) was calculated based on geometric measurements, obtained using a caliper, and mass measurements, recorded with an analytical balance.

Specimen density is calculated according to the formula:

Specimen Density (
$$\rho$$
s) = Mass of the sample (m)/ Total Volume (V) (1)

$$V = total \ volume, including \ voids \ (cm^3) = \frac{\mu. \ (width)^2.height}{4}$$

The mechanical strength and abrasion of the tablets are important, as they need to be resistant during transport. A laboratory ceramic-lined mill was used for the abrasion resistance test. 30 g tablets were tested for each sample. The machine operated at 30 rpm for 10 minutes, and after removing the material, it was sieved using a 1 mm opening size sieve for the fine fraction. The degree of the abrasion was calculated using Eq. (1) from the mass of the fine fraction and the feeding material (Faitli et al., 2017).

$$\Delta m_{abr} = \frac{m_{fine}}{m_{feed}} * 100 [\%]$$
 (2)

where:

 $\Delta m_{\rm abr}$ – the amount of abrasion (%),

 m_{fine} – the amount of material passed through the 1 mm sieve (g), m_{feed} – the feeding material (30 g).

Following the previously established procedure (**Fóris & Mucsi, 2023**), each tablet was subjected to a free-fall test by repeatedly dropping it from a height of 2 meters onto a concrete floor until fracture was observed. For each composition ratio, three tablets were tested to ensure reproducibility.

3. Results and discussion

3.1. Specimen density before and after heat treatment

Figure 2. (left) shows the densities of RM-only samples, ranging from 0.17 g/cm³ to 0.52 g/cm³, compared to 1.73 g/cm³ for untreated glass powder. At 750 °C, densities were highest (0.36 g/cm³ – 0.52 g/cm³), but decreased with temperature, reaching minimum values at 900 °C (0.17 g/cm³ at 10 °C/min). Higher heating rates consistently promoted lower densities by enhancing gas entrapment through rapid viscosity reduction and surface sealing (Guo et al., 2014), while slower rates and prolonged exposure favored gas escape and incomplete foaming. Holding time also influenced viscosity, with longer durations supporting further expansion and foam stabilization (Qin et al., 2018). Overall, heating rate, temperature, and holding time directly govern foaming efficiency (Bai et al., 2024).

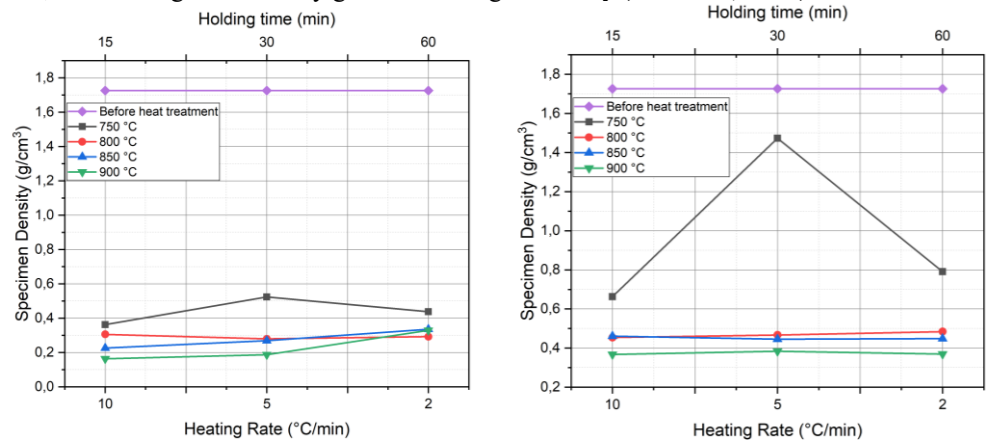


Figure 1. Specimen density of the samples containing only RM (left) and samples containing RM+FA (right)

At 750 °C, the high viscosity of glass limits foaming, producing higher densities. At this temperature, 10 °C/min yields the lowest density due to improved gas expansion, while 5 °C/min results in the highest density. At 2 °C/min, extended heating (60 min) partially compensates for slower heating, lowering density relative to 5 °C/min. At 800 °C, densities converge (0.28 g/cm³ – 0.30 g/cm³), suggesting a balanced state with minimal influence of heating rate. At 850 °C, a sharper density reduction is observed, with values of 0.22 g/cm³, 0.27 g/cm³ and 0.33 g/cm³ for 10 °C/min, 5 °C/min, and 2 °C/min, respectively. At 900 °C, the lowest density (0.17 g/cm³) occurs at 10 °C/min, whereas slower heating leads to higher densities (0.19 g/cm³ and 0.33 g/cm³ for 5 °C/min and 2 °C/min), as prolonged dwell promotes gas escape. Overall, optimal foaming is achieved at 10 °C/min with shorter holding times.

For RM+FA samples (**Figure 2. right**), densities ranged from 0.37 g/cm³ to 1.47 g/cm³. Fly ash reduced porosity and hindered gas entrapment, resulting in poor foaming, particularly at lower temperatures. At 750 °C, densities were 0.66 g/cm³ (10 °C/min), 1.47 g/cm³ (5 °C/min), and 0.79 g/cm³ (2 °C/min), mirroring the RM-only trend of highest density at the intermediate heating rate. At 800 °C, densities decreased to 0.45 g/cm³. – 0.48 g/cm³. with minimal variation across heating rates, while at 850 °C values stabilized around 0.45 g/cm³. – 0.46 g/cm³. At 900 °C, densities further declined to 0.37 g/cm³. –0.38 g/cm³., yet remained higher and less porous than RM-only foams. The restricted foaming is attributed to the high viscosity and softening temperature of FA, which limits liquid phase formation. While FA can enhance mechanical strength by increasing viscosity and reducing porosity, it negatively affects foaming efficiency. Previous studies suggest that this effect can be mitigated by incorporating fluxing agents, such as borax, to lower viscosity (**Chen et al., 2012; Song et al., 2021**).

3.2. Pore structure

Figure 3. (left) shows that porosity in RM-only samples increases with temperature and is highest at $10\,^{\circ}$ C/min, inversely reflecting density trends (**König et al., 2014**). At 750 °C, porosity peaked at 85.63 % ($10\,^{\circ}$ C/min) and was lowest at 5 °C/min (79.23%). From 800 °C onward, values stabilized (\sim 88 % - 93 %), with $10\,^{\circ}$ C/min consistently yielding the highest porosity. These results confirm that higher temperatures and faster heating rates promote pore formation and improved foaming.

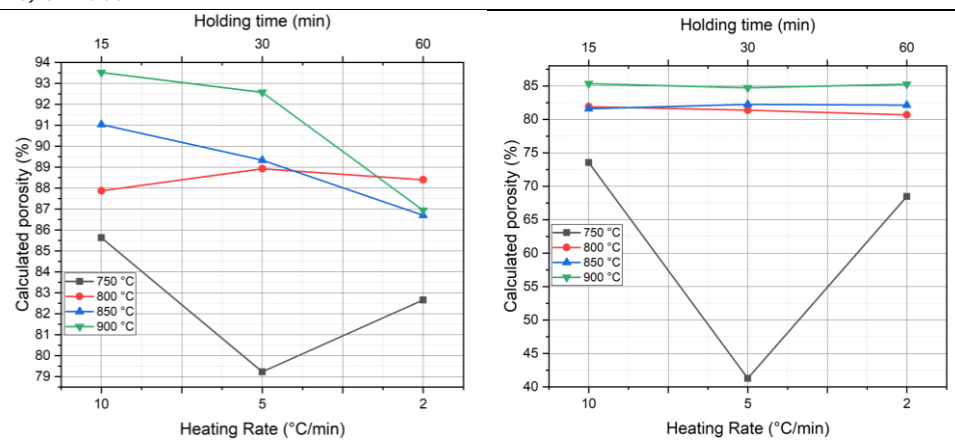


Figure 3. Calculated porosity values of the samples containing only RM (left), and samples containing RM+FA (right)

Figure 3. (right) shows that RM+FA samples had lower porosity than RM-only samples, confirming reduced foaming efficiency. At 750 °C, porosity dropped sharply at 5 °C/min (41.28 %), compared to 10 °C/min (73.56 %) and 2 °C/min (68.47 %). Porosity improved with temperature, reaching ~85 % at 900 °C, with reduced dependence on heating rate. At lower temperatures, foaming was limited and pore structures underdeveloped. From 800 °C onward, porosity increased due to liquid-phase formation, though slower heating still yielded less porous structures. At 850 °C, rapid heating caused structural breaks, while slow heating led to finer but uneven pores. At 900 °C, low viscosity allowed pore coalescence and thicker cell walls, which increased density but potentially lowered mechanical strength due to internal flaws (**Bui et al., 2025**).

3.3. Falling test and abrasion resistance test

Figure 4. shows that drop resistance of RM-based foams improved with temperature. At 750 °C, samples with all heating rates endured only 1-2 drops, while at 800 °C, performance increased to 6 drops for 10 °C/min and 2 °C/min. At 850 °C -900 °C, resistance varied by heating rate, with 10 °C/min (850 °C) and 2 °C/min (900 °C) showing the best results. These outcomes suggest that mechanical performance depends not only on density but also on pore structure and wall strength (**Guo et al., 2014**).

In contrast, RM+FA foams exhibited >50 drops across all conditions, confirming that FA markedly increases mechanical strength by refining pore structure and reducing critical flaws.

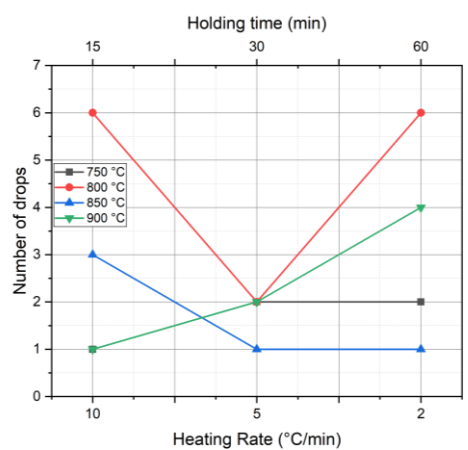


Figure 4. Falling test of the samples containing only RM

Figure 5 (left) shows that abrasion resistance of RM-only samples improves with temperature, peaking at 4.5% at 900 °C (10 °C/min). Lower temperatures (750 °C – 850 °C) yielded values between 2.9% – 3.6%, with minor variations across heating rates. The results indicate that temperature is the dominant factor, while heating rate and holding time have a lesser impact on surface wear resistance.

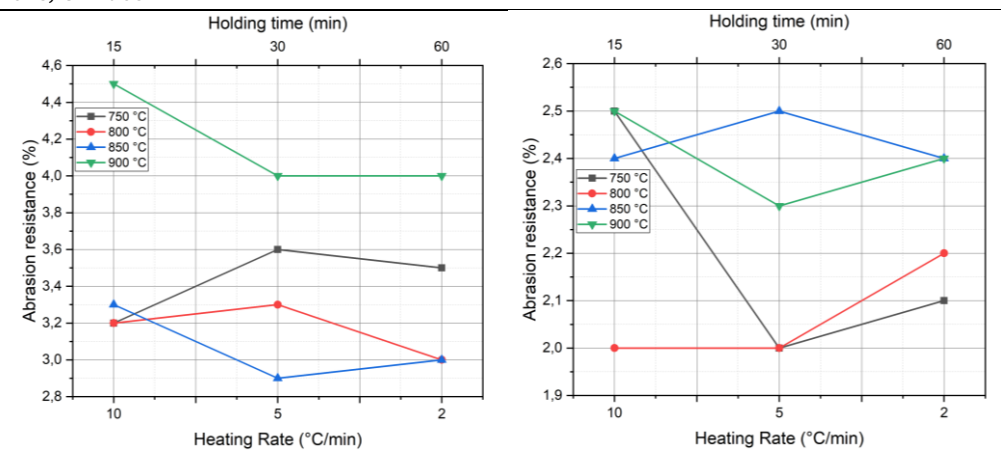


Figure 5. Abrasion resistance of the samples containing only RM (left), and the samples containing RM+FA (right)

Figure 5. (right) shows that RM+FA samples exhibited lower abrasion resistance, ranging from 2.0 % - 2.5%. Resistance improved at higher temperatures ($850 \degree C - 900 \degree C$), remaining around 2.4 % - 2.5 %, while it declined slightly at $750 \degree C - 800 \degree C$, reaching a minimum of 2.0 % - 2.2%. Overall, abrasion resistance increases with processing temperature.

The abrasion resistance results indicate that there is no direct linear relationship between heating rate, holding time, and abrasion resistance. However, abrasion resistance increased at higher temperatures, regardless of the heating rate or holding time employed. Temperature has a more pronounced effect in enhancing abrasion resistance. The observed relation was consistent across all samples, encompassing both those containing FA and those without.

4. Conclusions

This study demonstrated that end-of-life PV panel glass can be successfully recycled into lightweight glass foams using red mud (RM), fly ash (FA), and eggshell (ES) as additives.

For RM-only samples, the lowest density (0.17 g/cm³) was achieved at 900 °C with a heating rate of 10 °C/min, highlighting the importance of higher temperatures and rapid heating for effective foaming.

Porosity values exceeded 90% under these conditions, whereas slower heating rates led to gas escape and reduced efficiency.

The addition of FA significantly limited porosity (≤85 %) and increased densities (≥0.37 g/cm³), due to restricted liquid-phase formation, although it markedly improved mechanical strength, with samples exceeding 50 drops in the falling test. Mechanical performance might be governed by pore size distribution and wall integrity rather than density alone.

RM contributed to lowering the foaming temperature to \sim 800 °C, while FA acted as a reinforcing additive, although at the expense of porosity.

Overall, RM-containing samples provided the best balance of low density, while FA enhanced impact and abrasion resistance. These findings confirm that PV glass waste, combined with suitable secondary raw materials, offers a pathway to producing functional glass foams for insulation and structural applications, thereby contributing to circular economy principles by reducing primary resource demand and diverting waste from landfills.

These experiments served as preliminary investigations, and further research is required to validate and deepen the findings.

5. References

Bai, J., Li, C., Du, Q., & Dong, C. (2024). Fabrication and Properties of Self-foamed Glass Ceramics from Red Mud and Ceramic Tile Polishing Waste. Journal of Sustainable Metallurgy, 10(3), 1559–1571. doi:10.1007/s40831-024-00883-6

Barbosa, A.R.J., Lopes, A.A.S., Sequeira, S.I.H., Oliveira, J. P., Davarpanah, A., Mohseni, F., Amaral, V. S. & Monteiro, R. C. C. (2016). Effect of processing conditions on the properties of recycled cathode ray tube glass foams. J Porous Mater 23, 1663–1669. https://doi.org/10.1007/s10934-016-0227-7

Brykalski, M., Camaratta, R., Silveira, L., Ferraz de Azevedo, C., Ferreira Piazzi Fuhr, A. C., Goncalves Osorio, A. & Machado Machado, F. (2025). Utilizing waste glass from photovoltaic modules for glass foam production: a study on optimizing the processing parameters. Journal of Material Cycles and Waste Management. doi:10.1007/s10163-025-02285-6

Bui, T. K., Nhi, N. V. U. & Minh, D. Q. (2025). In-situ analysis on foaming behavior of foam glass produced from photovoltaic module waste. Journal of the Australian Ceramic Society. doi:10.1007/s41779-025-01160-9

- Chen, B., Wang, K., Chen, X. & Lu, A. (2012). Study of foam glass with high content of fly ash using calcium carbonate as foaming agent. Materials Letters, 79, 263–265. doi:10.1016/j.matlet.2012.04.052
- Faitli, J., Gombkötő, I., Mucsi, G., Nagy, S. & Antal, G. (2017). Mechanikai eljárástechnikai praktikum (Mechanical Processing Handbook). Miskolci Egyetemi Kiadó, 140-142. (in Hungarian there is no English abstract)
- Fóris, I., & Mucsi, G. (2023). Influence of raw material properties on waste-based glass foam. Rudarsko Geolosko Naftni Zbornik, 38(4), 75–83. doi:10.17794/rgn.2023.4.7
- Guo, Y., Zhang, Y., Huang, H., Meng, K., Hu, K., Hu, P. & Meng, X. (2014). Novel glass ceramic foams materials based on red mud. Ceramics International, 40(5), 6677–6683. doi:10.1016/j.ceramint.2013.11.128
- Hassan, A. M., Bunnori, N. M., Ramesh, S., Tan, C. Y., & Mo, K. H. (2024). Glass-based foam from alkali activation: A review on effect of primary foaming parameters on microstructure and density. Construction and Building Materials. Elsevier Ltd. doi:10.1016/j.conbuildmat.2024.136157
- König, J., Lopez-Gil, A., Cimavilla-Roman, P., Rodriguez-Perez, M. A., Petersen, R. R., Østergaard, M. B., Spreitzer, M. (2020). Synthesis and properties of open- and closed-porous foamed glass with a low density. Construction and Building Materials, 247. doi:10.1016/j.conbuildmat.2020.118574
- Lee, W. H., Lin, Y. W., & Lin, K. L. (2023). Optimization of synthesis parameters for the preparation of zeolite by reusing industrialwaste as raw material: Sandblasting waste and solar panel waste glass. Solid State Sciences, 143. doi:10.1016/j.solidstatesciences.2023.107277
- Qin, Z., Li, G., Tian, Y., Ma, Y., & Shen, P. (2018). Optimization of preparation process and performance analysis of fly ash foam glass. Functional Materials, 25, No:3, p. 554-563.
- Rodríguez, T., Vázquez, S., Valdés, R., Rodríguez, I., Figueroa, P., García, P., Álvarez Méndez, A. (2023). Recycling in the Development of Glass Substrates for Photovoltaic Applications. Materials, 16, 2848. doi:10.3390/ma
- Savvilotidou, V., Kritikaki, A., Stratakis, A., Komnitsas, K., & Gidarakos, E. (2019). Energy efficient production of glass-ceramics using photovoltaic (P/V) glass and lignite fly ash. Waste Management, 90, 46–58. doi:10.1016/j.wasman.2019.04.022
- Scheffler, Michael., & Colombo, Paolo. (2005). Cellular ceramics: structure, manufacturing, properties and applications. Wiley-VCH; John Wiley
- Smiljanić, S., Hribar, U., Spreitzer, M., & König, J. (2021). Influence of additives on the crystallization and thermal conductivity of container glass cullet for foamed glass preparation. Ceramics International, 47(23), 32867–32873. doi:10.1016/j.ceramint.2021.08.183
- Song, H., Chai, C., Zhao, Z., Wei, L., Wu, H., & Cheng, F. (2021). Experimental study on foam glass prepared by hydrothermal hot pressing-calcination technique using waste glass and fly ash. Ceramics International, 47(20), 28603–28613. doi:10.1016/j.ceramint.2021.07.019
- Thach, B.K., Tan, L.N., Minh, D.Q., Hung, L.C.& Tuan, P.D. (2023). Production of Porous Glass-Foam Materials from Photovoltaic Panel Waste Glass. In: Mohd Salleh, M.A.A., Che Halin, D.S., Abdul Razak, K., Ramli, M.I.I. (eds) Proceedings of the Green Materials and Electronic Packaging Interconnect Technology Symposium. EPITS 2022. Springer Proceedings in Physics, vol 289. Springer, Singapore. https://doi.org/10.1007/978-981-19-9267-4 34
- Thang, N. H., Binh, N. Q., Van Phuc, N., & Kien, P. T. (2024). Syntheses and characteristics of calcium-based geopolymer from solar-cell panel-glass waste by hydrothermal method. Materiali In Technologije, 58, 467-475. doi:10.17222/mit.2024.1153
- Weckend, S., Wade, A., & Heath, G. (2016). End-of-life management Solar Photovoltaic Panels. IRENA. Retrieved from IEA-PVPS Report Number: T12-06:2016

Acknowledgment

The authors are grateful to Ferenc Móricz for the XRF measurement.

Author's contribution

Ildikó Fóris (1) (PhD student) provided the raw materials preparation, presentation of the results and the evaulation of the experimental results. **Busra Karakas (2)** (Master student) performed the laboratory work, and presentation of the results. **Gábor Mucsi (3)** pProfessor) provided the evaluation of the experimental results and presentation of the results.



Mechanical Pretreatment of a Mild Hybrid Lithium-Ion Battery Pack – Recovery of Black Mass

DIM-ESEE Conference



Tamas Kurusta^{1*} ^⑤

— Sándor Márton Nagy¹ ^⑤

1-2 Institute of Raw Material Preparation and Environmental Technology, 3515 Miskolc, University of Miskolc

Abstract

Lithium-ion batteries (LiBs) are indispensable in modern technologies, powering devices from consumer electronics to electric vehicles and stationary storage systems. With the rapid growth of e-mobility, the accumulation of end-of-life (EoL) LiBs has become a pressing issue, posing both environmental hazards and resource recovery challenges. Their complex structure and composition make dismantling and recycling particularly demanding. Mechanical pretreatment plays a pivotal role, as it serves as the foundation for subsequent hydrometallurgical and pyrometallurgical processes.

This study investigates the mechanical dismantling and pretreatment of a lithium-ion battery pack from an F.T. mild hybrid commercial vehicle, focusing on black mass recovery. The workflow included manual disassembly, cell discharge, mechanical opening with rotary shears, electrolyte removal by thermal treatment at 60 °C, and size reduction using a hammer shredder. The <1 mm fraction was designated as black mass. ICP analysis confirmed that the recovered material originated from an NMC-type battery, containing nickel (17.3 wt%), cobalt (4.53 wt%), and lithium (3.39 wt%).

The recovery efficiency of black mass reached ~74 wt% with >90 % purity. Additional fractions enriched in aluminum and copper were recovered through air-flow separation. These findings highlight the potential of mechanical pretreatment as a scalable approach that prevents end-of-life batteries from landfilling and enables their reintegration into the circular economy. By producing high-quality recyclable fractions, the process contributes to resource recovery and the development of closed-loop battery recycling systems.

Keywords: lithium-ion batteries, mechanical processing, recycling, black mass

1. Introduction

Lithium-ion batteries (LiBs) were introduced to the market in the early 1990s and have since become the dominant technology for energy storage, owing to their high energy density, power capability, and long cycle life (**Heelan et al., 2016**; **Wu et al., 2022**). Initially, they were primarily used in portable electronic devices, but since 2010, their application has gradually expanded to larger systems, such as hybrid and fully electric vehicles. Market projections indicate that global LiB capacity will increase from 259 GWh in 2020 to 2500 GWh by 2030 (**Fan et al., 2020**), which will substantially raise both the demand for raw materials required for their production and the volume of end-of-life LiBs generated. Recycling of LiBs faces multiple technical and environmental challenges. Among the key issues are:

- Variety of Battery Types: The wide range of LiB types (such as LCO, LFP, LMO, NMC, and NCA) necessitates careful pre-classification and sorting to handle each type appropriately.
- Size of Battery Packs: The large size of battery packs and cells makes disassembly labor-intensive and challenging.
- Flammability Risks: LiBs are flammable and can ignite or explode as a consequence of mechanical stress or even improper storage.
- Harmful Substances: These batteries contain materials that are hazardous to human health and the environment, requiring careful separation, disposal, and recycling as part of a closed-loop or circular economy approach during mechanical preparation.

The European Union currently has technologies for processing EoL LiBs, with capacities ranging from several hundred tons to 20,000 tons per year. Various methods, including pyrometallurgical, hydrometallurgical, and metallurgical techniques, have been suggested for recovering metals from LiBs (Roy et al., 2021). LiB processing technologies involving mechanical pretreatment are considered environmentally friendly, as they reduce the need for downstream operations to separate pure metals at later stages. Mechanical processes are generally cost-effective and do not typically require specialized equipment (Javorsky da Costa et al., 2015). In hydrometallurgical processes, mechanical processing serves as the first step, involving battery comminution, separation of structural materials, and extraction of the black mass (Brückner et al., 2020).

Implementing specialized processes can address several technical issues. For example, discharging batteries is often necessary before shredding to prevent short circuits and fire hazards (Mádainé et al., 2020). However, discharging may not be required with wet shredding or freezing methods. Shredding can also be performed in inert atmospheres (e.g., CO₂ or nitrogen) or under vacuum, and wet technologies are available for electrolyte removal, which can be achieved through thermal treatment or vacuum application (**Greenwood et al., 2020**).

The primary objective of this research is to extract the black mass from battery cells. A comprehensive material balance of the entire hybrid system and battery cell processing was conducted to use the results as a foundation for practical applications.

2. Methods and Materials

2.1. Methods

The battery pack was manually dismantled using hand tools, which involved removing the releasable connection. After this, the battery cells were discharged by connecting them directly to a resistance (**Kwade and Diekman, 2018**), followed by manual and mechanical processing.

The battery cell was opened using a two-axis rotary shear shredder. Once opened, the electrolyte solvent was removed by heat treatment (**Colledani et al., 2023**) using the Memmert UFE 400 type drying oven at 60 °C for 24 hours.

After the electrolyte was removed, the battery cell was mechanically crushed using a hammer crusher with a 20 mm sieve. The crushed battery cell material was sorted using an airflow separator with an air speed of 2.54 m/s. Separation was carried out into the following particle size fractions: >16; 16-12; 12-8; 8-4 mm. Particles smaller than 1 mm are referred to as black mass. To recover the black mass adhering to the anode and cathode foils, the product fraction with high settling velocity was further comminuted using the same hammer crusher, equipped with a 6 mm sieve insert.

The qualitative analysis of battery cell cases and their identification were carried out using an FT/IR-4200 type A Fourier Transform Infrared Spectrometer (JASCO) equipped with a diamond ATR accessory. The spectra were obtained in a reflection mode.

The leached metals were analyzed using Varian Inc.'s 720-ES inductively coupled plasma (ICP) spectrometry. For the calibration of the device, a series of solutions was prepared from the certified multielement standard solutions, Certipur (distributed by Merck Ltd). and the Spectrascan (distributed by Teknolab).

2.2. Material

The experiments were carried out on an F.T. mild hybrid light commercial vehicle battery pack (**Figure 1**), from Auto Mandy Car Kft., Budapest (Hungary). The battery package weighed 16.02 kg and included the battery cells, inverter, battery management system (BMS), connection circuits, and cooling system. The pack also included safety fuses and protective housing to prevent overheating and ensure operational safety. These components illustrate the intricate design of modern hybrid battery systems, emphasizing the challenges involved in disassembling and processing these units.



Figure 1. Removed but intact F.T. battery pack

3. Results

3.1. Manual dismantling of the hybrid system

The system could be split into four main parts without causing any damage. The system consisted of four main components: the casing (Figure 1), the inverter (Figure 2a), the battery pack (Figure 2b), and the connecting structural elements, including screws, plugs, and sensors.

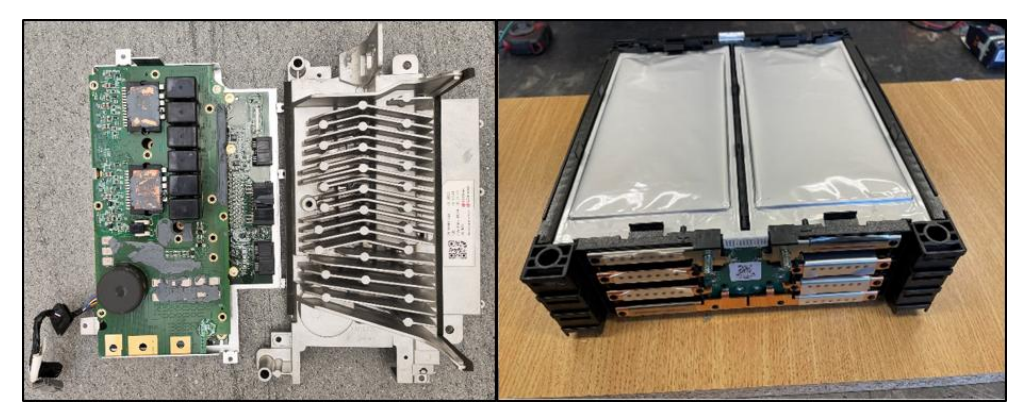


Figure 2. Central units of the hybrid system are a) the inverter and b) the battery pack.

The most significant part was the battery pack (40.60 wt%). The battery pack was treated separately and is, therefore, not included in the table. This is followed by the system case, which consists of an iron base plate (2.64 kg) to which the hybrid system is attached, and a plastic cover (2.06 kg) held together by screws, weighing a total of 4.70 kg. The air cooling fans and the aluminium-copper heat exchanger of the inverter are integrated into the plastic cover. Next to it is the inverter, which consists of a large aluminium heat exchanger, an AC/DC converter, and control electronics. During disassembly, the removed screws, cables, connectors, and sensors were collected; together, these weighed approximately 1.2 kg. The material balance after dismantling is shown in **Table 1**.

Table 1 Hybrid system units and their component materials (unit: wt%)							
	Units name (wt%)						
Material	System case	Inverter	Cooling system	Other parts			
	System case	IIIVCITCI	Cooling system	(screws, plugs, sensors)			
Plastic	39.06	5.00	63.46	4.10			
Iron	49.83	0.00	0.00	47.39			
Aluminum	6.44	46.29	23.27	1.46			
Glass	4.68	9.08	0.00	0.00			
PCB	0.00	38.41	0.00	0.00			
Rubber	0.00	0.00	3.24	7.23			
Copper	0.00	1.21	10.04	24.04			
Zinc	0.00	0.00	0.00	15.78			
Unit/Battery system	33.38	17.13	1.22	7.67			

Table 1 Hybrid system units and their component materials (unit: wt%)

3.2. Processing of the battery cells

During the research, both the mechanical processing of the battery cell and the manual disassembly of a cell were carried out. These processing steps aimed to obtain clear and detailed information about the structural composition of the cells, which cannot be achieved by mechanical methods alone. Manual dismantling enables the identification and quantification of the individual components (casing, anode, cathode, and separator foils, electrolyte, and active material layers), thereby providing a more accurate material balance of the battery cell.

3.2.1. Manual dismantling of the battery cell

The battery cell was manually disassembled in order to investigate its structural configuration as well as its quantitative and qualitative composition. In terms of construction, the battery is coated with a cellular composite casing, in which the anode, separator, and cathode foil are layered.

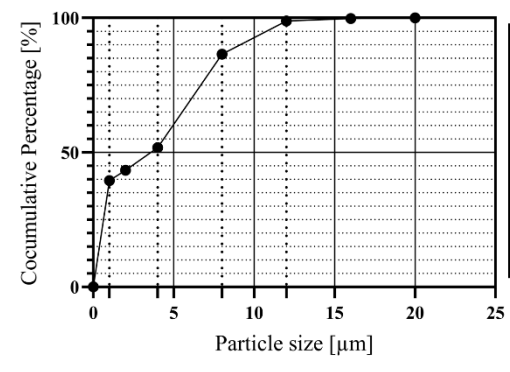
According to the FT-IR measurements, the cell coating is a composite material consisting of polyethylene terephthalate-aluminium-polypropylene, PET-Al-PP. The cell casing provides 16.19 wt% of the total mass, with an aluminum content of 19 wt% to 25 wt% based on volume concentration. The cathode foil consists of 28 aluminium plates, each 0.005 mm thick. It accounts for 2.51 wt% of the total cell mass. The anode foil consists of 29 copper plates, each 0.004 mm thick, making up 6.48 wt% of the cell. The separator foil between the anode and cathode plates provided 4.49 wt% of the total mass. Since the used technology could not separate the anode and cathode active materials, their mass fraction was determined to be one, which accounted for 54.1 wt% of the black mass.

During disassembly, the electrolyte content was determined by measuring the mass loss of the cells. The electrolyte content is 16.3 wt%, with a significant portion (10 wt%) removed shortly after the cell is opened. The composition of the gases released in this study was not examined. However, they may consist primarily of organic solvents such as ethyl methyl carbonate (EMC) and dimethyl carbonate (DMC), as well as CO₂ (Vetter et al., 2005; Aurbach et al., 2002).

3.2.2. Mechanical processing of the battery cell

Mechanical processing was carried out on electrically discharged batteries. The first stage of the process was to open the batteries and remove the electrolyte solvent with heat treatment. The 15.8 wt% electrolyte solvent left the cell, which is almost the same value as measured during manual dismantling. Since with this technology the electrolyte cannot be recovered, 100 wt% of the solid sample was used.

The particle size distribution and fractional composition of the battery cell after crushing in the hammer crusher are shown in **Figure 3**. According to the analysis, particles larger than 4 mm account for ~48 % of the sample's composition. Of these, 3/4 are metals with a partial black mass coating, and 1/3 is separator foil. The fraction between 1 and 4 mm was composed of anode and cathode foil particles that were almost completely free of separator foil, with a significant coating of black mass.



Material	4-8 [mm]	8-12 [mm]	12-16 [mm]
Composite case	3.43%	31.34%	40.43%
Cathode foil	26.52%	4.38%	23.40%
Anode foil	50.3%	3.60%	1.06%
Separator foil	19.78%	15.52%	35.11%
Weight ratio	34.69%	12.38%	0.94%

Figure 3. Crushed battery cell: particle size distribution a) and particle composition b)

The fraction below 1 mm, considered as a primary black mass, represented ~40 wt% of the sample. The composition of the extracted black mass, analyzed by ICP, is shown in **Table 2**. According to the analysis results, the processed battery is of the NMC type (**Winslow et al., 2018**). Upon analyzing the extracted black mass, it has been observed that it contains some amount of aluminum and copper foil fragments.

Table 2. Chemical composition of primary black mass

Chemical components	Ni	Mn	Cu	Ti	Al	Co	Fe	Li
wt%	17.3	3.49	3.95	0.98	0.91	4.53	0.07	3.39

3.2.3. Extraction of copper and aluminium

Valuable metals (aluminum and copper foil) with minor black mass coating were enriched in particle size fraction 4-16 mm. However, this fraction consisted of 70 % separator foil by volume. The separation of metal and plastic was carried out in an airflow separator, with particle size fractions of 12-16- and 8-12 mm. Results of the separation are shown in **Figure 3**. Based on the measurement results, the optimal airflow velocity is 2.68 m/s. At this velocity, the metal content loss is at its minimum; however, 95 wt% of the separator film will be transferred to the product, which has a low settling velocity.

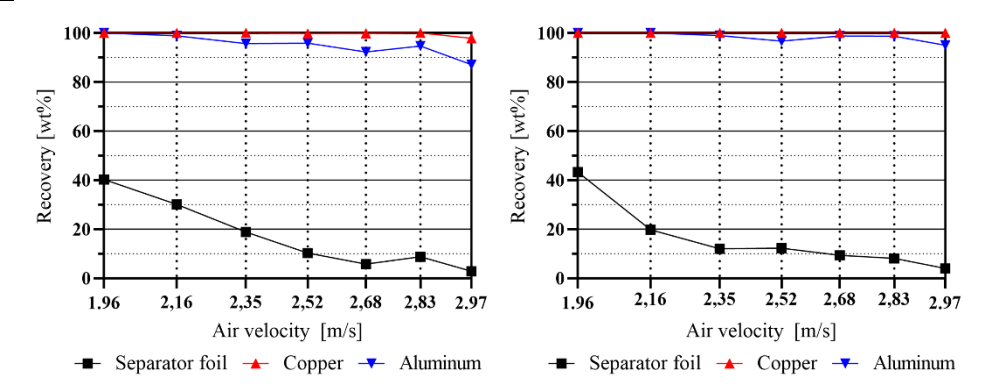


Figure 1. Material recovery in the high settling velocity products in the air separator by airspeed a) Particles between 4-8 mm; b) Particles between 8-12 mm

The residual black mass adhering as a coating on the surface of the 4–12 mm high-settling-velocity particles and the 4–1 mm size fraction was subjected to further mechanical treatment in order to enhance recovery. For this purpose, the previously used hammer shredder was equipped with a 6 mm sieve. The particle size distribution and composition of the resulting material are shown in **Figure 4**. Based on its composition, the crushed material could be divided into three different fractions: particles larger than 8 mm consisted of separator foil; the 1–8 mm fraction represented a heterogeneous mixture in which residual black mass coatings remained detectable on the anode and cathode surfaces; and the <1 mm fraction was considered as secondary black mass. Based on ICP measurements, this was heavily impurified with fine cathode (~43 wt%) and anode particles (~2 wt%).

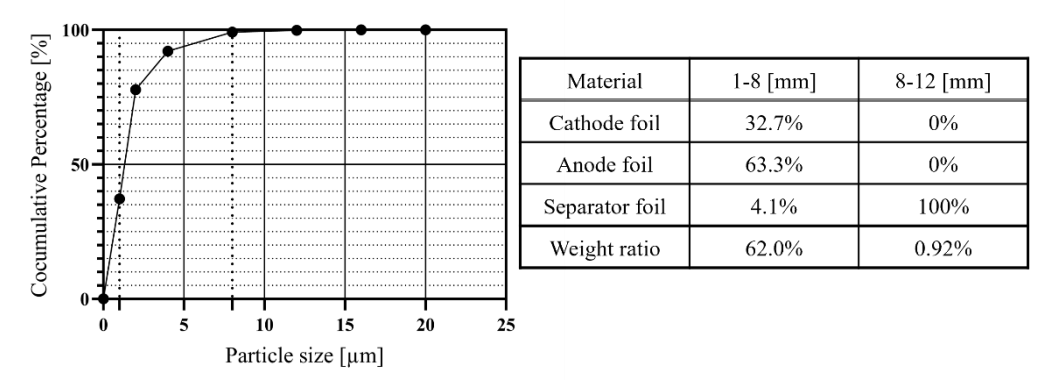


Figure 4: Crushed high-settling-velocity products: particle size distribution and particle composition

4. Discussion

The results of the present study demonstrate that the hammer shredder is an effective method for recovering black mass, while simultaneously enabling the retrieval of metallic fractions, primarily the anode and cathode foils. When operated with a 20 mm screen insert, the <1 mm fraction, considering the black mass, accounted for approximately 40 wt% of the total sample. This represents an improvement of ~10 wt% compared to slow-speed shredding mills (Werner et al., 2022; Wang et al., 2016) and ~5 wt% compared to high-speed shredding mills (Werner et al., 2022). The black mass contained approximately 5% metallic impurities (Cu, Al, and Fe), which is consistent with findings reported in other studies (Wilke et al., 2023). Among these, the elevated copper content poses potential challenges for hydrometallurgical processing (Pent et al., 2020), thereby necessitating additional purification steps. Nevertheless, the prepared material was shown to be suitable for bioleaching applications up to a solid concentration of 5 g/L (Mádainé et al., 2025).

Despite these advantages, mechanical pretreatment has limitations, as the secondary black mass fraction still contains residual anode- and cathode foil particles, reducing its suitability for further processing. Enhancing separation efficiency to achieve higher purity and yield of active material remains an essential focus for future research.

5. Conclusions

This study confirmed that the combined application of manual and mechanical disassembly represents a practical approach for recovering both black mass and structural components from lithium-ion battery cells. Manual disassembly provided a precise understanding of the internal architecture of the cells, offering essential reference data for subsequent processing steps. Mechanical pretreatment enabled the recovery of high-purity black mass suitable for further pyrometallurgical or hydrometallurgical treatment. The established material balance revealed that a substantial fraction of critical raw materials can be recovered during cell processing.

6. References

- Aurbach, D., Markovsky, B., Rodkin, A., Cojocaru, M., Levi, E., Hyeong-Jin, K. (2002): An analysis of rechargeable lithium-ion batteries after prolonged cycling. *Electrochimica Acta*, 47(12), 1899-1911. https://doi.org/10.1016/S0013-4686(02)00013-0
- Brückner, L., Frank, J., Elwert, T. (2020): Industrial Recycling of Lithium-Ion Batteries A Critical Review of Metallurgical Process Routes. *Metals*, 10(8), 1107. https://doi.org/10.3390/met10081107
- Colledani, M., Gentilinic, L., Mossalib, E., Picone, N. (2023): A novel mechanical pre-treatment process-chain for the recycling of Lilon batteries. *CIRP Annals*, 72(1), 17-20. https://doi.org/10.1016/j.cirp.2023.04.068
- Fan, E., Li, L., Wang, Z., Lin, J., Huang, Y., Yao, Y., Chen, R., Wu, F. (2020): Sustainable Recycling Technology for Li-Ion Batteries and Beyond: Challenges and Future Prospects. *Chemical Reviews*, 120(14), 7020-7063. https://doi.org/10.1021/acs.chemrev.9b00535
- Peng, C., Lahtinen, K., Medina, E., Kauranen, P., Karppinen, M., Kallio, T., Wilson, B.P., Lundström, M. (2020): Role of impurity copper in Li-ion battery recycling to LiCoO₂ cathode materials. Journal of Power Sources 450 227630. https://doi.org/10.1016/j.jpowsour.2019.227630
- Greenwood, D., Dowson, M., Unadkat, P., (2020). Automotive Lithium-ion Battery Recycling in the UK. Based on a feasibility study by Anwar Sattar. Canley, University of Warwick
- Heelan, J., Gratz, E., Zheng, Z., Wang, Q., Chen, M., Apelian, D., Wang, Y., (2016): Current and Prospective Li-Ion Battery Recycling and Recovery Processes. *The Journal of The Minerals*, 68, 2632-2638. https://doi.org/10.1007/s11837-016-1994-y
- Javorsky da Costa, A., Matos, J.F., Bernardes, A.M., Müller, I.L. (2015): Beneficiation of cobalt, copper and aluminum from wasted lithium-ion batteries by mechanical processing. *International Journal of Mineral Processing*, 145, 77-82. https://doi.org/10.1016/j.minpro.2015.06.015
- Kwade, A., Diekmann, J., (2018). Recycling of Lithium-Ion Batteries. Springer Cham
- Mádainé Üveges, V., Bokányi, L., Papp, R.Z., Szamosi, Z., Romenda, R.R., Nagy S., (2020). Valuable elements in waste electrical & electronic equipment (WEEE) and their possible recovery methods introduction. *Geosciences and engineering: a publication of the University of Miskolc*, 8(12), 71-83.
- Mádainé-Üveges, V., Butylina, S., Sethurajan, M., Nouaili, A., Spekker, D., Bokányi, L. (2025): Bioleaching of valuable metals from black mass originated from LFP and NMC Li-ion batteries. *Book of Extended Abstracts of the 18th European Symposium on Comminution & Classification : ESCC 2024*. 221-224. ISBN: 9786156018250
- Roy, J.J., Cao, B., Madhavi, S., (2021): A review on the recycling of spent lithium-ion batteries (LIBs) by the biobleaching approach. *Chemosphere*, 282, 130944. https://doi.org/10.1016/j.chemosphere.2021.130944
- Vetter, J., Novák, P., Wagner, M.R., Veit, C., Möller, K.C., Besenhard, J.O., Winter, M., Wohlfahrt-Mehrens, M., Vogler, C., Hammouche A., (2005): Ageing mechanisms in lithium-ion batteries. *Journal of Power Sources*, 147 (1-2), 269–281. https://doi.org/10.1016/j.jpowsour.2005.01.006
- Wanga, X., Gaustadb, G., Babbitt, C. W., (2016): Targeting high value metals in lithium-ion battery recycling via shredding and size-based separation. *Waste Management*, 51 204-2013. https://doi.org/10.1016/j.wasman.2015.10.026
- Werner, D. M., Mütze, T., Peuker, U. A., (2022): Influence of Pretreatment Strategy on the Crushing of Spent Lithium-Ion Batteries. *Metals*, 12(11) 1839. https://doi.org/10.3390/met12111839
- Winslow, K. M., Laux, S. J., Townsend, T. G. (2018): A review on the growing concern and potential management strategies of waste lithium-ion batteries. *Resources, Conservation and Recycling*, 129 263-277. https://doi.org/10.1016/j.resconrec.2017.11.001
- Wilke, C., Werner, D. M., Kaas, A., Peuker, U. A., (2023): Influence of the Crusher Settings and a Thermal Pre-Treatment on the Properties of the Fine Fraction (Black Mass) from Mechanical Lithium-Ion Battery Recycling. *Batteries* 9(10) 514. https://doi.org/10.3390/batteries9100514
- Wu, X., Ma, J., Wang, J., Zhang, X., Zhou, G., Liang, Z. (2022): Progress, Key Issues, and Future Prospects for Li-Ion Battery Recycling. Global Challenges, 6(12) 2200067. https://doi.org/10.1002/gch2.202200067

Acknowledgment and Funding

The authors would like to thank Tege Ficsór for his assistance with the dismantling, shredding, and preparation of the batteries, and Dr. Olivér Bánhidi for conducting the ICP analysis of the black mass. The research was funded by the Sustainable Development and Technologies National Programme of the Hungarian Academy of Sciences (FFT NP FTA). This project is funded by the European Union's Horizon Europe program under grant no. 101079354.

Author's contribution

Tamas Kurusta: conceptualization methodology, investigation, data curation, writing – original draft. Sándor Márton Nagy (associate professor): conceptualization, supervision, validation, visualization, writing – review & editing. All authors have read and agreed to the published version of the manuscript.



Investigation of Coal Reserve Recovery Indicators in Low-Capacity Mines Considering the Reprocessing of Mining Waste

DIM-ESEE Conference



Andrii Khorolskyi^{1*} [□]⊠, Oleksandr Mamaikin² [□]⊠, Iryna Lisovytska² [□]⊠, Ivan Sheka² [□]⊠, Svitlana Delehan³ [□]⊠

- ¹ Branch for Physics of Mining Processes of the M.S. Poliakov Institute of Geotechnical Mechanics the National Academy of Sciences of Ukraine, 15 Simferopolska St., 49005 Dnipro, Ukraine
- ² Dnipro University of Technology, 19 Yavornytskoho Ave., 49005 Dnipro, Ukraine
- ³Centre for Interdisciplinary Research of Uzhhorod National University, Uzhhorod National University, 88000 Uzhhorod, Ukraine

Abstract

The aim of this study was to investigate the production performance of low-capacity coal mines under different configurations of productive flows in the context of depleting industrial reserves, with specific attention to the feasibility of coal-mining waste processing. For the first time, operational indicators and exploitation parameters of low-capacity mines are examined in the broader framework of coal region transformation. The research scope covers low-capacity coal mines (up to 300 thousand tonnes/year) operating with mechanized extraction methods at depth. For the analysis, actual performance indicators of Ukrainian coal mining enterprises from 2008 to 2022 were used. The research could potentially be scaled to Eastern European countries with identical mining and geological conditions. The dataset includes mining-geological and technological parameters, as well as indicators of raw material quality measured by ash content. A central task was to assess the potential for waste processing and the recovery of associated minerals, which required substantiating the parameters for the completion of industrial reserves. These parameters are defined by the ratio of coal extraction volumes (as the main productive flow) to enrichment and coal-mining waste processing volumes (as additional productive flows), as well as by the quality of extracted coal. The study proposes a model for the efficient functioning of coal-mining enterprises under conditions of industrial reserve depletion. Using elasticity coefficients, simulations were conducted to explore the configuration of productive flows - coal, methane gas, rock, and water - under varying coal quality indicators.

Keywords: productive flow, waste utilization, Cobb–Douglas function, elasticity, heat map.

1. Introduction

The mining industry in Ukraine is undergoing transformational changes. Currently, there is a need not only to develop innovative approaches to optimize the parameters of rare earth metal deposit development but also to create conditions for the efficient extraction of industrial reserves. Coal mining in Ukraine exhibits specific characteristics that distinguish this sector from others. One of the primary challenges is the lack of effective reforms and development (or transformation) strategies for the industry. In the early 2000s, an attempt was made to modernize coal mining enterprises, resulting in a production increase of 15 % - 20 % (Bazaluk et al., 2022; Bondarenko et al., 2025). The article (Makarov et al. 2022) provides an analysis of the technical and economic performance of mines from 2004 to 2018, indicating that 57 % of enterprises could not achieve the minimum required loading level at the longwall. Active military operations in eastern Ukraine since 2014, followed by a full-scale military invasion, have accelerated trends of uncontrolled production capacity reduction. This has led to contradictory approaches ("recipes") proposed for the further development of the industry between 2014 and 2025 (Malashkevych et al., 2022; Petlovanyi et al., 2018; Boichenko, 2019). Additionally, there is an issue with the conceptual design approach. A coal mine is considered an enterprise focused on extracting a mineral resource-coal (Jeong et al., 2016; Calzada Olvera et al., 2023). If it is a mine, extraction occurs underground; if it is an open-pit, extraction is conducted open-cast methods. From an economic perspective, a mine is a single-profile enterprise. However, in reality, the end consumers of its products are the energy and metallurgical industries, and others (Matebese et al., 2024; Zhou et al., 2024). Even today, in 2025, vertically integrated companies exist that encompass a full cycle of mineral extraction and energy generation (Narkhede et al., 2023). Therefore, designing a mining operation for a specific type of mineral without assessing the feasibility of extracting associated minerals is economically unjustified (Rosa et al., 2024). We propose considering a mine as an enterprise whose efficiency is derived from primary and secondary productive flows (Lousada et al., 2024). For a coal mine, the primary flow is coal, while secondary flows include waste rock, methane gas, and water. Depending on the stage of the enterprise's lifecycle, the configuration of these productive flows varity. Finding a balance between these flows enables the achievement of maximum profitability.

At the design stage of mineral extraction (regardless of the mineral), certain assumptions are used that underlie evaluation models with either an economic or a physical meaning. An economic model was proposed by Harold Hotelling as early as 1931 (Hotelling, 1931) and has been further developed in contemporary studies (Henckens et al., 2016; Tilton, 2018). Hotelling conducted a series of studies on optimizing extraction parameters for non-renewable mineral resources. This made it possible to formulate the assumption that the final exploitation of mineral resources should correspond to the final demand for these resources and be equal to the initial stock. His assumptions were based on the hypothesis of a uniform spatial distribution of minerals, as well as on the idea that extraction costs increase with mining depth. All of this can be summarized by the general logic that "over time, technologies will make it possible to reduce the cost of mineral extraction, which will allow the development of deposits under more complex geological conditions and with lower quality." The Hotelling model does not account for exponential demand for minerals, which cannot be offset by technological progress as a response to the depletion of mineral deposits, and it also lacks a clear definition of the timing of transitions between states.

The model of Marion Hubbert, developed in 1956 and further elaborated in subsequent works (Scholz et al., 2013; Calvo et al., 2017), represents another class of models based on physical principles. The main idea is that the scale of mineral extraction depends on the size of reserves and the rate at which the mineral can be recovered. This model is predictive and therefore relies on two constraints: reserves and extraction are fixed. The reliability of the model depends on the information available; therefore, the Hubbert model is purely physical and can be used at the re-design assessment stage.

Currently, hybrid models are being developed. In the study (**Zhu et al, 2021**) was proposed to estimate the volumes of mineral extraction based on the marginal impact of extraction technology, which can be calculated using the Cobb—Douglas function and the coefficient of price elasticity of reserves. The research is grounded in the assessment of the availability of 13 types of strategic mineral resources in the People's Republic of China. As a result, four clusters of minerals were identified, and the hypothesis was confirmed that, over time, the availability potential of gold and tin will increase, while traditional minerals will be extracted to a lesser extent.

On the basis of this analysis, a relevant scientific task emerges: the rationalization of parameters for the completion of industrial reserves in coal-mining enterprises. For this purpose, it is necessary to determine the volumes of extraction of the primary mineral resource, as well as the feasibility of utilizing the potential of associated productive flows—methane gas, rock, and water.

The objective of this study is to investigate the production indicators of low-capacity underground coal mines under various configurations of productive streams during the final extraction of industrial reserves, with consideration of the feasibility of coal mining waste reprocessing. This work presents a novel approach by analyzing performance parameters of low-capacity coal mines (up to 300,000 tonnes per year) operating with mechanized technologies at depth, within the context of coal region transformation. The study covers mines in Ukraine and selected Eastern European countries (Czech Republic and Poland), where similar transitions of the coal sector are taking place. The analysis is based on empirical data from 2008 to 2022, including operations in Donetsk, Luhansk, Dnipropetrovsk, and Lviv regions. The dataset includes mining-geological and technological indicators, as well as information on raw material quality measured by ash content. The research also aims to assess the potential for waste reprocessing and extraction of associated mineral resources by justifying parameters for the depletion of industrial reserves, which are determined by the ratio of coal extraction (as the main productive flow), coal enrichment and waste reprocessing (as auxiliary streams), and the quality characteristics of extracted coal.

2. Methods

Before outlining the general statements of the mathematical model, a description of the research area should be given. The scope of research is coal-mining enterprises of Ukraine, Eastern Europe countries (Republic of Poland, Czech Republic, Republic of Slovakia), as well as those countries where coal is mined underground. The considered mines are characterized by the presence of a total or partial set of productive flows, that is, there is the probability of adverse hydrogeological conditions, the presence of rock interlayers, and the presence of methane gas accumulations. Different sets of parameters or only a few may be taken into account.

The proposed model should comply with the following requirements:

- 1) The level of profit as the main criterion. This is not surprising that the activities and feasibility of the enterprise's existence depend on economic factors.
- 2) The model should be "elastic". The term "elasticity" refers to the consideration of the influence of all productive flows on the level of the optimality criterion. Elasticity can be positive and negative. Positive elasticity means an unambiguous increase in the level of profit from an increase in flow volume, while negative elasticity means the presence of a restrictions on the level of productive flow, that is, an increase in volume is reasonable according to a certain limit. With zero elasticity, the productive flow has no influence on overall economic efficiency. "Zero" elasticity is common in mining operations, since the water inrush is conditionally constant and, regardless of the stage of the enterprise's development, there is a need for pumping out water. Even after the mine is closed, the water must be pumped out. The productive flow "water" in this case doesn't serve as a resource, as it does not enhance the target outcome. Unlike other flows (mining, processing, gas, etc.), which have positive or negative elasticities and shape profit distribution, water is more of a byproduct or external factor rather than an economic resource. From a management perspective, this means

that the costs of pumping or disposing of water should be treated as constraints or additional expenses, not as a source of profitability. The volume of water does not affect the overall efficiency of the enterprise, as its pumping is necessary regardless of the stage of mining operations. However, it should be noted that, with the implementation of demineralization technologies, water could become a valuable resource and a productive flow with positive elasticity. Thus, the zero elasticity is explained by the fact that, in the current production situation, water is not yet a source of additional profit.

- 3) The mutual influence of flows should be taken into account. This was noted in the introduction.
- 4) Alternative scenarios need to be analyzed, namely: a) all productive flows are available; b) there is no main productive flow; c) one of the auxiliary productive flows is missing; d) different productive flow levels. The "main" productive flow refers to coal, since mining is now underway. "Auxiliary" refers to alternative productive flows: rock, methane gas, water.
- 5) The model should take into account the diversity of production levels and the potential for increasing the volumes of auxiliary productive flows.

The Cobb-Douglas model is used to develop the model. This model takes into account the total profit level depending on the number of productive flows and their elasticity. In general terms, the Cobb-Douglas model can be described by the formula:

$$P = A \times C^{\alpha} \times M^{\beta} \times R^{\gamma} \times W^{\delta}, \tag{1}$$

Where are:

P – is the profit level, monetary units;

A – is the dimensionless scale factor;

 α , β , γ , δ , - elasticity of the respective flows C - coal, M - methane, R - rock, W - water.

Formula (1) for the profit maximization case can be written as follows:

$$\log(P) = \log A + \alpha \log(C) + \beta \log(M) + \gamma \log(R) + \delta \log(W). \tag{2}$$

Based on Equation (1) and Equation (2), an algorithm for studying production diversification scenarios can be determined:

- 1) First, it is necessary to use logarithmization to represent the function (1) in the form of a linear formula. In the general definition, the Cobb-Douglas function is piecewise linear, but in most cases, logarithmization yields a linear function, which greatly simplifies the analysis.
 - 2) Based on regression analysis, determine the elasticity coefficients.
- 3) Based on the coefficients, the maximum value of profit P can be calculated for different configurations of productive flows.

We have preliminarily determined the elasticity of productive flows. "Elasticity" is understood as the increment of the dependent variable resulting from a percentage increase in the independent variable. In other words, it reflects how the efficiency of the enterprise (in our case evaluated by profit) will change depending on variations in the configuration of the productive flow N. In the ideal approximation, the model is considered valid if the sum of elasticity coefficients equals one, P = 1.00. Our analysis produced elasticity values and confirmed the adequacy of the developed model. It was established that coal has negative elasticity, i.e., p(N) < 0, methane and rock have positive elasticity, i.e., p(N) > 0, while water is neutral, i.e., p(N) = 0. The physical interpretation is as follows: if elasticity is negative, it directly impacts the level of total profit—in other words, this is the primary productive flow. This is expected, since coal extraction volumes affect the quantities of both rock and methane gas. If elasticity is positive, it does not directly determine total profit but can enhance it—in other words, the productive flow acts as an additional resource. At zero elasticity, the productive flow does not affect overall efficiency. In our case, this is water; regardless of coal extraction volumes or the amount of processed rock, water pumping remains necessary. Information on elasticity was validated using the Analytic Hierarchy Process (Ait-Mlouk et al., 2019; Liao et al., 2023).

The next step is to proceed to modeling.

3. Results

At the first stage of the study, using software developed by one of the authors of this article, modeling of various production situations corresponding to different configurations of productive flows was performed. The program is designed to determine the ratio between productive flows as fractions of the total flow (i.e., from 0.00 to 1.00 for each flow). The physical meaning is as follows: if the share of a productive flow equals 0.00, it is absent in the overall balance; if the share equals 1.00, then the enterprise's profit is generated by a single productive flow. For example, with coal ash content A = 10 % and an annual extraction volume S = 300 thousand t/year, the share of coal amounts to 0.57, rock 0.38, and water 0.05. That is, under the initial modeling conditions of extraction, rock processing, and water treatment, coal provides 57 % of the enterprise's total profit, rock 38 %, and so forth. The program searches for balance among productive flows with a step of annual coal extraction of 50 thousand t/year. Figure 1 shows the ratio between productive flows for four production scenarios.

d)

ash, %	coal	rock	methane	water	ash, %	coal	rock	methane	water
50	0.22	0.74	0.00	0.04	50	0.22	0.70	0.02	0.06
40	0.27	0.69	0.00	0.04	40	0.26	0.64	0.02	0.08
30	0.32	0.64	0.00	0.04	30	0.32	0.59	0.02	0.07
20	0.41	0.55	0.00	0.04	20	0.39	0.52	0.03	0.06
10	0.57	0.38	0.00	0.05	10	0.54	0.34	0.05	0.07

ash, %	coal	rock	methane	water	ash, %	coal	rock	methane	water
50	0.20	0.76	0.02	0.02	50	0.82	0.00	0.08	0.10
40	0.26	0.68	0.02	0.04	40	0.83	0.00	0.07	0.10
30	0.32	0.60	0.03	0.05	30	0.83	0.00	0.06	0.11
20	0.39	0.52	0.04	0.05	20	0.83	0.00	0.06	0.11
10	0.54	0.32	0.06	0.08	10	0.86	0.00	0.05	0.09

a)

Figure 1. Ratio between productive flows under different production situations: (a) the mine is safe in terms of the gas factor, and the utilization of coal mining waste is feasible; (b) the mine is hazardous in terms of the gas factor, waste processing is feasible, and the mine is equipped with technologies for methane extraction from the underground space; (c) the mine is hazardous in terms of the gas factor, and the processing of mining waste is feasible; (d) the mine is safe in terms of the gas factor, technologies for methane extraction are available, but the utilization of waste is not feasible.

c)

As shown in **Figure 1**, various operational situations exist. We have considered 4 possible scenarios for the development of events. For conditions in Ukraine, mine methane is a significant limiting factor. The productivity of a mine depends on the concentration of methane in underground spaces. Therefore, for mines at risk of sudden methane outbursts or those with significant methane volumes in underground spaces, measures for methane extraction are mandatory. Additionally, the possibility of utilizing methane as an additional source of revenue was considered.

Based on the results of modeling the distribution of productive flows, four groups (clusters) of coal-mining enterprises were identified. The first cluster includes enterprises with a full set of productive flows and low coal ash content. For them, it is advisable to increase production scales and enhance efficiency. The second cluster – the largest in number—consists of mines where one of the flows is practically unused (most often methane). The strategy depends on ash content: at low levels, the focus should be on coal; at high levels, on waste rock processing. The third cluster reflects enterprises with limited growth potential. The main directions are either coal extraction or increasing waste rock processing volumes. The fourth cluster is characterized by the absence of feasibility in waste rock processing; the only development option is cost optimization and improvement of coal quality. Thus, the correct classification of mines according to the configuration of productive flows enables the application of targeted management decisions and reduces the risks of crisis phenomena in the sector. It has been established that in the process of completing industrial reserves, coal ash content plays a decisive role. The study focuses on enterprises that process their industrial reserves and may subsequently diversify their activities. We examined the issue of supporting enterprise operations from the perspective of engaging additional productive flows - rock, gas, and water. This approach enables maintaining a minimally required level of profitability, even under conditions of reduced coal production. In other words, the study of productive flow configurations helps determine the optimal volumes of mineral extraction and waste enrichment from coal mining, as well as assess the feasibility of utilizing other resources.

4. Discussion

It was necessary to carry out verification of the approach. As can be seen from **Figure 1**, the decisive factor is coal quality, expressed by ash content. It was established that when coal ash content A < 20%, the optimal strategy is to increase coal extraction.

As the research object, the performance indicators of the "Pavlogradska" mine (Ukraine) are analyzed. **Table 1** contains data on the ash content of coal seams. This allows the modeling of different production situations.

We've developed specialized software for analyzing industrial reserve development scenarios. Figure 2 illustrates a graph showing the search for the optimal configuration of production flows based on ash and coal production. For each scenario, the program generates 3D surfaces and creates profit heatmaps depending on coal ash and coal production.

Table 1. Information on the ash content of coal seams o	f the "Pavlogradska" mine of the State Holding Company
"Payloo	radugol"

			1 aviogradagoi		
Coal Seam	Coal Grade	Coal ash A _d , %		Mass fraction of	Coal washability by ash and
Symbol		range (min-max)		total sulfur S _{dt} ,	sulfur
		average		%,	
		coar seam groups	coal and rock	range (min-max)	
			interlayers	average	
C^{B}_{10}	G_6	2 - 18	2 – 29	0.7 - 4.2	easy washability
		8	9	2,1	
C^{B}_{8}	G_6	2-18	2 - 28	0.6 - 3.2	easy washability
		8	8	1,5	
C^{H_8}	G_6	2 - 18	2 - 25	0,6-3,0	easy washability
		7	10	1,3	
C^{H} 7	G_6	2 - 20	2 - 30	0.6 - 4.8	easy washability
		8	11	1,7	
C ₆	G ₁₁	2 - 20	2 - 29	0,3-3,9	easy washability
		$\frac{2-20}{9}$	10	1,9	
	_				
C_5	G ₁₁	$\frac{2-20}{-}$	$\frac{2-30}{1.0}$	0.4 - 3.1	easy washability
		7	10	1,4	
C^{B}_{4}	G_{11}	2 - 16	2 - 30	0.4 - 3.4	easy washability
		9	11	1,5	
C ₁	G ₁₁	2 - 19	2 - 30	0,4-3,7	easy washability
		10	15	1,2	

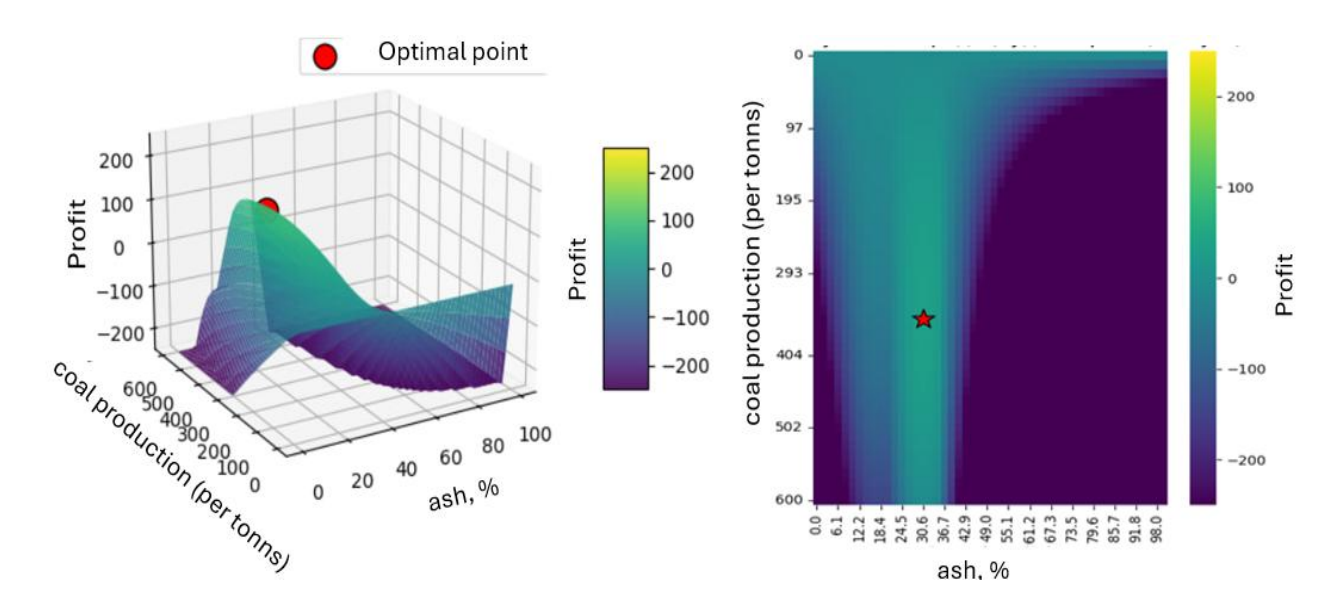


Figure 2. Graph for determining the optimal configuration of production flows and profit heatmap showing dependence on coal production and ash

The obtained results indicate that for the "Pavlohradska" mine, the optimal strategy is to scale up the volumes of waste beneficiation. This approach will allow achieving maximum profit as well as diversifying activities.

5. Conclusions

In the course of the research, a novel approach was developed for modeling the production performance of coal mining enterprises operating under conditions of industrial reserve depletion, with consideration of coal mining waste reprocessing. Four production scenarios were simulated, each representing a distinct operational context—ranging from conventional coal extraction with the absence of certain productive flows to scenarios lacking coal production entirely. It was established that as coal quality improves, its share in the overall production balance increases regardless of the operational scenario. When the ash content of coal is below 20 %, it is advisable to prioritize increased coal extraction, while the relevance of mining waste reprocessing declines, and wastewater treatment becomes economically unjustifiable. The study confirmed that under conditions of low ash content, coal remains the primary productive flow irrespective of extraction volumes. Furthermore, methane recovery from underground spaces in low-capacity coal mines appears economically unviable across all assessed ash content; levels. As a result, the configurations of productive flows were defined for various industrial scenarios.

The scientific novelty of the study lies in the development of a new approach for justifying the parameters of reserve depletion in low-capacity coal mining enterprises within the context of coal region transformation. Based on modeling, four types of low-capacity coal mines were identified according to the configuration of productive flows. For the first time, cluster boundaries were defined and accompanied by a corresponding technological description. Classifying an enterprise into a specific cluster enables the formulation of an appropriate operational strategy and the application of optimization and production management methods aimed at enhancing efficiency and rationalizing the parameters of coal deposit exploitation.

The practical significance of the study lies in the verification of an approach based on the application of the Cobb-Douglas function to identify optimal configurations of productive flows. Using the Analytic Hierarchy Process (AHP), the hypothesis regarding the elasticity of productive flows was confirmed. A decision support system in the form of dedicated software was developed to model performance indicators of low-capacity coal mines.

The presented study expands the frontier of research on the operational dynamics of coal mining enterprises in the context of post-mining and sustainable resource extraction management. The obtained results can be applied in the development of transformation strategies for coal-intensive regions.

6. References

Ait-Mlouk, A., & Agouti, T. (2019). DM-MCDA: A web-based platform for data mining and multiple criteria decision analysis: A case study on road accident. *SoftwareX*, 10, 100323. https://doi.org/10.1016/j.softx.2019.100323

Bazaluk, O., Ashcheulova, O., Mamaikin, O., Khorolskyi, A., Lozynskyi, V., & Saik, P. (2022). Innovative Activities in the Sphere of Mining Process Management. *Frontiers in Environmental Science*, 10. https://doi.org/10.3389/fenvs.2022.878977

Boichenko, M. (2019). Potential Ways of Innovative Development of Coal Mining Enterprises. *Herald of the Economic Sciences of Ukraine*, (2(37)), 78–81. https://doi.org/10.37405/1729-7206.2019.2(37).78-81

Bondarenko, V., Salieiev, I., Kovalevska, I., Chervatiuk, V., Malashkevych, D., Shyshov, M., & Chernyak, V. (2023). A new concept for complex mining of mineral raw material resources from DTEK coal mines based on sustainable development and ESG strategy. *Mining of Mineral Deposits*, 17(1), 1–16. https://doi.org/10.33271/mining17.01.001

Calvo, G., Valero, A., & Valero, A. (2017). Assessing maximum production peak and resource availability of non-fuel mineral resources: Analyzing the influence of extractable global resources. *Resources, Conservation and Recycling*, 125, 208-217. https://doi.org/10.1016/j.resconrec.2017.06.009

Calzada Olvera, B., & Iizuka, M. (2023). The mining sector: profit-seeking strategies, innovation patterns, and commodity prices. *Industrial and Corporate Change*. https://doi.org/10.1093/icc/dtad020

Henckens, M. L., van Ierland, E. C., Driessen, P. P., & Worrell, E. (2016). Mineral resources: Geological scarcity, market price trends, and future generations. *Resources Policy*, 49, 102-111. https://doi.org/10.1016/j.resourpol.2016.04.012

Hotelling, H. (1931). The economics of exhaustible resources. *Journal of political Economy*, 39(2), 137-175. https://doi.org/10.1086/254195

Jeong, A., Kim, S., Kim, M., & Jung, K. (2016). Development of Optimization Model for River Dredging Management Using MCDA. *Procedia Engineering*, 154, 369–373. https://doi.org/10.1016/j.proeng.2016.07.494

Liao, Y., Wang, T., Ren, Z., Wang, D., Sun, W., Sun, P., Li, J., & Zou, X. (2023). Multi-well combined solution mining for salt cavern energy storages and its displacement optimization. *Energy*, 129792. https://doi.org/10.1016/j.energy.2023.129792

Lousada, S., Delehan, S., & Khorolskyi, A. (2024). Application of Dynamic Programming Models for Improvement of Technological Approaches to Combat Negative Water Leakage in the Underground Space. *Water*, *16*(14), 1952. https://doi.org/10.3390/w16141952

Makarov, V. M., & Perov, M. O. (2022). Scenarios for the development of the coal industry with projected changes in the structure of the use of coal products in the country economy. *The Problems of General Energy*, 2), 2022(170–81. https://doi.org/10.15407/pge2022.01-02.070

Malashkevych, D., Petlovanyi, M., Sai, K., & Zubko, S. (2022). Research into the coal quality with a new selective mining technology of the waste rock accumulation in the mined-out area. *Mining of Mineral Deposits*, *16*(4), 103–114. https://doi.org/10.33271/mining16.04.103

Matebese, F., Mosai, A. K., Tutu, H., & Tshentu, Z. R. (2024). Mining wastewater treatment technologies and resource recovery techniques: A review. *Heliyon*, 10(3), Stattia e24730. https://doi.org/10.1016/j.heliyon.2024.e24730

Narkhede, G., Mahajan, S., Narkhede, R., & Chaudhari, T. (2023). Significance of Industry 4.0 technologies in major work functions of manufacturing for sustainable development of small and medium-sized enterprises. *Business Strategy & Development*. https://doi.org/10.1002/bsd2.325

Petlovanyi, M. V., Lozynskyi, V. H., Saik, P. B., & Sai, K. S. (2018). Modern experience of low-coal seams underground mining in Ukraine. *International Journal of Mining Science and Technology*, 28(6), 917–923. https://doi.org/10.1016/j.ijmst.2018.05.014

Rosa, A. G. F., Silva, W. D. O., Fontana, M. E., Levino, N., & Guarnieri, P. (2024). A GIS-based multi-criteria approach for identifying areas vulnerable to subsidence in the world's largest ongoing urban socio-environmental mining disaster. *The Extractive Industries and Society*, 19, 101500. https://doi.org/10.1016/j.exis.2024.101500

Scholz, R. W., & Wellmer, F. W. (2013). Approaching a dynamic view on the availability of mineral resources: what we may learn from the case of phosphorus? *Global Environmental Change*, 23(1), 11-27. https://doi.org/10.1016/j.gloenvcha.2012.10.013

Tilton, J. E. (2018). The Hubbert peak model and assessing the threat of mineral depletion. *Resources, Conservation and Recycling*, 139, 280-286. https://doi.org/10.1016/j.resconrec.2018.08.026

Zhou, G., Liu, Y., Liu, Z., Zhang, Y., Zhu, Y., Sun, B., & Ma, Y. (2024). Study on the characteristics of compound dust source pollution and foam dust suppression technology in coal mine anchor excavation production. *Process Safety and Environmental Protection*. https://doi.org/10.1016/j.psep.2024.03.119

Zhu, Y., Xu, D., Ali, S. H., & Cheng, J. (2021). A hybrid assessment model for mineral resource availability potentials. *Resources Policy*, 74, 102283. https://doi.org/10.1016/j.resourpol.2021.102283

Author's contribution

Andrii Khorolskyi (associate professor): scientific supervision, methodology design. Oleksandr Mamaikin (associate professor): critical review, funding acquisition, English language support. Iryna Lisovytska (associate professor): data curation & preprocessing. Ivan Sheka: (associate professor): model development and testing, formal analysis, validating results. Svitlana Delehan: (associate professor): conceptualization, supervising the scientific and technical aspects, English language support.

All authors have read and agreed to the published version of the abstract.



Development of Waste Risk Management Processes in the Mining Industry

DIM-ESEE Conference 15th – 17th October 2025, Dubrovnik, Croatia



Vitaliy Tsopa¹ [©]⊠, Olena Yavorska² [©]⊠, Serhii Cheberiachko² [©]⊠, Oleksandr Kovrov² [©]⊠, Yuliya Pazynich², ³ [©]⊠, Lidia Cheberiachko² [©]⊠

- ¹ International Institute of Management, 10/12B Shulyavska Str., 04116 Kyiv, Ukraine
- ² Dnipro University of Technology, 19 D. Yavornytskyi Ave., 49005 Dnipro, Ukraine
- ³ AGH University of Krakow, Al. Mickiewicza 30, 30059, Krakow, Poland

Abstract

The relevance of the work is related to the search for ways to reduce waste generation in organizations. It is proposed to consider a waste generation risk management process using a systemic approach to analyze it as a single, holistic system. The basis is taken from the study of the relationships between the generation of liquid, solid, and gaseous waste and greenhouse gas emissions that arise from hazardous events (production of low-quality products, incidents, accidents, etc.) in all organizational management systems. The proposed waste risk management process differs from the known ones in that it needs to identify hazardous events in various management systems related to product and service quality, environmental safety, health and safety of workers, energy consumption, etc. The waste risk management process consists of twelve steps, among which the main ones are: identification of hazards, hazardous factors, dangerous events, etc.; assessing the risks of waste generation from each hazardous event separately, determining the risk of waste generation of the organization as a whole across all management systems, developing preventive and protective measures to reduce the risks of waste generation, documenting these risks, conducting audits and periodic reviews of waste generation risk maps and the waste generation risk management process itself.

Keywords: waste, risk management, hazardous factors, dangerous events, occupational safety

1. Introduction

Management systems in organizations that cover environmental, health, safety and energy efficiency issues, especially in mining and mineral processing, operate in the presence of potential hazards. These hazards can lead to accidents or hazardous events, which are usually accompanied by the generation of industrial waste and emissions into the environment.

Hazardous events, such as incidents and accidents that occur during the mining processes and further mineral processing, lead to losses of thermal and electrical energy due to various emergency situations, which are significant problems that cause human and material losses. These hazardous events become sources of environmental pollution through the accumulation of solid waste, discharges of harmful liquids, emissions of pollution into the air, and emissions of greenhouse gases. (Pan et al., 2025). In the organization's management systems, these events are considered manmade and environmental risks that require control and management to ensure ecological safety at mining enterprises. To reduce the generation of waste and emissions, there is a need to identify all hazardous events that can lead to the formation of liquid, solid, and gaseous waste and greenhouse gas emissions into the atmosphere (Shvetsova et al., 2020). For this purpose, it is important to develop a new process for managing waste risks (the abbreviation waste risk should be understood as all existing waste and greenhouse gas emissions generated during the organization's activities) (Polyanska et al., 2024).

Currently, organizations are building an environmental management system based on the requirements of the ISO 14001:2015 standard and the Waste Framework Directive (WFD) 2008/98/EC, which provides for a five-step waste management hierarchy (Cerar et al., 2022). The main goal of such a system is to prevent or limit emissions of solid or liquid waste into air, water and soil, as well as greenhouse gases (Grobelak et al., 2024). At the same time, the built environmental management systems, although they include the environmental risk management process, are mostly reactive, since they are focused mainly on consistent adherence to the hierarchy of preventing their formation (Sobolev et al., 2025). Therefore, to eliminate this drawback, it is necessary to focus on eliminating the idea of "waste reduction" as the final result of production. Existing ways to solve the problem are to design products that are easily recyclable or capable of undergoing several use cycles (Josimović et al., 2022). However, there is a need to find the best solution from the existing proposals for reducing waste generation at enterprises involved in coal mining and its further benefication.

V. Tsopa, O. Yavorska, S. Cheberiachko, O. Kovrov, Yu. Pazynich, L. Cheberiachko

To do this, it is necessary to develop a new waste risk management process that will allow to achieve synergy between all systems.

An analysis of recent publications reveals a strong interest in developing effective waste management systems, particularly within mining companies that generate millions of tons of waste rock, tailings, and sludge (Pavlychenko et al., 2025). The investigation of modern technologies for reprocessing mining tailings (copper, silver, gold, tungsten, etc.) to extract critical metals integrate the circular economy principles into waste management reducing environmental risks, increasing resource efficiency, and promoting decarbonization and sustainable development (Kursunoglu, 2025). Based on the principles of the circular economy, production waste was converted into additional opportunities through additional processing of beet pulp to obtain raw materials for energy production. Studies on waste management emphasize the potential of integrated systems to generate social, environmental, and economic benefits when properly implemented (Shvetsova et al., 2020). Research also highlights persistent shortcomings, such as the mixing of hazardous and municipal waste, inadequate storage conditions, and outdated collection and transport systems, which necessitate comprehensive policy and management reforms (Oleniacz et al., 2025). The utilization of waste through thermochemical destruction is increasingly considered a promising approach, offering the potential to reduce volumes of difficult-to-recycle materials while recovering energy (Tabachenko et al., 2016). To address these issues, scholars propose strategic planning, improved segregation and recycling, enhanced financing, and the adoption of circular economy principles, including investment project management, restructuring of production and consumption, and the application of environmental technologies such as wastewater treatment and food waste utilization (Bonifazi et al., 2025; Ovander et al., 2017; Kovrov et al., 2025a; Kovrov et al., 2025b).

This article aims to develop a structured methodology for managing risks related to waste generation and greenhouse gas emissions across multiple organizational management systems. The analysis encompasses quality assurance, environmental management, occupational health and safety, and energy efficiency, reflecting the interconnected nature of these domains. By establishing an integrated risk management framework, the study contributes to advancing sustainability objectives while simultaneously improving the resilience and performance of organizations.

2. Methods

Each area of management (quality, energy conservation and occupational safety) of the organization is characterized by the presence of hazards, threats or non-conformities that can lead to the occurrence of dangerous events, which can be presented as negative environmental aspects in terms of increased emissions into the atmosphere, soil or water, as well as an increase in solid waste. The presence of negative environmental aspects leads to the need to develop a waste risk management process, which is convenient to build on the basis of the requirements of ISO 14001:2015, since in this case it can be integrated into the overall management system of the organization. At the same time, the solution to the task of developing a waste risk management process will be based on the High-Level Structure (HLS), which is defined in Annex SL of the ISO/IEC directives.

A systemic approach was applied to achieve the goal, which allows consideration of the waste risk management process not as a set of isolated actions but as a holistic system based on the study of the relationships between all management system elements. In this case, a comprehensive analysis of the requirements of international standards ISO 9001:2015; ISO 14001:2015; ISO 45001:2018; ISO 50001:2018 (Table 1), operational excellence methodologies and practices of leading organizations were used, which allowed us to formulate proposals for disassembling the waste risk management process in various management systems. A process approach was also applied based on the requirements of the standards: ISO 31000:2018 (Principles and framework), IEC 31010:2019 (Risk assessment methods) and ISO 31073:2022 (Terms and definitions) (Cerar et al., 2022), which transform the waste risk management process from discrete actions into a holistic, transparent and manageable process of achieving acceptable waste risks in management systems To increase the effectiveness of various management systems through early detection of non-conformities, the requirements of the international standard ISO 19011:2018 were taken into account for conducting internal audits. This made it possible to identify individual inconsistencies and systemic shortcomings in the interaction between various components of the organization's management systems (Standards E. BS EN 61882:2016). For the waste risk management process, it is proposed to use the "Bow-Tie" method, which allows identifying hazards and dangerous events in each organization's management system with subsequent analysis of the production process to find opportunities to reduce the risk of waste generation.

For an example of waste risk assessment, we will consider the risk of quality loss due to a violation of the mining technology, which will lead to a significant content of carbonaceous rock in the mined coal (we assume that 60% ash content is recorded per ton of coal, while up to 40 % sludge is formed during its enrichment, and up to 0.0205 t of CO2 emissions are formed during combustion, and up to 600 kg of gaseous harmful substances are formed, which are emitted into the air). The specified risk of quality loss can also manifest due to geotechnological violations, technical inconsistency, and differences in mining pressure. The ISO 17246:2010 standard "Coal. Technical analysis" is used to determine the acceptance criterion. To calculate the risk of waste generation, we will assume that the mine produces 1.2 million tons of coal annually. Violating coal mining technology is a complex threat that requires systematic risk management, quality control, environmental monitoring, and compliance with energy consumption standards.

3. Results

The **Figure 1** shows the developed process for managing waste generation risks in an organization. It involves, in the first step, identifying hazards, hazardous events, and consequences associated with waste generation and greenhouse gas emissions.

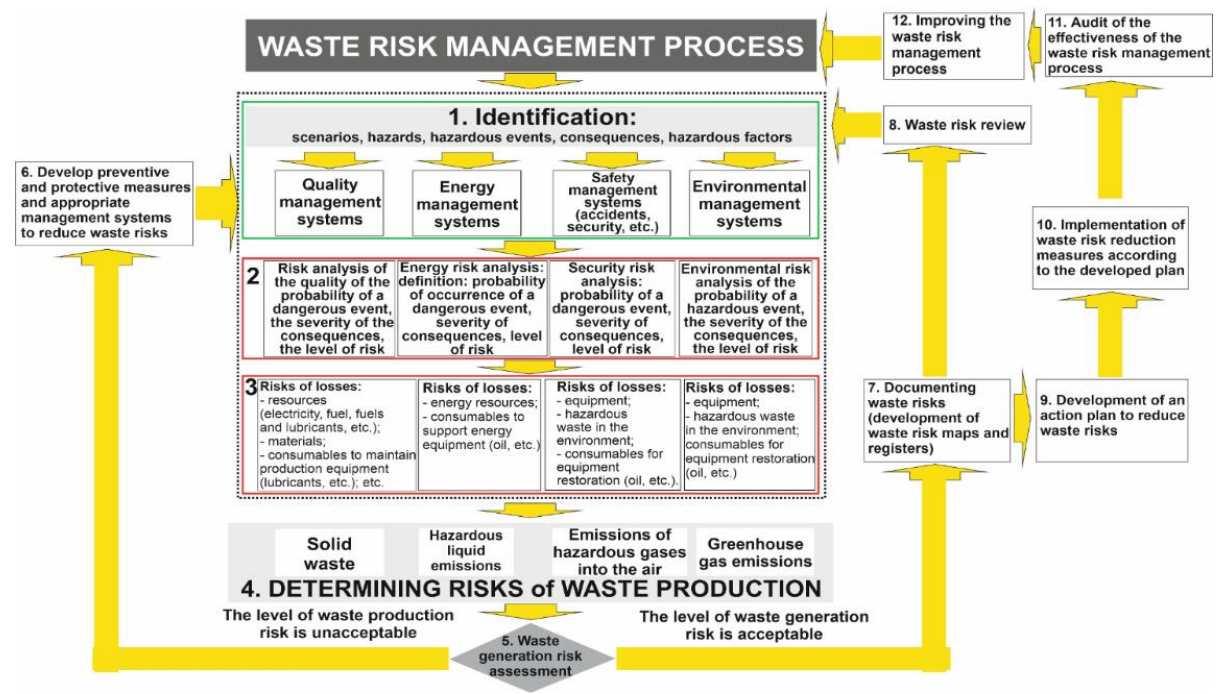


Figure 1. Waste risk management process

The second step involves assessing waste generation risks in each management system: quality, environmental management, occupational health and safety, and energy management. Then, in the third step, we determine the levels of waste and greenhouse gas emissions risks in each management system for each type of waste. In the fourth step, we determine the levels of waste generation risks of each kind of waste within the entire organization. In the fifth step, it is proposed to assess the risk of waste generation. If the risk of waste generation is unacceptable, then after documenting the current risk level in the seventh step (which is presented in **Table 1**), we proceed to the ninth step. In which we develop a plan of measures to reduce the risk of waste generation, that is, we determine the feasibility of applying specific preventive and protective measures to reduce the risks of waste generation to an acceptable level, which allows us to form **Table 2**.

Ta	Table 1. Fragment of the form for hazard identification, analysis and assessment of waste generation risk									
Identification			Prin	nary analysis	s - definition	Criterion	Risk assessment			
Danger $-i$ in the manage ment system $-j$	Dangero us event (DE)	Negative consequences of DE – by waste group	Severity (amount of waste) at one DE_{ii}	Frequency of occurrence of DE per year (probability)	Level of waste generation risk $R_{jl} = T_{jl}T^* N_{ji}$ $R_{jl} = T_{jl}P^* N_{ji}$ $R_{jl} = T_{jl}P^* N_{ji}$ $R_{jl} = T_{jl}P^* N_{ji}$ $R_{jl} = T_{jl}T^* N_{ji}$ $R_{jl} = T_{jl}T^* N_{ji}$	of Risk Unaccepta bility (allowable waste according to plan)	(if the risk is above the unacceptability criterion, the risk is unacceptable, if less than acceptable)			
ji	ji	Solid waste	T_{ji}^{T}	N_{ji}	$R_{ji}{}^{T}$	R^{nT}	Acceptable or unacceptable			
		Liquid waste	$T_{ji}^{\mathbf{P}}$	_	R_{ji}^{P}	R^{nP}	Acceptable or unacceptable			
		Greenhouse gases	T_{ji}^{I3}	<u>-</u>	$R_{ji}{}^{G}$	$R^{n\Gamma 3}$	Acceptable or unacceptable			
		Polluted air	T_{ji}^{CO}		R_{ji}^{co}	R^{nCO}	Acceptable or unacceptable			
	f waste nt system – <i>j</i> -	,	,	$+R_{ji}^{T}++R_{jn}^{T}$		R^{nT}	Acceptable or unacceptable			
managemer	it system j	R_{j}^{I}	$=R_{jl}^{P}++$	$+R_{ji}^{P}++R_{jn}^{P}$	•	R^{nP}	Acceptable or unacceptable			
				$+R_{ji}^{G}+\ldots+R_{jn}^{G}$		R^{nG}	Acceptable or unacceptable			
		$R_j^{CO} =$	$=R_{jl}^{CO}++$	$+R_{ji}^{CO}++R_{ji}$	₁ CO	R^{nCO}	Acceptable or unacceptable			
Risk o	f waste			$+R_j^T++R_k^T$		R^{nT}	Acceptable or unacceptable			
generation across all		R^{I}	$P = \overline{R_I P + \dots}$	$+R_j^P++R_k^P$	$R^{n\mathbf{P}}$	Acceptable or unacceptable				
management systems $ j=1k$		R^{G}	$G = R_1 G + \dots +$	$+R_i^G++R_k^G$		R^{nG}	Acceptable or unacceptable			
		R^{CO}	$=R_1^{CO}++$	$+R_i^{CO}++R_k^{CO}$	$R^{n}CO$	Acceptable or unacceptable				

V. Tsopa, O. Yavorska, S. Cheberiachko, O. Kovrov, Yu. Pazynich, L. Cheberiachko

Notes (Table 1). T_{ii}^{T} – severity of consequences is the amount of waste arising from i – hazard of j- system of the first waste group management

(solid waste); T_{ji}^{P} – severity of consequences is the amount of waste arising from i – hazard of j- system of the second waste group management (liquid waste); T_{ji}^G – severity of consequences is the amount of waste arising from i – hazard of j- system of the third waste group management (greenhouse gas emissions); T_{ii}^{CO} – severity of consequences is the amount of greenhouse gas emissions arising from i – hazard j- system of the fourth waste group management (greenhouse gas emissions); N_{ji} – frequency of occurrence of a hazardous event i – hazard of j- system of management; R_{ji}^{T} – risk arising from all i – hazards of j- system of the first waste group management (solid waste); R_{ji}^{P} – risk arising from all i – hazards of j- system of the second waste group management (liquid waste); R_{ji}^G – risk arising from j – hazard of i– system of the third waste group (air pollution); R_{ji}^{CO} – risk arising from all i – hazards of jsystem of the fourth waste group (greenhouse gas emissions); i –hazard; n – number of hazards; j – management systems; k – number of management systems.

Table 2. Fragment of the waste generation risk assessment form considering preventive and protective measures

Table	Z. Frag	ment of the waste ge						ective measures
		Risk assessment	Preventive	Re-a	nalysis of risk	taking into	Risk	Re-assessment of
-	uc	(if the risk is above	and protective	accour	nt preventive a	and protective	unacc	risk,
eve	rriteric plan)	the unacceptability	measures to		measure	es .	eptabil	(if the risk is
X 1	criterion o plan)	criterion, then the	reduce risk	$\widehat{\mathbf{g}}$	of (/		ity	above the
ris	ty c	risk is unacceptable,		/ast	nce ur Ility	ng ive ire	criteri	unacceptability
Waste generation risk level	Risk unacceptability c (waste according to	if less-acceptable)		verity (amount of was for a single hazardous event	requency of occurrence o emergency per year (emergency) (probability) emergency	Level of waste generation risk taking into account preventive and protective measures	on	criterion, then the
rat	pta			nt o aza t	cun rob	was sk t rev me	(allow	risk is
ene	acc			mound gle ha event	30 (b) (b) (b) (c)	of v nris nt p ive	able	unacceptable, if
9 20	mag ste			am ev	cy of occur gency per ency) (prob	rel ior our ect	waste accord	less-acceptable)
ast	k u was			.y (. 1 Sii	ncy erg gen er	Level of waste eration risk tak account prever protective meas		
≽	Ris (erit or a	ane Jery	I Sense Sense Sense d p	ing to the	
				Severity (amount of waste) for a single hazardous event	Frequency of occurrence of emergency per year (emergency) (probability) emergency	a ii a	plan	
R_{ji}^T	$R^{n}_{ji}^{T}$	Acceptable or		T_{ji}^{T}	N_{ji}^{3}	$R^{3}_{ji}^{T}$	R^{nT}	Acceptable or
ryı	re ji	unacceptable		1 Ji		It ji	11	unacceptable
R_{ji}^{P}	$R^{n}_{ji}^{P}$	Acceptable or	-	$T^{3}_{ji}^{P}$	-	$R^{3}_{ji}^{P}$	R^{nP}	Acceptable or
		unacceptable	Preventive		_			unacceptable
R_{ji} G	$R^n_{ji}^G$	Acceptable or	and protective measures	$T^{s}_{ji}G$		$R^{\scriptscriptstyle 3}{}_{ji}{}^{m{G}}$	R^{nG}	Acceptable or
		unacceptable	- Incasures		-			unacceptable
R_{ji}^{CO}	R^{n}_{ji} C	Acceptable or		T^{3}_{ji} CO		R^{3}_{ji} CO	R^{nCO}	Acceptable or
	0	unacceptable						unacceptable
Tota			$R_{j}^{3}T = R_{jl}^{3}T + \dots$	$+ R^{3}_{ji}^{T} + +$	$R^{3}_{jn}T$		R^{nT}	
environme			$R_{j}^{3}P = R_{jl}^{3}P + +$	$+R^{3}_{ii}^{P}++$	$R^{3}_{in}^{P}$		R^{nP}	
of the man	_		$R_{j}^{3} = R_{jl}^{3} + \dots +$	$R^{3}_{ji}G++$	$R^{3}_{in}G$		R^{nG}	
systen	n − <i>J</i>		$R_{j}^{3}CO = R_{jl}^{3}CO + +$	$+R^{3}_{ii}CO_{+}$	$+R^{3}_{in}CO$		R^{nCO}	Acceptable or
Total		$R^{3} = R^{3} I^{7} + \dots + R^{3} I^{7} + \dots + R^{3} I^{7}$				R^{nT}	unacceptable	
environme			$R^{3}P = R^{3}I^{P} + \dots +$				R^{nP}	
for all man			$R^{3} = R^{3}_{1} \stackrel{G}{G} + \dots + R^{3}_{k} \stackrel{G}{G} + \dots + R^{3}_{k} \stackrel{G}{G}$					
systems –	J=1k		$R^{3}CO = R^{3}_{I}CO + +$	$+R^{3}_{j}CO++$	$+R^3k^{CO}$		R^{nCO}	

In the tenth step, we introduce them. In the eleventh step, we conduct an audit of the implementation of the requirements of the developed waste risk management process and assess the effectiveness of the preventive and protective measures. Based on the results of the eleventh step - the audit of the implementation of the requirements, in the twelfth step, we develop measures to improve the waste risk management process and introduce them.

After that, we return to the beginning of the process to the first step. In the case of an acceptable level of waste generation risk in step 5, after documenting them, we proceed to the eighth step - reviewing the risks of waste generation for all management systems with periodicity in time, for example, at least once a year.

Identified hazardous events - i in management systems - j are a source of solid (T), liquid (P) or gaseous waste (G) generation, as well as greenhouse gas emissions (GHG), which allows us to calculate the risks of waste generation in each management system according to the **Equation (1)**:

$$R_{ji}^{\mathsf{T}} = N_{ji} \times T_{ji}^{\mathsf{T}}$$
; $R_{ji}^{\mathsf{p}} = N_{ji} \times T_{ji}^{\mathsf{p}}$; $R_{ji}^{\mathsf{G}} = N_{ji} \times T_{ji}^{\mathsf{G}}$; $R_{ji}^{\mathsf{CO}} = N_{ji} \times T_{ji}^{\mathsf{CO}}$ (1)
where are: R_{ji}^{T} ; R_{ji}^{p} ; R_{ji}^{G} ; R_{ji}^{CO} – level of risk of waste generation from hazards – and management systems – j , N_{ji} –

frequency of occurrence of a dangerous event from hazards -i and control systems -j, T_{ii}^{T} , T_{ji}^{G} ; T_{ji}^{G} ; T_{ji}^{G} – severity of waste generation from a hazardous event -ii.

In the fourth step, the risk of waste generation of each type (group) from one hazardous event -i for one of the control systems -i is determined by the **Equatios (2)-(9)**:

$$R_{ji}^{T} = R_{jl}^{T} + \dots + R_{ji}^{T} + \dots + R_{jn}^{T},$$

$$R_{ji}^{P} = R_{jl}^{P} + \dots + R_{ji}^{P} + \dots + R_{jn}^{P},$$
(2)

(3)

V. Tsopa, O. Yavorska, S. Cheberiachko, O. Kovrov, Yu. Pazynich, L. Cheberiachko

$$R_{ji}{}^{G} = R_{jl}{}^{G} + \dots + R_{ji}{}^{G} + \dots + R_{j}{}^{G}, \tag{4}$$

$$R_{ii}^{CO} = R_{i1}^{CO} + \dots + R_{ii}^{CO} + \dots + R_{in}^{CO}.$$
 (5)

while for the organization as a whole, i.e. all management systems:

$$R^{T} = R_{1}^{T} + R_{2}^{T} + R_{3}^{T} + R_{4}^{T}, (6)$$

$$R^{P} = R_{1}^{P} + R_{2}^{P} + R_{3}^{P} + R_{4}^{P}, \tag{7}$$

$$R^{G} = R_{1}^{G} + R_{2}^{G} + R_{3}^{G} + R_{4}^{G}, \tag{8}$$

$$R^{CO} = R_1^{CO} + R_2^{CO} + R_3^{CO} + R_4^{CO}. (9)$$

where are: $R_{ji}{}^T$, $R_{ji}{}^P$, $R_{ji}{}^G$, $R_{ji}{}^C$ — the level of risk of solid, liquid, gaseous waste generation and greenhouse gas emissions from a single hazardous event -ji in one of the organization's management systems -j; R^T , R^P , R^G , R^{CO} — the level of risk of solid, liquid, and gaseous waste generation and greenhouse gas emissions from all organization's management systems.

The determined levels of waste generation risks are compared with an acceptable level indicator, which is determined based on the size of the permissible amounts of waste and greenhouse gas emissions of the organization for the corresponding period of time. The developed waste generation risk management process differs from the known ones in the need to identify hazards and dangerous events in various management systems related to: the quality of products and services, environmental safety, health and safety of employees, energy consumption, etc. The proposed waste generation risk management process allows you to see how the risk of generation affects the entire organization as a whole, and not just one of its aspects (**Table 3**). That is, to move from reactive waste management (disposal) to proactive (prevention or reduction of its generation at all stages of the product or service life cycle).

Table 3. Interrelationship of management system standards ISO 9001 (quality), ISO 14001 (environment), ISO 45001 (occupational health and safety) and ISO 50001 (energy consumption) from the point of view of waste generation

(occupational ne	(occupational health and safety) and 150 50001 (energy consumption) from the point of view of waste generation						
Annex SL	Suggestions for developing a waste risk management process						
Organizational	Conduct a unified analysis of the organization's working environment, taking into account customer						
Environment	requirements for the purity of secondary raw materials, environmental standards for emissions, employee						
	safety expectations, and energy consumption reduction goals to reduce the corresponding losses that form						
	waste and emissions.						
Leadership	Develop a unified policy in the field of quality, ecology, safety, and energy efficiency, to reduce the						
	corresponding losses that form waste and emissions, signed by senior management, and bring it to the						
	attention of all employees.						
Planning	Create a unified register of hazards and opportunities, where quality hazards, occupational health and safety,						
	energy consumption, etc. are identified for the risks of waste generation.						
Support	Develop a unified personnel training program covering issues of sorting quality, hazardous waste						
	management rules, labor protection instructions, and energy saving methods, etc., to reduce the						
-	corresponding losses that form waste and emissions.						
Activity	Develop operational instructions that simultaneously regulate quality criteria for materials, safety rules for						
	operators, procedures in case of spillage of hazardous substances, and energy-efficient operating modes of						
-	equipment to reduce relevant losses that generate waste and emissions.						
Performance	Conduct an internal audit and a single analysis by management that comprehensively assesses performance						
Evaluation	in all areas: quality, ecology, safety, energy, etc., including reducing relevant losses that generate waste.						
Improvement	Implement a single non-conformity management procedure, where the incident is considered simultaneously						
	in all areas of management, including from the point of view of reducing relevant losses that generate waste.						

For example, consider a hazardous event in a coal mine related to analysis of the possible potential consequences of violating the coal extraction technology that is given in **Table 4**. Analysis of the effectiveness of preventive measures to reduce the risk of waste generation is presented in **Table 5**.

The considered example demonstrates that the loss of product quality (for example, a significant content of rock in coal) is the primary hazard that triggers the chain of formation of various types of waste - solid, liquid, gaseous. It indicates the systemic nature of the risk, where one technological error can cause a multi-component environmental load. The most effective way to reduce waste risk is the integration of modern technologies, which allows for the simultaneous influence of the causes and consequences of waste risk, ensuring the systemic stability of the technological process, and reducing the formation of all types of waste by substantiating the feasibility of implementing technologies. This approach requires a comprehensive analysis of the effect of the hazard on all kinds of waste. It leads to the determination of the relationships between the hazard (non-conformity) in the management systems for each type of waste, which will allow to establish the need to update technologies.

Table 4. Fragment of the analysis of possible potential consequences of mining technology violation

Identification		_	Prin	nary analysis - d	Risk	Risk assessment,	
Danger – i	Dangero	Negative	Severity	Frequency	Waste generation	unacceptabil	if the risk is above
in j-control	us event	consequenc	(amount of	of	risk level	ity criterion	the unacceptability
system	(NE)	es of the	waste) for one	emergency	$RJ^{T}=Tji^{T}*Nji$		criterion, then the
		emergency	NPji	occurrence	$RJ^{P}=Tji^{P}*Nji$		risk is unacceptable,
		 by waste 		per year	RJ ^{GZ} =Tji ^{GZ} *Nji		if less than
		groups		(probability)	RJ ^{SO} =Tji ^{SO} *Nji		acceptable)
		Solid waste	up to 600 kg	0	15.6 million tons	400	Unacceptable risk
	al)	(rock)	per ton of coal	with the		thousand	
	coal)			rith y		tons of rock	
gy	ts led			s s og.		per year	
olo	products in mine	water pollution		arises chnolo	624 million m3	1,500,000	Unacceptable risk
, hn	roc in 1	with sludge,	of sludge from	ar ech		m³/year	
tec	ig p		a ton of coal	g te			
ing	Non-conforming icant rock content	Air pollution	0.025 kg of	ies a year, a situation arises wi collapse of mining technology	130 thousand tons	500 tons per	Unacceptable risk
nin	ori C CC	by dust	particulate	ı sit		year	
ıf n	onf ock	impurities	matter	r, a of 1			
n c	n-c nt p		(PM10) per	year,			
utio	Nor		tonne of coal	a y		1.5.700	** 44 14
violation of mining technology	Non-conforming products (significant rock content in mined	Using	100 kg CO2	times	32.5 tons)	12,500 tons	Unacceptable risk
.2	sign	additional	per ton of coal	ti.		of CO ₂ per	
	8)	energy to clean		20		year	
		coal					

Table 5. Fragment of the analysis of the effectiveness of preventive measures to reduce the risk of waste

generation

Waste generati on risk	Risk unaccepta bility	Risk assessment, if the risk is	Preventive and protective measures to reduce risk				
level	criterion (waste according to plan)	above the unacceptabilit y criterion, then the risk is unacceptable, if less than acceptable)		Severity (amount of waste) for a single hazardous event	Frequency of occurr ence of emerg ency per year (emer gency)	Level of risk of waste generation taking into account preventive and protective measures	above the unacceptabilit y criterion, then the risk is unacceptable, if less than acceptable)
15.6 million tons	400 thousand tons of rock per year	Unacceptable risk	Automated process control Precision mining technologies Comprehensive training and certification of management systems	up to 100 kg per ton of coal	5	134 thousand tons	Acceptable
624 million m3	1,500,000 m³/year	Unacceptable risk	selective mining introduction of a closed water cycle Mine water treatment	up to 100 m3 of sludge from a ton of coal		234,000 m3	Acceptable
130 thousan d tons	500 tons per year	Unacceptable risk	Humidification and neutralization at the source Local aspiration Transport speed control	0.0005 kg of particulate matter (PM10) per tonne of coal		39 tons per year	Acceptable
32.5 tons)	12,500 tons of CO ₂ per year	Unacceptable risk	Degassing of coal seams Emissions monitoring Equipment update	30 kg CO2 per ton of coal		6.5 tons	Acceptable

4. Discussion

The need to develop a waste management process in organizations is due to the fundamental transformation of the model, which moves from traditional waste collection and disposal to the principles of a circular economy. This transition

V. Tsopa, O. Yavorska, S. Cheberiachko, O. Kovrov, Yu. Pazynich, L. Cheberiachko

is taking place under the influence of three key factors: regulatory pressure (EU Waste Framework Directive 2008/98/EC), which establishes a clear waste management hierarchy; economic and technological opportunities of the circular economy, which allow waste to be transformed from a burdensome liability into a valuable secondary resource and to create new environmental prospects; stakeholder demands focused on reliability, transparency, sustainability and environmental safety (**Perkumienė et al., 2023**). These factors determine the need to create a new waste risk management process that will ensure the sustainability and competitiveness of organizations.

The waste risk management process through integrated management systems (quality – ISO 9001:2015; ecology – ISO 14001:2015; occupational health and safety – ISO 45001:2018; energy consumption – ISO 50001:2018, etc.) is undergoing a significant fundamental transformation. The traditional model, focused on collection and disposal, is giving way to complex high-tech systems based on the principles of the circular economy.

The process of managing waste risks, especially in mining and mineral processing enterprises, through integrated quality management systems (ISO 9001:2015), environmental management (ISO 14001:2015), occupational health and safety management (ISO 45001:2018) and energy management (ISO 50001:2018) is the embodiment of the strategic responsibility of companies to future generations regarding the rational use of resources and sustainable development. (Lewicka, 2020).

The example provided in **Tables 4** and **5** demonstrates that violations of mining technology can lead to loss of product quality, and formation of various types of waste - solid, liquid, and gaseous. It indicates the systemic nature of the risk, where one technological error can cause a multi-component environmental load. All assessed risks (formation of rock, sludge, dust, CO₂) in the initial analysis had an unacceptable level, which requires an immediate response through the use of a complex of preventive and protective measures, automation, selective mining, aspiration, and degassing, which allowed reducing the amount of waste risk to an acceptable level.

The proposed approach provides a holistic, broader view of waste risks, which is impossible with an isolated approach. Often, a solution to improve one aspect may create a waste risk in another. For example, using a more aggressive chemical reagent to clean equipment (potentially improving quality) may pose an environmental risk (discharges) and a risk to personnel health (inhalation of vapors). The waste management process in the organization's management systems requires considering such solutions comprehensively within all management systems, balancing all factors and risks of quality, environmental, safety, and energy management systems, etc.

This approach allows an organization to identify and manage the relationships between different types of risks. These benefits are not isolated, but create a virtuous cycle, or "cascade of benefits". For example, integrating the audit process (Johnson et al., 2023) leads to direct cost savings. The freed-up resources can be invested in better waste reduction technologies that will reduce waste going to landfills and improve the quality of the secondary raw materials, which leads to savings (lower landfill fees) and increased revenue. Improved environmental performance strengthens the enterprise's reputation, which helps to win new tenders and receive investments. (Josimović et al., 2022; Lennon et al., 2024). Thus, the initial investment in the development and implementation of the waste risk management process starts a self-reinforcing mechanism, leading to sustainable development and increased competitiveness of organizations.

5. Conclusions

The developed waste risk management process at mining and mineral enrichment enterprises differs from the known ones in the possibility of full coverage (vision) of the problem as a whole, which allows making informed management decisions taking into account the conservation of resources and the environment based on the requirements of several international standards on the cyclicality and continuous improvement of organizational management systems and sustainable development.

The main advantage of the proposed waste risk management process from existing ones, especially at mining and mineral enrichment enterprises, is the integration of the consequences of waste generation in quality management systems (ISO 9001), ecology (ISO 14001), occupational health and safety (ISO 45001) and energy consumption (ISO 50001), etc. to reduce the loss of material and energy resources, which are the primary sources of waste generation.

The waste risk management process consists of twelve steps. The main ones are: determining the loss of material and energy resources from each hazard and hazardous event in all management systems: quality (ISO 9001), ecology (ISO 14001), occupational health and safety (ISO 45001) and energy consumption (ISO 50001), assessing the risk for each hazard and hazardous event in each management system from the point of view of waste generation; determining the overall risk of various types of waste generation of all management systems of the organization; developing preventive and protective measures to reduce the risks of waste generation; documenting the dangers of waste generation; conducting audits; periodic review of waste generation and continuous improvement of the waste risk management process itself.

6. References

Bonifazi, G., D'Adamo, I., Palmieri, R., & Serranti, S. (2025). Recycling-Oriented Characterization of Space Waste Through Clean Hyperspectral Imaging Technology in a Circular Economy Context. *Clean Technol.*, 7, 26. https://doi.org/10.3390/cleantechnol7010026.

Cerar, S., Serianz, L., Koren, K., Prestor, J., & Mali, N. (2022). Synoptic Risk Assessment of Groundwater Contamination from Landfills. *Energies*, 15, 5150. https://doi.org/10.3390/en15145150.

- V. Tsopa, O. Yavorska, S. Cheberiachko, O. Kovrov, Yu. Pazynich, L. Cheberiachko
- Grobelak, A., Całus-Makowska, K., Jasińska, A., Klimasz, M., Wypart-Pawul, A., Augustajtys, D., Baor, E., Sławczyk, D., & Kowalska, A. (2024). Environmental Impacts and Contaminants Management in Sewage Sludge-to-Energy and Fertilizer Technologies: Current Trends and Future Directions. *Energies*, 17, 4983. https://doi.org/10.3390/en17194983.
- Josimović, B., Manić, B., & Krunić, N. (2022). Strategic Environmental Assessment as a Support in a Sustainable National Waste Management Program—European Experience in Serbia. *Energies*, 15, 4568. https://doi.org/10.3390/en15134568.
- Johnson, R., Lee, K., & Martinez, P. (2023). Financial incentives for sustainablewaste practices in Germany and Sweden. *Waste Management & Research*, 41(4), 375-389.
- Lewicka, D. (2020). Employee institutional trust as an antecedent of diverse dimensions of organisational commitment. *Argumenta Oeconomica*, 2019(1), 321–340. https://doi.org/10.15611/aoe.2020.1.13
- Kovrov, O., Pavlychenko, A., & Kulikova, D. (2024). Development of the wastewater treatment technology for the mine 'Ternivska' of the Kryvyi Rih iron ore plant. *Environmental Technology*, 46(6), 908–921. https://doi.org/10.1080/09593330.2024.2371080.
- Kovrov, O., Malichenko, V., Kulikova D., Buchavyi, Y. (2025). Investigation of the spent coffee ground applicability for land phytoremediation via biotesting techniques. *IOP Conf. Series: Earth and Environmental Science*, 1481, 012001. https://doi.org/10.1088/1755-1315/1481/1/012001.
- Lennon, J.W.O., Pavlychenko, A., Tsopa, V., Deryugin, O., Khorolskyi, A., & Cheberiachko, L. (2024). Causal Relationship Between Environmental Aspect and Environmental Risk. *E3S Web of Conferences*, 567, 01013,. https://doi.org/10.1051/e3sconf/202456701013.
- Marych, K. (2024). Packaging waste management: European standards and Ukrainian legislation. *Visnyk Natsionalnoho Universytetu "Lvivska politekhnika"*, 11(2[42]), 89–95.
- Oleniacz, R., Grzesik, K. (2025). Assessment and Analysis of Waste Treatment and Environmental Management. *Energies*, 18, 138. https://doi.org/10.3390/en18010138.
- Ovander, N. (2021). Review of international and Ukrainian standards for risk management in the context of modern challenges and threats. *Ekonomika ta Suspilstvo*, 27. https://doi.org/10.32782/2524-0072/2021-27-26
- Perkumienė, D., Atalay, A., Safaa, L., & Grigienė, J. (2023). Sustainable Waste Management for Clean and Safe Environments in the Recreation and Tourism Sector: A Case Study of Lithuania, Turkey and Morocco. *Recycling*, 8, 56. https://doi.org/10.3390/recycling8040056.
- Pavlychenko, A., Sala, D., Pyzalski, M., Dybrin, S., Antoniuk, O., & Dychkovskyi, R. (2025). Utilizing Fuel and Energy Sector Waste as Thermal Insulation Materials for Technical Buildings. Energies, 18(9), 2339. https://doi.org/10.3390/en18092339
- Polyanska, A., Pazynich, Y., Petinova, O., Nesterova, O., Mykytiuk, N., & Bodnar, G. (2024). Formation of a Culture of Frugal Energy Consumption in the Context of Social Security, pp. 60-87. The Journal of the International Committee for the History of Technology, 29(2), 60–87. https://doi.org/10.11590/icon.2024.2.03
- Sobolev, V., Gubenko, S., Khomenko, O., Kononenko, M., Dychkovskyi, R., & Smolinski, A. (2025). Physical and chemical conditions for the diamond formation. Diamond and Related Materials, 151, 111792. https://doi.org/10.1016/j.diamond.2024.111792
- Shvetsova, O.A., & Lee, J.H. (2020). Minimizing the Environmental Impact of Industrial Production: Evidence from South Korean Waste Treatment Investment Projects. *Appl. Sci.*, 10, 3489.
- Tabachenko, M., Saik, P., Lozynskyi, V., Falshtynskyi, V., & Dychkovskyi, R. (2016). Features of setting up a complex, combined and zero-waste gasifier plant. Mining of Mineral Deposits, 10(3), 37–45. https://doi.org/10.15407/mining10.03.037

Funding

The authors declare that this research was conducted without any external funding.

Author's contribution

Vitaliy Tsopa (professor): conceptualization, data curation, Olena Yavorska (professor): formal analysis, Serhii Cheberiachko (professor): writing – original draft, Oleksandr Kovrov (professor): writing – review & editing, Yuliya Pazynich (ass. professor): reference analysis & data proceeding, Lidia Cheberiachko (postgraduate student): methodology verifying.

All authors have read and agreed to the published version of the manuscript.



Hydration and Carbonation Behaviour of Selected Recycled Materials from Slovenia

DIM-ESEE Conference



Vesna Zalar Serjun^{1*} ^{□⊠}, Primož Oprčkal¹ ^{□⊠}, Anton Meden² ^{□⊠} Marta Počkaj² ^{□⊠}, Romana Cerc Korošec² ^{□⊠}

¹ Slovenian National Building and Civil Engineering Institute, Dimičeva ulica 12, SI-1000 Ljubljana, Slovenia)²Faculty of Chemistry and Chemical Technology, University of Ljubljana, Večna pot 113, SI-1000 Ljubljana, Slovenia

Abstract

The European Union's shift towards a circular economy emphasizes the substitution of virgin materials with recycled alternatives, particularly in the construction sector, which can accommodate large volumes of industrial by-products. Ashes from coal, biomass, paper sludge, and co-combustion processes are abundant secondary materials whose variable chemical and mineralogical compositions necessitate careful assessment to enable safe and effective reuse.

This study investigates the hydration behaviour and early carbonation potential of ashes of different origin. The ashes were characterized using X-ray fluorescence, X-ray diffraction, and scanning electron microscopy coupled with energy-dispersive spectroscopy. Hydraulic reactivity was evaluated by preparing ash pastes at a 1:1 water-to-ash ratio and monitoring hydration product formation over time using XRD. Carbonation of co-combustion ash was studied under controlled CO_2 conditions (2 % CO_2 , 50 % RH, 20 °C \pm 1 °C) at different moisture contents (0 wt.%, 10 wt.%, 20 wt.%, and 40 wt.%) and early curing times (0 hours, 1 hours, 4 hours, and 24 hours).

Results indicate distinct differences among the ashes. Paper sludge ash exhibited the most extensive formation of calcium aluminate hydrates, coal and co-combustion ashes showed moderate hydration, while biomass ash produced only minor secondary phases. Carbonation of co-combustion ash proceeded concurrently with hydration, with lime depletion and calcite formation enhanced by higher moisture and longer curing. These coupled processes influenced both the kinetics and composition of hydration products. The findings demonstrate the potential of diverse combustion ashes for valorisation in construction materials and provide insight into their reactivity under early-age hydration and carbonation conditions, supporting circular economy initiatives.

Keywords: Combustion ash, Hydration, Carbonation, Circular economy, Construction materials

1. Introduction

The European Union is transitioning from a linear to a circular economy to extend material lifecycles and reduce waste. The 2020 Circular Economy Action Plan, part of the European Green Deal, emphasizes replacing virgin resources with recycled alternatives (European Commission, 2020). With global waste generation projected to rise by 70 % by 2050, an estimated 600 million tonnes of waste-based materials could be reused annually (European Commission, 2008; European Commission, 2015). The construction sector is particularly well suited for repurposing industrial by-products such as ashes, which enable large-scale material reuse while stabilizing harmful elements. In support of this, the SIST EN 16907-2 (2020) standard, introduced in 2019, allows the use of processed and recycled materials in construction composites.

Ashes produced in air pollution control systems of industrial and energy processes differ according to fuel source and combustion method. As coal use declines, biomass and co-combustion ashes (e.g. from sewage sludge, biomass, or municipal solid wastes) are becoming more prevalent. Although most ashes are still disposed of, only a small proportion is currently recycled (Hogg, 2022). Their composition varies with fuel type, plant operations, and storage conditions, which affects reuse potential and requires case-specific evaluation (Singh et al., 2016; Zhao et al., 2017).

Previous studies (Yao et al., 2015; Wei et al., 2023; Ding et al., 2024; Aboustait et al., 2016) have highlighted ash applications in cement production, lightweight aggregates, backfill, panel boards, and soil treatment. Standardization remains critical for safe and effective use, yet most regulations focus on coal fly ash, with limited provisions for other ash types. Nevertheless, practical applications demonstrate that a wider range of ashes can enhance geotechnical performance, for example by stabilizing soils or immobilizing contaminants (Zalar Serjun, 2024).

Recent studies have expanded understanding of ash reactivity, hydration, and carbonation mechanisms. For example, Shi et al. (2025) investigated how the amorphous phase content of recycled fly ash influences hydration kinetics, showing that higher amorphous content accelerates reaction rates and improves binding properties. Skevi et al. (2022) demonstrated that mechanochemical pre-treatment and mineral carbonation of biomass bottom ash enhance its pozzolanic activity and improve strength development when used as a supplementary cementitious material. Similarly, a review by

Gupta et al. (2024) on coal bottom ash reported that optimal fineness and controlled replacement ratios can yield concrete with comparable mechanical and durability performance to conventional mixes.

In terms of carbonation, Pihlajavaara et al. (2023) reviewed accelerated mineral carbonation processes in cementitious materials and industrial by-products, emphasizing the role of moisture and reactive calcium phases in CO₂ uptake. Laboratory-scale research by Li et al. (2024) found that CO₂ uptake in hydrated cementitious systems can reach up to 70 % of the theoretical capacity within the first 40 minutes, highlighting the importance of early carbonation kinetics. Moreover, Rahman et al. (2025) assessed wastewater sludge ash as a cement substitute and reported that controlled carbonation can improve durability while immobilizing potentially hazardous elements.

Compared with these studies, our work focuses specifically on industrial by-products from combustion processes, assessing both their hydration behaviour and mineral carbonation potential at early curing stages. Several types of combustion ashes were hydrated, with curing monitored over time, while the carbonation capacity of co-combustion ash (wood chips added to coal during combustion) was evaluated under different moisture contents at early time intervals (up to 24 hours). This approach contributes to understanding the short-term reactivity and CO₂ sequestration potential of co-combustion ashes — a topic that remains underexplored in current literature.

2. Materials and Methods

Four different ashes from various incineration processes were investigated in this study, namely from coal, cocombustion, paper sludge and biomass incineration. Macroscopic appearance with the microstructure of investigated ashes is shown in **Figure 1**.

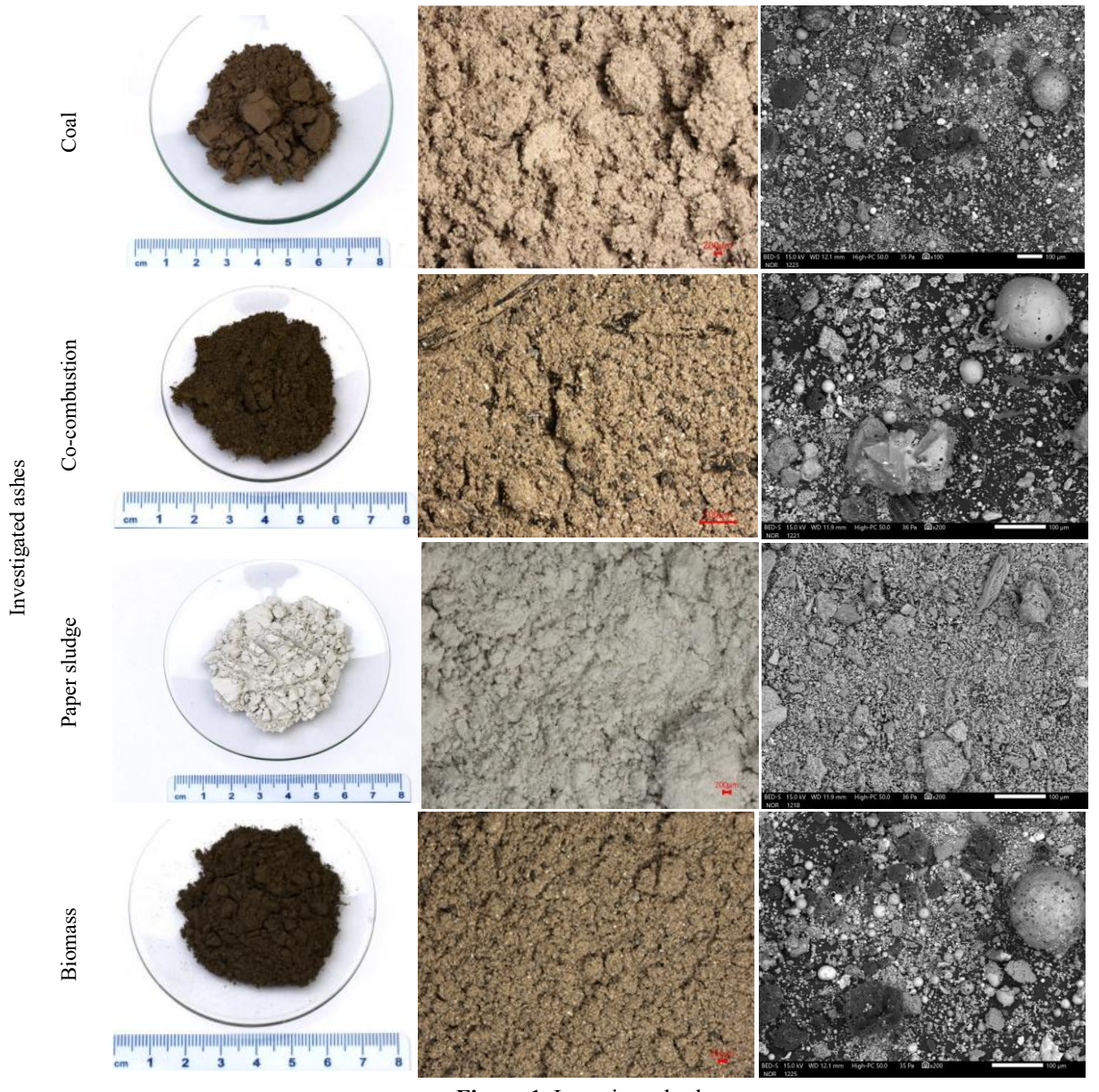


Figure 1. Investigated ashes

Ashes were characterized for their phase and chemical composition. Phase composition was determined using the quantitative powder X-ray diffraction (QXRD), using an Empyrean (PANalytical, Netherlands) diffractometer with Cu-Kα radiation. Powder diffraction data were collected at a tube tension of 40 kV and a tube current of 45 mA using a 2θ step size of 0.02° and measurement time of 100 s per step. Quantitative phase analysis was performed using the Rietveld refinement method, employing the external standard approach and the K-factor method. NIST alumina (corundum SRM 676a) was used as the external standard Bulk chemical composition was analysed by X-ray fluorescence (XRF), using Perform-X ARL (Thermo Fischer, USA). The samples were prepared as glass disks. The sample-to-flux ratio was 1:10. The flux used for this study was 50 % lithium tetraborate with 50 % of lithium metaborate. The microstructural and mineralogical features were investigated further by scanning electron microscopy (SEM) using a JEOL JSM-IT500LV (Tokyo, Japan) microscope equipped with energy dispersive spectroscopy (EDS) (Oxford Instruments, UK).

To study the hydraulic reactivity, ash pastes were prepared by mixing ash with water at a 1:1 ratio. The formation of hydration products was monitored by XRD at selected time intervals.

The carbonation of co-combustion ash was investigated on a sample collected directly from the production process (rather than obtained through conventional process handling) to assess its maximum CO_2 sequestration capacity under varying moisture contents and controlled CO_2 levels at early-age time intervals of up to 24 hours (0 hours, 1 hours, 4 hours, and 24 hours). Water was admixed with ash at different contents (0 wt.%, 10 wt.%, 20 wt.%, and 40 wt.%), and the samples were conditioned in a CO_2 chamber under the following parameters: $CO_2 = 2$ %, RH = 50 %, and T = 20.0 °C \pm 1°C.

3. Results and Discussion

The results of the XRF analyse is shown in Table 1 (according to Snellings et al., 2023).

The differentiation into four groups is determined by the fuel type used in combustion. Coal and co-combustion are characterized by silico-aluminous ashes with the lowest (earth) alkali contents, biomass ashes are characterized as more calcareous, whereas paper sludge combustion is characterized by ashes with the highest alkali concentrations.

The results of the QXRD analysis is shown in **Figure 2**. Coal ashes exhibit the highest proportion of amorphous phases, followed by co-combustion and biomass ashes, with paper ashes containing the least. In contrast, paper ashes are enriched in calcium-bearing phases, including calcite, portlandite, and lime. Apart from weakly hydraulically active phases such as gehlenite, no other well-defined cementitious phases were identified in investigated ashes.

Table 1. The results of the XRF bulk chemical composition

ASH	Chemical composition (wt.%)		
	CaO+MgO+Na ₂ O+K ₂ O	SiO ₂	Al ₂ O ₃ +Fe ₂ O ₃
Coal	14.4	47.9	34.6
Co-combustion	27.4	31.1	20.8
Paper sludge	46.9	12.2	13.3
Biomass	34.3	19.7	9.0

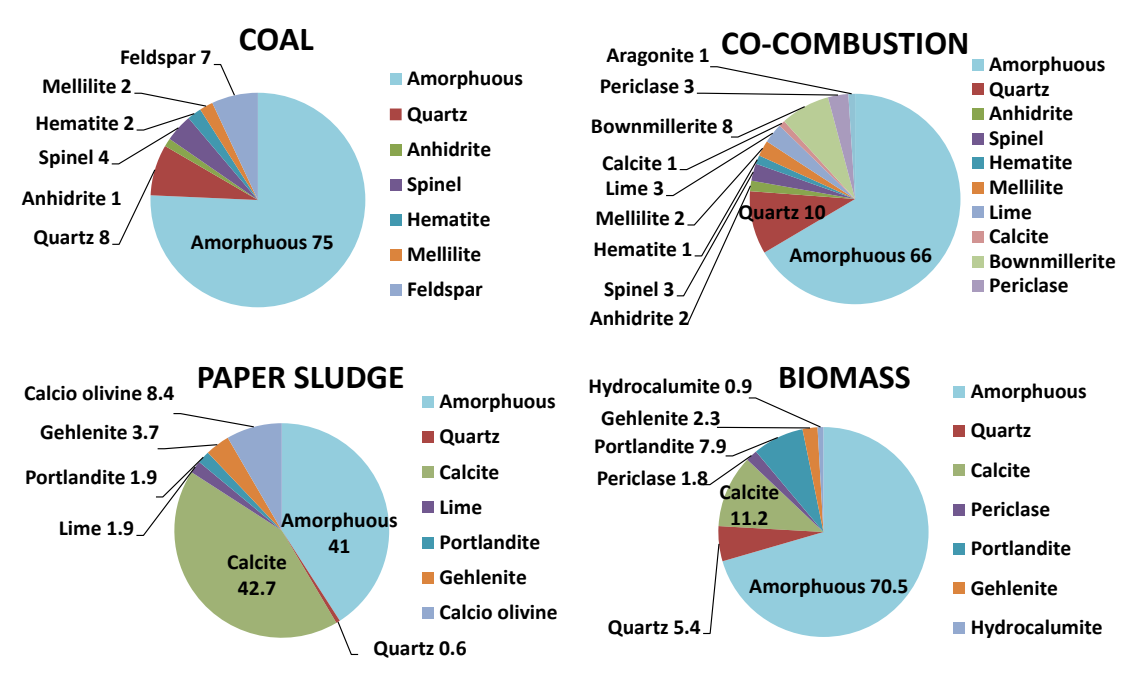


Figure 2. QXRD analysis of investigated ashes.

The morphology of grains composed of amorphous phases varies among the ashes. Coal and co-combustion ashes contain well-rounded spherules, whereas biomass and paper sludge ashes exhibit more irregularly shaped grains with rounded pores (Mohebbi et al., 2022, Oprčkal et al., 2020). In the latter, the amorphous phase is more finely interspersed with the fine-grained matrix, and spherules are absent. Amorphous grains are often highly heterogeneous, comprising different elements in varying ratios, making it difficult to define their overall composition for each ash type. Figure 3 illustrates various types of amorphous grains, together with EDS analyses (averaged from 20 measurements of amorphous grains per sample, taken from points like those designated as "x" in the illustration) for coal and paper sludge ashes. The results, expressed in atomic percentages (at.%), show the maximum and minimum values of selected elements, highlighting the broad compositional variability of the amorphous phases.

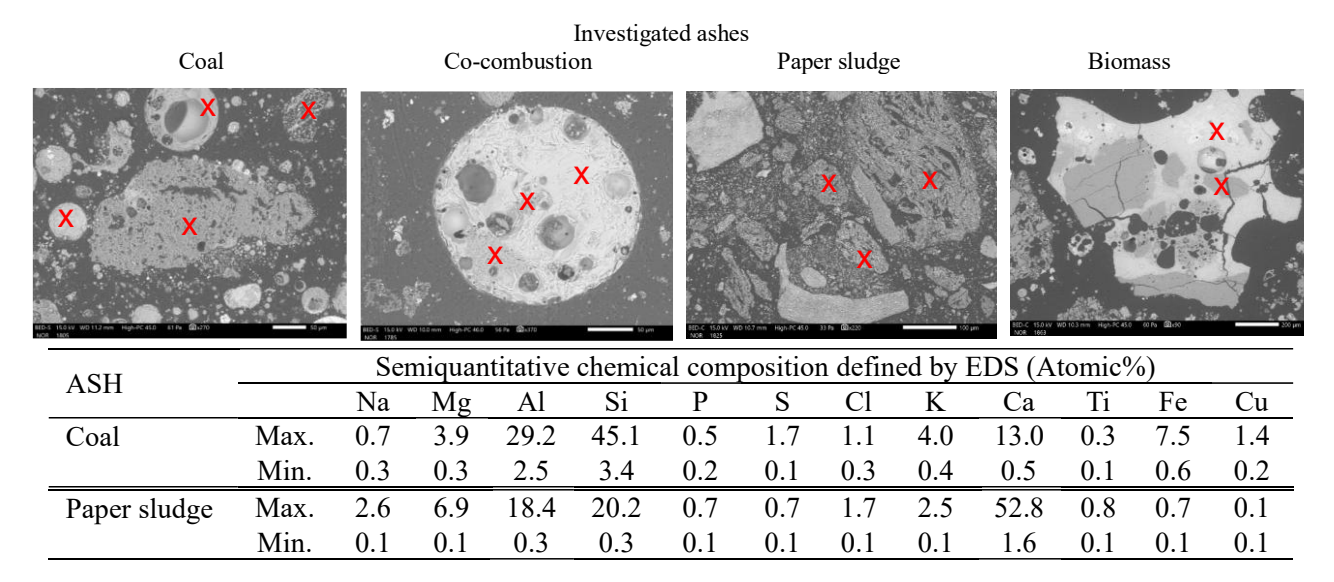


Figure 3. Variations in the appearance of amorphous phase grains among ashes

Time-resolved XRD analysis (2D, 7D, 14D, 28D, 56D, 90D, and 180D, corresponding to 2, 7, 14, 28, 56, 90, and 180 days) of ash paste hydration products (example of co-combustion ash shown in Figure 4) revealed the formation of various calcium aluminate hydrates (CAHs) characteristic of cementitious hydration, including Aft (ettringite) and AFm phases (hemicarboaluminate, monocarboaluminate and hydrocalumite). Paper ash pastes exhibited the most extensive formation of CAHs. In coal and co-combustion ash pastes, CAH development increased over time and was clearly detectable. In contrast, biomass ash pastes exhibited only minor amounts of newly formed phases.

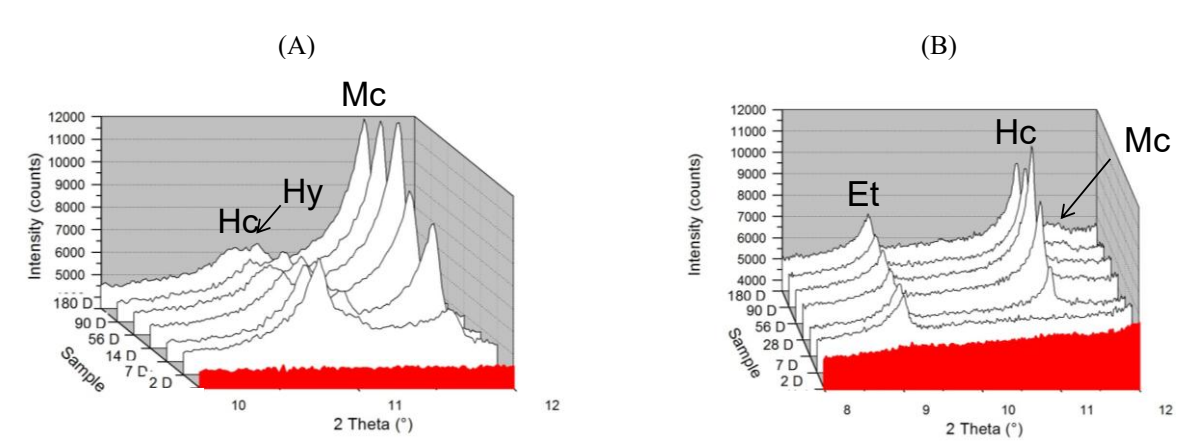
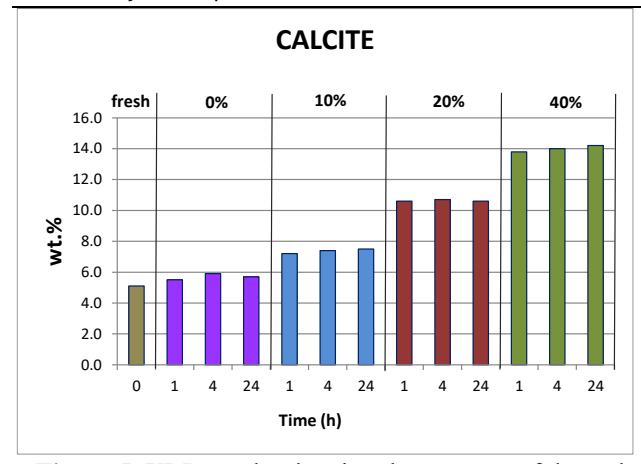


Figure 4. Time dependent XRD results of paper sludge (A) and co-combustion ash (B) pastes; Et- ettringite; Hc-hemicarboaluminate; Mc-monocarboaluminate; Hy-hydrocalumite

The results of the carbonation of co-combustion ash show a clear transition of lime into hydrated and carbonated forms (**Figure 5**), primarily calcite. Higher moisture content (wt.%) and longer curing times enhanced the carbonation process, confirming the positive carbonation potential of this ash. The findings also indicate that hydration and carbonation occur simultaneously and can influence one another. Their interaction under curing conditions is often complex. Hydration products such as Ca(OH)₂, ettringite, and C–S–H are prone to carbonation, while the main carbonation product, CaCO₃, can in turn affect both the kinetics of hydration and the composition of the hydration phases. A comprehensive understanding of these coupled processes is therefore essential for describing the hardening behaviour.



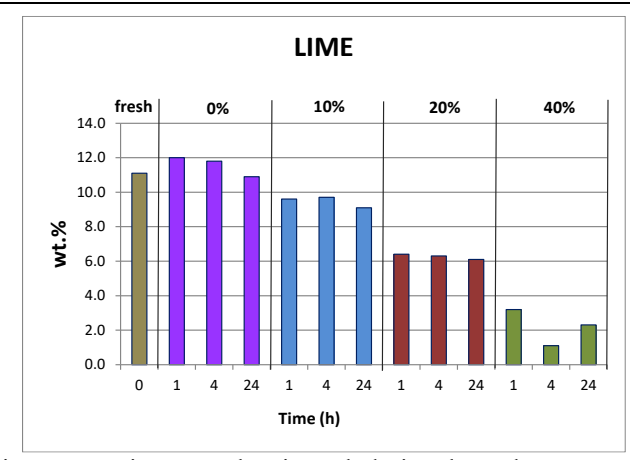


Figure 5. XRD results showing the progress of the carbonation process in co-combustion ash during the early stages (up to 24 hours), highlighting lime depletion and calcite formation.

5. Conclusions

This study evaluated the hydration behaviour and early carbonation potential of four combustion ashes—coal, co-combustion, paper sludge, and biomass—emphasizing their chemical, mineralogical, and microstructural variability. XRF and QXRD analyses showed that coal and co-combustion ashes are predominantly silico-aluminous, paper sludge ash is highly calcareous with elevated alkali content, and biomass ash is also calcareous. SEM/EDS observations confirmed differences in grain morphology as well as in the distribution and appearance of amorphous phases, both of which are critical for reactivity.

Hydration experiments demonstrated that paper sludge ash exhibited the most extensive formation of calcium aluminate hydrates, while coal and co-combustion ashes showed moderate hydration, and biomass ash formed only minor newly formed phases. Carbonation tests on co-combustion ash showed that lime transformed into calcite and other hydrated products, with higher moisture content and longer curing times (24 hours) enhancing slightly the carbonation process. Hydration and carbonation were observed to occur simultaneously, influencing both the kinetics and composition of hydration products.

These findings highlight the potential for valorising diverse combustion ashes in construction applications, supporting circular economy objectives. Understanding the coupled processes of hydration and carbonation is crucial for optimizing the performance and durability of ash-containing materials.

Future work will focus on identifying and clarifying the key factors controlling these processes, including the influence of ash amorphous phase composition, particle morphology, and environmental conditions, to enable more efficient and safe utilization of industrial by-products in construction materials.

6. References

Aboustait, M.; Kim, T.; Ley, M.T.; Davis, J.M. Physical and chemical characteristics of fly ash using automated scanning electron microscopy. *Constr. Build. Mater.*, 106, 1–10 (2016).

Ding, X.; Du, H.; Wu, E.; Yi, P.; Li, Y.; Luo, Y.; Liu, W. Investigating the hydration, mechanical properties, and pozzolanic activity of cement paste containing co-combustion fly ash. *Buildings*, 14, 1305 (2024).

European Commission. *The Raw Materials Initiative—Meeting Our Critical Needs for Growth and Jobs in Europe*; 699 final; COM: Brussels, Belgium, 2008.

European Commission. Closing the Loop—An EU Action Plan for the Circular Economy; 614 final; COM: Brussels, Belgium, 2015.

European Commission. Critical Raw Materials Resilience: Charting a Path towards Greater Security and Sustainability; 474 final; COM: Brussels, Belgium, 2020.

Gupta, S.; Kumar, A.; Singh, V.P.; Patel, P. Coal bottom ash and its applications in cement and concrete technologies: a review. *J. Mater. Circular Econ.*, 6(1), 23–45 (2024).

Hogg, D. *Incineration residues in the EU: quantities and fates*. Edited by E. Favoino, J. Vähk and A. Oliveira. Brussels: Zero Waste Europe (2022).

Li, C.; Zhang, Q.; Shi, C. Evolution of CO₂ uptake degree of ordinary Portland cement during accelerated aqueous mineralisation. *Minerals*, 7(4), 109 (2024).

Mohebbi, M.; Rajabipour, F.; Madadian, E. A framework for identifying the host phases in coal-derived fly ash. *Fuel*, 314, 122806 (2022).

NEPN. Celoviti Nacionalni Energetski in Podnebni Načrt Republike Slovenije; NEPN: Ljubljana, Slovenia (2020).

Oprčkal, P.; Mladenovič, A.; Zupančič, N.; Ščančar, J.; Milačič, R.; Zalar Serjun, V. Remediation of contaminated soil by red mud and paper ash. *J. Clean. Prod.*, 256, 120440 (2020).

Pihlajavaara, T.; Andersson, R.; Johansson, K. Enforced carbonation of cementitious materials: mechanisms and applications for industrial by-products. *Cem. Concr. Res.*, 176, 107028 (2023).

Rahman, A.; Torres, L.; Kim, S. Durability and environmental impact of wastewater sludge ash as a cement replacement in concrete: challenges and future directions. *Clean Technol. Recycl.*, 7(2), 145–162 (2025).

Shi, L.; Müller, A.; Koyanaka, S. Influence of amorphous content in recycled fly ash on binder hydration characteristics. *J. Mater. Cycles Waste Manag.*, 27, 112–124 (2025).

Singh, G.B.; Subramaniam, K.V. Quantitative XRD study of amorphous phase in alkali activated low-calcium siliceous fly ash. *Constr. Build. Mater.*, 124, 139–147 (2016).

SIST EN 16907-2. Zemeljska Dela—2. Del: Klasifikacija Materialov. iTeh Standards: Toronto, ON, Canada (2019). Skevi, A.; Tsiampousi, A.; Papatzani, S. Biomass bottom ash as supplementary cementitious material: the effect of mechanochemical pre-treatment and mineral carbonation. Sustainability, 14(24), 16480 (2022).

Snellings, R.; Suraneni, P.; Skibsted, J. Future and emerging supplementary cementitious materials. *Cem. Concr. Res.*, 107199 (2023).

Wei, G.; Dong, B.; Fang, G.; Wang, Y. Understanding reactive amorphous phases of fly ash through the acidolysis. *Cem. Concr. Compos.*, 140, 105102 (2023).

Yao, Z.T.; Ji, X.S.; Sarker, P.K.; Tang, J.H.; Ge, L.Q.; Xia, M.S.; Xi, Y.Q. A comprehensive review on the applications of coal fly ash. *Earth-Sci. Rev.*, 141, 105–121 (2015).

Zalar Serjun, V. Recycling of different incineration ashes in the construction sector: perspectives from Slovenia. *Materials*, 16(12), 5065 (2024).

Zhao, P.; Liu, X.; De La Torre, A.G.; Lu, L.; Sobolev, K. Assessment of the quantitative accuracy of Rietveld/XRD analysis of crystalline and amorphous phases in fly ash. *Anal. Methods*, 9, 2415–2424 (2017).

Acknowledgment

Special thanks to dr. Mateja Štefancič for conducting the XRF analysis, Sabina Drmovšek for technical support and to dr. Ana Mladenović for her contributions to the conceptualization of part of this work.

Funding

This research was funded by Slovenian Research and Innovation Agency (ARIS), grant numbers P2-0273, J1-4413 and J7-50228.

Author's contribution

All authors have contributed to: conceptualization, investigation, draft, and manuscript preparation. All authors have read and agreed to the published version of the manuscript.



Circular Economy In Mining

Predrag Šinik¹, Ivo Galić², Metka Gostečnik³, Viktor Kovačič⁴, Lana Šteko², Dora Kolobara²

- ¹ Ekomineral d.o.o., Slovenia
- ² University of Zagreb, Faculty of Mining, Geology and Petroleum Engineering, Pierottijeva 6, 10000 Zagreb, Croatia
- ³ Nerinvest d.o.o., Slovenia
- ⁴ Štore Steel d.o.o., Slovenia

DIM-ESEE Conference 15th – 17th October 2025, Dubrovnik, Croatia



Keywords: "circular economy", "sustainable development", "metallurgical waste recycling", Andraž Quarry

Abstract

The traditional linear economic model: "take, make, use, dispose" is unsustainable, and it is necessary to adopt and implement a new approach to preserve the planet.

The transition from a linear to a circular economy is becoming the foundation of sustainable development in resource-intensive industries. This paper presents the model and principles, as well as an example of good practice in applying the circular economy in mining.

As a case study of the circular economy, the Andraž Quarry (Ekomineral & Nerinvest) is analyzed, where, in cooperation with the company Štore Steel, circular economy principles have been practically applied for 15 years in mining, metallurgy, and construction. The circular economy approach includes innovative technologies and cross-sector collaboration aimed at transforming metallurgical and construction waste into valuable secondary raw materials.

A key initiative, the SWIM project (Sustainable Waste Industry Management), enabled the development of new construction products, advanced recycling technologies, and environmental remediation strategies. However, implementation faced significant challenges, including legislative barriers, complex spatial planning requirements, high initial investment costs, and market resistance to recycled materials. Despite these difficulties, the Andraž Quarry and its partners have demonstrated that circular solutions can deliver ecological, economic, and social benefits when supported by systemic changes in legislation, infrastructure investments, and increased public awareness. The need for stronger cooperation between industry, government, and research institutions is emphasized to fully unlock the potential of the circular economy model.

The collaboration between Andraž Quarry and Štore Steel represents a leading example of circular economy application in Slovenia. Since the late 1990s, these companies have adopted practices that turn waste into resources, with particular focus on the reuse of metallurgical slag and construction waste as secondary raw materials for the construction sector. Through projects such as SWIM, innovative technologies have been developed, including mobile modular machines (HEFAJST) for industrial waste processing, specialized concrete mixtures, and asphalt solutions successfully applied in infrastructure projects.

The initiative has resulted in significant environmental benefits, including reduced waste disposal, lower greenhouse gas emissions, and conservation of natural resources. In addition, it has fostered economic resilience by creating new jobs and strengthening regional competitiveness. Nevertheless, the wider application of these practices is hindered by fragmented legislation, slow permitting processes, high implementation costs, and public distrust of recycled products.

Achieving a functional circular economy requires more than just technological advancements—it also demands legal reforms, investment incentives, and collaboration among all stakeholders in society. By aligning the efforts of government institutions, industry, and the scientific community, it is possible to overcome systemic barriers and advance sustainable practices in industry.

1. Introduction

Mining is a key sector for the global economy as it provides raw materials for industry, energy, and infrastructure. However, resource exploitation is associated with a range of environmental and social challenges: environmental degradation, generation of large amounts of waste, greenhouse gas emissions, and conflicts with local communities.

According to the latest research: 90% of biodiversity loss is caused by resource extraction and processing, up to 80 % of a product's environmental impact is determined at the design stage, and the current rate of circular material use in the EU stands at 11.8% (European Commission, 2025).

The linear economy model (take-make-dispose) is becoming unsustainable in the context of growing demand for raw materials and resource scarcity. Therefore, the need for a transition towards a circular economy in mining is increasingly emphasized (Geissdoerfer et al., 2017; EC, 2025).

The sustainable development model prioritizes the maximum reuse of materials and energy, transforming the waste of one industry into valuable raw materials for other sectors. In this way, it goes beyond the linear mindset of consumption and creates a more efficient, sustainable, and economically stable system, in which natural resources do not end up in landfills but continuously circulate among different users.

In this paper, the circular economy (CE) model is examined with a focus on quarries, highlighting the Andraž Quarry as an example, where the adopted principles have been successfully implemented for 15 years (**Šinik et al., 2025**).

2. Circular economy principles in mining

The circular economy is an economic system that promotes the design of products and processes in such a way as to maximize the usability of resources, minimize waste, and reduce negative environmental impacts (see **Figure 1**).

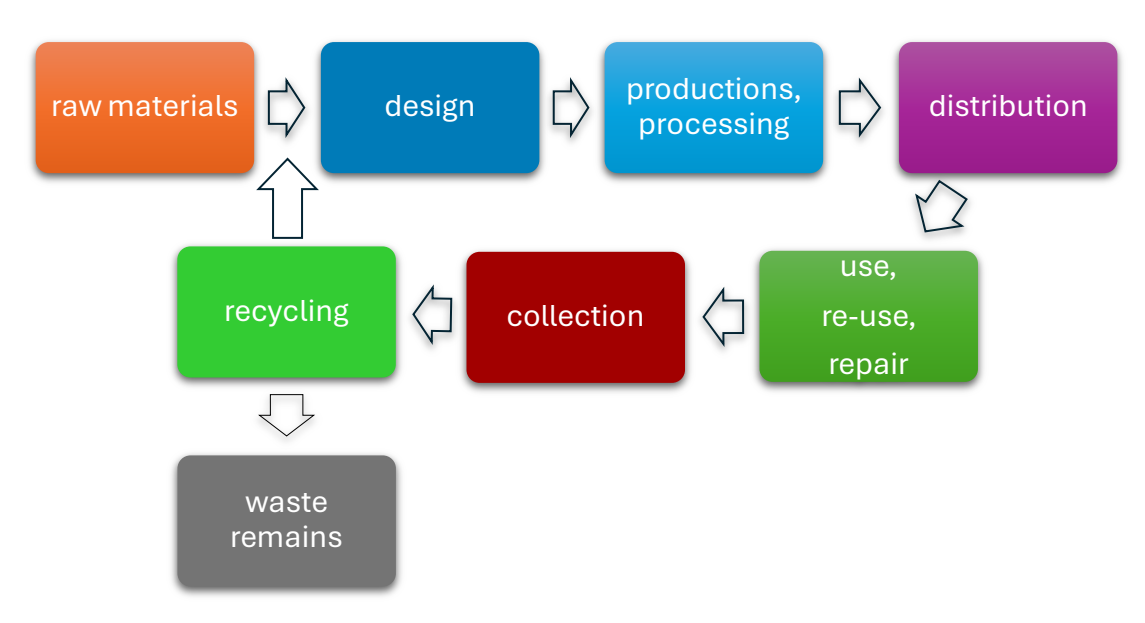


Figure 1. Circular economy model (CCIŠ)

Circular economy principles applicable to mining include:

- Waste prevention and process optimization
- Reuse of by-products and recycling of materials
- Reclamation and repurposing of mining areas for new economic or ecological purposes
- Integration of renewable energy sources in mining operations, in exploitation fields
- Digitization and monitoring of material flows

The circular economy can be represented as a mineral raw materials value chain that can be applied in any area where mining activities are carried out (Galić et al., 2024).

The guidelines for achieving sustainable and environmentally responsible exploitation of mineral resources are based on the document Extractive Industries Transition to Sustainable Systems (United Nations Economic Commission for Europe, 2021).

The mining and related processing and construction industry is an important driver of recovery in the process of transition to green and sustainable economies. However, this transition must be aimed at creating sustainable and socially responsible value chains of mineral raw materials, which seek a balance between environmental protection, the development of mining activity and the rights of local communities (Ndlovu et al., 2017). Therefore, the green transition brings an opportunity to transform the mining and related processing and construction industries towards a more sustainable, fairer and more inclusive development based on the circular economy.

The application of the principles of the circular economy in mining is shown in the **Table 1**.

Table 1. Applying the principles of the circular economy in mining

Input stream / by-product	Applications	Benefits
Fine fractions and rock dust	Production of aggregates for concrete mixtures; soil stabilization	Reduction of waste, added value of secondary raw materials
Overburden (unusable pieces of rock)	Use in local road construction	Less need to exploit new resources; reducing disposal costs
Industrial and construction waste (slag, etc.)	Production of aggregates for concrete mixtures for various purposes; metal extraction	Reduction of waste, added value of secondary raw materials
Used quarry areas	Recultivation into green areas and recreational zones	Improving the landscape, increasing social acceptability
Inactive exploitation zones	Installation of photovoltaic panels	Production of renewable energy, reduction of CO ₂ emissions
Cooperation with the local community	Donations, joint projects, transparent communication	Strengthening the social license to work, reducing conflicts

Mining waste management

The mining industry generates billions of tons of waste annually, including tailings, sludges and slag. Instead of disposal, these streams are increasingly used for:

- production of construction materials,
- soil stabilization,
- filling of abandoned underground and surface spaces.

Secondary raw materials

Mining by-products can become a source of secondary metals and minerals, thus reducing the need for primary exploitation. Examples include the recycling of metal from tailings or the use of slag in the cement industry.

Recultivation and reuse of space

Abandoned quarries and mines are being converted into recreational areas, lakes, solar and wind farms. This practice contributes to reducing the negative perception of mining.

Energy efficiency and renewable sources

The integration of photovoltaic systems, wind farms and the exploitation of geothermal energy in mining areas represents a synergy between mining and the low-carbon transition.

3. Case study of good practice: Circular economy in the Andraž Quarry

As a good practice example in implementing the circular economy approach, the Andraž Quarry (Ekomineral & Nerinvest), in cooperation with the company Štore Steel, has been introducing sustainable solutions for 15 years, proving that sustainability is the future of industry. Their innovative practice transforms waste into raw materials, reduces the ecological footprint, and sets the foundation and new standards for the economy of the future.

The following section presents the achievements and challenges of the circular economy faced by the Andraž Quarry, as well as the research and development program SWIM (Sustainable Waste Industry Management), which integrates research, innovation, and ecology with the mining, metallurgical, construction, and agricultural sectors. The SWIM program fosters business competitiveness and paves the way toward a more sustainable future (Šinik et al., 2025).

Description of location and activity

The Andraž Quarry is located about 15 kilometers northwest of Celje (Slovenia), between the towns of Polzela and Velenje (see **Figure 2**). The exploitation field covers an area of approximately 17.4 hectares. The quarry exploits carbonate rocks that are used as technical and construction stone, i.e. for construction purposes. The exploitation reserves of technical and construction stone amount to approximately 5 million tons, with a large share of overburden (30%) in

the total rock mass. The implementation of the circular economy principle in the Andraž quarry is visible through several dimensions:

- Use of fine fractions and dust: Materials that would otherwise end up as waste are used to produce aggregates for concrete mixes and stabilize the soil.
- Recycling of tailings: Tailings are used in local road construction, reducing the need for primary material.
- Recycling (processing) of industrial and construction waste: Mineral aggregates are used for concrete mixes for various purposes; metals are reused in industry.
- Land reclamation: During exploitation, the open pit is shaped (rehabilitated) and recultivated in phases. After exploitation, parts of the quarry are converted into green areas or zones for recreational purposes, in cooperation with the local community.
- Energy innovations: The possibility of installing photovoltaic panels on inactive quarry surfaces is being explored.
- Social dimension: Active cooperation with the local population through donations and projects strengthens the social license to operate.

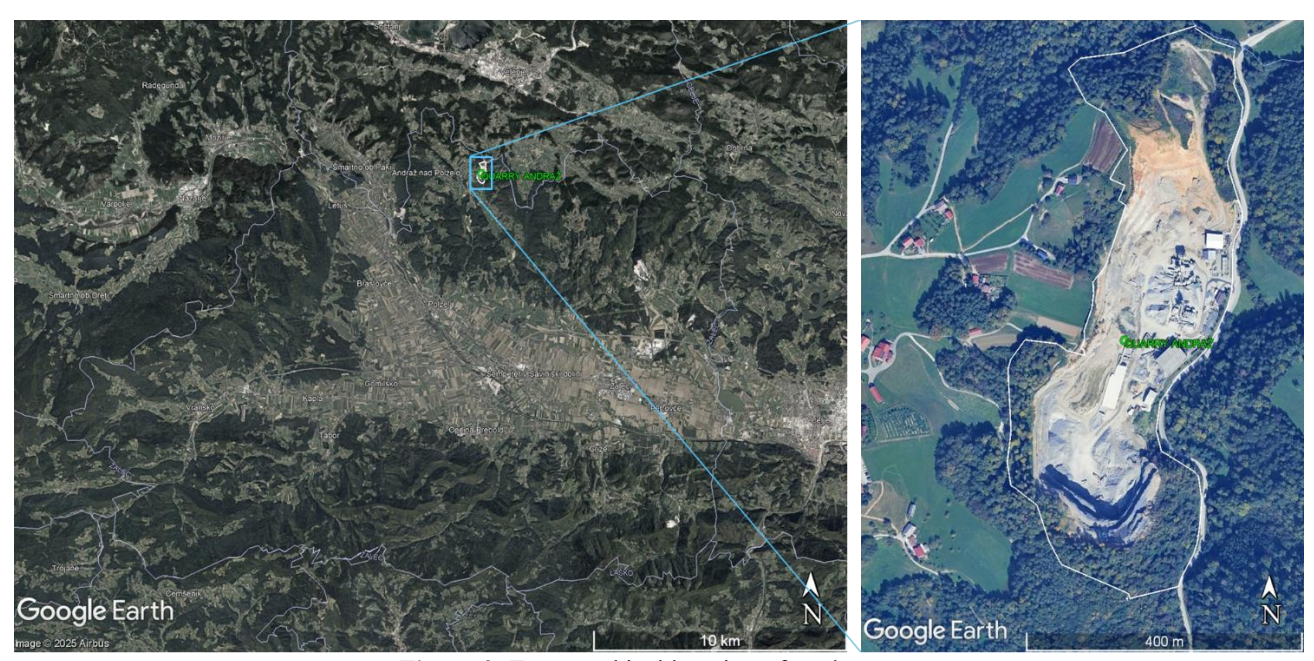


Figure 2. Topographical location of Andraž quarry

Waste processing at the Andraž Quarry: an opportunity for success

At the Andraž Quarry, it was recognized 30 years ago that waste is not just waste, but a valuable source of alternative raw materials. By incorporating the principles of the circular economy into the quarry's core operations, metallurgical byproducts and construction waste are transformed into new construction products that replace primary raw materials.

The Andraž Quarry consists of two parts: the technical and construction stone deposit and the industrial complex.

The deposit covers rocks of carbonate origin in which the primary mineral raw material is exploited using an elevated open pit. The open pit has developed floors with a height of 12 m to 15 m, with a base plateau at 321.5 m above sea level and a total mine height of about 70 m. The industrial complex is located on the base plateau, approximately at 321.5 m above sea level.

Technological equipment is located in the industrial circle - facilities for secondary processing of waste and production of building materials, as well as a landfill for storage of finished products (see **Figure 3**).

Less waste disposal means less burdened landfills, cleaner soil and water, and lower emissions of substances into the air and greenhouse gases. Every recycled material is a step towards preserving natural resources and reducing the negative impact of industry on the environment.

But the benefits go further. The circular economy not only brings environmental benefits, but also connects communities and creates new jobs. The processing of metallurgical and construction waste and other secondary materials opens the door to innovation and increases the need for specialized personnel. Thus, the Andraž Quarry actively participates in shaping a stronger regional economy and contributes to the well-being of the local community.

In addition to environmental benefits, the circular approach should also contribute to economic efficiency. However, economic advantages are no longer self-evident today - due to changes in legislation in recent years, the positive economic trend has reversed. The Andraž Quarry is facing new challenges that may threaten the sustainability of circular business. These include insufficient knowledge of the principles of the circular economy among the professional public and the

restraint and caution of the profession when reusing products made from recycled materials. Such an attitude further hinders the implementation of otherwise effective solutions in practice.



Figure 3. Presentation of the existing contours of the surface mine and the Andraž industrial area (Šinik et al., 2025)

Innovation and development

Technological development and innovation play a key role in realizing a circular economy. Andraž Quarry actively develops sustainable solutions for the reuse of recycled materials in construction and industry. The development and research project SWIM has so far led to advanced solutions, such as new construction products REMIX, special concrete and asphalt, and HEFAJST technology. In the future, new activities are planned within the SWIM and LIFE IP RESTART projects, including re-mining on metallurgical landfills.

SWIM – sustainable use of metallurgical waste

The SWIM project, implemented by Ekomineral & Nerinvest together with Štore Steel, is aimed at the sustainable processing of metallurgical waste, where black and white steel slag play a key role (see **Figure 4**). These secondary raw materials are used in construction as a substitute for natural mineral raw materials, because they have good physical-mechanical and chemical properties that contribute to their usability in various applications, especially for special concrete (see **Figure 5**). The use has been tested and confirmed in various test projects.



Figure 4. Processed black slag

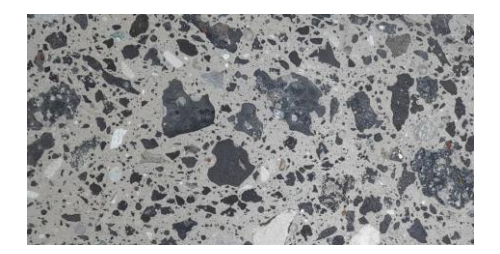


Figure 5. Special concrete ČBŽ100

HEFAJST – innovative technological solutions

As part of the SWIM project, the HEFAJST program was developed, the main achievement of which is the construction of a modular mobile machine for the processing of metallurgical waste, with the HH/HDTRS 1200/AFCFL 1000/2.46 complex. Advanced separation technology enables efficient separation of various metals and mineral raw materials. It is also designed to work on landfills, as a mobile unit, which would reduce the environmental burden of degraded areas, and at the same time open up new opportunities for sustainable resource management.

In the past 9 years, the production and sale of recycled materials has been variable, from an initial 40,000 tons (2016) to a maximum of 265,000 tons (2019). In the last five years, there was a drop in production, which was caused by the reduced activity of the construction sector, so that last year the placement of recycled materials amounted to about 80,000 tons.

Integration of renewable energy sources

The Andraž quarry is located in an isolated area that is not sufficiently supplied with electricity to start the plant in the industrial area. In the current circumstances, for the supply of electricity to the industrial area, our own capacity, i.e. diesel electric generators, with a total power of about 1 MW, is used.

However, there is a possibility of integrating renewable energy sources on areas that have already been excavated or will be excavated in the near future and on facilities in the industrial area. Such systems would enable independent sources of energy to power mining machines and plants, which makes mining operations even more environmentally friendly.

The transition of the mine from the classic form, with the dominant use of energy from diesel fuel or a hybrid network, to the model of the so-called "green mine" can be implemented by gradual integration of renewable energy sources. Mining facilities in segregated areas are particularly vulnerable due to their energy dependence and consequently less resistance in the market. Therefore, in order to improve the sustainability and resilience of mining facilities in isolated areas, the integration of renewable energy sources is necessary. In this way, the final results will be reflected through positive economic and ecological effects (**Kronja et al., 2025**).

Rehabilitation and reclamation of the Andraž Quarry

The principles of the circular economy in mining also include complementary spatial planning solutions, which presuppose the rehabilitation and reclamation of the Andraž Quarry, during the exploitation of primary raw materials and the recycling of industrial and other types of waste.

According to the plans of the economic company, the identified exploitation reserves are sufficient for about 20 years of quarry operation. Successively with the exploitation of technical and construction stone, the shaping (rehabilitation) of the final contours of the Andraž open pit mine will be carried out.

According to the detailed spatial plan, the Andraž exploitation field needs to be biologically rehabilitated or recultivated in order to achieve a landscape composition with the immediate environment (see **Figure 6**). For this purpose, project documentation has been prepared with spatial planning and repurposing solutions for the Andraž Quarry.

The development of mining works at the Andraž Quarry is divided into several phases. Upon completion of each phase of mining works, biological remediation of the terrain will begin, which primarily consists of filling empty spaces and forming surfaces (terraces and slopes) for recultivation. Filling the empty spaces will be carried out with unusable waste residues, which will be generated in the recycling process of metallurgical and construction waste. The final, surface layer of the terrain (0.5 m to 1.0 m) will be formed by spreading a mixture of humus and substrates that are suitable for the development of plant cover.

Rehabilitation of the quarry and appropriate reclamation of the terrain will return the area to its natural state, and the qualitative and quantitative damage to the environment will be minimal.



Figure 6. Spatial representation of the exploitation field Andraž after biological remediation

4. Results and discussion

The application of the principle of circular economy in the Andraž quarry brought a number of benefits, of which the following stand out:

- Waste reduction through the use of by-products.
- Reduced consumption of primary resources in road construction and civil engineering.
- Disposal of unusable waste and reclamation (repurposing) of space

- Positive effects on the perception of the local community and increased social acceptance of mining activities.
- Potential for the integration of renewable energy sources in the future...

The result of a balanced circular economy in the Andraž Quarry is a symbiosis (joint action) of all relevant participants, process stakeholders that can be represented by a circular flow (see **Figure 7**).

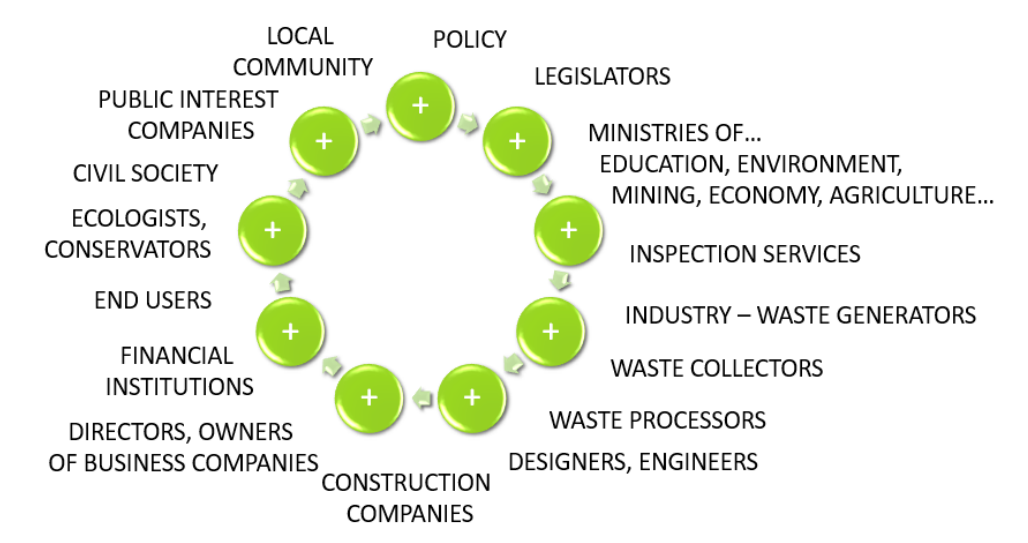


Figure 7. The result of a balanced circular green economy

There are numerous obstacles and challenges for the application of circular economy principles, such as:

- 1. Technical and Technological Challenges
 - Technical limitations in the reuse of waste material in construction (quality regulations, standards).
 - Required investments in new technologies (crushing, screening, stabilization, sludge treatment).
- 2. Economic Challenges
 - High initial costs for the development of circular economy infrastructure.
 - Low market value of by-products (e.g., fine fractions, quarry dust).
 - Dependence on demand in the construction sector recycled aggregates are often not competitive with primary ones.
- 3. Regulatory and Administrative Challenges
 - Insufficiently clear legal framework regarding the status of by-products and waste.
 - Complex procedures for obtaining permits for secondary products.
 - Lack of national and local policies to encourage closed material flows.
- 4. Environmental Challenges
 - Compliance with environmental protection measures near settlements and natural areas.
- 5. Social and Organizational Challenges
 - Lack of qualified personnel for managing circular processes.
 - Insufficient awareness and education on the benefits of the circular economy in the mining sector.

5. Conclusion

Circular economy in mining represents a necessary step in the transition toward sustainable development. The application of CE principles can significantly reduce the sector's ecological footprint, open new markets for secondary raw materials, and increase the social acceptability of mining projects. Good practices, such as the integration of byproducts into the construction industry and the reclamation of extraction sites, demonstrate that this model is both feasible and economically viable.

The symbiosis between the Andraž Quarry and Štore Steel is a prime example of good practice, proving that innovation and collaboration can generate sustainable benefits. This partnership has pushed the boundaries in the sustainable use of raw materials and the efficient processing of industrial by-products.

Nevertheless, numerous obstacles hinder the implementation of the circular economy in practice. Among the key challenges are legislative inconsistencies across different sectors, administrative barriers, and decision-making inertia, all of which slow down the transition to a circular economy. In addition, high initial costs, the lack of adequate infrastructure,

and market skepticism toward recycled products are factors that further constrain the development of sustainable practices.

To unlock the full potential of the circular economy on a broader scale, legislative adjustments are necessary to remove administrative barriers, harmonize regulations across different governmental bodies, and streamline bureaucratic procedures. Additional incentives are also needed for investments in new technologies and infrastructure development, which would enable more efficient recycling and reuse of materials. Furthermore, certain benefits or exemptions for companies that use recycled-material products would be highly meaningful.

Achieving a circular economy requires close cooperation among government institutions, industry, the research sector, and the wider community. Local communities, civil associations, educational institutions, the construction profession, and end-users also play an essential role. Only through the inclusion of all levels of society can there be a deeper understanding and more effective implementation of circular economy principles in practice.

References

- Chamber of Commerce and Industry of Štajerska (CCIŠ). The Strategic Research and Innovation Partnership (SRIP). Available online: https://srip-circular-economy.eu/ (accessed on 10 September 2025).
- European Commission (EC). Circular Economy. Available online: https://environment.ec.europa.eu/strategy/circular-economy en (accessed on 10 September 2025).
- Galić, I., Bohanek, V., Farkaš, B., Pavičić, I., Duić, Ž., Borojević Šoštarić, S., Garašić, V., Brenko, T., Bilić, Š., Kurevija, T., Macenić, M. (2024). Mining and Geological Study of Karlovac County. Faculty of Mining, Geology and Petroleum Zagreb. Available online: https://www.kazup.hr/images/RGS K%C5%BD-compressed.pdf (accessed on 10 September 2025).
- Geissdoerfer, M., Savaget, P., M.P. Bocken, N., Hultink, E. J. (2017). The Circular Economy A new sustainability paradigm? Journal of Cleaner Production. 143, 757-768. https://doi.org/10.1016/j.jclepro.2016.12.048.
- Kronja, J., Galić, I., 2025., Integration of Renewable Energy Sources to Achieve Sustainability and Resilience of Mines in Remote Areas. Mining, 5, 51. https://doi.org/10.3390/mining5030051.
- Ndlovu, S., Simate, G.S., Matinde, E. (2017). Waste Production and Utilization in the Metal Extraction Industry. CRC Press, Boca Raton, 230. https://doi.org/10.1201/9781315153896.
- Šinik, P., Gostečnik, M. (2025). 15-let krožnega gospodarstva v praksi Kamnolom Andraž –Štore Steel in projekt SWIM Pasti in prednosti. 28. strokovni posvet "Slovenska okoljska modernizacija in zeleni prehod". Moravske Toplice, 10-11 april 2025.
- United Nations Economic Commission for Europe (2021). Extractive Industries-Transition to Sustainable Systems. https://www.un.org/sites/un2.un.org/files/2021/05/final_regional_brief_on_extractive_industries.pdf (accessed on 10 September 2025).



Training needs of copper sector employees in the context of digital and environmental transformation: results of the SkiComCu project

DIM-ESEE Conference



Jolanta Religa¹ ©⊠, Ireneusz Woźniak² ©⊠, Malwina Kobylańska³©⊠, Katerina Adam⁴©⊠, Małgorzata Kowalska⁵©⊠

- $^{1\,2\,5}$ Łukasiewicz Research Network Institute for Sustainable Technologies Centre for Vocational Education Research and Innovation Management, ul. Pułaskiego 6/10, 26-600 Radom
- ³ KGHM CUPRUM Ltd. Research and Development Centre, Gen. Wł. Sikorskiego 2/8, 53-659 Wrocław
- ⁴ National Technical University of Athens School of Mining and Metallurgical Engineering, Zografou 157 72, Greece

Abstract

The research work presented in the article focuses on identifying competency gaps among employees in the copper sector, a sector strategically crucial for the development of the EU economy, particularly in the context of the green transition. Within the challenges facing the copper sector, the human resource and skills shortages are becoming increasingly urgent. The present research, conducted within the SkiComCu-LL project funded by EIT RM, aimed to identify the competency gaps of selected groups of current and future employees in the European copper industry. The methodological approach included a triangulation of methods: desk research, an online survey (conducted directly in the work environment for key competence profiles selected by the project partnership as strategic for the future of the sector), and participatory assessment - interviews with representatives of different groups of copper sector employees (Focus Group Interviews). Competence gaps were analysed in two categories: technical and social competencies. It has been demonstrated that copper processing is a highly specialised field, requiring the integration of fundamental knowledge and skills in STEM disciplines, such as physics, chemistry, and mechanics, with modern automation and digitalisation, including virtual and augmented reality (VR, AR) applications. The results obtained serve as the basis for formulating a proposal for training topics and developing training materials that align with the real expectations of both current and future employees in the copper sector companies.

Keywords: lifelong learning, competences, competence gaps, competency profiles, copper industry

1. Introduction

Available reports, academic data and industry studies indicate that the European copper labour market is shaped by the interaction of four megatrends: technological progress, sustainable development, demographic change and globalisation (Marszowski, Jarosławska-Sobór, 2025; OECD, 2024; WEF, 2023). Other researchers have emphasised that the most critical changes in mining include improved safety, increased productivity, environmental care, and more efficient resource utilisation (Beloglazov et al., 2020; Kazanin, 2017). This reflects the aim of transformation towards Industry 4.0. It is based on the consolidation of systems and the integration of people with digitally controlled machines that extensively utilise wireless networks, information, and communication technologies.

The copper industry is shifting towards innovative solutions, including automation and artificial intelligence, as well as digital and climate-neutral activities, to enhance operational efficiency. To achieve these goals, the changes are also expected to create specific skills, new job positions, and innovative methods of working.

The undersupply of skills in Europe is attributed to declines in education and training systems that are failing to prepare the workforce for technological change. According to the Draghi Report (EC, 2024), the EU should overhaul its approach to skills, making it future-oriented and focused on emerging skill shortages. As was shown in this report, despite a significant EU's current investment in skills development and training, results have been limited due to, e.g. limited industry involvement in shaping job-specific training, lack of systematic evaluations of training results, hindering strategy refinement and underuse of skills intelligence, i.e., reliable, granular data on skill needs and gaps.

In the copper sector, addressing the crucial problems in the HR area should focus on modifying staff recruitment and retention strategies, as well as prioritising the upskilling and retraining of existing employees (EY, 2023). This is also supported by forecasts from the World Economic Forum, which indicate the need for higher investment in developing the professional competences of existing employees and in retaining employees with specialised skills and qualifications, as talent availability during hiring is expected to be significantly lower (WEF, 2023). On the other hand, different training

and education requirements sometimes hinder the free flow of workers from one region or industry to another (Religa et. al., 2024).

The research work to identify, recognise and understand gaps in skills and competences in the copper value chain has been implemented within the 'SkiComCu-Lifelong Learning (LLL) Course for skills & competences in the Copper sector' project. The project proposal was based on research conducted in selected RIS (Regional Innovation Schemes) countries. The project focuses on the development and delivery of advanced training materials and innovative tools to support them, corresponding to the requirements of digital and green transformation, among others.

The key aspects of the project is to provide through LLL the necessary skills related to industry 4.0 & 5.0, green transition and circular economy that boost the responsible sourcing of critical and strategic raw materials in Europe thereby securing their supply and advance innovation, and education related to circular economy and closing materials' loops for the Cu-sector in the EU, in parallel with facing technological, structural and human changes management.

2. Methods

The primary objective of the undertaken activities presented in this article was to identify and analyse the training needs of selected occupational groups employed in the copper (Cu) sector, with particular emphasis on countries covered by the EIT Regional Innovation Scheme (RIS), where the need to foster innovation capacity is greater.

The research methods employed included desk research, online surveys, and focus group interviews (FGIs). The research covered employees working in the following enterprises: KGHM Polska Miedź S.A., ELVALHALCOR Hellenic Copper and Aluminium Industry S.A., Aurubis Bulgaria AD.

The methodological approach adopted in this study aimed to identify competency gaps among employees in the copper (Cu) sector, with reference to a set of strategic competency profiles defined by the SkiComCu partnership as essential for the sector's sustainable development.

Due to the complexity of the copper industry—characterised by diverse operational domains and a correspondingly broad spectrum of skills required to ensure both effective job performance and sectoral competitiveness—the scope of the research was limited to selected, representative occupations and key competencies within copper ore extraction, processing, manufacturing and recycling. This targeted approach enabled a focused analysis of skill requirements in core industry segments, ensuring the relevance and applicability of the findings.

2.1. Development of Key Competency Profiles for the Copper Sector

Based on document analysis, a review of relevant source materials, and the methodological expertise of the project team, six competency profiles were identified as strategic for the further development of the copper sector, as defined by the SkiComCu partnership:

- 1. Miner Operator of Self-Propelled Mining Machines (EQF Level 3)
- 2. Mineral Processing Technician (copper ore) (EQF Levels 4 and 5)
- 3. Mining Engineer (Senior Mining Supervisor) (EQF Levels 6 and 7)
- 4. Mining Geologist (EQF Levels 6 and 7)
- 5. Metallurgical Engineer Non-Ferrous Metals (EQF Levels 6 and 7)
- 6. Copper Recycling Process Engineer (EQF Levels 6 and 7)

The selection of profiles was guided by the specific criteria: alignment with the European Qualifications Framework (EQF), inclusion of diverse employee categories (foremen and operational staff, professionals, managers and senior specialists), holistic understanding of the sector, alignment with industrial partner needs, and evidence-based and forward-looking, future-safe approach.

The descriptions of selected profiles were developed according to a standardised structure agreed upon within the partnership. Learning outcomes were categorised into two domains: technical skills and social competencies.

2.2. Identification of Skill Gaps (Online Survey - CAWI)

The second stage involved an online survey (Computer-Assisted Web Interviewing – CAWI), designed specifically for each of the six strategic competency profiles. A diagnosis of both professional skills and social competences was undertaken.

As previously noted, the survey targeted employees in the copper sector working in mining and processing companies operating in countries covered by the RIS scheme. Respondents included employees at various organisational levels whose job roles aligned with the identified profiles, as well as their direct supervisors. A total of 250 complete responses were collected. The questionnaires were made available via a hyperlink or QR code. Due to the limited length of this publication, the survey questionnaires (separate for each of the six profiles studied) could not be included. They are available in the research report at the project website: https://skicomcu.eu/work-packages/.

2.3. Identification of Skill Gaps (Focus Group Interviews - FGIs)

The third stage consisted of focus group interviews (FGIs), aimed at deepening the insights obtained through the online survey and identifying current and future skill gaps in the copper sector workforce. FGIs were conducted using a semi-structured interview format. An interview scenario and guidelines for the interviewers were developed.

The focus group interviews were organised and conducted (May-June 2024) with the involvement of key industrial partners of the SkiComCu project, with the participation of employees of the copper companies representing three RIS countries: Poland, Greece and Bulgaria. We employed a stratified purposive sampling strategy, coordinated with the HR units of the partner companies, to ensure that each focus group reflected the organisational structure and key functions of the copper sector in the three RIS countries. The target groups in each country (8-12 selected people) included: middle management and technical staff, senior management, administrative and office staff, and HR staff. Eligible candidates were current employees with role-relevant knowledge and direct exposure to the topics under study, able to participate in the interview in the designated language, and available on the scheduled dates. HR departments compiled preliminary nominee lists per stratum; the research team then screened and invited participants to: 1) meet inclusion criteria, 2) avoid direct reporting lines within the same group (to reduce social-desirability and dominance effects), and 3) maximise heterogeneity (company/site, function, tenure, and gender). Participation was voluntary and based on informed consent, with confidentiality assured.

Participants met face-to-face in each of the three countries. They discussed the situation of human resources in the copper sector, focusing on several neutral and unambiguous exploration questions that do not allow for "yes/no" answers:

- What are the most urgent competency gaps in the sector?
- Is the training offer for developing the competences of current workers of the copper sector (reskilling, upskilling) accessible, satisfactory, and based on the latest technical developments? How should it be improved?
 - How to attract new employees to the Cu sector?
- What difficulties do Cu sector companies face in recruitment processes? Does the development and/or updating of job descriptions and vacancies require competence development of HR staff?

Discussions were run by a moderator/ facilitator (as an active participant), according to the scenario. The moderators were experienced researchers representing the SkiComCu project partnership institutions, familiar with the full context of the research being conducted. After the interviews, the moderators prepared summaries of the discussion results, which were further analysed by the research team responsible for the project's research component.

3. Results

3.1. Survey results (CAWI)

Respondents performing work in accordance with the analysed competency profile were asked to assess the level of individual professional and social competencies included in that profile. This assessment covered both their own skills and those observed in their coworkers. In turn, respondents in managerial positions were asked to provide a similar evaluation regarding the employees under their supervision.

Competencies were assessed using a five-point Likert scale, with the following weightings: very low (weight = 1), low (weight = 2), satisfactory (weight = 3), high (weight = 4), and very high (weight = 5).

In cases where the respondent was unable to evaluate a particular competency, the option "Not applicable" (weight = 0) was available. Responses marked as "Not applicable" were excluded from the calculation of the mean scores.

Table 1 presents the competencies that received the lowest ratings, indicating the areas requiring further development within the selected 3 (out of 5) analysed competency profiles. The profiles with the highest percentage of respondents were selected for presentation in the table.

A unified threshold of 4.0, representing the average value, was adopted.

3.2. Results of Focus Group Interviews (FGI)

The data obtained during focus group interviews were the subject of qualitative analysis (SkiComCu report on the assessment & validation of needs for Cu-oriented education chain selected groups, not published yet). The most relevant elements of this analysis are presented in the following paragraphs.

According to the Polish interviewees, technological challenges in the copper industry are primarily related to the process of automation and remote control of machines. The biggest challenge facing the industry is adapting company operations to technological changes, as well as changing organisational culture, social culture, and generational differences. Special emphasis was placed on methods of communication, task performance in the workplace, and the implementation of new technologies. On the other hand, social challenges faced by the Cu sector are primarily demographic changes – an ageing society and the need to implement solutions that ensure the replacement of generations. FGI participants forecast the need for technological changes in workplaces to adapt them to the capabilities of the ageing workforce. The lack of basic technical skills among younger workers was considered a significant challenge in Poland. Similar views were shared by participants in the Greek focus group, who generally cited attracting and retaining young people as a significant challenge

for the sector. Replacing the skills of experienced existing staff with skills available in the labour market was reported as a significant difficulty today.

The Bulgarian participants of FGI identified the industry's ability to leverage technological development as a primary challenge facing the cooperative sector. As the most essential competency gap in the sector in Bulgaria, which need immediate actions, "the lack of overall view of the business by the employees" (most of the employees in the sector are not familiar with the method of working of the business as well as of key sectors in connection with its operation, e.g., the financial operations, the logistic operations) was identified. The importance of the green transition and ESG reporting was also highlighted as a significant topic that needs attention in the professional development process of sector employees.

Regarding the most urgent competency gaps in the sector, Greek experts, like their Bulgarian counterparts, pointed out the lack of knowledge of basic Cu properties and characteristics. Additionally, they highlighted the need for the following soft skills at all levels and all work positions: communication (including intergenerational), collaboration, and flexibility. The importance of soft skills was also emphasised during the interview in Poland, where, in addition to the skills reported by the Greek FGI's participants, the following skills were mentioned: involvement, motivation for change, and stress resistance. Polish members of the focus group identified the most urgent gaps among employees in the copper ore mining and processing sector into several categories. Next to the soft skills mentioned above, they underlined basic technical skills, as the most urgent, digital skills and several managerial skills, like e.g., transfer of instructions/ orders, searching for "talents" and recruiting them within the organisation, building clear pathways to professional development, and building competency-based teams. They also pointed out the lack of commitment and identification with the company among young people, which strongly distinguishes them from older generations of workers.

Attraction and retention of new employees in the Cu sector was a "hot subject" of discussion during FGI in all participating countries. It was suggested that efforts should focus on branding and marketing for copper sector companies, enhancing their image in the market to attract young specialists. It is essential to provide employees with opportunities for career development to ensure they have a solid career path within the company.

Participants of focus groups in different countries confirmed the conclusions of literature reports, that there is a serious problem of replacing experienced employees in the copper sector companies, where jobs are not very attractive for young employees in terms of working conditions (including payments).

Analysis of competences in the sector provides supporting evidence that copper processing is a highly specialised field that requires material and technical knowledge on the one hand (physical and chemical properties of copper and operating parameters of metallurgical processes), whereas on the other hand, special skills to face the challenges of advanced green and digital transformation.

Through the work conducted within SkiComCu, it was also demonstrated that training needs in the field of soft skills are equally important and urgent. Participants identified skills such as communication, cooperation and teamwork, leadership, analytical thinking (including data interpretation), and flexibility as essential for sustainable operations.

Table 1. Professional skills and social competencies require development within the given competency profile.

Competency	Number of	Lowest-rated professional skills	Lowest-rated social competencies
profile The Miner Self- Propelled Mining Machine Operator	respondents 50	Maintains the operational logbook of the self-propelled mining machine on an ongoing basis.	 Applies stress management techniques. Utilises problem-solving methods and techniques. Adapts behaviour with consideration for other team members.
The Solid Mineral Processing Technician	82	 Operates storage and loading processes for solid copper mineral processing products. Operates raw material storage systems. Defines operational procedures for the use of machinery and equipment for grinding solid minerals. Performs preliminary treatment and dosing of raw materials for core solid mineral processing operations. 	 Proposes solutions to challenges encountered during the execution of professional tasks under unpredictable conditions. Adjusts behaviour with consideration for other team members. Actively participates in the implementation of collaborative team tasks. Applies principles of effective interpersonal communication. Utilises methods and techniques for problem-solving.
The Metallurgical Engineer – Non- Ferrous Metallurgy	75	 Plans and organises both individual and team-based work for solving materials-related problems in the metallurgical and copper industries, including interdisciplinary challenges. Designs manufacturing technologies for advanced materials specific to the copper and nonferrous metals industries. Applies logistics principles in metallurgical enterprise management. Designs and optimises material processing operations in the non-ferrous metals industry, particularly in areas related to traditional and advanced metallurgical process engineering, copper processing, and materials engineering. Utilises basic IT tools for processing measurement data in materials engineering. Manages production processes of copper-based semifinished products and multi-material composites based on non-ferrous metals, using various synthesis techniques. Collaborates with specialists and expert teams to address complex technical and organisational problems in the workplace. Applies knowledge of mathematics, physics, and chemistry in the design of processes specific to materials and metallurgical engineering, particularly in metallurgy, recycling, and the processing of copper and other non-ferrous metals, including process automation. Applies the fundamentals of physics, mathematics, and statistics necessary for interpreting and processing measurement data. Analyses properties and selects appropriate non-ferrous metals for technical applications. Utilises basic techniques used in the analysis of materials and processes related to copper and non-ferrous metals processing. Applies specialised knowledge in the design and optimisation of tools for various production processes in copper tube manufacturing plants. Demonstrates expertise in selecting appropriate tools at different stages of the production process. Understands phase transformations and their implications f	 Is prepared to make decisions within the scope of assigned responsibilities. Is prepared to assess the risks and consequences associated with mining activities. Demonstrates awareness of the significance of the extractive industry for socio-economic development. Motivates colleagues and subordinates to achieve goals effectively, comply with regulations, and implement best practices and professional ethics. Builds and maintains strong relationships with various stakeholder groups (local communities, subordinates, clients, and subcontractors) by fostering mutual trust, respect, and improved communication. Demonstrates social and entrepreneurial initiative in the workplace. Is prepared to take responsibility for assigned tasks and decisions made. Is willing to share knowledge and expertise. Is committed to engaging in actions that promote sustainable development.

4. Discussion

The studies on competence gaps among employees in the copper sector in selected European countries, conducted within the SkiComCu project and presented in this article, were innovative. They focused on a specific group of employees of a larger sector (non-ferrous metals sector), i.e. employees of copper ore mining, processing and manufacturing. This research was undertaken due to the importance of copper as a strategic raw material for the development of the European economy, as well as the ongoing challenges faced by companies in this sector in attracting and retaining suitably qualified staff (EY, 2023; WEF, 2023; Religa et al., 2024).

The survey covered five employee group profiles that the project partnership identified as key for the future of the sector. The selection and description of key competence profiles for selected employee positions were preceded by indepth desk research, as well as expert knowledge of the industrial partners of the SkiComCu project, which included key industrial companies in the European copper industry (Bator A., 2012).

The proposed methodology enabled the identification of competence gaps for selected groups of employees representing the profiles mentioned above.

Research has shown that the professional skills gaps differ for each of the profiles studied. Some of them are consistent with the data available in publications and reports, primarily regarding skills resulting from global technological changes that affect the competency requirements of employees, such as the automation and digitisation of processes (WEF, 2023). These processes are associated with, for example, remote control of activities, virtual and augmented reality (VR, AR) applications, and real-time monitoring and analysis of production (Chirgwin, 2021). However, the respondents to the surveys and FGIs also indicated many particular skills closely related to the key competence profiles for the copper sector, e.g., a comprehensive understanding of metallurgical principles and processes, as well as storage, loading, and transport processes for solid copper mineral processing products.

The survey consisted, to a considerable extent, of self-assessment given that more than 80% of respondents were employees in the surveyed profession. It is noticeable that the results align with the general correlation that, as the educational level of the respondents increases, their level of awareness and critical view of their own competences and the need for development also increase. In the SkiComCu study, the respondents indicated the fewest deficiencies in the skills possessed when commenting on the competences of a mining machinery operator (EQF 3). They indicated that, in their opinion, the level of professional skills and social competencies they currently possess is very high and does not require further development.

5. Conclusions

Based on the survey results, it was deduced that in the copper ore mining and processing sector, the working positions related to the recycling of copper-containing materials are not considered as a separate profession. Professional tasks related to this vital area of operation of copper industry enterprises are performed by representatives of professions, such as metallurgical engineers. The increasing importance of recycling processes in the overall management of copper resources justifies the assumption that this will likely prove insufficient in the near future, where engineers specialising in the recovery of copper from production waste will be needed.

Gaps in soft skills, both in literature reports and in research within the SkiComCu project, were unanimously recognised as essential and urgent professional competences. The following skills were identified as the most important for future employees in the Cu sector, including analytical and creative thinking, flexibility and agility, motivation and self-awareness, as well as curiosity and a commitment to lifelong learning (Barbara, 2021; WEF report, 2023). When analysing the responses of SkiComCu project participants, a specific pattern of repeated indications for employees whose qualifications are at different levels of EQF was noticed. The competences identified as in need of urgent development, and were common for EQF levels 3 and 4, and for EQF levels 5 and 7, include:

- a) for competences of EQF levels 3 and 4: Applies problem-solving methods and techniques; Modifies behaviour taking into account other team members
- b) for competences of EQF levels 6 and 7: Demonstrates social and entrepreneurial activity in the workplace; Initiates actions for sustainable development; Builds and maintains good relationships with different stakeholder groups; Assess the risks and consequences of undertaking mining activities.

Moreover, the dynamic transformation processes occurring within companies necessitate that employees continually adapt to new situations and conditions. These skills will become increasingly important in the future.

Copper sector companies, especially those from RIS EU territories, should continually invest in training programs to develop the skills and expertise necessary to meet the demand for sustainable copper production. This could include apprenticeships, internships, Lifelong Learning programs, or specialised programs to move across sectors. Therefore, the results obtained and presented in the present study provide a basis for formulating proposals for training topics and developing training materials that align with the real expectations of current and future employees, as well as those of copper sector companies.

6. References

- Barbara A., Tauš P. (2021). Mining Engineer Competencies for an Innovative Economy. In E3S Web of Conferences: The Second Interregional Conference Sustainable Development of Eurasian Mining Regions (SDEMR-2021), vol. 278
- Bator A. (2012). Competency profiles as a tool used in the recruitment and selection process of the mine workforce. AGH Journal of Mining and Geoengineering, vol. 36, No. 3.
- Beloglazov, I. I., Petrov, P. A., Bazhin, V. Y. (2020). The concept of digital twins for tech operator training simulator design for the mining and processing industry. Eurasian Mining, 2020(2), 50–54. https://doi.org/10.17580/em.2020.02.12
- Chirgwin P. (2021). Skills development and training of future workers in mining automation control rooms. Computers in human behaviour report, volume 4, August-December 2021. Elsevier. https://doi.org/10.1016/j.chbr.2021.100115
- Deloitte (2022). Future of Work in mining: Attracting, developing and retaining talent. https://www.deloitte.com/content/dam/assets-shared/legacy/docs/deloitte-norcat-future-work-in-mining.pdf
- EIT Raw Materials Strategic Agenda (2021-2027). https://eitrawmaterials.eu/sites/default/files/2024-11/EIT RM Strategic Agenda 2021-2027.pdf
- Ernst & Young (2019). The future of work: the changing skills landscape for miners. A report for the Minerals Council of Australia. https://minerals.org.au/wp-content/uploads/2023/01/The-Future-of-Work-The-Changing-Skills-Landscape-for-Miners-February-2019.pdf
- Ernst & Young (2023). Building a better working world. Top 10 business risks and opportunities for mining and metals in 2024. EYGM Limited.
- European Commission (2024). Report on the Future of European Competitiveness. https://commission.europa.eu/topics/eu-competitiveness/draghi-report_en#paragraph_47059 (accessed 24th July 2025).
- Kazanin O.I, Drebenshtedt (2017). Mining education in the XXI century: global challenges and prospects. Journal of Mining Institute Vol. 225. St. Petersburg.
- Marszowski R., Jarosławska-Sobór S. (2025). Forecasting future skills and the internal potential of entrepreneurs from the perspective of mining transformation in Poland and the global labour market megatrend. Scientific Papers of Silesian University of Technology, Organisation and Management Series. DOI: 10.29119/1641-3466.2025.216.21
- OECD (2024), OECD Employment Outlook 2024: The Net-Zero Transition and the Labour Market, OECD Publishing, Paris, https://doi.org/10.1787/ac8b3538-en
- Religa J., Kobylańska M., Lopes L. (2024). Trends in changes in competency expectations towards employees in the copper sector. Edukacja Ustawiczna Dorosłych. Journal of Continuing Education nr 4/2024,13-28, DOI: 10.34866/fpp0-sz39
- SkiComCu Report on the assessment & validation of needs for Cu-oriented education chain selected groups (Del. 2.1: chrome-extension://efaidnbmnnnibpcajpcglclefindmkaj/https://skicomcu.eu/wp-content/uploads/2025/07/SkiComCu_Deliverable_2.1_final.pdf).
- Włoch R., Śledziewska K. (2020). Kompetencje przyszłości. DELab UW, Polski Fundusz Rozwoju.
- World Economic Forum (2023). Future of the Jobs Report. Insight report.

Acknowledgment

This research work was carried out within the 'SkiComCu-Lifelong Learning Course for skills & competences in the Copper sector' project. The authors also acknowledge the SkiComCu project industrial partners: ElvalHalcor Hellenic Copper and Aluminium Industry S.A., KGHM Polska Miedź S.A. and Aurubis Bulgaria AD, who provided input in the surveys and the FGIs, as well as other partners not included in the affiliations, who, according to the authors, contributed to drafting this article.

Funding

EIT RawMaterials, grant number 23043, funded this research.

Author's contribution

Jolanta Religa (PhD): conceptualisation, formal analysis, investigation, methodology, project administration, supervision and writing — original draft. **Ireneusz Woźniak** (PhD): data curation, investigation, methodology, visualisation and writing — original draft. **Malwina Kobylańska** (PhD Eng.): formal analysis, funding acquisition, project administration, resources and writing — original draft. **Katerina Adam** (Professor): formal analysis, investigation, funding acquisition, resources, supervision and writing — review & editing. **Malgorzata Kowalska** (PhD): data curation, investigation, resources, validation and writing — review & editing.

All authors have read and agreed to the published version of the manuscript.